Universitat Autònoma de Barcelona

DEPARTMENT OF BIOCHEMISTRY AND MOLECULAR BIOLOGY

SCHOOL OF VETERINARY MEDICINE

CENTER OF ANIMAL BIOTECHNOLOGY AND GENE THERAPY

PROLIFERATIVE RETINOPATHY: STUDY OF THE CONTRIBUTION OF NEUROGLIAL ALTERATIONS AND DEVELOPMENT OF GENE THERAPY APPROACHES

PILAR VILLACAMPA ALCUBIERRE

This PhD thesis has been carried out under the direction of
Dr. Fàtima Bosch i Tubert and Dr. Virginia Haurigot Mendonça
at the Biochemistry and Molecular Biology Department
of the School of Veterinary Medicine and at the
Center of Animal Biotechnology and Gene Therapy
(CBATEG).

PILAR VILLACAMPA ALCUBIERRE FATIMA BOSCH I TUBERT VIRGINIA HAURIGOT MENDONÇA

APRIL 2012
BELLATERRA

En primer lugar, me gustaría agradecer a mi directoras de tesis su dedicación y empeño en este trabajo. Gracias a la Dra. Fàtima Bosch por darme la oportunidad de hacer esta tesis y formar parte de su grupo de investigación. También por contagiarme su energía y pasión por el trabajo. Gracias a la Dra. Virginia Haurigot por iniciarme en la ciencia, enseñarme muchas cosas, dentro y fuera del laboratorio, por motivarme y por estar siempre ahí.

Gracias a todos mis compañeros por hacerme reír cada día de este largo camino. Especialmente a Albert y Sandra, por estar siempre dispuestos a ayudar.

Gracias a todos los servicios del CBATEG por hacer posible nuestro trabajo cada día: técnicos, estabulario, mantenimiento, limpieza y seguridad. Gracias al resto de los compañeros del CBATEG, especialmente al grupo del Dr. Jesús Ruberte.

Gracias al Dr. Pedro de la Villa y su equipo por la colaboración en los estudios de electroretinografía.

Y por último, pero no menos importante, gracias a Víctor, a mi familia y a mis amigos por su apoyo incondicional.

Esta tesis ha sido realizada mediante una beca predoctoral de la Fundación Ramón Areces. Las investigaciones de este trabajo se han financiado gracias a las siguientes instituciones: Instituto de Salud Carlos III (Proyecto de Investigación FIS PI061417) y CIBERDEM: Diabetes y Enfermedades Metabólicas (CB07/08/0037); Ministerio de Educació y Ciencia, Plan Nacional I+D+I (SAF2005-01262, SAF2008-00962); Agència Gestió d'Ajuts Universitaris i de Recerca (2005SGR 00673, 2009SGR 224); Unión Europea: EUGENE2 Network of excellence-NoE (LSHM-CT-2004-512013), CLINIGENE Network of excellence-NoE (LSHB-CT-2006-018933) y EUMODIC (LSHG-CT-2006-037188); European Foundation for the Study of Diabetes/Juvenile Diabetes Research Foundation/Novo Nordisk.

ABBREVIATIONS

AAV	Adeno-asociated virus
ABC	Avidin-biotin complex acid
Ad	Adenovirus
ADP	Adenosine diphosphate
AGE	Advanced glycation end-products
Akt	PKB, protein kinase B
AMD	Age-related macular degeneration
ATP	Adenosine-5'-triphosphate
AU	Arbitrary units
BB	BioBreeding
BBB	Blood-brain barrier
BC	Bipolar cells
Bcl-2	B-cell lymphoma 2
BM	Basal membrane
BRB	Blood-retinal barrier
Brn3a	Brain-specific homeobox/POU domain protein 3A
BSA	Bovine serum albumin
CAG	Cytomegalovirus enhancer and chicken beta actin hybrid promoter
CaCl2	Calcium chloride
CD-1	Caesarian Derived-1
CD105	Endoglin
cDNA	Complementary DNA
$cd \cdot s/m^2$	candela per second/square metre
cGMP	Cyclic guanosine monophosphate
CMV	Cytomegalovirus
CNS	Central nervous system
CNTF	Ciliary neurotrophic factor
CNV	Choroidal neovascularization
Col-IV	Collagen type IV
cpm	Counts per minute
CTGF	Connective tissue growth factor
DAB	3’3’-diaminobenzidine
DAG	Diacylglycerol
DAPI	4',6-diamidino-2-phenylindole
DCCT	Diabetes Control and Complications Trial
dCTP32	Deoxycytidine triphosphate-32
DEPC	Diethylene pyrocarbonate
DME	Diabetic macular edema
DNA	Desoxi-ribonucleic acid
DNAse	Deoxyribonuclease
DNPH	2,4-Dinitrophenylhydrazine
dNTPs	2'-deoxynucleosides5'-triphosphate
DR	Diabetic Retinopathy
DRS	Diabetic Retinopathy Study

e	Exponential base
EDTA	Ethylenediamine tetraacetic acid
ELISA	Enzyme-kinked inmunoassay
eNOS	Endothelial nitric oxide synthases
ERG	Electroretinography
ETDRS	Early Treatment Diabetic Retinopathy Study
fa/fa	obese Zucker rats
Fas	TNF receptor superfamily, member 6
FasL	Fas ligand
$FeCl^3$	Ferric chloride
Fig	Figure
FITC	Fluorescein isothiocyanate
Fw	Forward
g	Grams
g	Gravity
G	Gauge
GABA	Gamma-aminobutyric acid
GADPH	Glyceraldehyde-3 phosphate dehydrogenase
GL	Ganglion cell layer
GFAP	Glial Fibrillary Acidic Protein
GFP	Green fluorescein protein
Gja1	Gap junction protein alpha 1
GK rat	Goto-Kakizaki rat
GLAST	Glutamate Aspartate Transporter
GLUT1	Glucose transporter 1
GS	Glutamine synthetase
GSH	Gluthatione (reduced form)
h	Hour
H_20_2	Hydrogen peroxide
HC	Horizontal cells
HCl	Hydrogen chloride, Hydrochloric acid
HEK 293	Human embryonic kidney 293
HIF-1α	Hypoxia inducible factor-1 alpha
HIV-I	Human immunodeficiency virus
hPEDF	Human Pigmented Epithelium Derived Factor
HRP	Horseradish peroxidase
HSC	Hematopoietic stem cell
Hz	Hertz
ICAM-1	Intracellular adhesion molecule-1
IGF-1	Insulin-like Growth Factor I
IGF-1 R	Insuline-like growth factor I receptor
IL-1β	Interleukin 1 beta
IL-6	Interleukin 6
INL	Inner nuclear layer
iNOS	Inducible nitric oxide synthases
$Ins2^{Akita}$	insulin-deficient Akita mice

IP	Paraffin inmunohistochemistry
IPL	Inner plexiform layer
IS	Outer segment
ISCEV	International Society for the Clinical Electrophysiology of Vision
ITR	Inverted terminal repeat
K^+	Potassium cation
KDa	KiloDalton
kg	Kilograms
kHz	KiloHertz
Kir 4.1	Inward rectifying potassium channel 4.1
KOH	Potassium hydroxide
l	Litre
LCA	Leber Congenital Amaurosis
log	Logarithm
LPS	Lipopolysaccharide
LV	Lentivirus
M	Molar (mol/l)
MCP-1	Monocyte Chemotactic Protein-1
mg	Milligrams
$MgCl^2$	Magnesium chloride
MHC	Major histocompatibility complex
min	Minute/s
ml	Millilitre
mM	Millimolar
mm	Milimeter
mm^2	Square millimeter
MMPs	Matrix Metalloproteinases
mRNA	RNA messenger
n	Number of animals
Na2HPO4	Disodium hydrogen phosphate
NaCL	Sodium chloride
NAD^+	Nicotinamide adenine dinucleotide
NADH	Nicotinamide adenine dinucleotide reduced
NADPH	Nicotinamide adenine dinucelotide phosphate
NaOH	Sodium hydroxide
NF-kB	Factor nuclear kappa B
ng	Nanogram
NIDDM	Non-insulin-dependent diabetes mellitus
nm	Nanometre
nNOS	Neuron nitric oxide synthases
NO	Nitric oxide
NOD	Non-obese diabetic
NOS	Nitric oxide synthases
OD	Optical density
OIR	Oxygen-induced models
OLEFT rat	Otsuka Long-Evans Tokushima fatty rat

ONL	Outer nuclear layer
OP	Oscillatory potentials
OPL	Outer plexiform layer
OS	Outer segment
P	Postnatal day
P^{32}	Phosphor 32
PARP	Poly(ADP-ribose) polymerase
PAS	Periodic Acid Schiff
PBS	Phosphate-Buffered Saline
PBT	Phosphate buffer tween
PC	Photoreceptors cells
PCR	Polymerase Chain Reaction
PDGF	Platelet Derived Growth Factor
PDR	Proliferative diabetic retinopathy
PEDF	Pigmented Epithelium Derived Factor
PEI	Polyethylenimine
pH	Potential Hydrogen
PI3	Phosphatidylinositol *3*
PKC-α	Protein kinase C alpha
PVDF	Polyvinylidene difluoride
qPCR	quantitative PCR
RIP-I	Rat insulin-I promoter
RNA	Ribonucleic acid
RNase	Ribonuclease
ROP	Retinopathy of prematurity
ROS	Reactive oxygen species
RPE	Retinal pigmented epithelium
rpm	Revolutions per minute
RT-PCR	Reverse transcription polymerase chain reaction
Rv	Reverse
s	Seconds
s100b	S100 calcium binding protein B
SDS	Sodium Dodecyl Sulphate
SDS-PAGE	Sodium dodecyl sulfate polycrylamide gel electrophoresis
SDT rat	Spontaneously Diabetic Torii rat
SEM	Standard error from the mean
SER-CBATEG	Servei d'Estabulari de Ratolins-CBATEG
SSC	Sodium chloride and sodium citrate solution
STR	Scotopic threshold response
STZ	Streptozotocin
TAE	Tris acetate EDTA
TBS	Tris buffered saline
TBS-T	Tris buffered saline tween
Tg	Transgenic
TgIGF-I	Transgenic mice overexpressing IGF-I
Tub	Tubuline

TK	Thymidine kinase
TNF-α	Tumor necrosis factor alpha
Tris	THAM, tris(hydroxymethyl)aminomethane
TRITC	Texas red isothiocyanate
t test	Student's t-test
UAB	Universitat Autònoma de Barcelona
UKPDS	United Kingdom Prospective Diabetes Study
USA	United States of America
UV	Ultraviolet
V	Volt
VE-cadherin	Vascular endothelial cadherin
VEGF	Vascular Endothelial Growth Factor
VEGF-R	Vascular Endothelial Growth Factor Receptor
vol	Volume
vg	Vector genomes
VSV-G	Vesicular stomatitis virus
v/v	volume/volume
WB	Western blot
WHO	World Health Organisation
WPRE	Woodchuck post-transcriptional regulatory element
Wt	Wild-type
w/v	weight/volume
ZDF rat	Zucker diabetic fatty rat
º C	Degree centigrade
µg	Microgram
µl	Microlitre
µm	Micrometre

I. Presentation

Diabetic retinopathy (DR) is the most common cause of acquired blindness in developed countries, with a high prevalence in diabetic patients. Available treatments are invasive and only partially efficacious in halting the progression of the disease. The development of new effective therapies requires further investigations on disease pathogenesis and good animal models are essential to this end.

Several rodent models of diabetes, spontaneous or drug-induced, have been used for studying the pathogenesis of retinopathy and for testing new therapeutic approaches. However, the majority of these models do not develop a complete phenotype of proliferative retinopathy, but only some mild vascular alterations. In our lab we have developed a new animal model, a transgenic mouse overexpressing Insulin-like Growth Factor I (IGF-I) in the retina (TgIGF-I), which despite not being hyperglycaemic presents a progressive vascular disease resembling that of human diabetic patients. Thus, these mice can be considered a good model for the study of the physiopathology of retinopathy and for the assessment of the efficacy and safety of new therapeutic approaches.

It has been described that neuronal and glial cells are affected by hyperglycaemia and their dysfunction contributes to the development of diabetic retinopathy. To fully characterize the eye pathology of TgIGF-I, the first part of this work was focused on the study of the alterations in these cell types in transgenic retinas. We found that TgIGF-I retinas showed a progressive decline in their electroretinographic responses that resulted in significantly impaired

neuronal functionality in old animals. Gliosis and microgliosis were also detected in transgenic retinas at early ages. Gliosis is associated with the loss of essential neuron-supportive functions performed by Müller cells. We found that transgenic retinas showed changes in normal retinal metabolism, such as alterations in the metabolism of glutamate and signs of oxidative stress and impaired potassium buffering, all of which may underlie the neuronal dysfunction of transgenic retinas that could be further exacerbated by the increased production of pro-inflammatory cytokines.

The progressive nature of the pathology in the TgIGF-I model allows the long-term evaluation of new therapeutic approaches. The second part of this work was dedicated to the study of the efficacy of a gene therapy approach aimed at counteracting neovascularization and neurodegeneration. Adeno-associated (AAV) vectors of serotype 2 were chosen to overexpress Pigmented Epithelium Derived Factor (PEDF), a protein with potent antiangiogenic and neuroprotective properties. AAV2-mediated PEDF gene transfer led to long-term production of PEDF and to a striking inhibition of intravitreal neovascularization, normalization of retinal capillary density, and prevention of retinal detachment. This was parallel to a reduction in the intraocular levels of Vascular Endothelial Growth Factor (VEGF). Normalization of VEGF was consistent with a downregulation of downstream effectors of angiogenesis. These results demonstrate long-term efficacy of AAV-mediated PEDF overexpression in counteracting retinal neovascularization and provide evidence towards the use of this strategy to treat angiogenesis in DR and other chronic proliferative retinal disorders.

II. Introduction

1. DIABETES MELLITUS

1.1. INTRODUCTION

Diabetes mellitus is the most common metabolic disease in humans. The estimated worldwide prevalence of diabetes among adults was 285 million in 2010, a 6.4% of the world's total population, and this value is predicted to rise to 430 million by 2030 (7.7%) (Shaw et al., 2010).

Type 1 diabetes is generally developed in childhood or early adulthood and is defined as a condition in which immune-mediated pancreatic β-cell destruction leads to absolute insulin deficiency (ADA, 2005). Although only 5-10% of diabetic patients are type 1, the incidence is increasing at 2-5%/year worldwide (Gale, 2002). The abnormal activation of self-reactive T-cells in susceptible individuals leads to an inflammatory response within the islets as well as to a humoral response with production of antibodies against auto-antigens (Daneman, 2006). Several susceptibility genes have been identified (Devendra et al., 2004), and the influence of environmental factors is also currently under study. The absence of insulin has serious metabolic effects such as reduced uptake of glucose by peripheral tissues and increased hepatic glucose production due to high glucagon levels, both leading to hyperglycaemia. In addition, the lack of insulin also causes release of fatty acids from the adipose tissue, and these are converted to ketone bodies in the liver, with the risk of development of ketoacidosis.

Type 2 diabetes is the worldwide predominant form and accounts for at least 90% of diabetic patients. Type 2 diabetes is characterised by inadequate insulin secretion to compensate for insulin resistance. The onset of type 2 diabetes is later in life compared to type 1, but the tendency is changing, and the incidence in young people is continuously increasing (Reinehr et al., 2010), frequently associated with obesity. Type 2 diabetes results from an interaction between genetic and environmental factors (Nolan et al., 2011). Insulin resistance in peripheral tissues and impaired insulin secretion are characteristic features (Defronzo, 2009). Individuals with normal glucose tolerance progress to impaired glucose tolerance (IGT) that worsens to overt type 2 diabetes in association with a progressive deterioration in β-cell function (Defronzo, 2009).

1.2. LONG-TERM COMPLICATIONS OF DIABETES MELLITUS

Long-term complications of Diabetes Mellitus are the major cause of mortality and morbidity of the disease (Daneman, 2006). Several clinical studies as the Diabetes Control and Complications Trial (DCCT) (DCCT, 1993) and the UK Prospective Diabetes Study (UKPDS) (UKPDS, 1998) have shown that the development and progression of diabetic complications is directly related with the severity and duration of hyperglycaemia in both type 1 and 2 diabetic patients. Secondary complications of diabetes are classified in three categories: macrovascular complications, cardiomyopathy and microvascular complications.

Diabetes-associated macrovascular disease is the major cause of mortality and morbidity in diabetic patients and is characterised by coronary artery disease, atherosclerosis and peripheral vasculopathy (ADA, 2010). Intensive glycemic, blood pressure and lipid control are crucial for reducing cardiovascular risk in both type 1 and type 2 diabetic patients (Golden, 2011).

Diabetic cardiomyopathy is defined by structural changes in the heart, such as increased left ventricular mass, fibrosis and dilation of ventricles (Spector, 1998). This complication is highly associated with hyperglycaemia and, although the prevalence of this disease without any other cardiovascular co-morbidities is still quite rare in type 2 diabetes, it might be a factor that aggravates other macrovascular complications resulting in increased mortality and morbidity (Bell, 2003).

Microvascular complications mainly affect the vascular system of the retina and the kidney and neural perfusion. Diabetic nephropathy is the most common cause of renal failure in the developed world (Friedman, 1996). About the 30-40% of diabetic patients progress to end-stage renal disease. The earliest detectable phase is characterized by the presence of microalbuminuria, which can progress to macroalbuminuria or nephropathy. This is the consequence of hemodynamic changes in renal blood-flow and glomerular alterations, such as basement membrane thickening, which are considered to be the consequence of hyperglycaemia-induced oxidative stress (Cooper, 1998).

Diabetic retinopathy is the most common cause of acquired blindness in developed countries, with a prevalence of 86% of patients in type 1 diabetes and 42% in type 2 diabetes in US (Kempen et al., 2004). It progresses from early non-proliferative retinopathy, characterized by alterations in the retinal vasculature such as pericyte loss and thickening of the basement membrane, to proliferative retinopathy, associated with overt neovascularization, vitreous haemorrhage and risk of retinal detachment and visual loss (Cai and Boulton, 2002). Other ocular complications with lower prevalence are glaucoma, cataracts and neovascularization of the iris (Rand et al., 2004).

Diabetic neuropathy comprises a complex group of pathological conditions, but the most common form is peripheral polyneuropathy (Harati, 1996). It mainly affects the sensorimotor system but may also progress to autonomic impairment, with cardiac and erectile dysfunction (Daneman, 2006). Diabetic neuropathy is characterised by loss of nerve fibres, demyelination, axonal thickening and capillary alterations, all of which are associated with hyperglycaemia (Harati, 1996). Peripheral neuropathy, in association with macrovascular alterations, can lead to ulceration and poor healing in the lower limbs, with a high risk of amputation (Daneman, 2006). Some authors have considered diabetic retinopathy a form of diabetic neuropathy due to the presence of neuronal alterations in the retina of diabetic patients before the observation of any vascular pathology (Barber et al., 2011; Fletcher et al., 2007).

2. THE EYE

The eye is an asymmetrical complex organ responsible for vision, with important regional anatomic variations between species that should be taken into account when studied. The eye structure can be divided in three layers and two chambers (Figure 1):

- the external layer, with structural and protective properties, is formed by the sclera and the cornea.
- the intermediate layer, which can be separated in the anterior part, composed by the iris and the ciliary body, and the posterior part, the choroid.
- the internal layer, comprising the retina, which is the sensory part of the eye.
- the anterior chamber, filled with aqueous humour, located between the lens and the cornea.
- the vitreous chamber: filled with vitreous humour, located between the lens and the retina.

In addition to these structures, the lens is suspended between the anterior and the vitreous cavity by ligaments attached to the ciliary body. The whole eyeball is maintained in position by the extraocular muscles that attach the eye to the bony orbit of the skull and allow rotation of the eye and image focusing.

All the structures listed above are functionally designed for supporting and protecting visual function, a task carried out by retinal neurons.

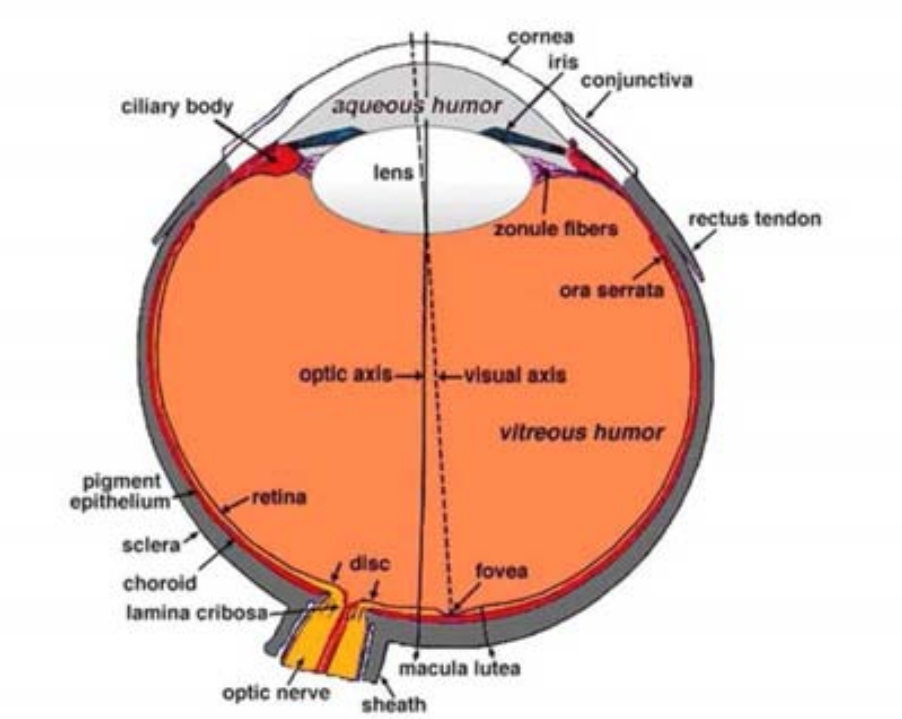

Figure 1. Schematic representation of an adult human eye. From Kolb et al. 1995.

2.1. THE NON-SENSORY PARTS OF THE EYE

- The **sclera** is the principal part of the outer fibrous coat of the eye and is formed by dense connective tissue, constituted mainly by collagen types I and III. It protects intraocular structures and maintains the shape of the eyeball.

- The **cornea** represents the air-tissue interface of the anterior part of the eye, and is composed by a multilayered epithelium in the outer surface and endothelium in the posterior surface. The corneal stroma between them is a dense connective tissue of high regularity. Clear vision depends on cornea transparency, which in turn depends on avascularity and strict organization of

its components. The cornea is responsible for the refraction of the light, but it also acts as a physical barrier against trauma and infections.

- The **iris** controls the diameter of the pupil, providing a variable diaphragm that controls the amount of light that reaches the retina. The iris is composed by two layers of pigmented epithelium containing a fibrovascular stroma.

- The **lens** is a highly organized structure that allows the change of the refractive index of the light entering the eye to focus on the retina. The lens is enclosed by a capsule, which is covered by an epithelium that produces lens fibres. The fibres are composed of long epithelial cells that have lost their nuclei and all their organelles. Again, the transparency of the lens is crucial for visual acuity and depends on the high organization of the fibres and avascularity.

- The **ciliary body** can be divided into the cilliary epithelium, the cilliary body stroma and the cilliary muscles. The latest are attached to the lens by the suspensory ligaments and are responsible for the accommodation movements of the lens to ensure correct focusing of the light on the retina. The processes of the cilliary epithelium continuously produce and secrete aqueous humour.

- The **choroid** is a highly vascularized layer of connective tissue that provides the blood supply for the external, avascular layers of the retina. In addition, due to its high pigmentation, the choroid is responsible for the absorption of light, preventing reflections through the retina.

- The **aqueous humor**, a colourless fluid secreted by the ciliary body, passes across the anterior chamber and leaves the eye through the trabecular meshwork and the Schlemm's canal. It helps maintaining hydrostatic pressure and provides nutrients to the avascular structures of the anterior part of the eye.

- The **vitreous humor** is a transparent gel mainly composed of glycosaminoglycans, hyaluronic acid and water. It fills the vitreous cavity, between the lens and the retina, and maintains the shape of the ocular globe. The vitreous cavity is notably smaller in mice compared to humans or other species.

2.2. THE RETINA

The retina is the innermost of the three layers of the eye and is responsible for transforming the information of light into neural impulses that are transmitted to the brain. The retina is a highly organized tissue; in which several cell types are located in specific cell layers to ensure optimization of light pass with minimal diffraction. The lamellar architecture of the retina is composed of three neuronal layers: the outer nuclear layer (ONL), the inner nuclear layer (INL) and the ganglion cell layer (GCL), with two plexiform layers where neurons establish synaptic contacts (outer and inner, OPL and IPL, respectively) located in between (Figure 2).

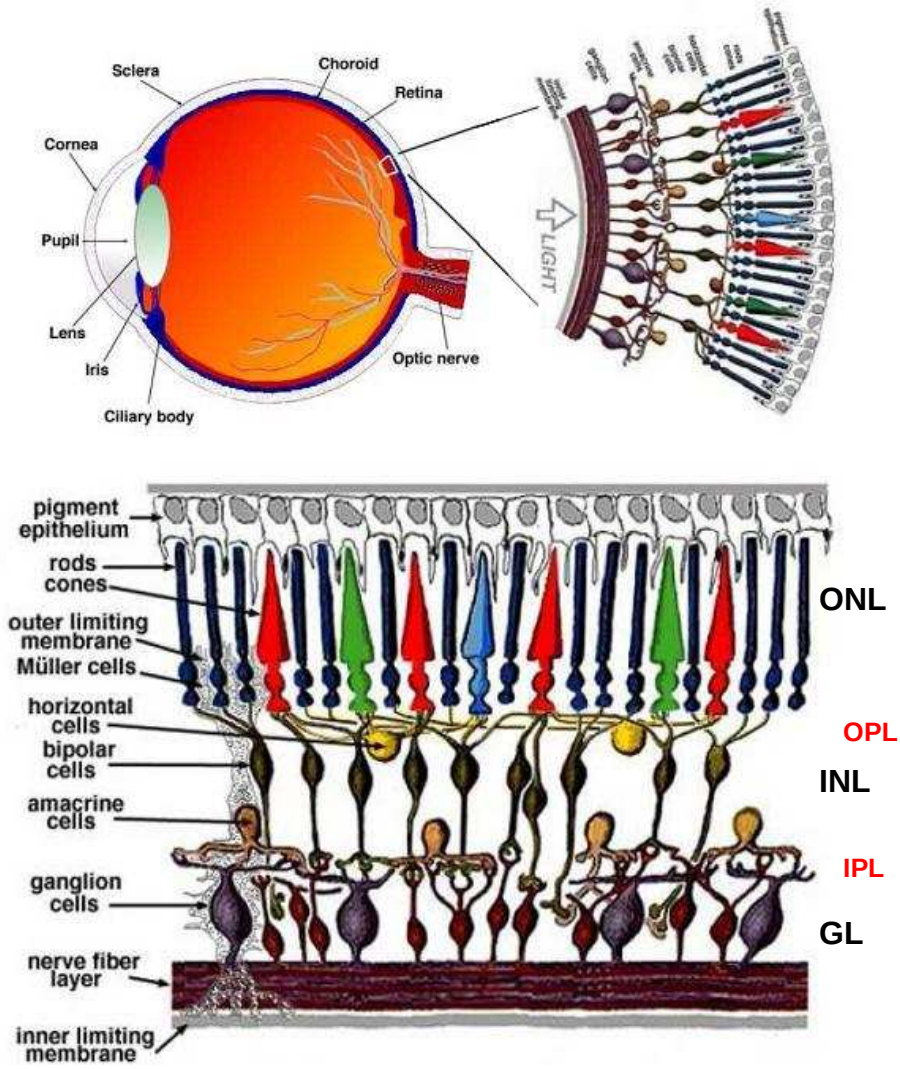

Figure 2. Diagram of the organization of the human retina. The different cell types present in the retina are organized in nuclear layers, from outside to inside: pigmented epithelium; neurons: photoreceptors in the outer nuclear layer (ONL), horizontal, amacrine and bipolar neurons in the inner nuclear layer (INL) and ganglion and amacrine in the ganglion cell layer (GL); Müller glial cells processes span from ONL to GL. Neurons establish synapses in the inner and outer plexiform layers (IPL and OPL). Adapted from Kolb et al. 1995.

Located between the retina and the choroid, the retinal pigmented epithelium (RPE) is a monolayer of cells with critical functions in the normal visual process; maintaining adhesion of the neuroretina to the posterior part of the eye, supplying nutrients and oxygen to photoreceptors, providing a

protective barrier to the highly permeable vessels of the choroid, as well as recycling products of phototransduction are amongst them (Strauss, 2005).

2.2.1. Neurons and visual function

Photoreceptor cells convert light stimuli in electric impulses that can be transmitted to other retinal neurons and ultimately to the brain. Nuclei of both rod and cone photoreceptors constitute the outer nuclear layer of the retina, whereas their inner and outer segments span to the RPE. The outer segment is the important visual pigment-bearing portion of the photoreceptor and the inner segment is rich in organelles, specially mitochondria, an evidence of the high metabolical activity of these cells. Rods are specialized in vision under low light conditions, whereas cones are responsible for colour and detailed vision. In humans, there are different types of cones that are sensitive to different wavelengths, allowing colour discrimination. In the mouse retina, rod photoreceptors are predominant and represent 95% of the photoreceptors (Jeon et al., 1998). The synaptic terminals of rods, named spherules, and those of cones, known as pedicles, are located in the outer plexiform layer, where photoreceptors establish contact with second order neurons through synaptic vesicles (Forrester, 2002).

Bipolar cells are second order neurons that receive signals from photoreceptors and transmit them to ganglion cells. Their nuclei are located in the inner nuclear layer and their cell bodies are oriented in a radial pattern parallel to photoreceptors. The dendrites of each bipolar cell can receive

information from 50-100 rods or a single cone (which explains the high sensitivity of rods in dim light). Nine types of bipolar neurons have been reported, one for rod bipolar cells and eight for cone bipolar cells. Their unique axon synapses with ganglion cells and also with amacrine neurones in the inner plexiform layer.

Ganglion cells are the last step in the retinal visual pathway and are placed in the innermost nuclear layer of the retina, the ganglion cell layer. Their axons converge in the surface of the retina (nerve fibre layer) and synapse with neurones in the lateral geniculate nucleus of the thalamus. Ganglion cells have morphological and functional diversity, and more than ten types of this population of retinal neurons have been described (Masland, 2011).

In addition to the neurons forming the visual pathway (photoreceptors-bipolar cells-ganglion cells) there are other types of “interneurons” or associate neurons in the retina. In the outer part of the inner nuclear layer, two types of horizontal cells can be identified morphologically. Type A horizontal cells are axonless and only interact with cones, whereas type B cells have axons and make synapses also with rod photoreceptors. In the mouse retina, only type B horizontal cells can be found (Forrester, 2002). Horizontal neurons mediate interactions between photoreceptors, providing feedback signals that modulate the gain of the visual pathway signals. Horizontal cells also interact with bipolar neurons, regulating and adapting responses.

Amacrine cells are the most diverse population of interneurons in the retina. More than twenty classes of amacrine neurons have been described (Masland, 2011) and their functions are also diverse, from establishing inhibitory synapses with bipolar cells, neuromodulating responses releasing dopamine or adjusting retinal responses to light intensity. Amacrine neurons are located in both the inner nuclear layer and the ganglion cell layer, making synaptic contacts with bipolar and ganglion cells.

There are some regional variations in cell distribution within the retina. In the case of human beings, the central retina is rich in cones and more than a single layer of ganglion cells can be found. The macula, laterally displaced from the optic disc in humans, is an avascular area in which neuronal populations are highly concentrated to increase visual acuity. The fovea is a small retinal depression located in the centre of the macula; it only contains cone photoreceptors and the inner nuclear neurons are displaced to avoid light dispersion and facilitate detailed vision. The peripheral retinal is dominated by rods photoreceptors and necessary for low-light vision. It is important to note that these topographical differences of the human retina are not present in the mouse retina, where nor avascular areas, such as macula or fovea, nor cone-enriched areas are found (Smith et al., 2002).

2.2.2. Glia and microglia

Glia cells fulfil supportive functions in the retina, as they do in the rest of the CNS. In general, the mammalian retina contains two types of macroglial

cells: astrocytes and Müller cells. *Astrocytes* are found in the nerve fiber layer of the retina, where their radiating processes are covering ganglion cell axons and interacting with blood vessels. Astrocytes perform support functions for neuronal homeostasis, such as provision of metabolites, regulation of ionic concentrations and recycling of neurotransmissors (Holländer et al., 1991). About their interaction with blood vessels, astrocytes are known to participate in the regulation of blood flow and to be part of the blood-retinal barrier (Bringmann et al., 2006). *Müller cells* are elongated cells that span between the inner and the outer limiting membrane, creating an architectural supportive structure for retinal neurons. These cells have a range of functions vital to neuron survival similar to those of astrocytes (Figure 3). Metabolic support, clearance of neural waste products, control of ionic homeostasis, production and recycling of neurotransmitters and also phagocytosis of neuronal debris are amongst Müller cells functions (Bringmann et al., 2006). Glial cells, and specially Müller cells, respond to any retinal damage by becaming “reactive”. This reaction is called gliosis and in early, acute phases is characterized by the secretion of neuroprotective and antioxidant molecules with the aim of protecting the tissue (Bringmann et al., 2006). But when gliosis becomes a chronic process it evolves with de-differentiation of Müller cells, which may alter glial functions, specially K+ conductance and glutamate detoxification (Bringmann et al., 2000, 2006).

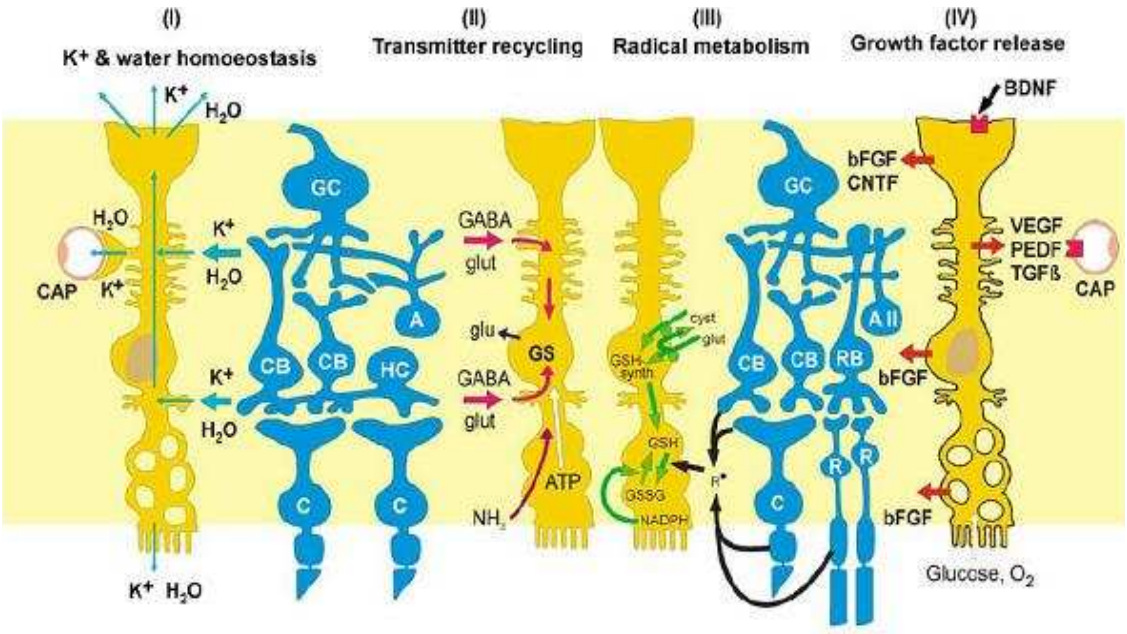

Figure 3. Müller glial cells carry out multiple functions for the maintenance of retinal homeostasis. Müller cells maintain retinal homeostasis and contribute to normal neuron function by regulating processes like (I) ion and water homeostasis, (II) recycling of neurotransmitters, such as glutamate and γ-aminobutyric acid (GABA) (III) detoxification of free radical or (IV) production neurotrophins that support neuronal survival, such as Pigmented Epithelium Derived Factor (PEDF) or Ciliary Neurotrophic Factor (CNTF) . From Giaume et al. 2007.

Microglia constitutes the resident macrophage population of the retina. These cells are found in the inner and outer plexiform layers, where they perform immunomodulating functions, realising cytokines and phagocytising apoptotic cells (Karlstetter et al., 2010). Microglial cells also become activated after local injury, but persisting activation may result in chronic and deleterious inflammatory processes (Karlstetter et al., 2010; Langmann, 2007).

2.2.3. Vascular structure

The retina is an extremely metabolically active tissue with the highest oxygen consumption rate of any human tissue (Yu and Cringle, 2005). At the same time, the retinal capillaries have a relative sparse distribution and their size is small in order to minimise optical interference with the light path. The

outer layers of the retina are avascular and directly nourished by the choroid vasculature through the RPE. The supply of oxygen and nutrients to the superficial layers of the retina is guaranteed by the central artery, which enters the eye by the optic disc and radiates in four major arterioles. In humans, three plexus of capillary networks coming from these branches irrigate the inner layers of the retina: the peripapillary plexus, in the nerve fiber layer; the inner capillary plexus, situated in the ganglion cell layer, and the outer capillary plexus, located in the inner nuclear layer (Kolb, 1995).

The endothelial cells (EC) of retinal vessels are joined by non-leaky tight junctions, a component of the blood-retinal barrier (Dejana, 2004). These vessels are covered by a thick and continuous basal membrane and stabilized by the presence of pericytes. As mentioned previously, the blood-retinal barrier is a selective barrier that isolates the retina from blood. Not only endothelial cells and pericytes but also the glial processes of astrocytes and Müller cells are known to play a role in the maintenance of the blood-retinal barrier. The inner BRB is formed by the endothelial cells of blood vessels, with tight junctions that reduce the permeability of the vasculature. The RPE cells constitute the outer BRB, which separates photoreceptors from choroidal vessels.

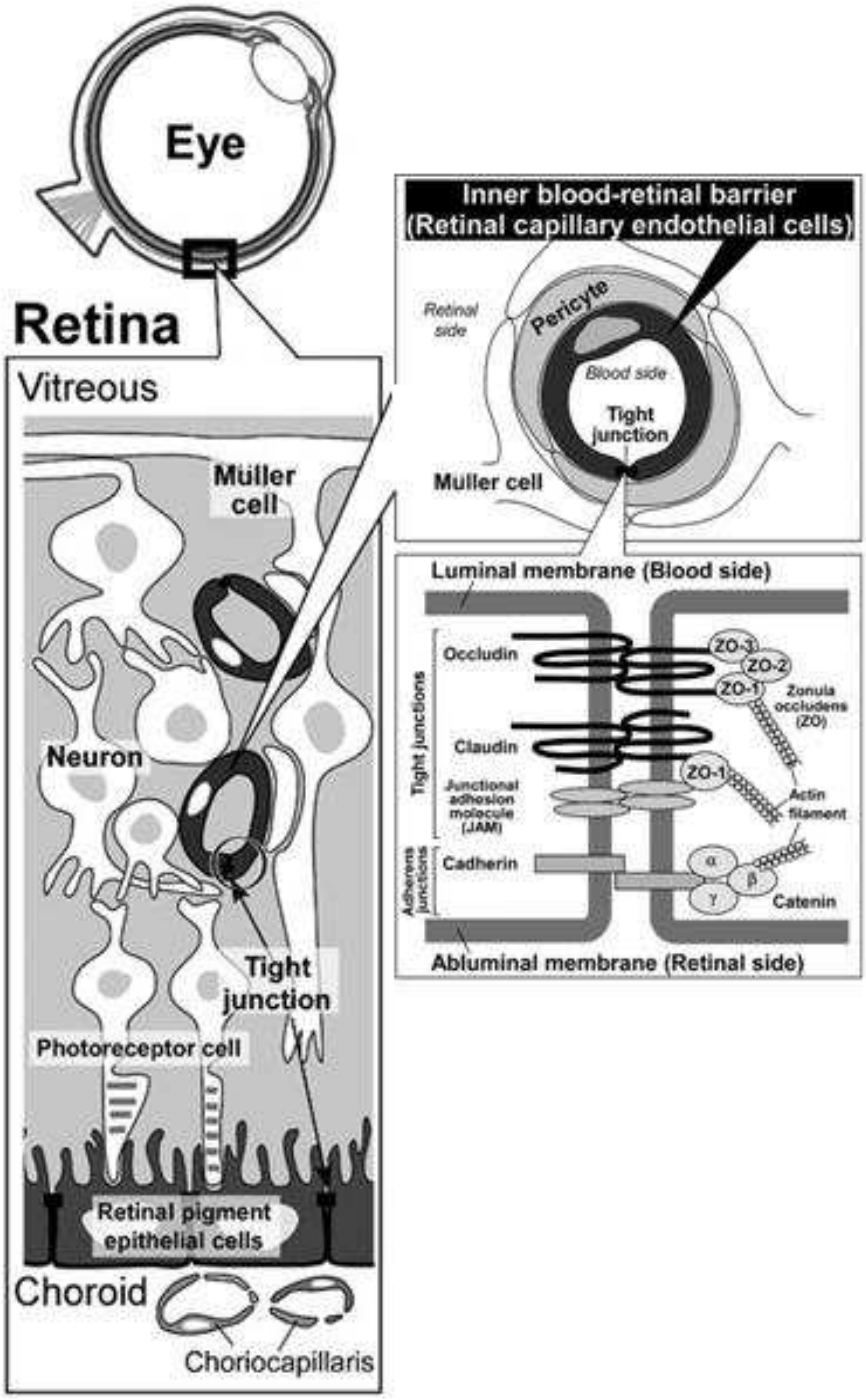

Figure 4. Schematic representation of the inner and outer blood-retinal barriers. Tight junctions are found in between adjacent cells in both retinal capillaries and pigment epithelium, constituting a selective barrier that protects neurons from blood-derived deleterious factors. Adapted from Hosoya et al. 2012.

3. DIABETIC RETINOPATHY

Diabetic retinopathy is the most common and serious ocular long–term complication of diabetes, although chronic hyperglycaemia can cause other deleterious alterations in the eye, such as cataracts and iris neovascularization (Porta and Bandello, 2002). Diabetic retinopathy is the most frequent cause of adult blindness in many countries, including Western Europe, USA, India and China (Cheung et al., 2010). The prevalence and severity of this pathology is higher in some ethnic groups, such as African Americans or South Asians (Wong et al., 2006; Raymond et al., 2009). Genetic susceptibility, hypertension or obesity are considered risk factors associated with diabetic retinopathy (Cheung et al., 2010).

3.1. PATHOLOGICAL FEATURES AND PROGRESSION OF DIABETIC RETINOPATHY

Diabetic retinopathy has been classically defined and diagnosed as a vascular pathology, and the stages of its evolution have been specified according to the progression of the alterations in retinal vessels. Chronic exposure to hyperglycaemia initiates a cascade of biochemical and physiological changes that lead to microvascular damage and retinal dysfunction (Cheung et al., 2010). However, there is evidence that the functionality of retinal neurons is compromised by hyperglycaemia before the onset of vascular lesions (Antonetti et al., 2006). In addition, it is known than glial cells are activated in human diabetic retinopathy (Mizutani et al., 1998) and impaired glial metabolic and homeostatic functions, essential for neuronal

activity and vascular integrity, have been described in experimental diabetes (Barber et al., 2000; Lieth et al., 2000). Complex functional and metabolic interactions between neurons, vessels and glial cells are required for proper retinal functionality (Figure 5). This suggests that the processes set in motion by hyperglycaemic damage in diabetic retinopathy may have pathoglogical consequences in different retinal cell types.

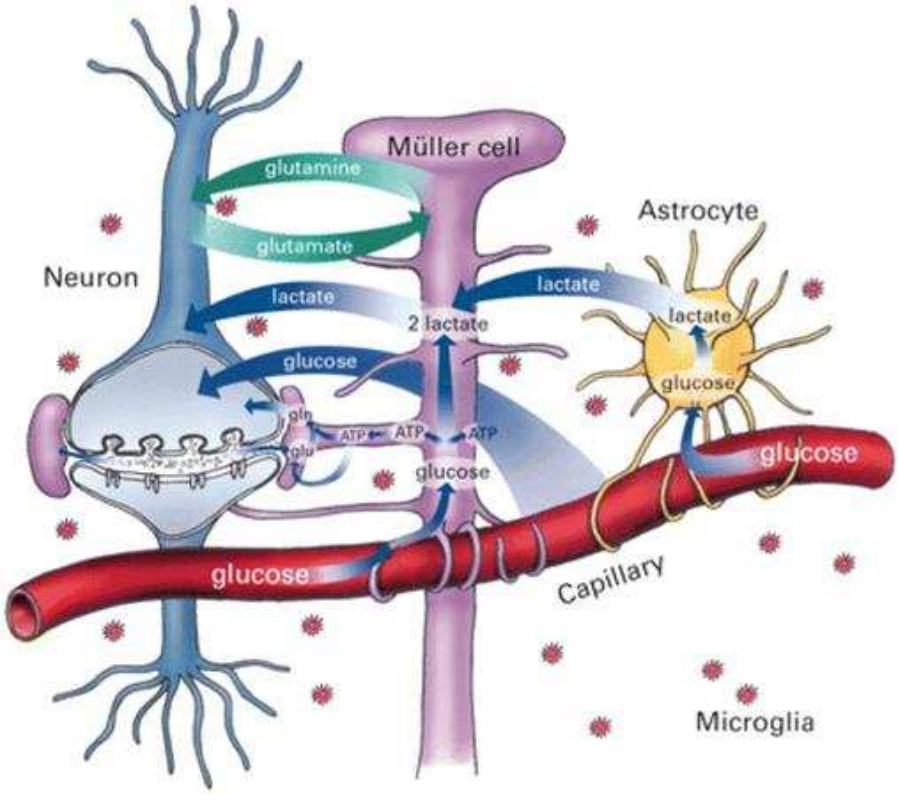

Figure 5. Schematic representation of the interactions between vascular, neuronal and glial cells in the retina. Complex functional and metabolic interactions between neurons, vessels and glial cells are required for proper retinal functionality. Glucose can pass directly from vessels to neurons or can be converted to lactate by glial cells and then transferred to neurons. Neurons and Müller cells participate in the metabolization and recycling of glutamine and glutamate. From Antonetti et al.2006.

3.1.1. Biochemical changes in diabetic retinopathy

Both type 1 and type 2 diabetes are associated with hyperglycaemia, which can be toxic to cells, specially to those that cannot regulate the entrance of glucose, such as retinal endothelial cells or mesangial cells (Heilig et al., 1995; Kaiser et al., 1993). Four classical pathways of hyperglycaemic damage have been described: polyol pathways, hexosamine pathway, PKC activation and advanced glycation end-products (AGEs) formation (Brownlee, 2005).

1. In the *polyol pathway,* the enzyme aldose reductase converts the excess of glucose in sorbitol, consuming NADPH molecules that are essential for antioxidant defences, which, in turn, increases the susceptibility to oxidative stress (Lee and Chung, 1999).

2. The *hexosamine pathway i*s characterized by the production of N-acetyl glucosamine, which covalently binds serine and threonine residues of proteins. The increased flux of hexoses through this pathway during hyperglycaemia leads to accumulation of N-acetyl glucosamine that can negatively alter gene expression (Wells and Hart, 2003).

3. Another mechanism is based on *PKC activation*. Intracellular hyperglycaemia is associated with high levels of diacylglycerol (DAG), which activates several isoforms of PKC (Xia et al., 1994). When PKC is activated, changes in gene expression occur that have impact on several aspects of vascular functionality, such as blood-flow, permeability or vessel occlusion (Brownlee, 2005).

4. Finally, excess of intracellular glucose can lead to the *formation of AGE* precursors (glyoxal, methylglyoxal or 3-edoxyglucosone) that can covalently modify intracellular, extracellular and plasmatic proteins impairing their function. These modifications may include changes in gene expression, activation of

transcription factors such as NF-kB (Brownlee, 2001) and changes in the interactions amongst cells due to modifications of the extracellular matrix (Charonis et al., 1990).

A few years ago a unifying mechanism was proposed to explain why oxidative stress and excessive ROS production were the initiating insult in cells affected by hyperglycaemia, and how this was associated with the activation of the four mechanisms implicated in hyperglycaemic damage (Brownlee, 2005). Both type 1 and type 2 diabetes are associated with induction of oxidative stress caused mainly by hyperglycaemia, but also by other metabolic alterations, such as dyslipidemia or accumulation of metabolic products (Kuroki et al., 2003). The circulating levels of lipid peroxides, a byproduct of increased production of reactive oxygen species (ROS), are known to correlate with the severity of diabetic retinopathy in diabetic patients (Augustin et al., 2002), and ROS oxidation products are also increased in experimental animal models of diabetes and in vascular cells cultured in high-glucose conditions (Kuroki et al., 2003; Brownlee, 2001). Increased ROS production is a consequence of glucose overload and increased amounts of glucose being oxidized in the tricarboxylic acid cycle, which results in the collapse of the mitochondrial electron transport chain and donation of the remaining electrons to molecular oxygen, generating ROS (Brownlee, 2005). ROS can induce the formation of DNA strand breaks that activate the poly(ADP-ribose) polymerase (PARP) (Du et al., 2003). PARP activation leads to the inhibition of glyceraldehyde-3 phosphate dehydrogenase (GADPH) activity, a key glycolytic enzyme (Du et al., 2003). This decreased activity of GADPH slows down glycolysis, with the concomitant accumulation of

intermediate products that feed and activate the four classical pathways of hyperglycaemic damage (Brownlee, 2005).

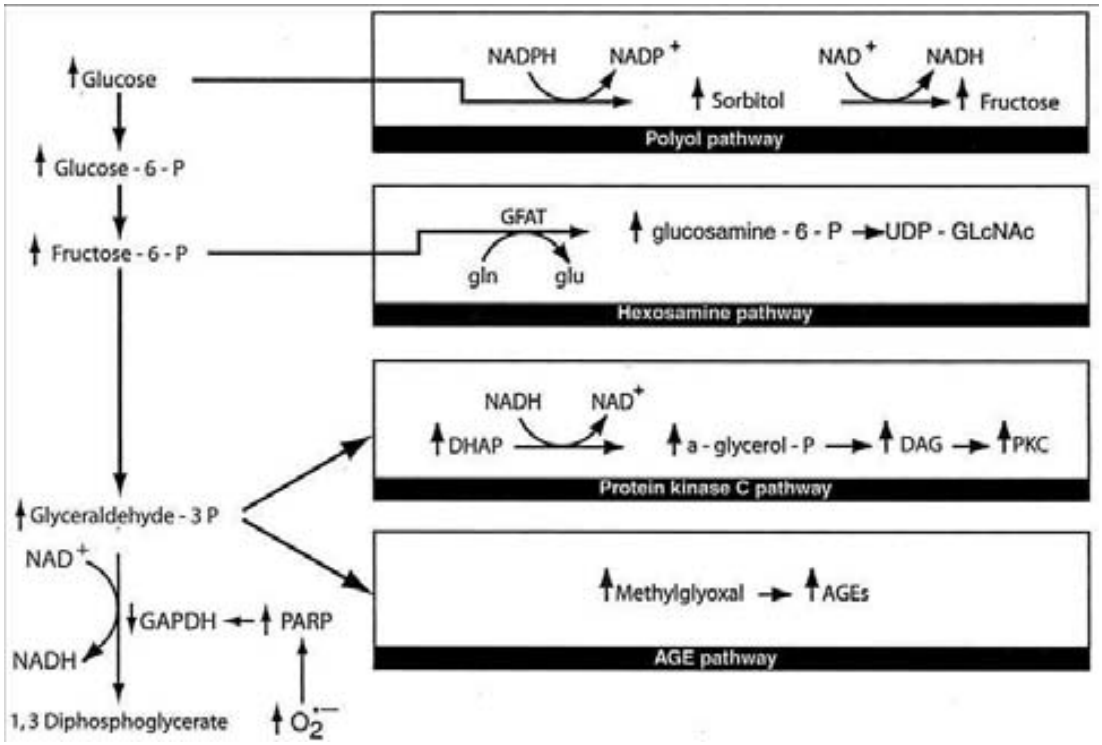

Figure 6. A unifying mechanism for hyperglycaemia-mediated cell damage in diabetic complications. Mitochondrial overproduction of superoxide activates the four major pathways of hyperglycemic damage by inhibiting GAPDH. From Brownlee et al.2005.

3.1.2. Vascular changes in diabetic retinopathy

Hyperglycaemia-induced biochemical changes cause functional alterations in the retinal microvasculature. The progression and severity of the vascular lesions is clearly associated with the levels of hyperglycaemia, and tight glycaemic control is the most effective approach to prevent them, as reported for several clinical studies (DCCT, 1993; UKPDS, 1998). The progression of diabetic retinopathy has been classically divided in non-proliferative and proliferative retinopathy. Loss of pericytes, thickening of the

basement membrane of retinal capillaries and formation of microaneurysms are the alterations characteristic of non-proliferative stages at the level of retinal capillaries. In addition, platelet aggregation, and leukostasis also contribute by promoting vascular occlusion (Agardh and Agardh, 2004). Vascular permeability is increased, due to a compromise in the integrity of the blood-retinal barrier (Agardh and Agardh, 2004). If vascular leakage occurs, fluids accumulate in the retinal tissue, leading to edema and formation of lipid deposits; when the edema affects the macular region it can result in decreased visual acuity and risk of loss of vision (Kent et al., 2000). It is believed that all these alterations lead to tissular hypoxia and the appearance of non-perfused areas, which stimulate the growth of new retinal vessels, the key feature of proliferative retinopathy (Agardh and Agardh, 2004). Vascular Endothelial Growth Factor (VEGF), a potent angiogenic factor, plays a key role in the progression of vascular alterations in diabetic retinopathy. Increased levels of VEGF have been found in the vitreous and the retina of diabetic patients (Aiello et al., 1994; Malecaze et al., 1994) and this increase is thought to be the consequence of retinal hypoxia (Malecaze et al., 1994). VEGF promotes endothelial cell-mediated degradation of the extracellular matrix through the activation of matrix metalloproteinases (MMPs) (Kosano et al., 1999; Wang and Keiser, 1998a) and also stimulates EC migration, proliferation and association for tube formation (Ferrara, 2000), contributing to retinal neovascularization. VEGF is also involved in the fibrotic processes that can be concomitant with retinal angiogenesis, through the induction of connective tissue growth factor (CTGF) (Kuiper et al., 2008). Retinal neovessels initially grow within the retina but can invade the vitreous cavity where, due to their fragility, they may rupture causing

haemorrhages that affect vision. Moreover, these neovessels, associated with fibrous tissue, form epiretinal membranes that can traction the retina, causing retinal detachment from the RPE (Agardh and Agardh, 2004), with a high risk of loss of vision.

In addition to VEGF, Insulin-like Growth Factor I (IGF-I) is also increased in the vitreous of patients with proliferative diabetic retinopathy (Merimee et al., 1983; Grant et al., 1986; Inokuchi et al., 2001). Moreover, pharmacological inhibition or genetic deletion of IGF-I in the retinal vasculature prevent the development of retinal neovascularization in hypoxic conditions (Smith et al., 1999; Kondo et al., 2003). These observations suggest a role of IGF-I in retinal neovascularization in diabetic retinopathy. A role of intraocular IGF-I, in association with VEGF, has also been proposed for the development of vascular hyperpermeability in retinopathy (Haurigot et al., 2009). Moreover, IGF-I induces VEGF expression (Punglia et al., 1997) through HIF-1α stabilization, the main hypoxia-responsive transcription factor, which activates the expression of VEGF in retinal epithelial cells (Treins et al., 2005). These interactions suggest that both IGF-I and VEGF contribute to retinal neovascularization in diabetic retinopathy.

3.1.3. Neuronal changes in diabetic retinopathy

Visual dysfunction has been described in human diabetic retinopathy (Bearse et al., 2006), suggesting that biochemical and vascular changes in the diabetic retina can have effects on neuronal functionality. Alterations in spatial,

colour and dynamic vision and delayed responses after light stimuli are the most common alterations found in diabetic patients (Bearse et al., 2006). Electroretinographic recordings in diabetic patients showed reduced amplitudes of the scotopic b-wave and increased latency times in the oscillatory potentials (OPs) and the scotopic a-wave (Coupland, 1987; Shirao and Kawasaki, 1998; Tyrberg et al., 2011), both related to reduced neuronal activity in the inner retinal layers. Moreover, photoreceptor dysfunction has been also detected in these patients (Holopigian et al., 1997). Importantly, these pathological changes are present in diabetic patients at early stages of the disease, with no signs of vascular retinopathy in funduscopic examinations, and get worse as vascular pathology advances (Shirao and Kawasaki, 1998). In agreement with these clinical observations, apoptotic neurons have been detected in the INL and the GCL in post-mortem retinas from diabetic patients (Barber et al., 1998; Abu-El-Asrar et al., 2004). Evidence has pointed out towards the activation of the polyol pathway and the concomitant accumulation of sorbitol as one of the possible mechanisms underlying neuronal degeneration in diabetic retinas (Asnaghi et al., 2003).

3.1.4. Glial changes in diabetic retinopathy

Müller cells, the main macroglial cell type in the retina, are a possible target of hyperglycaemia; these cells have an unregulated uptake of glucose, via glucose transporter 1 (GLUT1), and a high rate of glycolisis (Kumagai et al., 1994; Poitry-Yamate et al., 1995). Glial fibrillary acidic protein (GFAP) up-regulation, a hallmark of reactive gliosis, is found in retinas from diabetic

patients (Mizutani et al., 1998). In experimental diabetes in rats, increased GFAP expression in Müller cells is an early event of retinopathy, present even when no vascular alterations can be detected, and maintained during the animal's life (Lieth et al., 1998). Studies in diabetic rats indicate that chronic glial activation results in impaired glutamate metabolism due to the reduction of glutamine syntethase activity (Lieth et al., 2000), and altered potassium conductance, associated with the deslocalization from Müller cell membrane of Kir4.1 potassium channels (Pannicke et al., 2006). This loss of supportive glial functions may contribute to neuronal dysfunction in diabetic retinas (Bringmann et al., 2006). In addition, activated Müller cells produce pro-inflammatory molecules potentially citotoxic for neurons, such as Tumor Necrosis Factor alpha (TNF-α) and Interleukin 1 beta (IL-1β), whose expression is known to be activated by hyperglycaemia in rat retinas (Joussen et al., 2002; Gerhardinger et al., 2005). Some of these alterations have been recently linked with AGEs accumulation and oxidative stress in Müller cells (Curtis et al., 2011). Furthermore, VEGF production is increased in Müller cells in human diabetic retinas before vascular abnormalities can be detected (Amin et al., 1997), a fact that may contribute to increased vascular permeability and, later, to retinal neovascularization.

Microglial cells may also play an important role in the onset and development of diabetic retinopathy. Activation of microglial cells has been reported for human diabetic retinas (Zeng et al., 2008) and rats with experimental diabetes (Krady et al., 2005). Activated microglial cells contribute to the inflammatory milieu of the diabetic retinas by releasing IL-1β, TNF-α,

interleukin 6 (IL-6), VEGF and nitric oxide (Krady et al., 2005). The accumulation of these cytokines and growth factors may induce neuronal death (Venters et al., 1999) and breakdown of the blood-retinal barrier (Joussen et al., 2002). Treatment with anti-inflammatory drugs counteracts neurodegeneration and other features of early retinopathy in diabetic rats through downregulation of the expression of pro-inflammatory cytokines (Krady et al., 2005; Joussen et al., 2002).

4. ANIMAL MODELS FOR THE STUDY OF DIABETIC RETINOPATHY

Rodents are the most commonly used small animal models for research in diabetes and its secondary complications. Several rat and mouse models of diabetes have been used in the study of retinopathy, although most of them do not fully develop advanced stages of disease; particularly, they do not show abnormal growth of vessels and are therefore not good models of proliferative retinopathy. For that reason, rodent models of retinal neovascularization have been developed in order to study this process, central to proliferative retinopathy and other ischemic retinopathies, and to test the efficacy of potential antiangiogenic therapies.

4.1. SPONTANEOUS MODELS OF TYPE 1 DIABETES

- **Non-obese diabetic (NOD) mice.** NOD mice are the most commonly used mouse model in the study of type 1 diabetes. Due to a mutation in a MHC complex molecule, 20% of males and 80% of females present autoimmune diabetes at 12-14 weeks of age. However, few reports on the development of secondary complications in this model have been published. Mild nephropathy (Maeda et al., 2003) and susceptibility to macrovascular disease (Zimmerman et al., 2011) have been reported, but no features of diabetic retinopathy have been described to date in these mice.

- **Ins2^{Akita} mice.** These mice contain a point mutation in the insulin 2 gene at the *Mody4* locus, resulting in hyperglycaemia at 4 weeks of age (Yoshioka et

al., 1997). $Ins2^{Akita}$ mice show increased vascular permeability, leukostasis and mild neuronal death in adult age but neither gliosis nor pericyte loss have been observed (Barber et al., 2005).

- **BB (BioBreeding Worcester) rats.** This autoimmune model of type 1 diabetes is characterized by the development of hyperglycaemia between 10-12 weeks of age with an incidence of 60-90%, regardless of sex (Like et al., 1982). Although these rats are a good model of nephropathy and peripheral neuropathy, only early features of retinopathy are observed in these animals (Sima et al., 1985; Barber et al., 2000). Loss of pericytes, increased thickness of the basement membrane, microaneursyms and GFAP upregulation have been described in hyperglycaemic BB rat retinas (Sima et al., 1985; Barber et al., 2000).

4.2. SPONTANEOUS MODELS OF TYPE 2 DIABETES

- ***db/db*** **mice.** These leptin receptor deficient mice are obese and develop hyperglycaemia at 8 weeks of age (Kodama et al., 1994). *db/db* mice are a good model of diabetic nephropathy (Sharma et al., 2003) and peripheral neuropathy (Calcutt et al., 1988). At 6 months of age these mice show early retinopathy, characterized by perycite and endothelial cell loss (Midena et al., 1989) and basement membrane thickening (Clements et al., 1998). At 15 months of age, *db/db* mice also present breakdown of the blood-retinal barrier, glial reactivity, neuronal apoptosis and increased capillary density (Cheung et

al., 2005). In contrast, leptin-deficient mice (*ob/ob*) are only mildly hyperglycaemic and do not develop secondary complications (Lindström, 2007).

- **Goto-Kakizaki rats.** The Goto-Kakizaki (GK) rat is a model of spontaneous type 2 diabetes without obesity. The diabetic state of GK rats is moderate, with glucose intolerance developing early and significant hyperglycaemia present at 4 weeks of age in most of the animals (Goto et al., 1988). As in other rodent models, albuminuria and decreased peripheral nerve conductance, but no advanced proliferative retinopathy, have been described in these rats. Only increased vascular permeability (Carmo et al., 2000) and altered endothelial/perycite ratio (Agardh et al., 1997) have been reported in the Goto-Kakizaki rats.

- **Zucker diabetic fatty (ZDF) rats.** ZDF rats are derived from obese Zucker rats (*fa/fa*), which carry a mutation in the leptin receptor and become hyperglycaemic at 6-7 weeks of age (Clark et al., 1983), developing both nephropathy and neuropathy (Kasiske et al., 1985; Peterson, 2001). Basement membrane thickening and increased capillary cellular density have been described in retinas of 7 months-old ZDF rats, but neither loss of pericytes nor microaneurysms were found (Danis and Yang, 1993).

- **Otsuka Long-Evans Tokushima fatty (OLEFT) rats.** OLEFT rats are a spontaneous model of non-insulin-dependent diabetes (Kawano et al., 1992) that develops hyperglycaemia at about 20 weeks of age. Despite the fact that these rats are prone to glomerular lesions (Kawano et al., 1992), few features of early retinopathy have been described. Microaneurysms and reduced retinal

layer thickness are found in adult OLEFT rats (Lu et al., 2003), but no loss of pericytes or acellular capillaries has been reported.

- **Spontaneously Diabetic Torii (SDT) rats.** SDT are non-obese type 2 diabetic, with chronic severe hyperglycaemia from 15-20 weeks of age (Shinohara et al., 2007). Aged STD rats (between 35 and 82 weeks) have acellular capillaries, pericytes loss, venous dilation and increased permeability in the retina, and also several important proliferative features such as retinal haemorrhage, tractional retinal detachment with fibrous proliferation and iris neovascularization (Kakehashi et al., 2006; Sasase, 2010). About 50% of rats present intravitreal vessels when analysed at more than 80 weeks of age (Yamada et al., 2005). However, there is not a clear temporal evolution from early retinopathy to advanced stages of the retinal complications in this model (Kakehashi et al., 2006).

4.3 STREPTOZOTOCIN (STZ)- INDUCED RODENT MODELS OF DIABETES

Streptozotocin (STZ), an antibiotic extracted from *Streptomyces achromogenes*, is the most commonly used drug to induce experimental diabetes in rodent models. STZ toxicity causes β-cell death by several mechanisms, such as DNA methylation and ROS and NO production (Wilson et al., 1984). Depending on the protocol and the dose, a few days after STZ administration rodents develop overt hyperglycaemia (Rossini et al., 1977).

.

- STZ-induced diabetic rats. These models develop diabetic nephropathy and neuropathy but only early features of retinopathy. Amongst them are: ERG abnormalities, neuronal apoptosis and GFAP upregulation in early stages of diabetes (Kern and Barber, 2008a; Lieth et al., 1998). Vascular alterations in STZ-treated rats appear about eight months after the onset of hyperglycaemia, when pericyte loss, capillary degeneration and vascular hyperpermeability are found (Kern et al., 2010). Some differences in the susceptibility to STZ-induced retinal complications have been described in different rat strains (Kern et al., 2010).

- STZ-induced diabetic mice. Only transient apoptosis of ganglion neurons, two weeks after STZ injection, has been described in STZ-treated mice. However, no GCL cell loss could be detected 2 and 6 months post STZ treatment (Feit-Leichman et al., 2005). Moreover, transient GFAP upregulation has only been observed 1 month after STZ administration and it comprised only astrocytes, with no involvement of Müller cells (Feit-Leichman et al., 2005). After 6 months of STZ-induced diabetes, vascular cell apoptosis, acellular capillaries and pericytes ghosts have been observed; with no significantly increases in basement membrane thickness even 15 months after the induction of diabetes (Feit-Leichman et al., 2005).

4.4. ANIMAL MODELS OF RETINAL NEOVASCULARIZATION

- **Oxygen-induced models of retinopathy (OIR).** Rat and mouse OIR models try to mimic the pathology of retinopathy of prematurity (ROP) in humans. When

an infant is born prematurely, the process of retinal vascular maturation can be disrupted, due to the environmental hyperoxia (compared with intrauterine conditions) and the supplemental oxygen therapy that may be required to treat lung immaturity in these patients. Hyperoxia induces vaso-obliteration and stops the growth of existing retinal vessels. In the first phase of the pathology, increased metabolic requirements of the retina cause the induction of compensatory uncontrolled neovascularization that develops in the second, proliferative phase of the disease. These neovessels are immature and do not oxygenate the retina, causing neuronal degeneration (Ashton, 1966). This process is recapitulated in the OIR mouse model (Smith et al., 1994), in which mouse pups are placed in 75% oxygen atmosphere from postnatal day 7 (P7) to P12. Afterwards, mice are returned to normal oxygen tension, which causes relative hypoxia compared to the previous condition, and five days later retinal neovascularization is present in the 100% of the mice, evidenced as vascular tufts in the vitreous cavity that can be easily visualized and quantified (Smith et al., 1994). In the case of the OIR rats, the animals are exposed to alternative 12-hour cycles of 80% and 40% oxygen for the first 14 days of life (Penn et al., 1993). After this protocol, 66% of rats develop retinal neovascularization (Penn et al., 1993). In both models of OIR, an spontaneous regression of the intravitreal neovessels occurs after few weeks of normal oxygen exposure (Smith et al., 1994; Penn et al., 1993).

- **Vascular occlusion models.** Retinal vein occlusion by laser has been described as a good model for the induction of preretinal neovascularization in rats (Saito et al., 1997). Laser photocoagulation of retinal veins induces

alterations in the vasculature that cause reduced blood flow and retinal ischemia, leading to pre-retinal neovascularization (Saito et al., 1997).

- **Transgenic mouse models of retinal neovascularization.** Several transgenic mouse models of retinal neovascularization have been developed. Overexpression of VEGF in photoreceptors (Ohno-Matsui et al., 2002) and RPE cells (Oshima et al., 2004a) has resulted in different phenotypes. Rho/VEGF transgenic mice, in which VEGF is produced by rod photoreceptors, show atypical neovascularization in the photoreceptor layer and the subretinal space, with a pattern that resembles more choroidal neovascularization (CNV) than the preretinal vessels characteristic of diabetic retinopathy (Ohno-Matsui et al., 2002). Transgenic mice overexpressing VEGF in the RPE do not present any alteration in the retinal and choroidal vasculatures unless overexpression of angiopoietin 2 is also present (Oshima et al., 2004a). Again, this model shows a pattern of neovascularization similar to CNV (Oshima et al., 2004a).

In summary, rodent models of diabetes do not develop overt proliferative retinopathy. Only Torii rats present proliferative retinopathy in very long-lived animals, which makes the assessment of new therapies in this model difficult. The OIR models present pre-retinal neovascularization resembling proliferative retinopathy but do not allow the long-term evaluation of the efficacy of new therapeutic approaches owing to the early regression of neovessels. Thus, an adult model of proliferative retinopathy would be required for the assessment of new experimental therapies.

5. TRANSGENIC MICE OVEREXPRESSING INSULIN-LIKE GROWTH FACTOR I IN THE RETINA (TgIGF-I)

The intraocular levels of IGF-I are increased in diabetic patients with proliferative retinopathy (Merimee et al., 1983; Grant et al., 1986; Inokuchi et al., 2001) and IGF-I contribution to retinal neovascularization has been clearly demonstrated (Smith et al., 1999; Kondo et al., 2003). Transgenic mice overexpressing Insulin-like Growth Factor I (IGF-I) under the control of the rat insulin promoter I (RIP-I) were initially designed to study the role of IGF-I in pancreatic β-cells (George et al., 2002). These mice are normoglycemic, normoinsulinemic, have normal body weight, and their circulating levels of IGF-I are similar to that of Wt littermates (George et al., 2002). Surprisingly, it was observed that, with age, some of these transgenic mice developed cataracts and buphthalmos. Further analyses demonstrated that IGF-I is also overexpressed in the retinas and accumulated in the aqueous humour of transgenic mice (Figure 7) (Ruberte et al., 2004; Haurigot et al., 2009). Detailed molecular and morphological studies revealed the presence of ocular alterations in TgIGF-I mice similar to those of diabetes-induced eye complications (Ruberte et al., 2004; Haurigot et al., 2009).

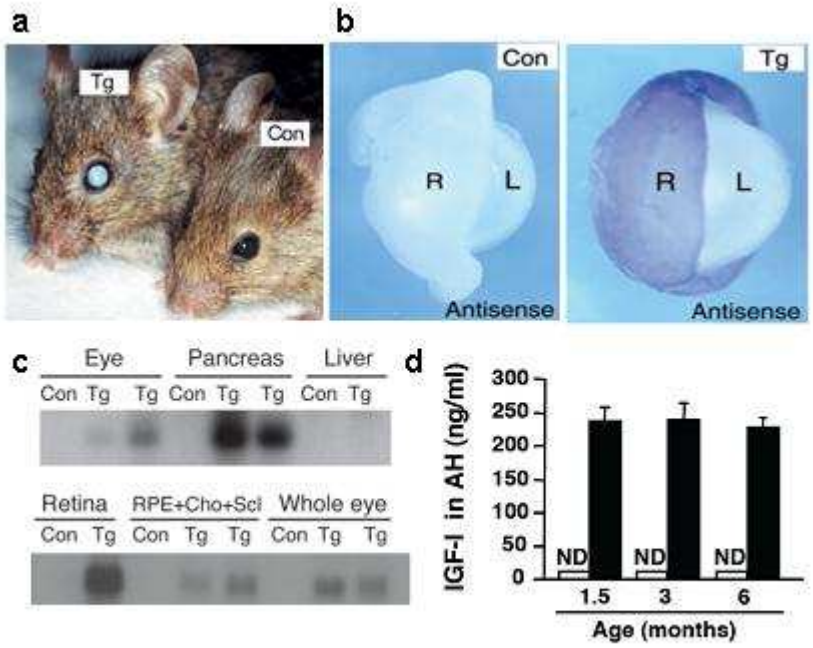

Figure 7. Retinal IGF-I overexpression in TgIGF-I. (a) Macroscopic alterations in the eyes of transgenic mice overexpressing IGF-I, with cataracts and buphthalmos, which prompted the investigation of whether the transgene was being expressed in the eye. **(c)** *In situ* hybridization of IGF-I mRNA in transgenic retinas, The left panels shows that's IGF-I expression was undetectable in Wt mice. **(b)** Northern blot demonstrating increased IGF-I expression under the control of the RIP-I promoter in pancreas and retina of TgIGF-I but not control mice. **(d)** ELISA measurements revealed IGF-I life-long accumulation in the aqueous humor of transgenic mice White bars represent control healthy animals, black bars represent Tg-IGF-I. Adapted from Ruberte et al. 2004 and Haurigot et al. 2009.

5.1. NON-PROLIFERATIVE RETINOPATHY IN TgIGF-I MICE

Loss of pericytes was observed in retinal digestions in TgIGF-I mice aged 2-3 months; endothelial cell number, however, remained unchanged (Figure 8a) (Ruberte et al., 2004). In addition, using both confocal and electron microscopy, a clear thickening of the basement membrane was described in retinal capillaries from transgenic retinas at this age (Figure 8b) (Ruberte et al., 2004). Both alterations are present in the non-proliferative phase of human diabetic eye disease (Agardh and Agardh, 2004).

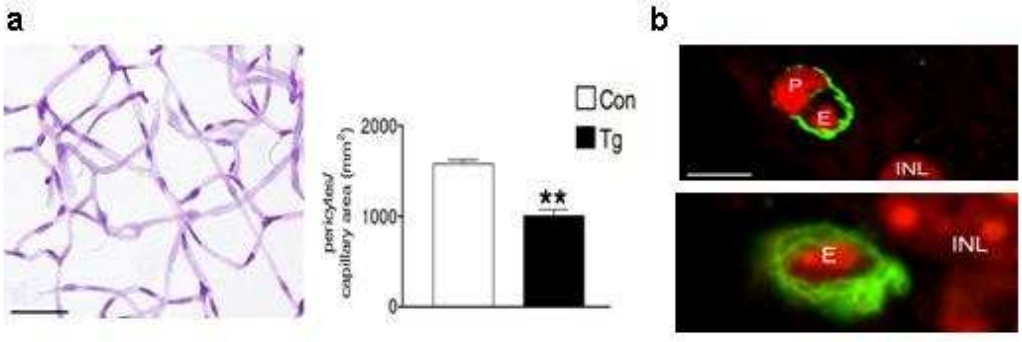

Figure 8. Vascular non-proliferative alterations in TgIGF-I. (a) Representative images of trypsin retinal digests. Only basement membrane-surrounded vessels are protected from digestion. The histogram indicates that a decreased number of pericytes was determined in transgenic retinal vessels **(b)** Laser confocal microscopy analysis demonstrating basement membrane thickening in TgIGF-I retinal vessels in sections immunolabeled for the basement membrane marker collagen type IV (green). Nuclei are counterstained in red with propidium iodide. Adapted from Ruberte et al. 2004.

These pathological features of non-proliferative retinopathy correlate with increased VEGF expression in transgenic retinas at 3 months of age and the presence of reactive gliosis, determined by the upregulation of GFAP in these retinas (Figure 9) (Ruberte et al., 2004).

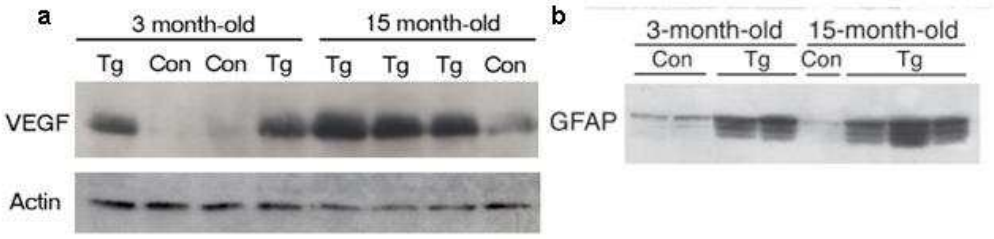

Figure 9. Increased VEGF and GFAP levels in TgIGF-I retinas. Western blot revealed increased retinal levels of **(a)** VEGF and **(b)** GFAP in transgenic animals at 3 and 15 months of age. Adapted from Ruberte et al. 2004.

Increased vascular permeability, another hallmark of diabetic retinopathy, is observed in 3 months-old transgenic mice owing to the disruption of the blood-retinal barrier (BRB), with alterations in the integrity of tight junctions in

retinal vessels (Figure 10a) (Haurigot et al., 2009). Retinal inflammation has been associated with the pathogenesis of BRB breakdown (Adamis, 2002). ICAM-1 mediates key steps of the transmigration of circulating leukocytes into tissues and is increased in human diabetic retinas (McLeod et al., 1995). Similarly, ICAM-1 is increased in TgIGF-I retinas (Figure 10b) (Haurigot et al., 2009). In accordance with the rise in retinal ICAM-1, TgIGF-I showed increased number of BM-derived microglial cells, suggesting the existence of a inflammatory process in transgenic retinas that recruited macrophages from the bone marrow (Figure 10c) (Haurigot et al., 2009).

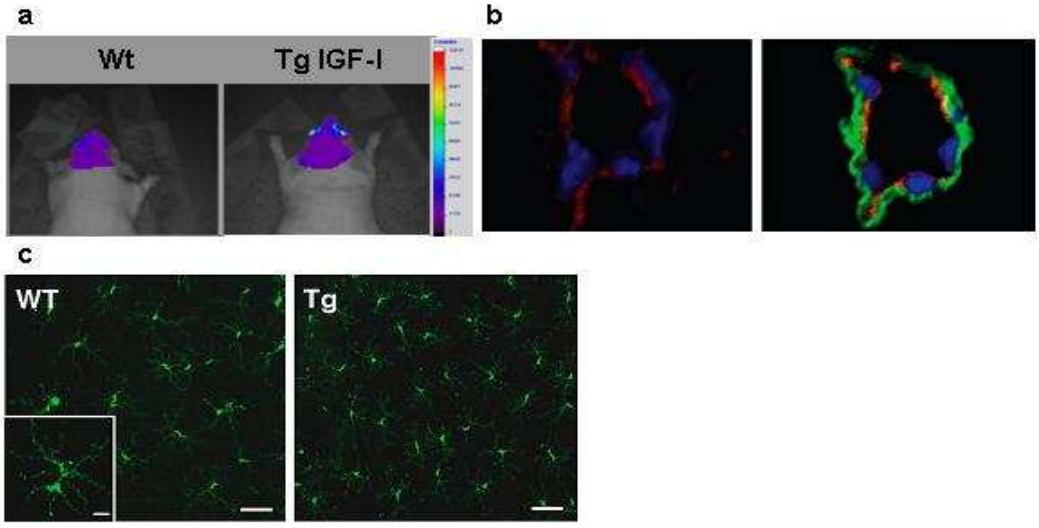

Figure 10. BRB breakdown and inflammation in TgIGF-I. (a) Representative images of *in vivo* fluorescence assay demonstrating increased retinal vascular permeability in TgIGF-I mice. The intravascularly-injected cy5.5 dye accumulated in the eyes of transgenic but not WT mice. **(b)** Immunofluorescent detection of ICAM-1 (green) overexpression in transgenic vessels co-labelled for the vascular marker Collagen Type IV (red). Nuclei (blue) were counterstained with Topro 3 **(c)** Increased number of bone marrow-derived microglial cells in transgenic retinas suggested the existence of an inflammatory process in transgenic retinas. Transgenic and WT mice received a bone marrow transplant from healthy transgenic mice ubiquitously expressing the Green Fluorescent Protein (GFP) and microglial infiltration in the retina was analysed 4 months after engraftment. GFP immunodetection (green) was used to identify bone-marrow origin of microgial cells Adapted from Haurigot et al. 2009.

5.2. PROLIFERATIVE RETINOPATHY IN TgIGF-I MICE

The non-proliferative alterations present in the retinal vasculature of transgenic mice progress to vessel degeneration and retinal vascular abnormalities; with non-perfused areas observed in old transgenic mice (Figure 11a) (Ruberte et al., 2004). Increased activity of metalloproteinases is detected in aqueous humour of transgenic mice (Llombart et al., in preparation), indicating remodelling of the tissue. Retinal and pre-retinal neovascularization is observed in old animals (Figure 11a-b) (Ruberte et al., 2004). Rounded vascular structures with lumen and positive for collagen type IV and Von Willebrand factor, a marker of endothelial cells, are identified as intravitreal vessels (Figure 11b). By intravascular injection of resine, these intravitreal neovessels were confirmed to be functional (connected to the general circulation), and the observation of the patter of the imprints left by endothelial nuclei confirmed the neovascular nature of these structures, excluding the possibility of a hyaline origin (Figure 11b) (Ruberte et al., 2004). These intravitreal vessels, likely through the exertion of tractional forces, may be the cause of the high incidence of retinal detachment in TgIGF-I mice, which is present in 75% of old transgenic animals (Ruberte et al., 2004).

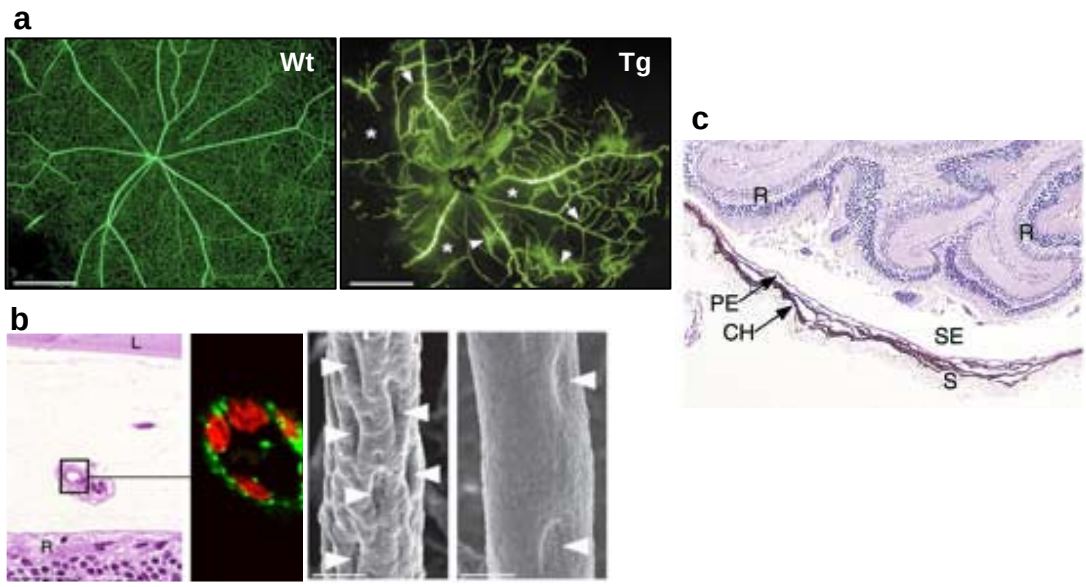

Figure 11. Neovascularization in transgenic retinas overexpressing IGF-I. (a) Fluorescein angiographies showed vascular abnormalities and non-perfused areas in transgenic retinas from old animals. **(b)** Hematoxilin-eosin staining demonstrating the presence of neovessels in the vitreous cavity of transgenic eyes, characterized by collagen IV (green) and Von Willebrand factor (red) expression (right panels). Nuclear imprints observed in the resina cast confirmed the neovascular origin of these vessels. **(c)** Retinal detachment is observed in old transgenic mice. Adapted from Ruberte et al. 2004.

5.3. NON-RETINAL ALTERATIONS IN TgIGF-I MICE

As previously mentioned, TgIGF-I mice show cataracts and buphthalmos with high incidence in old animals (Ruberte et al., 2004). Iris neovascularization is also observed, with synechias that preclude drainage of aqueous humour, causing an increase in the size of the anterior chamber (Figure 12) (Ruberte et al., 2004).

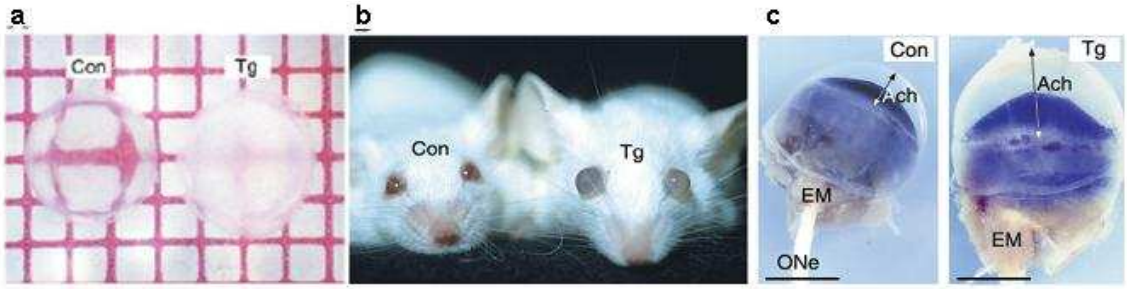

Figure 12. Non-retinal alterations in TgIGF-I mice. (a) Lens opacities were observed in transgenic mice after macroscopical observations. **(b)** Buphthalmos are clearly observed in TgIGF-I mice **(c)** Increased size of the anterior chamber is observed in transgenic eyes. Adapted from Ruberte et al. 2004.

Then, TgIGF-I presents the majority of the vascular alterations observed in the human diabetic eye with a temporary evolution that resembles that of the human disease, allowing the long-term evaluation of therapeutic strategies and facilitating the translation to the clinical setting of a chronic pathology such as retinopathy, when compared with OIR or laser-induced models.

6. TREATMENT OF DIABETIC RETINOPATHY

The guidelines for the treatment of diabetic retinopathy have been established following the conclusions of three large clinical trials: the Diabetic Retinopathy Study (DRS, 1971-1978), the Early Treatment Diabetic Retinopathy Study (ETDRS, 1980-1989) and the Diabetic Vitrectomy Study (1976-1983) (Agardh and Agardh, 2004). The recommendations set up by these studies are still applicable, although laser and surgical technologies have since then been considerably improved. Furthermore, the results of several clinical trials of anti-VEGF agents have recently been published (Nicholson and Schachat, 2010; Boscia, 2010), suggesting an important role of this new treatment in the management of diabetic retinopathy.

6.1. LASER PHOTOCOAGULATION

Panretinal laser treatment is the main therapy for the vascular alterations of diabetic retinopathy, specially in proliferative stages. This treatment is recommended for patients with neovessels and vitreous haemorrhage or patients with neovessels near the optic disc (DRS Report 8, 1981). However, laser photocoagulation is not clearly indicated for patients in non-proliferative stages of diabetic retinopathy, and the risk/benefit for each patient should be carefully evaluated (DRS Report 8, 1981). Current protocols include 2 or 3 sessions over a period of 4-6 weeks, using a 500 µm spot size, with 1200-200 laser burns separated 0.5 burn-widths from each other and with a duration of 0.1-0.2 seconds per burn (Neubauer and Ulbig, 2007). The DRS trial demonstrated a reduction of 50% in the rate of severe visual loss during a 5-

year follow-up period after panretinal photocoagulation (DRS Report 8, 1981). The mechanisms underlying the beneficial effects of photocoagulation are not clear. Laser burns result in reduced thickness of the retina due to cell loss, which may improve oxygen diffusion, reducing ischemia (Gottfredsdóttir et al., 1993). In addition, VEGF vitreous levels are reduced after photocoagulation, contributing to the halt in the growth of new vessels (Aiello et al., 1994). However, panretinal laser photocoagulation has serious side-effects, amongst which are loss of visual field and reduced visual acuity that occurs in most cases, specially after intensive, high-density treatments (Towler and Lightman, 2003).

6.2. VITRECTOMY

The removal of the vitreous gel and its replacement by a balanced salt solution is indicated for non-clearing vitreous haemorrhage and advanced proliferative retinopathy with severe fibrovascular proliferation (Towler and Lightman, 2003), improving the visual acuity in 25% of treated patients (DRSV Report 5, 1990). The removal of a partially deattached vitreous reduces the growth of neovessels associated to fibrovascular membranes (Helbig, 2007). However, the removal of intravitreal neovessels may exacerbate the angiogenic process and intense photocoagulation is often required immediately after surgery (Helbig, 2007). Other side-effects of vitrectomy are acceleration of cataract formation and iris neovascularization (Agardh and Agardh, 2004).

6.3. ANTI-VEGF TREATMENTS

VEGF plays a central role in the pathogenesis of diabetic retinopathy, being involved in the alteration of vascular permeability, inflammation and neovascularization. Thus, agents blocking VEGF action have been extensively tested for the treatment of both proliferative diabetic retinopathy and diabetic macular oedema (Nicholson and Schachat, 2010). Three anti-VEGF commercial products are currently available: 1. *pegaptanib* (Macugen, OSI/Eyetech), a pegylated $VEGF_{165}$ aptamer; 2. *ranibizumab* (Lucentis, Genentech Inc.), a humanized antibody fragment for all VEGF isoforms and 3. *bevacizumab* (Avastin, Genentech Inc.), a full-length, humanized antibody also specific for all VEGF isoforms.

Intraocular administration of *pegaptanib* (Macugen) has demonstrated its efficacy in the treatment of diabetic macular oedema (DME) and proliferative diabetic retinopathy (PDR) in several clinical trials. A phase II trial on DME patients, with and without PDR, who received 5 injections (every 3 weeks) demonstrated an improvement in visual acuity, reduced need for photocoagulation and complete regression of neovascularization (Cunningham et al., 2005; Adamis et al., 2006). Reduced vascular leakage and regression of neovascularization have also been reported in PDR patients after two administrations of pegaptanib, separated 6 weeks, and evaluated 6 and 12 weeks after the last injection (González et al., 2009). However, these small and short-term studies do not give enough information regarding adverse effects or persistence of the benefits observed. An ongoing phase II/III, multicenter trial,

with two-year follow up, will likely provide more conclusive information (NCT00605280, clinicaltrials.gov).

Ranibizumab (Lucentis), administered locally, has been tested in several phase I/II trials for DME (Chun et al., 2006; Nguyen et al., 2009; Elman et al., 2010), demonstrating improvements in visual acuity outcomes when compared with sham or laser treatments. Best results have been obtained when ranibizumab is administrated as an adjunct to laser photocoagulation in DME patients, with the possibility of retreatment evaluated at monthly visits (Elman et al., 2010). As in the case of pegaptanib, no long-term results have been reported yet, and phase III studies with ranibizumab that include PDR patients are currently in progress (NCT00545870, clinicaltrials.gov).

Although it was initially indicated for cancer therapies, several off-label studies have been reported on the use of intravitreal injections of *bevacizumab* (Avastin) for the treatment of DME and PDR. In general, improvement of visual acuity has been reported in short-term trials with bevacizumab, alone or in combination with laser therapy (Cho et al., 2009; Tonello et al., 2008). Moreover, PDR patients treated with bevacizumab + laser presented reduced vascular leakage and significant improvement of vitreous haemorrhage (Cho et al., 2009; Tonello et al., 2008). Yet again, these are short-term results that have to be validated by longer studies and the frequency of repeated administrations needs to be set up, due to the short-life of these molecules (Nicholson and Schachat, 2010).

.

7. GENE THERAPY FOR OCULAR DISORDERS

Gene therapy is defined as the correction of diseases by the introduction of foreign nucleic acids in target cells or tissues. The genetic modification of cells provides continuous therapeutic effects, generally, after one single administration, offering certain clinical advantages over conventional pharmacological therapies. Different strategies can be performed, such as gene replacement (by addition of a correct copy of a mutated gene), gene silencing (by suppression of the pathological overexpression of a gene), gene addition (by supply of a therapeutic gene independent of the primary genetic or non-genetic nature of disease) or gene correction (by *in situ* repair of a mutated gene in its chromosomal locus).

Two main categories of gene therapy have been defined depending on the strategy used for the modification of the target cells or tissues. In an *ex vivo* approach, target cells are obtained from the individual, cultured and genetically modified *in vitro* and the re-implanted to the patient. In an *in vivo* strategy, the target cells are genetically modified *in situ* inside the organism.

For both *ex vivo* and *in vivo* approaches, a vector capable of introducing the therapeutic nucleic acid with an efficacy enough to produce a biological effect is required. There are two types of vectors for gene transfer: non-viral and viral vectors. Non-viral gene transfer is based on physical/chemical methods of nucleic acid transfer. Electrotransference or encapsulation of nucleic acids in liposomes or cationic polymers are amongst the most commonly used non-viral

strategies. On the other hand, viral vectors are derived from wild-type viruses and take advantage of their natural ability to introduce genetic material into the cells, transfer it to the nucleus and express the encoded proteins. Several families of viral vectors have been engineered and used for gene therapy strategies, in all of which most or all of the viral genome has been replaced for a therapeutic cassette of expression. The choice of vector depends on the characteristics of each disease, the target tissue or the route of administration to be used.

7.1. OCULAR GENE THERAPY

The eye presents several advantages as target organ for gene therapy approaches. It is a small, enclosed organ that allows the delivery of reduced quantities of vectors with minimal risk of dissemination to the rest of the body (Smith et al., 2009). In addition, immune responses that normally follow vector administration are attenuated in the eye, due to the presence of the blood-retinal barrier and the immune-privileged status of the eye (Colella et al., 2009).

The delivery of therapeutic genes to the eye structures can be performed by both viral and non-viral methods. However, ocular non-viral gene transfer shows low efficacy of transfection and transient expression of the transgenes (Andrieu-Soler et al., 2006). On the other hand, viral vectors have demonstrated a high efficacy of transduction and long-lasting expression in ocular structures (Colella et al., 2009). An important issue in ocular gene transfer is the route of administration, due to the high compartmentalization of the eye. Different injection procedures result in exposure of the vector to different ocular cell types

and, subsequently, different transduction patterns. The ocular tropism of viral vectors can vary depending on the route of administration. The same vector administrated by two different routes will probably result in the transduction of different ocular structures. Five routes of delivery can be performed in the eye, as depicted in Figure 13. After subretinal injection, photoreceptors and RPE cells are exposed to the vector preparation, whereas cells located on the retinal surface, including ganglion cells, are in contact with the vector solution after intravitreal administration. For the treatment of corneal diseases, modification of corneal epithelium or endothelium can be achieved by topical application, periocular or anterior chamber injection.

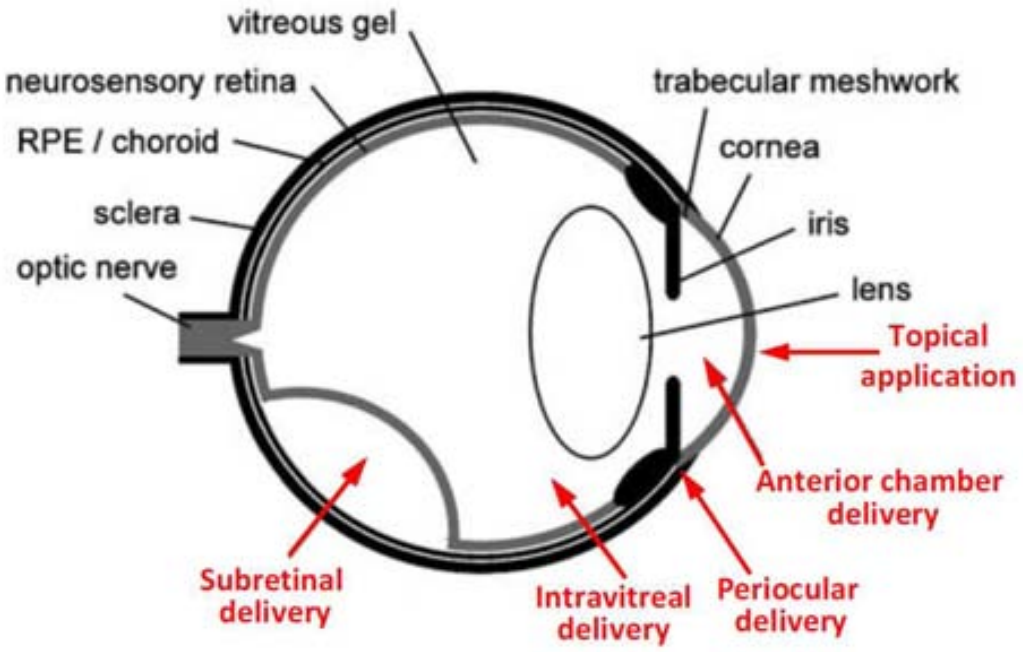

Figure 13. Routes of vector delivery to the eye. Intravitreal and subretinal injections allow transduction of several cell types in the retina, whereas anterior chamber administration is commonly used for corneal and/or trabecular meshwork transduction. Periocular and topical treatments are mainly used for corneal pathologies. Modified from Bainbridge et al., 2006.

The most commonly used viral vectors for ocular gene transfer are lentiviral, adenoviral and adeno-associated virus-derived vectors. Each vector presents advantages and disadvantages that are summarized in Table 1.

Vector	Advantages	Disadvantages
Adenovirus	• Long encapsulation capacity • Infects quiescent and dividing cells • Remains episomal • Production in high titers • High levels of transgene expression	• Immunologic and inflammatory response • Unselective tropism, uncontrolled infection
Adenoassociated Virus	• High stability in specific cell types • Infects quiescent and dividing cells • Remains episomal • Production in high titers • Low immunogenicity • Non pathogenic	• Low encapsulation capacity (4.8 kb)
Retrovirus	• Stable expression in dividing cells • Production in high titers	• Random integration into the host genome • Limited encapsulation capacity (8 kb) • Infects only dividing cells
Lentivirus	• Infects quiescent and dividing cells • Stable expression for long periods of of time • Non immunogenic	• More studies are needed to assess the lack of pathogenicity • Random integration into the host genome

Table1. General characteristics of the most commonly used viral vectors in gene therapy. The table summarizes the advantages and disadvantages of the most commonly used viral vectors. Adapted from Verma et al. 2005.

Lentiviral (LV) vectors, derived from human immunodeficiency virus (HIV-1), are able to transduce the corneal endothelium and the trabecular meshwork after anterior chamber injection in rodents (Challa et al., 2005). When administrated subretinally, RPE cells are transduced and long-term expression with therapeutic effects has been reported (Tschernutter et al., 2005). Lentiviral vectors, however, do not transduce in adult mice photoreceptors, the target cells for most inherited forms of blindness (Kostic et al., 2003). Vesicular

stomatitis virus (VSV-G) pseudotyped LV vectors have been demonstrated to infect Müller cells after subretinal delivery, but no transduced cells where found when the administration was intravitreal (Greenberg et al., 2007).

Adenoviral (Ad) vectors are able to transduce several cell types in the eye depending on the route of administration. If injected intracamerally or intravitreally, high infection of the anterior segment is observed, but minor retinal transduction is detected, mainly in Müller cells (Mori et al., 2002b; Budenz et al., 1995). After subretinal administration, RPE is strongly transduced but the expression of transgenes in photoreceptors is very low (Bennett et al., 1994). It is been described that external ocular tissues can be transduced by Ad vectors when injected in the conjunctive (Tsubota et al., 1998). However, these vectors are not suitable for long-term expression due to the immune response that they elicit, particularly in the case of first-generation Ad vectors, which results in the elimination of the cells expressing adenoviral proteins (Reichel et al., 1998). In contrast, Ad vectors have been clinically tested for transient expression of toxic molecules with the objective of eliminating malignant cells, as in the case of thymidine kinase expression for the treatment of retinoblastomas (Chévez-Barrios et al., 2005). In an attempt to reduced inmmune responses against Ad vectors and ensure long-term expression, a new generation of Ad in which all viral coding sequences have been eliminated has been developed, these are known as helper-dependent Ad vector or gutless Ad vector (Kochanek et al., 2001). Gutless Ad vectors show decreased immunogenicity, reduced toxicity, and prolonged transgene expression (Morsy et al., 1998). Subretinal injection of gutless Ad vectors results in high efficient

transduction of RPE cells (Takahashi et al., 2003), whereas intravitreal administration induces widespread corneal transduction and scattered transduced cells in the retina, mainly Müller cells (Oshima et al., 2004b). In one report sustained transgene expression was maintained for at least 6 months after subretinal injection (Kreppel et al., 2002).

Vectors derived from adeno-associated viruses (AAV) are the most promising vectors for ocular gene transfer, due to their ability to transduce different ocular cell types in mice, dogs and primates (Bennett et al., 1997; Stieger et al., 2008a). As a consequence of the low immunogenicity of these vectors, AAV-mediated transgene expression is sustained for long periods of time (Stieger et al., 2008b). AAV vectors are derived from non-pathogenic parvoviruses that require a helper adenovirus to promote replication (Gonçalves, 2005). The wild-type virus is composed of a 4.9 kb single-stranded DNA genome with two open reading frames: rep (regulatory proteins for replication) and cap, encoding the capsid proteins (Xie et al., 2002) (Figure 14). In the recombinant vectors both genes are removed and replaced by an expression cassette flanked by the ITRs, the only viral sequences remaining in the vector genome, which are needed for the assembly of the particle.

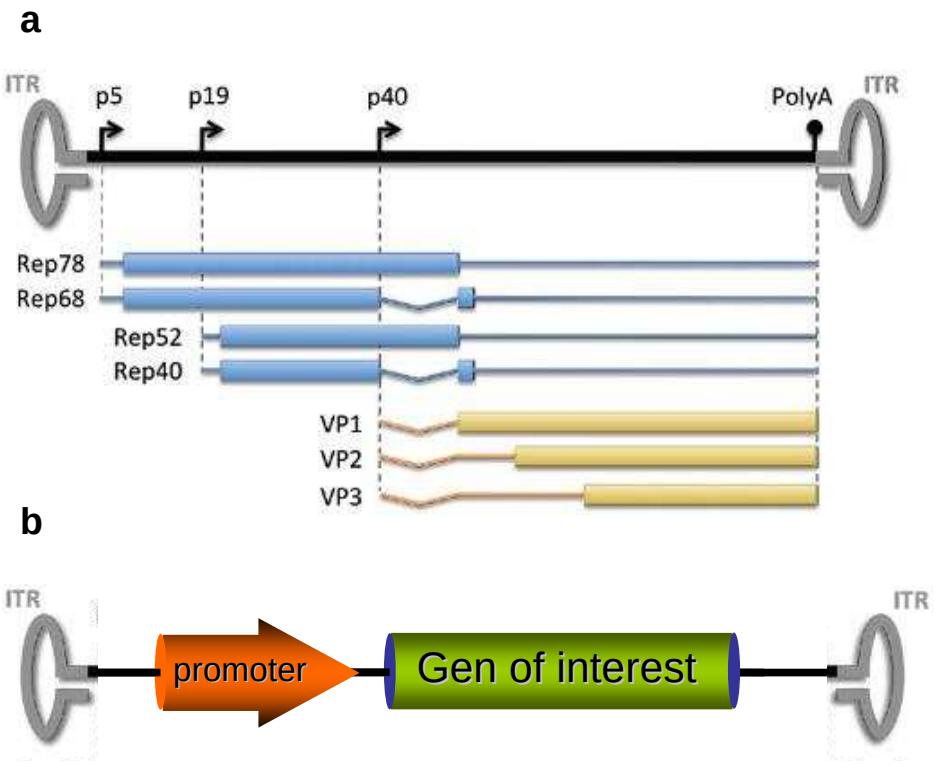

Figure 14. Structure of the wild-type AAV genome. (a) Flanked by the ITRs are the only two genes of the AAV genome: rep, which encodes functions required for replication, and cap, which encodes structural proteins of the capsid. Different proteins are generated by alternative splicing. **(b)** In recombinant AAV vectors, all the viral gens are deleted and replaced by an expression cassette that carries a promoter to drive expression and the gene of interest. Ojo que en el esquema no se lee gene of interest. AL menos en mi mac. Mirar al imprimir.

Several AAV serotypes have been characterized, with variants in the capsid proteins that result in different patterns of infection and kinetics of expression; combining the ITRs of AAV2 and the capsid protein of the serotype of choice, “pseudotyped” AAV vectors can be obtained (Auricchio, 2003). In terms of eye gene therapy, the combination of a particular serotype with a route of administration will result in specific patterns of transgene expression (Colella et al., 2009). The specific tropism of the most common AAV serotypes administrated by intravitreal or subretinal delivery is summarized in Table 2:

Route	AAV1	AAV2	AAV4	AAV5	AAV6	AAV7	AAV8	AAV9
Intravitreal	low, GC	GC	low, GC	low, GC	GC, INL	low, AS	low, GC, AS	GC, MC
Subretinal	RPE	PR, RPE	RPE	PR, RPE	RPE	PR, RPE	PR, RPE	PR, RPE, MC

Table 2. Tropism of AAV vectors in the rodent eye depending on serotype and route of administration. GC, ganglion cells; INL, inner nuclear layer cells; AS, anterior segment cells; MC, Müller cells; RPE, Müller cells; PR, photoreceptors. Summarized from Buch et al. 2008, Hellstrom et al. 2009; Lebherz et al. 2008.

Preclinical gene therapy approaches in rodents, dogs or non-human primates based on AAV have demonstrated the efficacy and the safety of these vectors, in diseases ranging from neuronal degeneration to neovascular or inflammatory disorders (Acland et al., 2005; Broderick et al., 2005; Lukason et al., 2011; Mori et al., 2002c). These studies have paved the way for the clinical translation of ocular gene therapy.

7.2. CLINICAL STUDIES IN EYE GENE THERAPY

The first clinical trial in ocular gene therapy was designed for the treatment of retinoblastoma, the most common intraocular tumour of childhood (Devesa, 1975). Remaining vitreous seeds (small pieces of tumour) often compromise the success of the standard clinical practice, based on chemotherapy and surgery (Shields et al., 1996). Suicide gene therapy using an Ad vector carrying the thymidine kinase gene (Ad-TK) followed by systemic administration of gangcyclovir had been previously reported to be safe and efficient in the treatment of human malignancies (Sung et al., 2001; Alvarez et

al., 2000). Eight patients with vitreous seeds resistant to chemotherapy and radiation were enrolled and received from 1 to 5 intravitreal injections of Ad-TK, with doses ranging from 10^8 to 10^{11} viral particles per eye (Chévez-Barrios et al., 2005). Patients treated with the highest doses presented mild to moderate inflammation and all the patients receiving more than 10^{10} vp showed resolution of the vitreous seeds, which delayed the time of enucleation by several months in most of the cases (Chévez-Barrios et al., 2005).

In 2006, Campochiaro and colleagues reported the first clinical gene transfer approach for a non-malignant ocular disease, neovascular age-related macular edema (AMD), using an Ad vector carrying the antiangiogenic factor PEDF (Campochiaro et al., 2006). Several doses between 10^6 and $10^{9.5}$ viral particles were tested in 28 patients who received a single intravitreal injection of Ad-PEDF (Campochiaro et al., 2006). Transient ocular inflammation was observed in 25% of the patients, but no serious adverse events were reported (Campochiaro et al., 2006). Twelve months after administration, patients receiving the high dose showed improvement or no change of their neovascular lesions (Campochiaro et al., 2006), suggesting the antiangiogenic potential of PEDF. However, the authors have suggested that further clinical investigations should be performed using a vector that provides long-term expression of the therapeutic factor (Campochiaro et al., 2011).

The most promising clinical gene transfer protocols have been focused in the treatment of Leber Congenital Amaurosis (LCA), a group of severe inherited retinal degenerations that result in impaired vision from birth progressesing to

blindness in young adults (Paunescu et al., 2005). Type 2 LCA is caused by a mutation in the RPE65 gene, an essential enzyme present in RPE cells, whose lack results in impaired vision and retinal degeneration (Redmond et al., 1998). Three independent clinical trials published in 2008 were based on RPE65 replacement using AAV2 vectors via subretinal delivery (Hauswirth et al., 2008; Maguire et al., 2008; Bainbridge et al., 2008). All three studies reported no adverse effects and improvements in visual functions in the treated eye compared to the non-treated eye (Hauswirth et al., 2008; Maguire et al., 2008; Bainbridge et al., 2008). One of these trials was extended in time and number of patients, revealing that the beneficial effects were correlated with the age at treatment of the patients (Maguire et al., 2009). The results of the re-administration trial, in which patients treated in the phase I study received vector in the contralateral eye, have recently been published (Bennett et al., 2012). Three adult patients received the highest dose of vector tested in the phase I trial in their previously non-treated eye. The main concern of AAV re-administration was that immune responses mounted against the vector during the first administration would be boosted with the second administration. However, re-administration reported no adverse effects, recovery of functionality in the second-treated eye and maintenance of benefits in the first-treated eye, indicating that re-administration of AAV vector by subretinal delivery in the contralateral eye is safe (Bennett et al., 2012). These encouraging results demonstrate the safety and efficacy of AAV-based gene transfer approaches for ocular diseases.

8. PIGMENTED EPITHELIUM DERIVED FACTOR (PEDF)

New therapeutic genes capable of counteracting neovascularization and neurodegeneration have to be identified, in order to test their efficacy in gene therapy approaches for proliferative retinopathies. Pigmented Epithelium Derived Factor (PEDF) is a good candidate, given that its potential to inhibit the development of neovessels and to counteract neuronal death has been well – described in different pre-clinical and clinical studies.

PEDF is a glycoprotein of 50 KDa that was initially identified in conditioned media from human RPE cells (Tombran-Tink and Johnson, 1989). It belongs to the serpin proteins, a large family of protease inhibitors (Becerra et al., 1995). The human PEDF gene, with a size of 16 Kb, was cloned in 1993, and 8 exons and 7 introns were identified (Steele et al., 1993). The PEDF gene is located in chromosome 17, included in a cluster of cancer-related genes (Steele et al., 1993; Tombran-Tink et al., 1994).

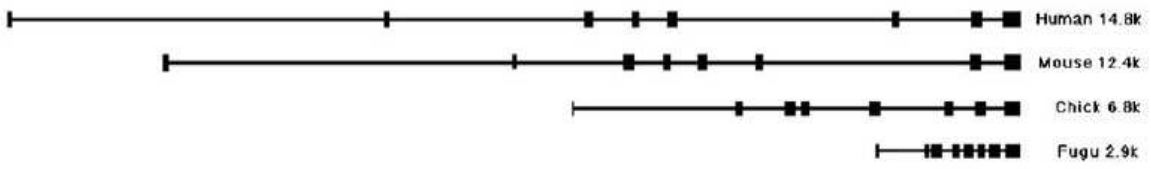

Figure 15. Comparison of the PEDF genes in human, mouse and chicken. Each species has eight exons of similar size and seven introns of variable size. Adapted from Barnstable et al. 2004.

Although it was initially isolated in RPE cells, PEDF expression has been detected in many tissues: in the eye, in the central nervous system (CNS) and

in the rest of the body, in both fetal and adult stages (Filleur et al., 2009). In the eye, PEDF is found in the cornea and the ciliary epithelium and in other retinal and choroidal cells, but at lower levels (Tombran-Tink et al., 1996; Karakousis et al., 2001; Ogata et al., 2002). PEDF levels in the vitreous of different species have been determined to be about 1-2 µg/ml (Tombran-Tink et al., 1995; Ogata et al., 2002; Wu and Becerra, 1996). In the nervous system, PEDF expression has been found in ependymal cells and motor neurons (Bilak et al., 1999) and PEDF is detected in cerebral spinal fluid (Barnstable and Tombran-Tink, 2004). PEDF transcripts have also been found in liver, stomach, testis, heart and colon (Filleur et al., 2009) and plasmatic levels of PEDF are around 5 µg/ml (Petersen et al., 2003). In tissues like the eye, PEDF is expressed very early in development, but no clear evidences of its developmental role have been reported (Barnstable and Tombran-Tink, 2004). The PEDF-knockout mouse is not lethal but presents retinal abnormalities that can be related to deficient cell differentiation (Doll et al., 2003).

8.1. NEUROPROTECTIVE PROPERTIES OF PEDF

PEDF was initially isolated as the differential factor in the RPE conditioned media that was able to differentiate retinoblastoma cells into neurons (Tombran-Tink and Johnson, 1989). Since then, the ability of PEDF to induce differentiation and neurite growth has been reported for other neuronal cultures, and PEDF trophic effects have also been observed in RPE or Müller cells (Jablonski et al., 2001; Houenou et al., 1999; Malchiodi-Albedi et al., 1998). Due to the links that exist between differentiation and survival

mechanisms, PEDF has extensively been tested for its neuroprotective properties in several conditions of neuronal injury. PEDF demonstrated to increase neuronal survival in ischemic retinas (Stellmach et al., 2001; Takita et al., 2003), in axotomized motor neurons (Houenou et al., 1999) and in neurons exposed to high glutamate or H_20_2 (Cao et al., 1999; Taniwaki et al., 1995). PEDF has also been tested in retinal neurodegeneration models, such as in the rd mutant mice, in rats exposed to constant bright light and in Royal College Surgeon rats (Murakami et al., 2008; Cao et al., 2001; Cayouette et al., 1999).

8.2. ANTIANGIOGENIC PROPERTIES OF PEDF

In addition to its neurotrophic properties, PEDF has also been described as a potent anti-angiogenic factor (Dawson, 1999). PEDF inhibits the migration and proliferation of endothelial cells, and induces their apoptosis only if endothelial cells are activated (Volpert et al., 2002). In addition, PEDF expression is lost or down-regulated in several types of tumours; this decrease is associated with increased metastatic activity (Doll et al., 2003; Crawford et al., 2001; Takenaka et al., 2005; Uehara et al., 2004). Besides the indirect influence of PEDF on tumour growth and metastatic potential achieved through the reduction of vascular support, a direct pro-apoptotic effect of PEDF on tumour cells has also been reported (Broadhead et al., 2009). This action is probably mediated by de Fas/FasL ligand (Broadhead et al., 2009). In the eye, PEDF is thought to be the major anti-angiogenic factor, contributing to the maintenance of the avascularity of ocular tissues (Bouck, 2002). The unbalance between intraocular PEDF and VEGF levels has been associated with risk of

neovascularization in diabetic retinopathy (Ogata et al., 2002; Funatsu et al., 2006). Retinal overexpression of PEDF counteracts neovascularisation in animal models (Mori et al., 2002c; Raisler et al., 2002).

8.3. MOLECULAR ACTIONS OF PEDF

The molecular mechanism by which PEDF exerts its multiple actions has not been completely elucidated yet. It is not known if the neuroprotective and the antiangiogenic properties are induced via the same receptor or through the activation of different receptors (Filleur et al., 2009). Another possibility that could explain this multi-functionality would be the interaction with the receptor of separate domains of the protein, such as the 44-mer peptide linked with neuroprotection and the 34-mer peptide involved in anti-angiogenesis, to mediate different effects (Meyer et al., 2002). The phosphorylation state of PEDF has also been associated with differential activity (Maik-Rachline and Seger, 2006).

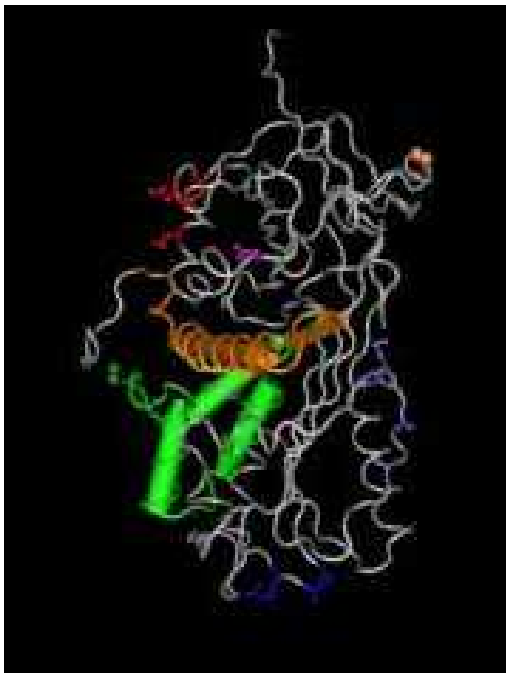

Figure 16. 3D structure of PEDF depicting structural components associated to specific functions. The 34-mer peptide region associated with antiangiogenesis (green) and the 44-mer peptide region associated with neuroprotection (orange) are shown in tube representations. The acidic residues required for collagen binding (red), the basic residues required for heparin binding (blue), and the phosphorylation sites Ser114 and Ser227 (green and orange, respectively) are also shown. Adapted from Broadhead et al. 2010.

In 2006, a phospholipase membrane protein was identified as a specific receptor for PEDF in RPE and hepatocytes (Notari et al., 2006). It has been proposed that the phospholipase activity of the PEDF-R may release several types of lipid mediators that could mediate neurotrophic, anti-angiogenic or anti-tumorigenic actions (Notari et al., 2006). However, in 2009, Bernard and colleagues reported the existence of a 60 kDa receptor in endothelial cells, which is activated after interaction with the 34-mer region of PEDF and mediates apoptosis and inhibition of migration in endothelial cells (Bernard et al., 2009).

Despite the fact that the characterization of the PEDF receptor remains elusive, it is known that the neuroprotective effects of PEDF are mediated by the activation of NF-kB, which in turn induces the expression of genes involved in survival, such as Bcl-2 (Yabe et al., 2001). The mechanisms underlying the anti-angiogenic actions of PEDF are also under intense study. Evidence suggests that the antiangiogenic effects of PEDF may rely on the disruption of VEGF signalling, by either impairing VEGF binding to VEGF-R2 (Wang et al., 2006b) or by degrading VEGF-R1, preventing signalling down this receptor (Cai et al., 2006). Moreover, it has been reported that the Fas/FasL pathway is

responsible for the PEDF-mediated induction of apoptosis in proliferating endothelial cells, which are Fas positive (Volpert et al., 2002).

8.4. PRECLINICAL STUDIES BASED ON PEDF OVEREXPRESSION

The *in vivo* studies in which recombinant PEDF was administered intraocularly for the treatment of induced or inherited neuronal death have been useful as first proof-of concept of PEDF actions, but the window of neuroprotection was very limited due to the rapid clearance of PEDF in the eye (Barnstable and Tombran-Tink, 2004). To ensure long-term expression and effects on neurodegeneration and/or neovascularization several gene therapy approaches based on ocular PEDF overexpression have been developed. Adenoviral or lentiviral vectors encoding PEDF have demonstrated effective neuroprotection in the ischemia-reperfusion mouse model and in RCS rats, respectively (Takita et al., 2003; Murakami et al., 2008). The intravitreal administration of Ad-PEDF vectors has been tested to achieve inhibition of ocular neovascularization in several mouse models, such as the oxygen-induced retinopathy model, the laser-induced choroidal neovascularization model and a transgenic model overexpressing VEGF in photoreceptors (Mori et al., 2001). Choroidal neovascularisation was also inhibited after periocular administration of PEDF-enconding vectors in both mice and pigs (Saishin et al., 2005; Gehlbach et al., 2003). AAV vectors carrying the PEDF gene have also proven successful in counteracting neovascularization in mouse models of neovascularization, such as the oxygen-induced retinopathy model and the

laser-induced choroidal neovascularization model (Mori et al., 2002c; Raisler et al., 2002).

8.5. CLINICAL USE OF PEDF

The promising results obtained in the preclinical studies using Ad-PEDF for the treatment of choroidal neovascularization (Mori et al., 2001, 2002a; Gehlbach et al., 2003; Saishin et al., 2005) led to the development of a clinical protocol for neovascular age-related macular degeneration (AMD). As previously described, 28 patients with advanced neovascular AMD refractive to standard treatment were enrolled in a PI/II dose-escalating trial (Campochiaro et al., 2006). After the intravitreal administration of Ad-PEDF, no serious adverse effects were observed for any of the doses tested and patients treated with the highest dose showed mild improvement or stabilization of the neovascular lesions in the 12 months follow-up (Campochiaro et al., 2006), confirming the antiangiogenic potential of PEDF-based therapies for the treatment of ocular neovascularization. This clinical study has not been continued, due to the transient expression of the gene of interest mediated by Ad vectors, and the impossibility of re-administration imposed by the immune responses developed against the Ad vectors that could put into risk the initial beneficial effects of the therapy (Campochiaro et al., 2011).

9. TOWARDS NEW THERAPIES FOR DIABETIC RETINOPATHY

As previously stated, the treatment of diabetic retinopathy is still an unmet medical need. Standard clinical practises, such as laser therapies or vitrectomy, only provide palliative solutions to diabetic retinopathy which are unable to halt the progression of the disease. The development of new, effective therapeutic approaches is highly necessary. Nevertheless, a full characterization of the molecular mechanisms underlying diabetic retinopathy is required to identify new targets. Although it has been classically diagnosed as a vascular pathology, the potential contribution of neuronal and glial alterations to the development of retinopathy in human diabetic patients has been extensively discussed (Antonetti et al., 2006; Shirao et al., 1998; Mizutani et al., 1998; Curtis et al., 2011) and it is not fully understood. However, the lack of suitable animal models precludes proper investigations and testing of experimental drugs for diabetic retinopathy.

Diabetic rodents do not develop advanced stages of retinopathy. Only Torii rats present proliferative retinopathy in very long-lived animals (Yamada et al., 2005). For this reason, non-diabetic models in which retinal neovascularization is experimentally induced, such as the oxygen-induced retinopathy (OIR or ROP) models, have been widely used for testing anti-proliferative drugs (Smith et al.,1994; Penn et al., 1993). However, early neovessel regression occurs in these animals (Smith et al.,1994; Penn et al., 1993), making them not suitable for long-term evaluation of new therapeutics. In contrast, despite not being hyperglycaemic, TgIGF-I mice develop most of the

vascular alterations present in diabetic retinas, with a progressive evolution resembling that of the human disease (Ruberte et al., 2004; Haurigot et al., 2009). In addition to its well-described vascular pathology, neurons and glial cells are probably affected in TgIGF-I retinas and may participate in the progression of the vascular alterations. A comprehensive characterization of the pathology underlying the ocular phenotype of TgIGF-I mice could contribute to the understanding of the molecular mechanisms that lead to proliferative retinopathy. In addition, the study of the non-vascular alterations present in TgIGF-I retinas would reinforce the value of this model as a model of retinopathy, allowing the assessment of new therapies aimed at counteracting proliferative retinopathies.

Pre-clinical and clinical studies have proven gene therapy successful in the treatment of retinal diseases, specially in chronic pathologies that require continuous delivery of therapeutic agents (Bainbridge et al., 2008; Hauswirth et al., 2008; Maguire et al., 2008). Gene transfer of antiangiogenic agents may then be a promising therapy to counteract proliferative retinopathy. In this regard, the testing in TgIGF-I retinas of a therapeutic approach based on AAV-mediated long-term overexpression of the antiangiogenic and neuroprotective factor PEDF is proposed.

III. Objectives

The currently available treatments for diabetic retinopathy are invasive and only partially efficacious. The development of new effective therapies requires further investigations on disease pathogenesis. Appropriate animal models are essential to elucidate the mechanisms leading to retinopathy and to assay the potential efficacy of innovative therapies.

Therefore, using the TgIGF-I mouse as a model, the ***general aim*** of this work was to ***determine the molecular mechanisms responsible for the development of retinal alterations leading to proliferative retinopathy, as a key step towards the development of effective therapies for diabetic retinopathy***. This general aim was divided into two specific aims:

1. To examine the development and progression of early, non-vascular alterations in TgIGF-I retinas. This study can be divided in two parts:

1.1. To analyze neurological function in TgIGF-I retinas

1.2. To determine glial alterations in TgIGF-I retinas

2. To evaluate the long-term efficacy of AAV-mediated overexpression of the anti-angiogenic and neuroprotective factor PEDF in counteracting proliferative retinopathy in TgIGF-I mice.

IV. Results and Discussion

Part I: Characterization of Neuroglial Alterations In Retinas Overexpressing IGF-I

Recent clinical evidence has placed the focus on the non-vascular aspects of diabetic retinopathy, especially those affecting neuronal functionality, and studies in patients and several different animal models of diabetes have demonstrated the presence of neurodegeneration before the onset of serious vascular disease.

Transgenic mice overexpressing IGF-I in the retinas present vascular alterations that progress as animal age from non-proliferative to proliferative disease, with development of intrareptinal and intravitreal neovascularization, making these mice an excellent animal model of proliferative vascular retinopathy (Ruberte et al., 2004). In addition to neovascularization, gliosis, inflammation and disruption of the BRB have also been described in this model (Ruberte et al., 2004; Haurigot et al., 2009).

Whether the retinas of Tg-IGF-I develop neurophysiological alterations and their impact on disease progression remains to be determined. In order to study this, the first part of the study analyzed the temporal evolution (from 1.5 to 7.5 months of age) of neuronal and glial changes in TgIGF-I retinas, attempting to determine the sequence of pathological events that occur in TgIGF-I mice previous to overt vascular alterations.

1. STUDY OF NEURONAL FUNCTIONALITY IN TgIGF-I RETINAS

1.1. ASSESSMENT OF NEURONAL FUNCTION

To determine the neurophysiological activity of the retina of the TgIGF-I mice, electroretinographic recordings were obtained. The technique of electroretinography (ERG) allows the recording of post-stimulo electrical activity in the retina with an active electrode positioned in the cornea of the animal. This electrode is usually a metal wire that forms a loop and contacts the center of the mouse eye. When stimulated with light, changes in retinal potential take place as a consequence of neuronal electrical activity within the retina, resulting in complex responses with two primary components, the a-wave and the b-wave. Photoreceptor hyperpolarization is reflected by the negative a-wave, caused by light absorption in the photoreceptor outer segments and closure of cGMP-gated channels (Robson and Frishman, 1998). Under dark-adapted conditions, the response of rod photoreceptors dominates the a-wave, while under light-adapted conditions this component reflects only cone photoreceptor responses. Following the a-wave, the positive b-wave represents the activity of depolarizing bipolar cells (Robson and Frishman, 1998). In the transition between the a and the b wave, six oscillations corresponding to the oscillatory potentials (OPs) are observed in the mouse ERG, which reflect the activity of amacrine and other INL neurons (Wachtmeister, 1998) (Scheme 1).

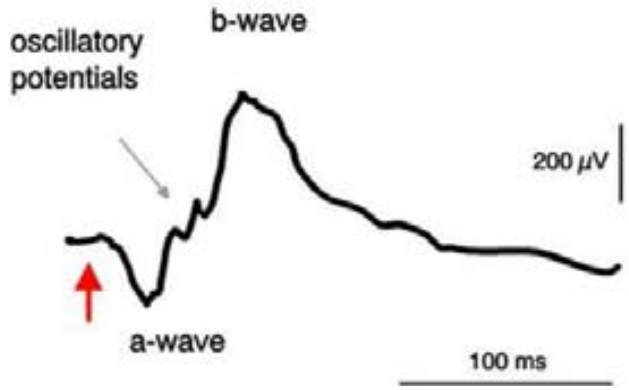

Scheme 1. Schematic representation of an ERG recording obtained from a mouse. The different waves reflect the activity of different retinal neuronal types. Adapted from Fletcher et al.2005.

1.1.1. ERG responses at 3 months of age

Standard protocols from ISCEV (International Society for the Clinical Electrophysiology of Vision) were followed. The maximum amplitude of each wave was measured and averaged in each experimental group tested. The rod-driven circuitry was tested under scotopic conditions stimulating with low-light intensities, at which only rod photoreceptors are able to react. Scotopic threshold response (STR) is the most sensitive waveform, induced with very dim light stimuli (-4log cd·s/m^2). In mice, it is composed of a small amplitude positive potential. First, 3 month-old Wt and TgIGF-I mice were analyzed (the STR is indicated by a bidirectional arrow in Figure 1a, arrow). With higher light stimuli but still under cone stimulation threshold (-2log cd·s/m^2), the scotopic b-wave reflecting rod activity was also obtained and measured (Figure 1b, arrow). Mixed responses (rod and cones) in scotopic conditions were evoked using stimuli of high intensity (1.5log cd·s/m^2), where both a-waves (negative wave in, Figure 1c, indicated by a bidirectional green arrow) and b-waves (from bottom

of the a-wave to maximum of the b-wave, Figure 1c, indicated by a bidirectional blue arrow) were observed and quantified. Oscillatory potentials were recorded at the same light intensity that the mixed responses but changing the frequency of the analyzer (Figure 1d). After light adaptation, photopic activity, exclusively driven by cones, was studied using high, rod-saturating light intensities. As in scotopic conditions, no a-wave was observed in these responses. Photopic b-wave amplitude was determined after a stimuli of 2log cd·s/m^2 (Figure 1e, arrow). The flicker test was performed with a frequency of 20Hz and the maxim amplitude of waves was measured (Figure 1f, arrow). At 3 months of age, transgenic mice did not show any differences in comparison with Wt littermates in the amplitudes of the responses in any of the tests performed, neither in scotopic nor in photopic conditions with different light intensities (Figure 1g).

Figure 1. Electroretinographic responses in Wt and TgIGF-I mice aged 3 months. Average ERG recordings from Wt (black line) and TgIGF-I (pink line) mice at 3 months of age. Each graph corresponds to a different ISCEV protocol, with specific settings that induce the response of different neuronal types. Arrows indicate the amplitudes measured in each test. **(a)** STR wave, that allows the analysis of highly sensitive responses in rod photoreceptors; **(b)** scotopic b-wave, for testing rod responses; **(c)** mixed scotopic response, resulting form the stimulation of both rods and cones under scotopic conditions; **(d)** oscillatory potentials, that measure the activity of INL neurons; **(e)** photopic b-wave, for testing of cone responses; **(f)** flicker response, repetitive photopic stimulations for analysis of cone's recovery. **(g)** Histogram representation of the amplitude of the averaged responses obtained in a-f. Transgenic mice showed responses similar to those of Wt mice, indicating they had preserved visual function at this age. Values are expressed as the mean ±SEM of 7 animals/group.

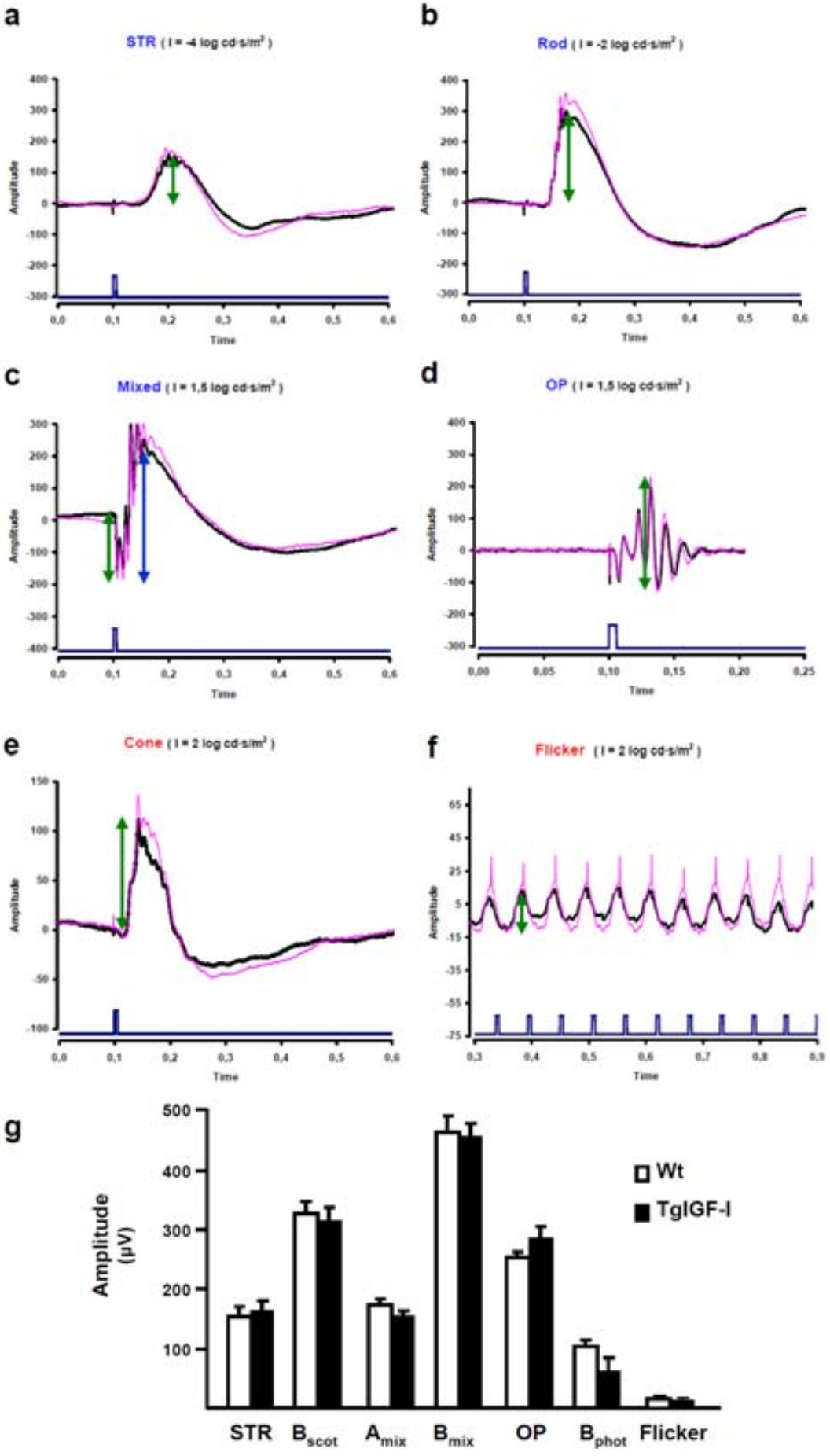
a
STR (I = -4 log cd·s/m²)
b
Rod (I = -2 log cd·s/m²)
c
Mixed (I = 1,5 log cd·s/m²)
d
OP (I = 1,5 log cd·s/m²)
e
Cone (I = 2 log cd·s/m²)
f
Flicker (I = 2 log cd·s/m²)
Amplitude
Time
g
Amplitude (µV)
Wt
TgIGF-I
STR
B scot
A mix
B mix
OP
B phot
Flicker

1.1.2. ERG responses at 6 months of age

At 6 months of age, responses were heterogeneous. Some TgIGF-I retinas showed reduced amplitudes in all conditions, whereas others had totally normal responses (Figure 2), demonstrating a great variability in recorded responses at this age.

Figure 2. Electroretinographic responses in 6 month-old Wt and TgIGF-I mice. ERG from Wt and TgIGF-I mice at 6 months of age. Recordings from Wt animals were averaged (black line). Recordings from TgIGF-I are depicted individually (colored lines). Each plot corresponds to a different ISCEV protocol, with specific settings that measure the response of different neuronal types. **(a)** STR (rod photoreceptors), **(b)** scotopic b-wav (rod responses) **(c)** mixed scotopic (stimulation of rods and cones under scotopic conditions), **(d)** oscillatory potentials (INL neuron activity) **(e)** photopic b-wave (cones); **(f)** flicker, repetitive photopic stimulations (cone recovery). A few transgenic mice presented a marked reduction in retinal responses in all tests performed, whereas others showed normal responses. **(g)** Quantification of the amplitude of the responses obtained in the ERG recordings. The averaged amplitude of the different parameters recorded showed non-statistically significant differences between 6 month-old Wt and transgenic mice. Values are expressed as the mean ±SEM of 7-9 animals/group.

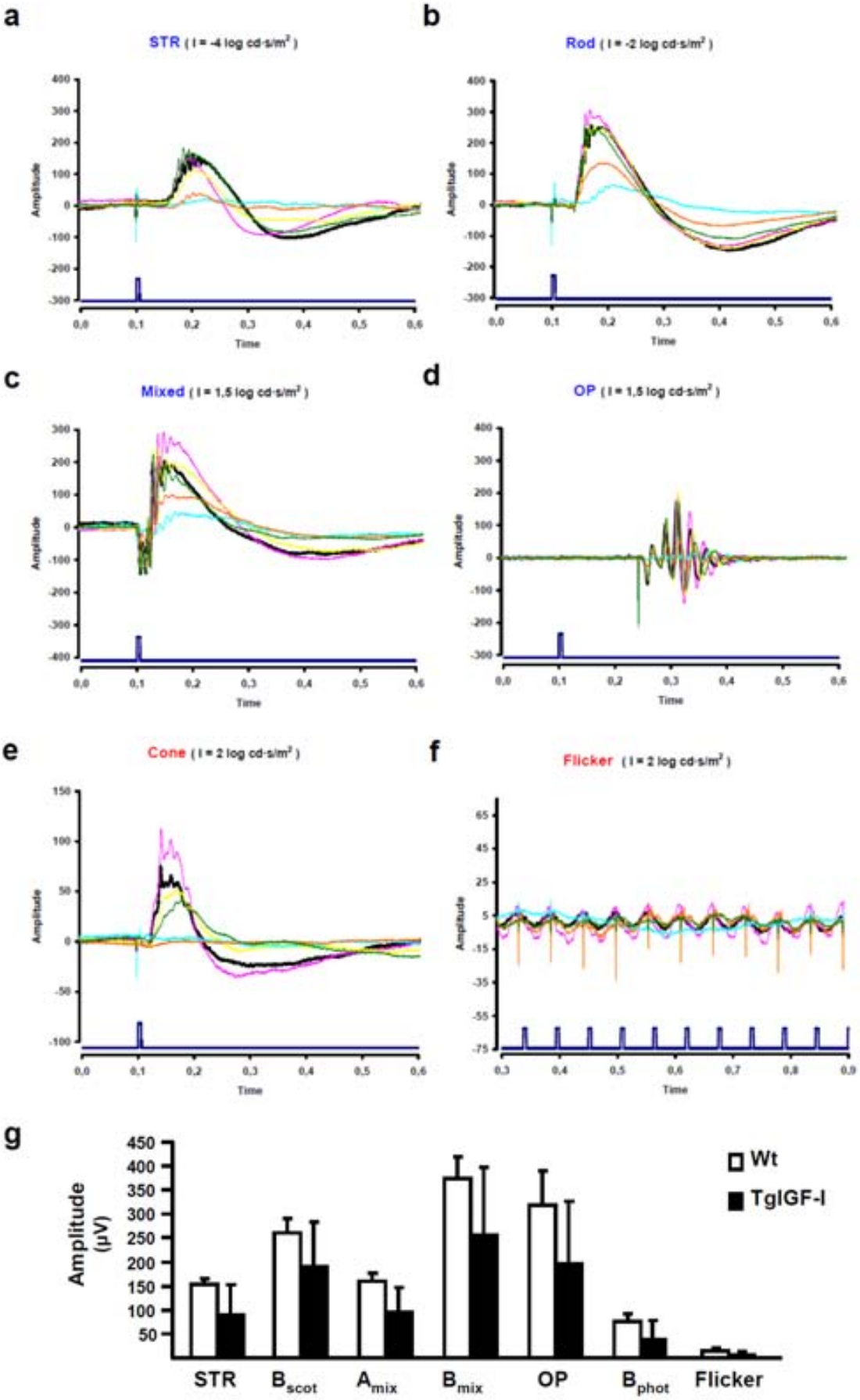
a
STR (I = -4 log cd·s/m²)
b
Rod (I = -2 log cd·s/m²)
c
Mixed (I = 1,5 log cd·s/m²)
d
OP (I = 1,5 log cd·s/m²)
e
Cone (I = 2 log cd·s/m²)
f
Flicker (I = 2 log cd·s/m²)
Amplitude
Time
g
Amplitude (µV)
Wt
TgIGF-I
STR
B scot
A mix
B mix
OP
B phot
Flicker

1.1.3. ERG responses at 7.5 months of age

The alterations in the electrophysiological responses in TgIGF- I retinas became clearly apparent at 7.5 months, with statistically significant differences between Wt and TgIGF-I in all parameters measured (Figure 3). However, there still existed some variability in the degree of reduction in the amplitudes recorded for individual transgenic animals, suggesting differences in the rate of evolution of the pathology.

Figure 3. Electroretinographic responses in Wt and TgIGF-I mice at 7.5 months of age. ERG responses from 7.5 month-old Wt and TgIGF-I mice. Each plot corresponds to a different ISCEV protocol, with specific settings that induced the response of different neuronal types. **(a)** STR (rod photoreceptors), **(b)** scotopic b-wave (rod responses) **(c)** mixed scotopic, (stimulation of rods and cones under scotopic conditions), **(d)** oscillatory potentials (INL neuron activity) **(e)** photopic b-wave (cones); **(f)** flicker, repetitive photopic stimulations (cone recovery) The black line represents the average response of Wt animals, whereas colored lines represent individual recordings obtained for transgenic mice. At this age, all transgenic mice showed reduced responses compared with age-matched Wt littermates, with different degrees of reduction among individual transgenic animals. **(g)** Statistically significant differences were observed in the averaged amplitudes obtained for all tests performed in transgenic and Wt mice at 7.5 months of age. Values are expressed as the mean ±SEM of 5 animals/group. $p^{*}<0.05$, $p^{**}<0.01$

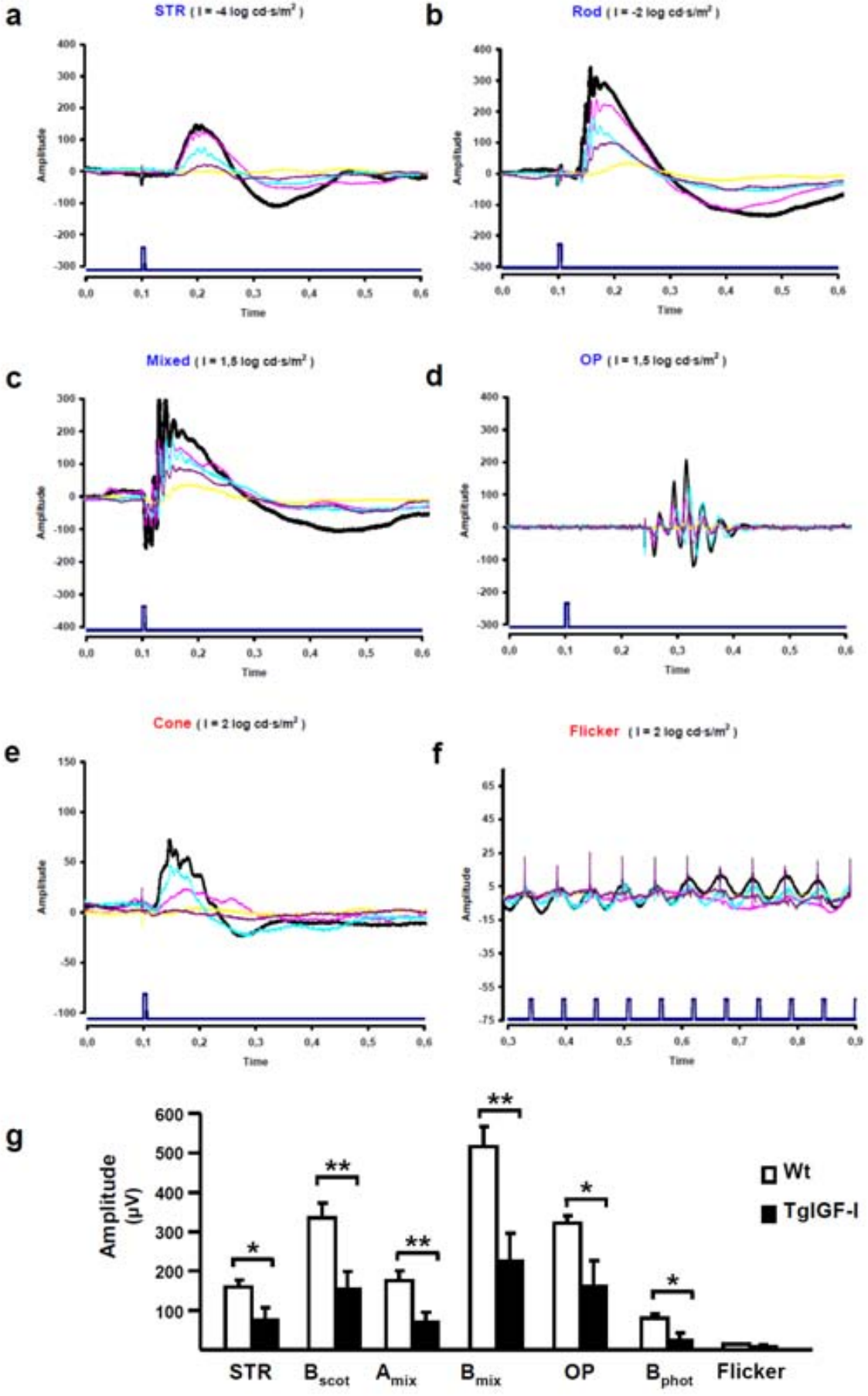
a
STR (I = -4 log cd·s/m²)
b
Rod (I = -2 log cd·s/m²)
c
Mixed (I = 1,5 log cd·s/m²)
d
OP (I = 1,5 log cd·s/m²)
e
Cone (I = 2 log cd·s/m²)
f
Flicker (I = 2 log cd·s/m²)
Amplitude
Time
g
Amplitude (µV)
Wt
TgIGF-I
STR
B scot
A mix
B mix
OP
B phot
Flicker

1.1.4. ERG responses at 9 months of age

By 9 months of age, the ERG responses recorded in all transgenic mice were reduced by approximately 80% (Figure 4).

Figure 4. Electroretinographic responses in Wt and TgIGF-I mice at 9 months of age. ERG responses from 9 month-old Wt (black line) and TgIGF-I (pink line) mice. Each plot corresponds to a different ISCEV protocol, with specific settings that induced the response of different neuronal types. **(a)** STR (rod photoreceptors), **(b)** scotopic b-wav (rod responses) **(c)** mixed scotopic, (stimulation of rods and cones under scotopic conditions), **(d)** oscillatory potentials (INL neuron activity) **(e)** photopic b-wave (cones); **(f)** flicker, repetitive photopic stimulations (cone recovery). Lines represent the averaged response of 5 animals per group. ERG recordings showed that the neurophysiologic activity in transgenic retinas of 9 month-old mice was reduced by 80% of normal in all parameters analyzed **(g)** The quantification of amplitudes revealed a marked impairment of neuronal activity in transgenic retinas at this age. Values are expressed as the mean ±SEM of 5 animals/group. p*<0.05, p**<0.01

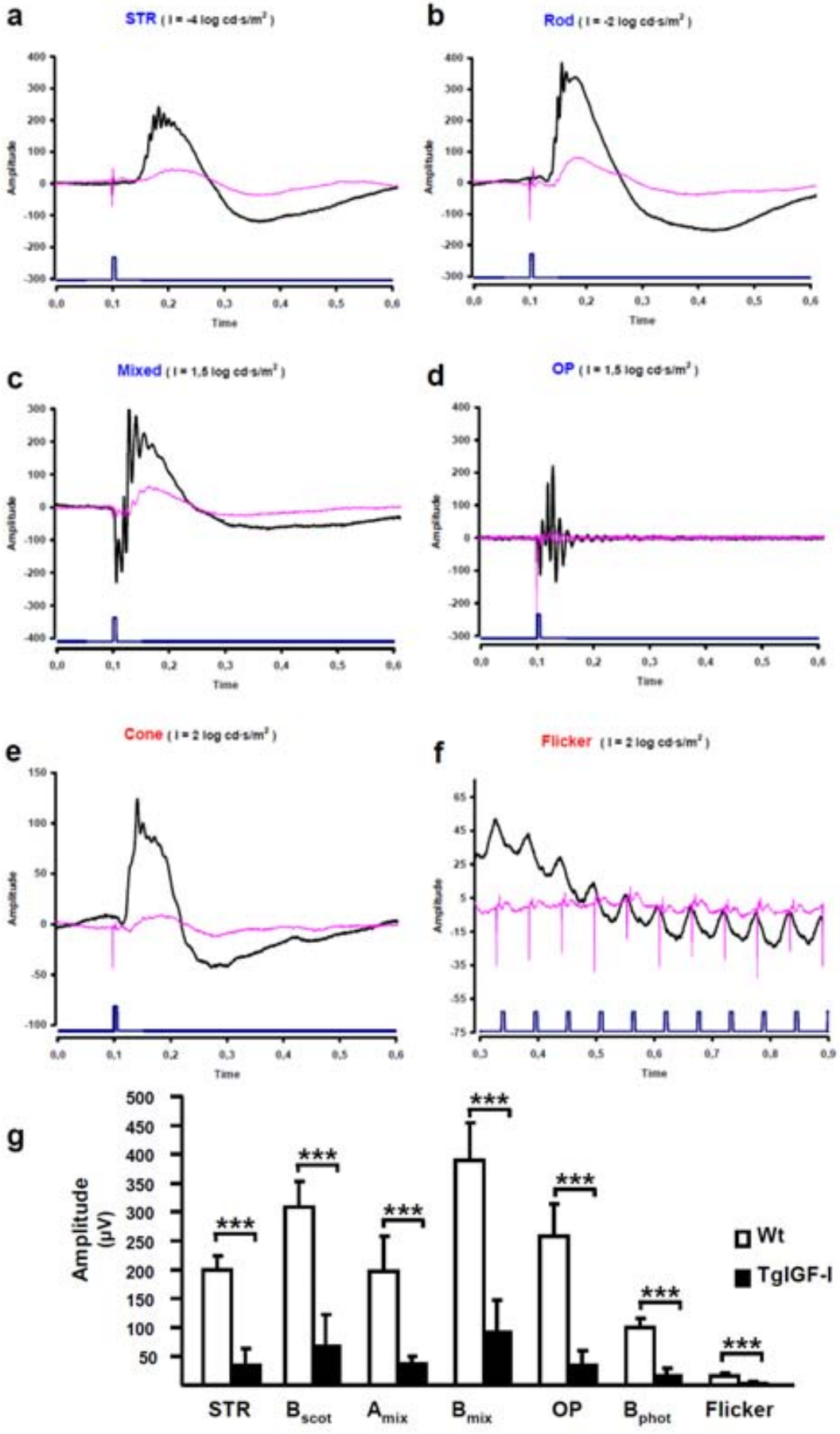
a
STR (I = -4 log cd·s/m²)
b
Rod (I = -2 log cd·s/m²)
c
Mixed (I = 1,5 log cd·s/m²)
d
OP (I = 1,5 log cd·s/m²)
e
Cone (I = 2 log cd·s/m²)
f
Flicker (I = 2 log cd·s/m²)
Amplitude
Time
g
Amplitude (µV)
***
Wt
TgIGF-I
STR
B scot
A mix
B mix
OP
B phot
Flicker

1.1.5. Chronological progression of ERG responses in TgIGF-I

The progression of retinal neurological dysfunction in TgIGF-I mice is represented in Figure 5, which shows the decline in all recorded parameters as transgenic mice aged, with statistically significant differences emerging at 7.5 months of age. These results demonstrated the progressive nature of retinal neurodegeneration in transgenic mice overexpressing IGF-I in the retina and suggested it paralleled the evolution of vascular alterations in this model. At three months of age, transgenic mice only present mild vascular alterations (increased vascular permeability and pericyte loss) and neovascularization is overt in animals aged more that 6 months (Ruberte et al., 2004).

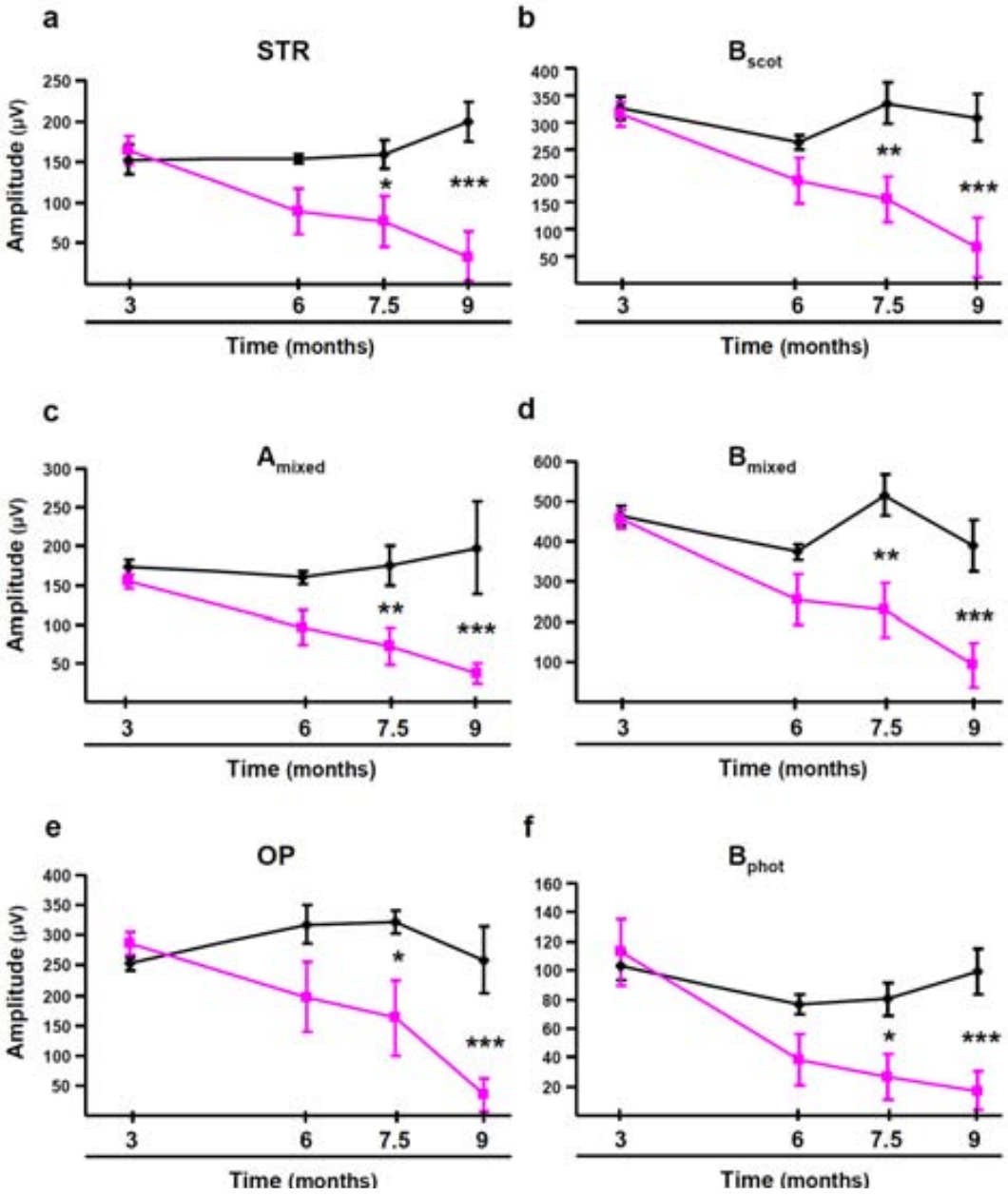

Figure 5. Progressive alteration of electroretinographic responses in TgIGF-I mice. With age, TgIGF-I mice (pink lines) showed a progressive decline in the amplitudes of responses to all ERG stimuli with respect to healthy littermates (black line): **(a)** STR, for analyzing high sensitive responses of rod photoreceptors; **(b)** scotopic b-wave, for testing rods response; **(c)** mixed scotopic, from stimulation of both rod and cones under scotopic conditions; **(d)** oscillatory potentials, that measure INL neuronal activity; **(e)** photopic b-wave, for testing cone responses; **(f)** flicker, repetitive photopic stimulations for analyzing cone recovery. These were statistically significant reductions in the responses in animals aged more than 7.5 months. Values are expressed as the mean ±SEM of 5-9 animals/group. p*<0.05, p**<0.01, p***<0.01

1.2. ANALYSIS OF NEURONAL POPULATIONS IN TgIGF-I RETINAS

The alterations observed in the electrophysiological responses in TgIGF-I mice were progressive and affected both rod and cone-driven visual pathways, suggesting that more than one type of neuron was affected in transgenic retinas. The retina is organized in a very specific arrangement of cells, with different neuronal types located in different nuclear layers. Thus, the thickness of each of these layers can be used as an indicator of the loss of one or a few specific cell types.

The ONL and INL thickness were analyzed in both peripheral and central retina (in retinal sections showing the optic nerve) stained with DAPI (nuclear marker) in Wt and TgIGF-I retinas (Figure 6a). In agreement with the functional observations, at 3 months of age, TgIGF-I retinas did not present any differences in the thickness of the retinal layers when compared with age-matched wild-type retinas (Figure 6b). A slight, non-statistically significant decrease was observed in 6 month-old animals, mainly in the ONL (Figure 6c). At 7.5 months of age, the retinas from TgIGF-I mice were clearly thinner than wild-type retinas, with a statistically significant reduction in both ONL and INL width (Figure 6d). These observations suggested that both photoreceptor and INL neuronal populations were altered in TgIGF-I at this age.

Figure 6. Thickness of the different retinal layers in mice overexpressing TgIGF-I in the eye. (a) Representative image of a retinal section that includes the optic nerve (arrows). Bidirectional arrows in the inset indicate how the measurement of the thickness of the layer was performed. Nuclei were stained with DAPI (blue). **(b-d)** The thickness of retinal layers was measured at (b) 3, (c) 6 and (d) 7.5 months of age. At 3 and 6 months of age there were no differences in the thickness of retinal layers when compared to Wt. At 7.5 months of age, retinal layers were clearly thinner in TgIGF-I mice when compared with Wt retinas, with statistically significant reductions in both ONL and INL thickness in both the central and the peripheral retina. Values are expressed as the mean ±SEM of 5-9 animals/group. p*<0.05, p**<0.01. Scale bar: 35.51 µm.

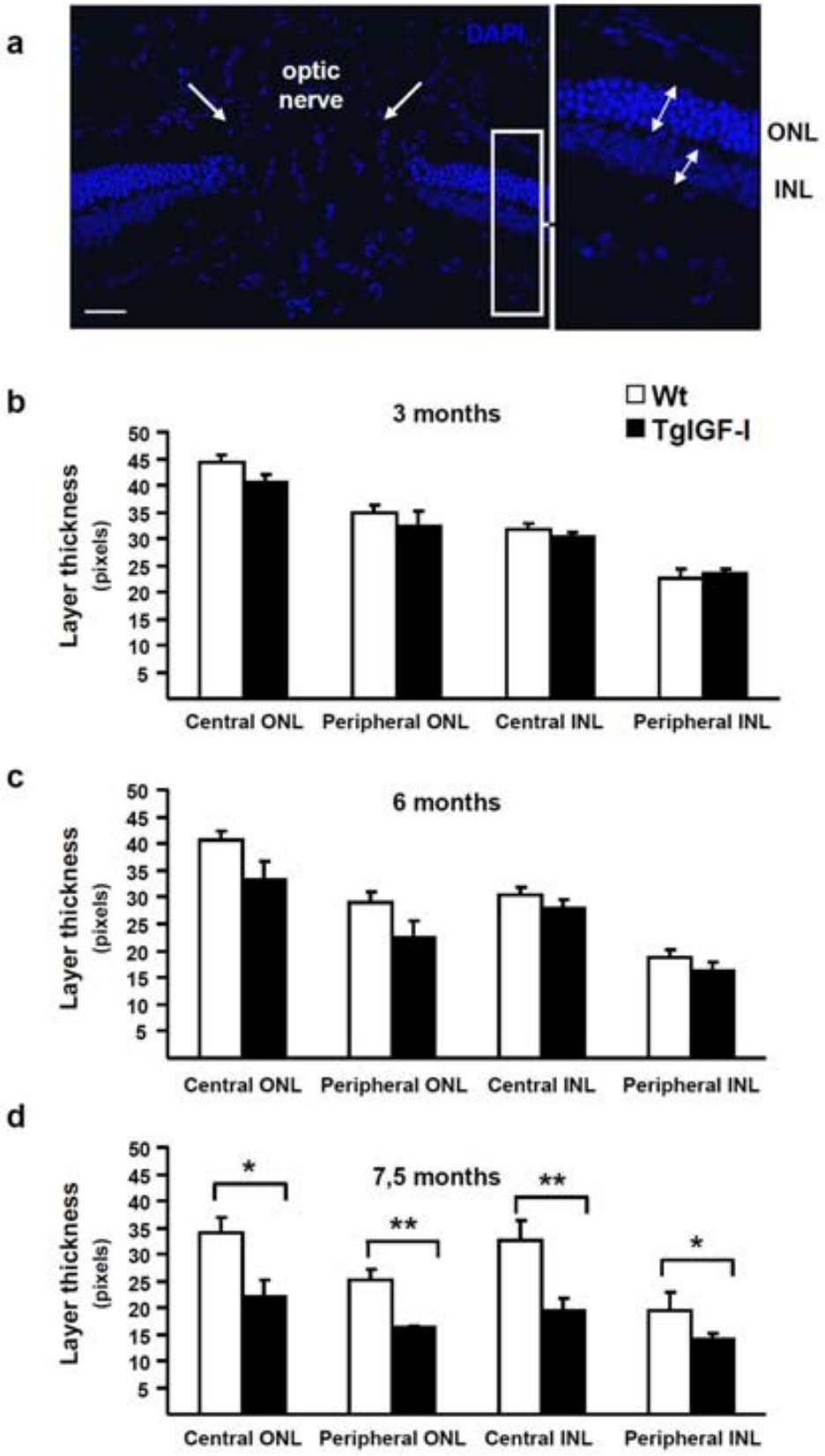
a
DAPI
optic nerve
ONL
INL
b
3 months
Wt
TgIGF-I
Layer thickness (pixels)
50
45
40
35
30
25
20
15
10
5
Central ONL
Peripheral ONL
Central INL
Peripheral INL
c
6 months
Layer thickness (pixels)
Central ONL
Peripheral ONL
Central INL
Peripheral INL
d
7,5 months
*
**
**
*
Layer thickness (pixels)
Central ONL
Peripheral ONL
Central INL
Peripheral INL

1.2.1. Analysis of rod photoreceptors

The observation that retinal layers thinned with age suggested that neurons from TgIGF-I retinas were progressively dying. To elucidate which type of neurons were degenerating, specific markers were used to detect and quantify different neuronal populations in the retina. Rhodopsin is synthesized in the inner segment (IS) of rod photoreceptor cells and then transported to the outer segment (OS), where it plays a key role in visual phototransduction (Terakita et al., 2005).

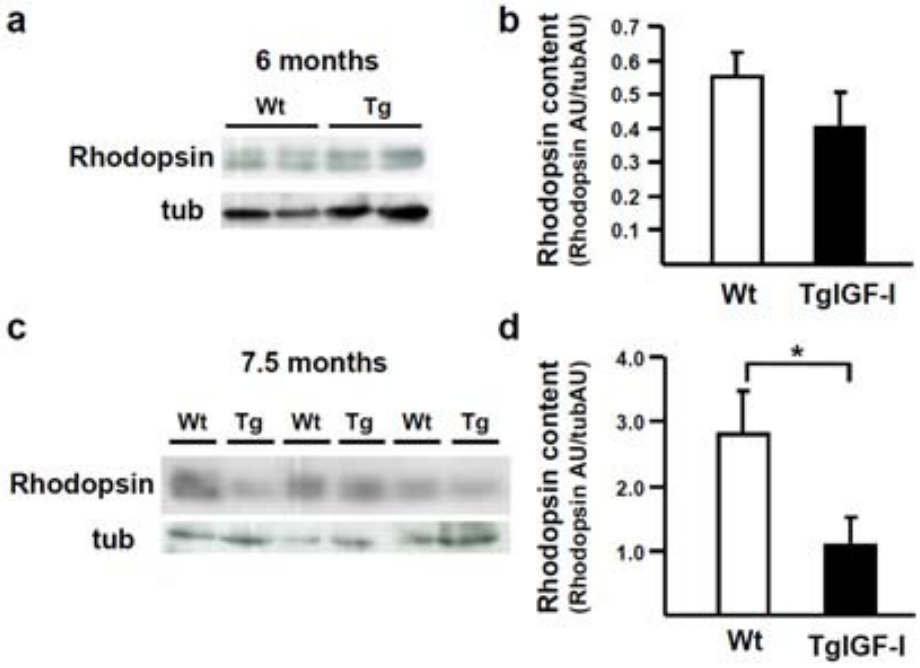

Figure 7. Rhodopsin content in Wt and TgIGF-I retinal extracts. Representative blots **(a,c)** and quantification **(b,d)** of rhodopsin in 6 month-old and 7.5 month-old Wt and TgIGF-I retinas after load normalization by tubulin levels. Rhodopsin content was significantly reduced in TgIGF-I retinas from 7.5 month-old but not 6 month-old mice. AU: arbitrary units. Tubulin immunoblotting served as loading control. Values are expressed as the mean ±SEM of 5 animals/group. p*<0.05

Rhodopsin is then considered a specific marker of rods. Total retinal rhodopsin levels were determined by Western blot in 6 and 7.5 month-old mice. Although a tendency towards decreased content of rhodopsin was observed at 6 months of age, a significant reduction in the content of retinal rhodopsin was only observed in mice of 7.5 months of age (Figure 7). This reduced rhodopsin content observed in 7.5 month-old transgenic mice was in agreement with the reduction in the length of the photoreceptor outer segments in transgenic mice, determined by morphometric analysis on central retina sections immunostained for rhodopsin (Figure 8).

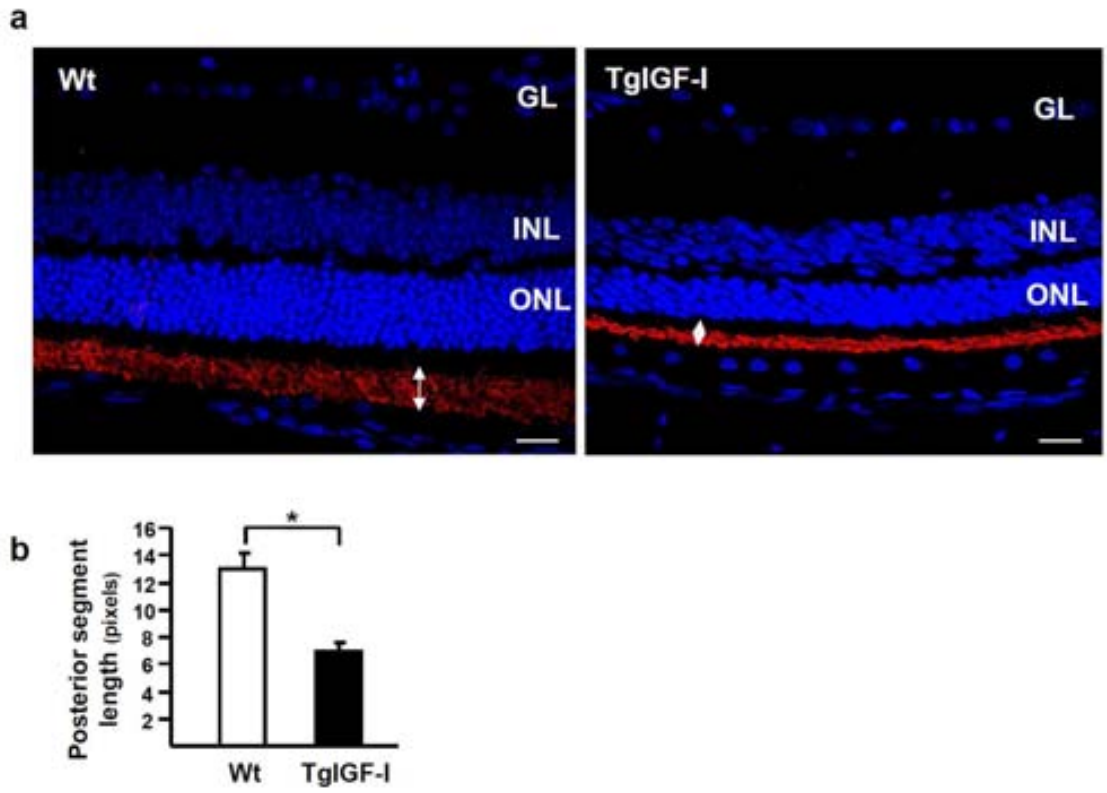

Figure 8. Morphometric quantification of the length of photoreceptor outer segments in Wt and TgIGF-I retinas. (a) Rhodopsin immunelabelling (red) in retinal sections from Wt and transgenic mice, showing positive staining in the outer segment (OS) of photoreceptors. **(b)** OS length (arrows) was measured in medial retinal sections. The length of the OS was significantly reduced in transgenic retinas when compared with Wt littermates at 7.5 months of age. Nuclei were stained with DAPI (blue). Values are expressed as the mean ±SEM of 5 animals/group. p*<0.05. Scale bar: 18.37 µm.

1.2.2. Analysis of cone photoreceptors

Cone photoreceptors are also located in the ONL and can be specifically detected with antibodies recognizing arrestin (Fujimaki et al., 2004). Arrestin content was studied in protein extracts of Wt and TgIGF-I mice at 7.5 months of age. There were no differences in the levels of arrestin between Wt and TgIGF-I retinas (Figure 9), suggesting that cone photoreceptors were not altered in transgenic retinas at this age.

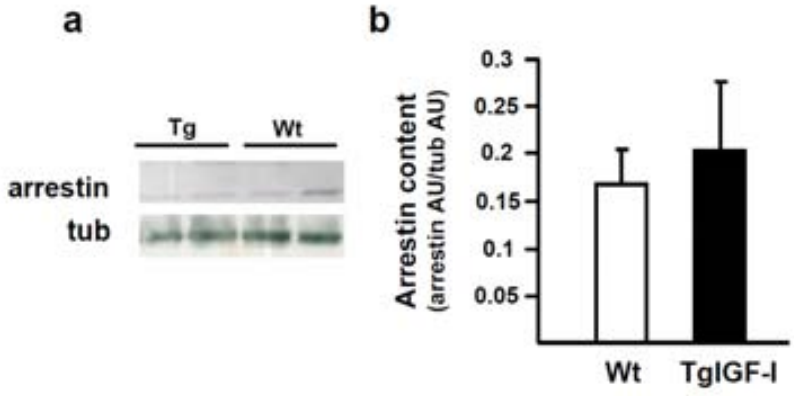

Figure 9. Arrestin content in Wt and TgIGF-I retinal extracts. (a) Western blot analysis and **(b)** densitometry quantification showing no differences in the retinal content of arrestin between Wt and TgIGF-I retinas at 7.5 months of age. Normalization by tubulin corrected for unequal sample loading. AU: arbitrary units. Values are expressed as the mean ±SEM of 5 animals/group.

This result suggested that the reduction in the thickness of the ONL (Figure 6), indicative of cell number, observed in TgIGF-I retinas at 7.5 months of age was most likely due to the loss of rod but not cone photoreceptors. Moreover, cone photoreceptors represented less than 5% of total photoreceptors in the mouse retina. In addition to the reduction in rod numbers, the alteration of the length of the OS evidenced the presence of structural alterations in the cell architecture that could impact neuronal functionality.

1.2.3. Analysis of bipolar cells

Bipolar cells are INL second-order neurons that receive input from photoreceptors and transmit it to ganglion cells. They specifically express the protein kinase C alpha (PKCα) (Grunert et al., 1994). When analysed by Western Blot, a lower amount of PKCα was observed in retinal extracts from transgenic mice as early as 3 months of age (Figure 10). This decrease was also observed in samples from animals aged 6 months.

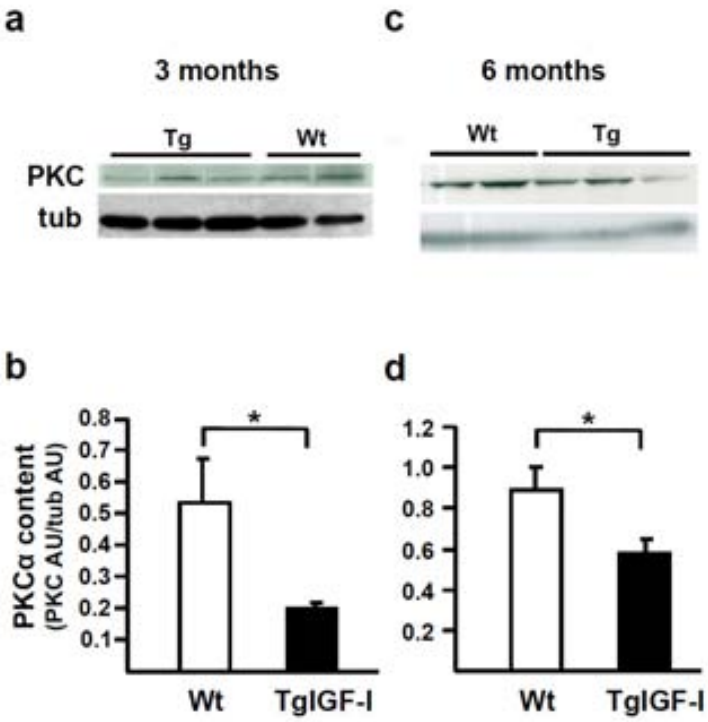

Figure 10. Analysis of PKC retinal content in Wt and TgIGF-I mice. (a, c) Immunoblot detection showed decreased levels of PKCα in Tg mice at 3 and 6 months of age. No apparent differences were observed in older animals. **(b, d)** Quantification of band intensity corresponding to the immunoblots depicted in a-c confirmed a statistically significant decrease in PKCα levels in transgenic eyes at 3 and 6 months of age. Normalization by tubulin content ensured independence of loading differences. AU: arbitrary units. Values are expressed as the mean ±SEM of 5 animals/group. p*<0.05

Immunostaining with PKCα antibody allowed the identification of bipolar neurons in the INL of retinal sections (Figure 11a). These cells were strongly positive for PKCα in their terminals at the outer plexiform layer, where they establish contacts with photoreceptors (Figure 11a, lower inset). Bipolar cells span to the inner plexiform layer, where their other terminals, also strongly positive for PKCα, contact with ganglion cells (Figure 11a, upper inset). The counting of the number of PKCα+ cells per retinal section confirmed a reduction in the number of bipolar cells in TgIGF-I retinas at both 6 and 7.5 months of age (Figure 11b), an observation that was in agreement with the previously determined reduction in the thickness of INL in transgenic retinal sections (Figure 6).

1.2.4. Analysis of amacrine neurons

Amacrine neurons are found both in the INL and in the GL and integrate and modulate interactions between bipolar and ganglion cells (Forrester, 2002). Calretinin can be used as a specific marker for this subtype of neurons in the retina (Kolb et al., 2002). Retinal levels of this protein presented a marked decrease in transgenic mice of 7.5 months of age, but not in younger animals (Figure 12).

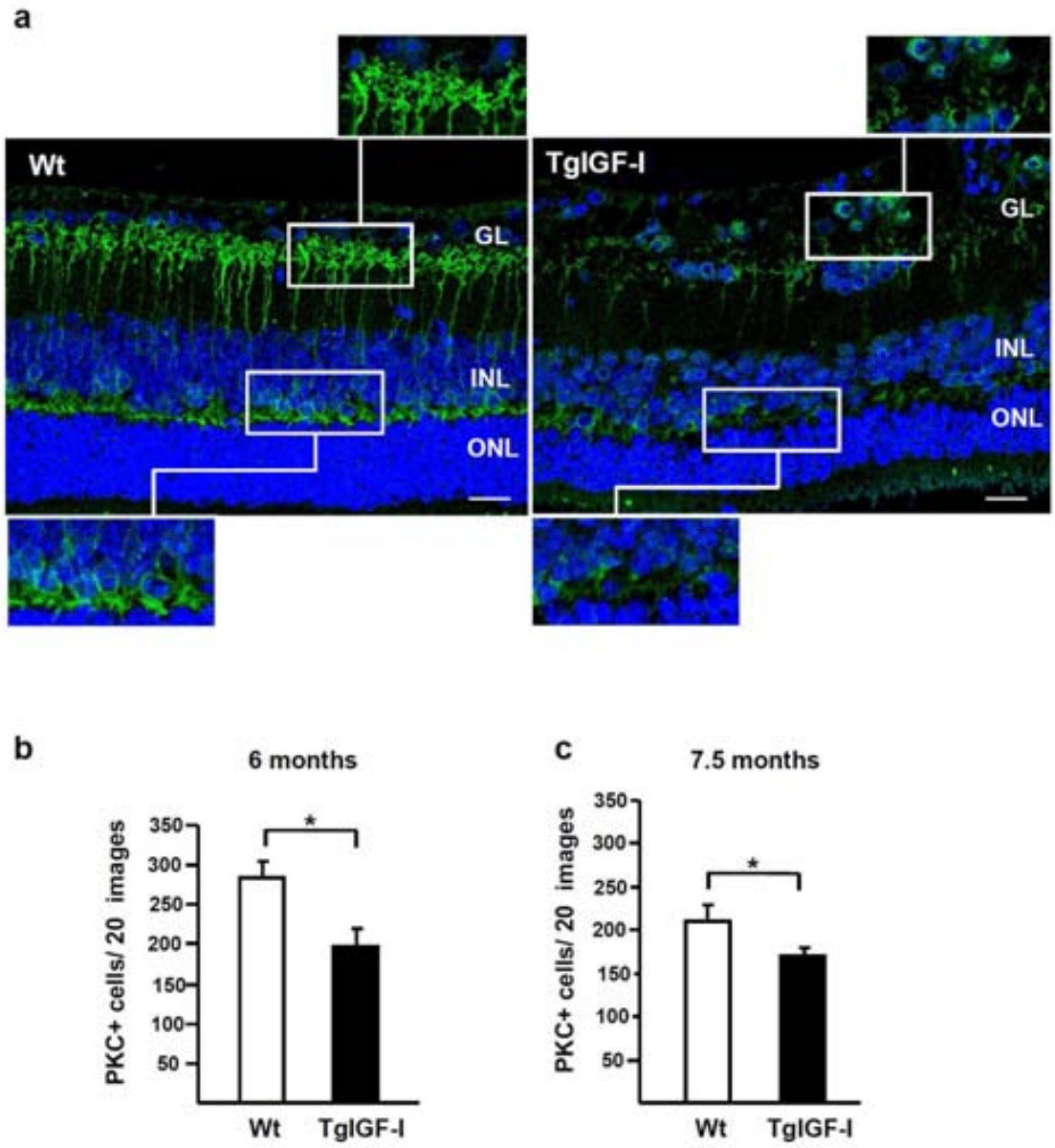

Figure 11. Bipolar cell loss in TgIGF-I retinas at 6 and 7.5 months of age. (a) Representative images of PKCα immunostaining (green) in retinal sections from Wt and TgIGF-I mice aged 7.5 months. Bipolar cells were strongly positive in their terminals located in the outer and the inner plexiform layers (upper and lower insets). The cell bodies spanning from the INL to the GL were also labelled. Transgenic retinas showed reduced PKC reactivity and there was a lower number of positive cells in the INL in transgenic versus Wt mice. **(b)** Quantification of the number PKC positive cells (INL nuclei with PKC positive cytoplasm) per retinal section in 6 and 7 month-old transgenic mice revealed a significant loss of bipolar PKC+ cells. Nuclei were stained with DAPI (blue). Values are expressed as the mean ±SEM of 5 animals/group. p*<0.05. Scale bar: 18.37 µm.

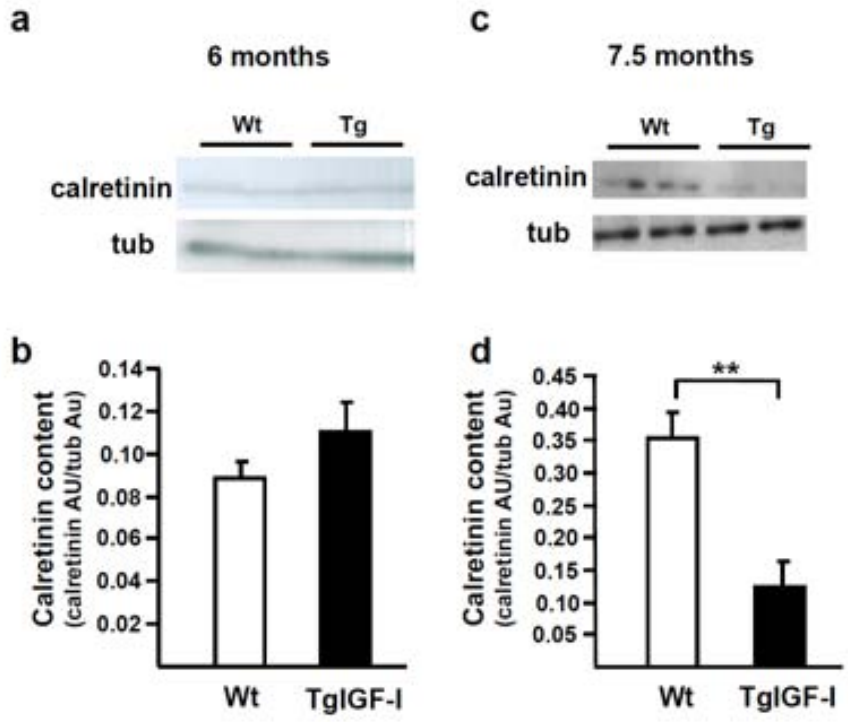

Figure 12. Calretinin retinal levels in Wt and TgIGF-I mice. Western blot analysis **(a)** and quantification of band intensities **(b)** did not show any differences in calretinin retinal levels between Wt and TgIGF-I mice at 6 months of age, after load normalization by tubulin levels. Representative blot **(c)** and densitometric quantification **(d)** of calretinin content revealed a marked decreased in 7.5 month-old transgenic mice when compared with aged-matched Wt animals. AU: arbitrary units. Values are expressed as the mean ±SEM of 5 animals/group. p**<0.01

Amacrine cells can be easily observed after calretinin staining in retinal sections both in the INL and the GL. The cell bodies of amacrine cells as well as their dendrites located in the inner plexiform layer are positive for calretinin (Figure 13a). When the number of calretinin positive neurons was quantified in retinal sections from 7.5 month-old mice, a smaller number of cells could be identified per retinal section in transgenic mice. This result agreed with the previously observed reduced content of calretinin (Figure 13b).

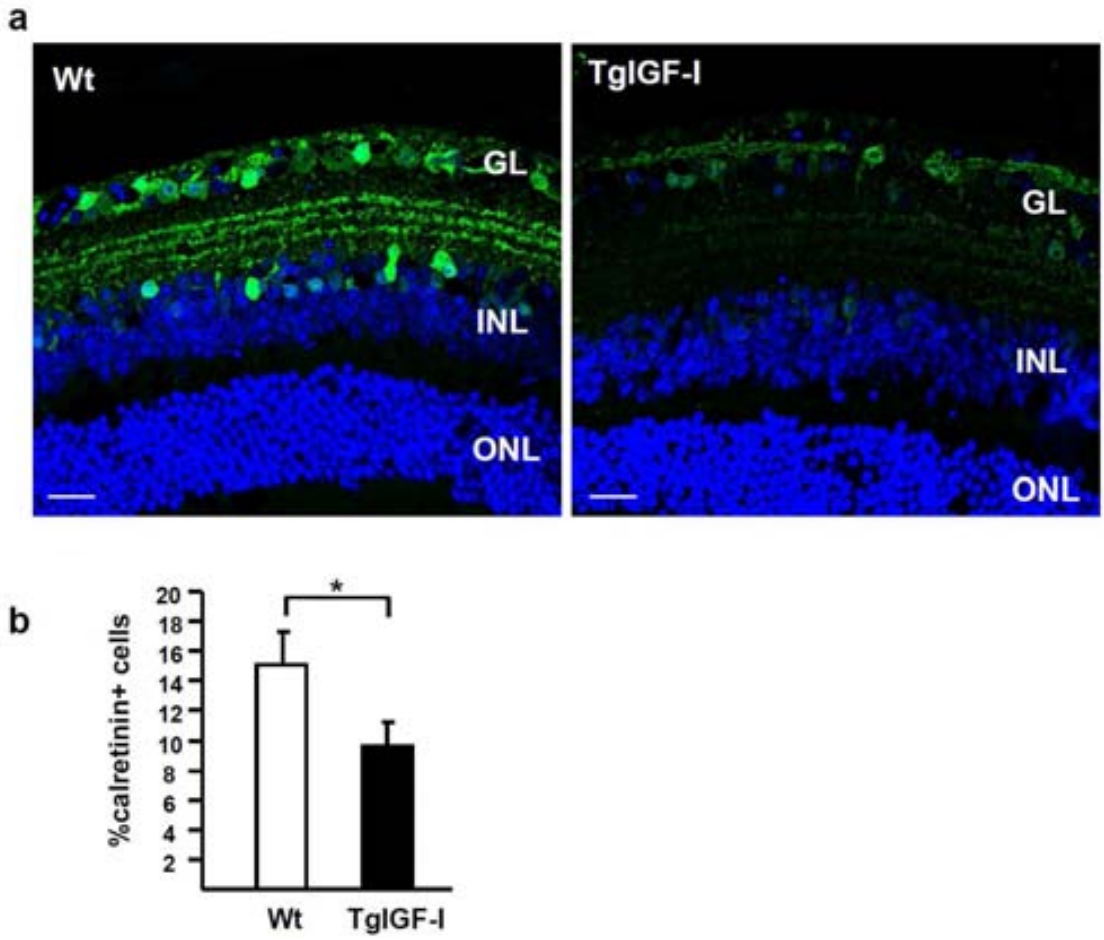

Figure 13. Decreased number of retinal amacrine neurons in TgIGF-I mice at 7.5 months. (a) Representative images of calretinin immunofluorescent detection (green) in retinal sections from Wt and TgIGF-I mice at 7.5 months of age showed reduced staining in both the GL and the INL. **(b)** Quantification of the number of cells inmmunostained with calretinin per retinal section demonstrated a reduction in the number of amacrine neurons in transgenic retinas at 7.5 month of age, in comparison with Wt retinas at the same age. Nuclei were stained with DAPI (blue). Values are expressed as the mean ±SEM of 5 animals/group. p*<0.05. Scale bar: 18.37 µm.

1.2.5. Analysis of horizontal neurons

Horizontal neurons are also located in the INL and involved in the modulation of photoreceptors and bipolar cell signals (Forrester, 2002). These cells can be identified using an antibody specific for calbindin (Haverkamp and Wässle, 2000). Western blot analysis in retinal extracts obtained from animals

at 7.5 months of age did not show any differences in calbindin content between Wt and TgIGF-I mice (Figure 14).

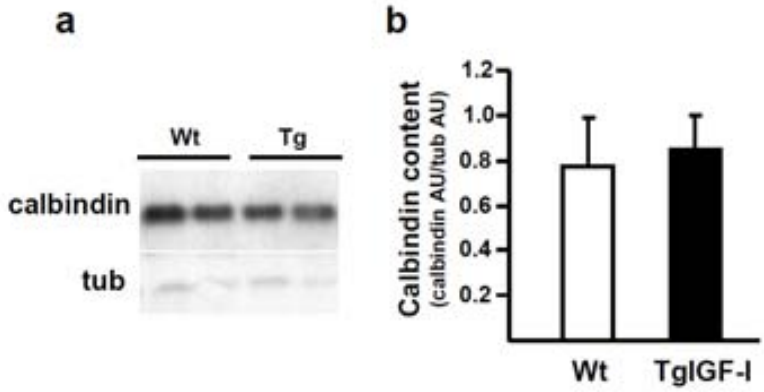

Figure 14. Retinal levels of calbindin in 7.5 month-old Tg IGF-I mice. (a) Representative western blot and **(b)** densitometric quantification of band intensity did not reveal any differences in calbindin content between Wt and TgIGF-I mice at 7.5 months of age, after load normalization by tubulin content. AU: arbitrary units. Values are expressed as the mean ±SEM of 5 animals/group.

1.2.6. Analysis of ganglion cells

Ganglion neurons receive electric input from bipolar cells and their axons project to the brain forming the optic nerve (Forrester, 2002). Retinal levels of Brn3a, a transcription factor expressed specifically in ganglion cell nuclei, were determined in 6 and 7.5 month-old Wt and transgenic mice. As shown in Figure 15, 7.5 month-old mice had a significant reduction in Brn3a retinal content, which was not observed at 6 months of age. The presence of Brn3a reactivity within the nuclei after immunostaining for Brn3a of retinal sections allowed the identification of cells of the GL as ganglion cells (Figure 16a). Quantification of

the number of Brn3a+ cells in retinal sections stained with anti-Brn3a evidenced a decrease in the number of ganglion cells in transgenic retinas at 7.5 moths of age (Figure 16b).

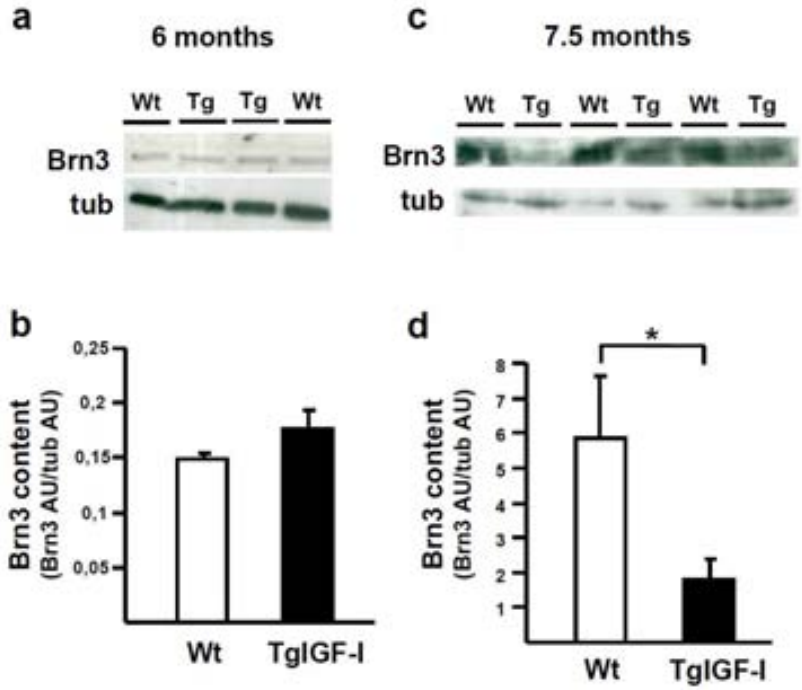

Figure 15. Study of Brn3a content in Tg IGF-I retinas. Brn3a immunoblot detection **(a)** and densitometric quantification of band intensity **(b)** in Wt and TgIGF-I retinas at 6 months of age. Representative blot of Brn3a content **(c)** and densitometric quantification of band intensity **(d)** at 7.5 months. When compared with age-matched Wt animals, TgIGF-I showed no differences in Brn3a content at 6 months, but a marked decrease was evident in 7.5 month-old transgenic retinas. Normalization by tubulin content corrected for loading differences. AU: arbitrary units. Values are expressed as the mean ±SEM of 5 animals/group. p*<0.05

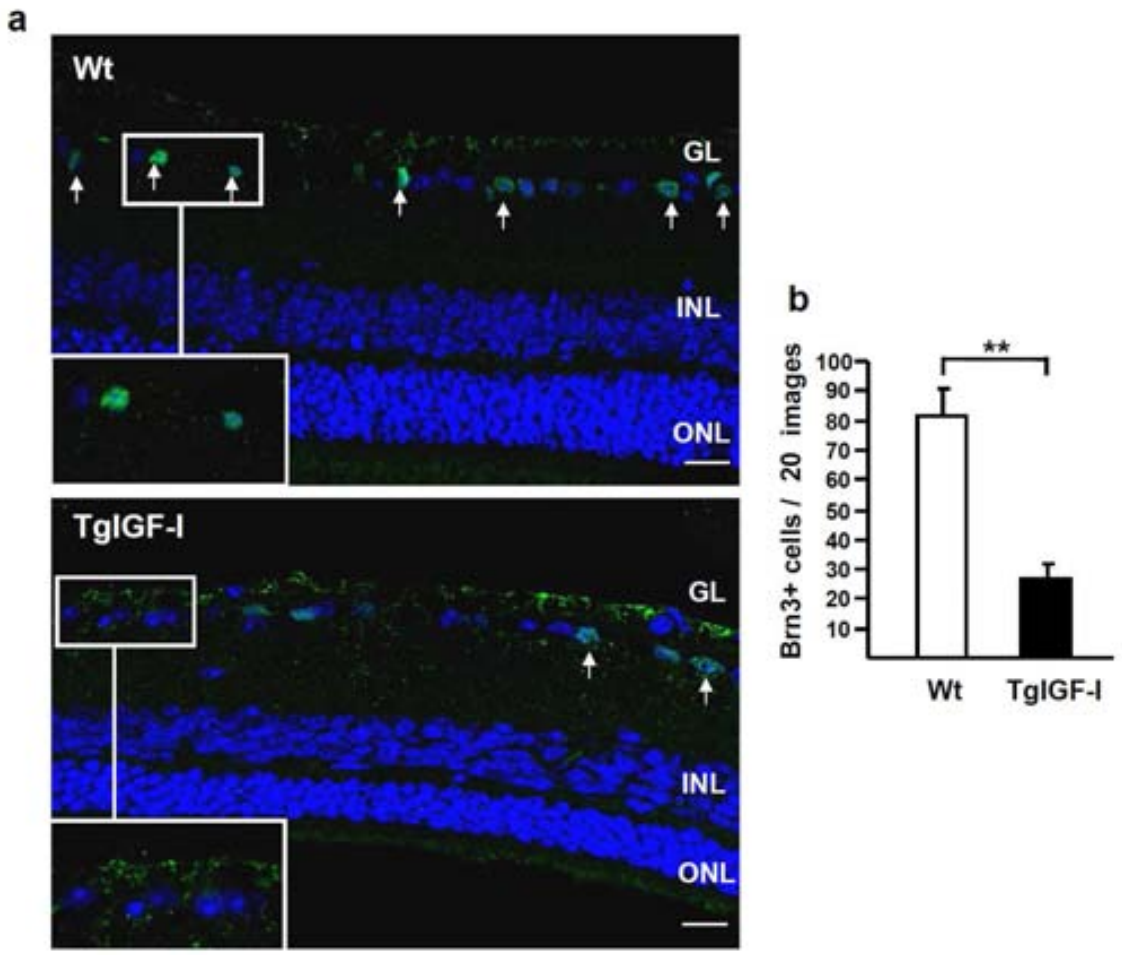

Figure 16. Ganglion cell loss in TgIGF-I retinas at 7.5 months of age. (a) Immunofluorescent detection of Brn3a (green), expressed specifically in the nuclei of ganglion neurons (arrows), in Wt and transgenic retinas at 7.5 months of age. Transgenic retinas showed less positive nuclei, despite the presence of more background signal (insets). **(b)** Brn3a+ cell counting revealed loss of ganglion cells in transgenic retinas at 7.5 months of age. Nuclei were stained with DAPI (blue). Values are expressed as the mean ±SEM of 5 animals/group. p**<0.01. Scale bar: 18.37 μm.

1.3. DETECTION OF NEURONAL DEATH IN TgIGF-I RETINAS

Reductions in most neuronal populations were observed in retinas of old TgIGF-I mice. Rod photoreceptors, bipolar, amacrine and ganglion neurons were affected, particularly at 7.5 months of age, but earlier in the case of bipolar cells. These findings, together with the observations of reduced ERG responses, suggested that there was a progressive loss of neurons in

transgenic retinas, likely due to cell death. To confirm the increase in neuron apoptosis, immunofluorescent detection of cleaved-caspase 3, an early marker of cell death, was performed in retinas of 3, 6 and 7.5 month-old transgenic mice and age-matched wild-type littermates. A few caspase-3 positive cells were found in 6 month-old transgenic eyes, mainly located in the ganglion cell layer, whereas no positive cells were observed in sections from wild-type animals (Figure 17). No caspase-3 positive cells were observed in either transgenic or in wild-type retinas at the other ages analysed, suggesting that retinal neuronal death peaked at around 6 months of age in TgIGF-I mice.

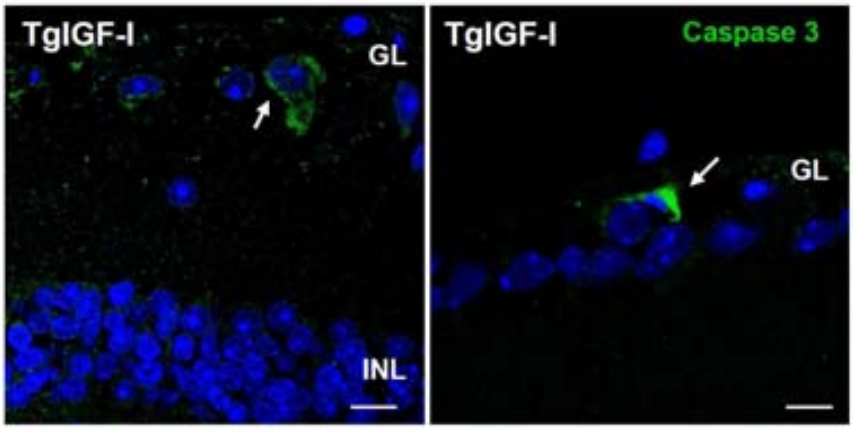

Figure 17. Cleaved-caspase 3 positive cells in transgenic retinas overexpressing IGF-I. Some apoptotic cells, positive for cleaved-caspase 3 (green, arrows), were found in the ganglion cell layer of transgenic mice at 6 months of age. Cleaved-caspase 3 positive cells could not be detected in retinal section from wild-type retinas at the same age. Nuclei were stained with DAPI (blue). Scale bar: 7.6 µm (left panel), 11.43 µm (right panel).

2. STUDY OF GLIAL AND MICROGLIAL ALTERATIONS IN TgIGF-I RETINAS

2.1. ANALYSIS OF THE GLIAL AND MICROGLIAL ACTIVATION

The integrity and function of retinal neurons is dependent on the normal function of retinal glial cells; these cells play a key role in maintaining the retinal milieu optimal for proper neuronal functionality, controlling processes such as the homeostasis of ions, the recycling of neurotransmitters, the production of neurotrophic factors or the detoxification of free-radicals (Giaume et al., 2007). Gliosis and increased microglial infiltration have been previously described in human diabetic retinopathy (Mizutani et al., 1998) and also in TgIGF-I mice (Ruberte et al., 2004; Haurigot et al., 2009). In addition, IGF-I directly induces gliosis in Müller cells in experimental models (Fischer et al., 2010).

As a first step in the study of the temporal progression of glial alterations in TgIGF-I retinas, GFAP inmunohistochemistry was perfomed in retinal sections from transgenic and Wt mice at different ages. The detection of GFAP is normally confined to retinal astrocytes unless gliosis is present, a condition in which GFAP is strongly upregulated in Müller cells (Eisenfeld et al., 1984). In wild-type retinas, GFAP positivity in Muller cell processes was barely detected in old animals. On the contrary, TgIGF-I retinal sections showed increased GFAP staining in both astrocytes and Müller cells in animals as young as 1.5 months of age (Figure 18). In addition to astrocytes, located in the superficial layer of the retina, GFAP-positive Müller cell processes were observed

spanning through transgenic retinas at all ages analyzed, which demonstrates the gliotic status of these retinas.

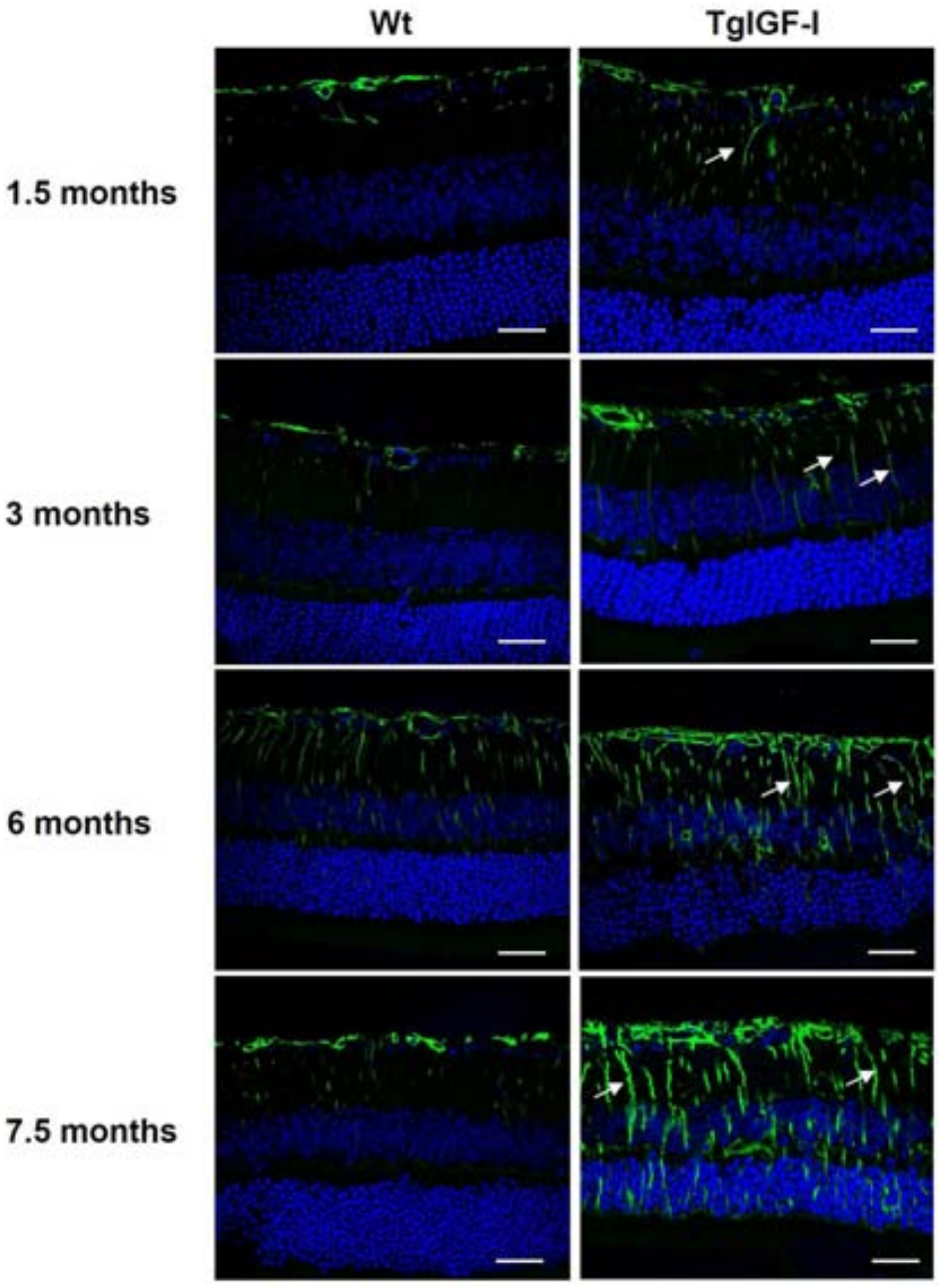

Figure 18. GFAP inmunostaining in Wt and TgIGF-I retinas at different ages. GFAP immunohfluorescent detection (green) in retinal sections from Wt and TgIGF-I at 1.5 months, 3 months, 6 months and 7.5 months of age. At all ages analyzed, transgenic retinas showed overexpression of GFAP, especially in Müller cells processes radially spanning the retina (arrows), where GFAP is not normally expressed. This pattern of GFAP staining indicated the presence of reactive gliosis in transgenic retinas. Scale bar: 31.27 µm.

The quantification of GFAP retinal levels by Western blot confirmed a marked increase in GFAP in transgenic animals (Figure 19). As soon as 1.5 months of age there was a 2.5 fold-increase in the retinal content of GFAP in TgIGF-I. A clear trend suggesting that the content of GFAP increased with age was observed (Figure 19).

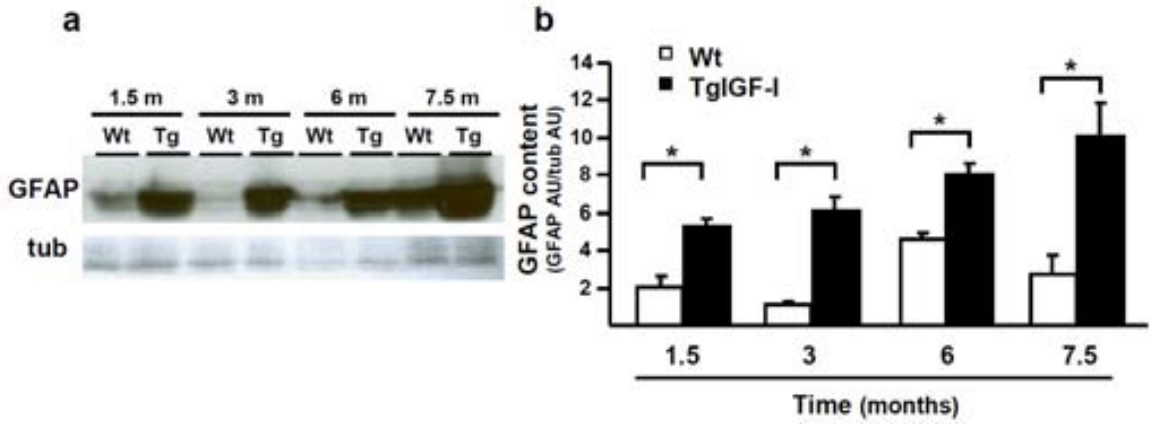

Figure 19. Retinal GFAP levels in Wt and TgIGF-I mice at different ages. (a) GFAP content was analyzed by Western blot in retinal extracts from Wt and TgIGF-I mice at 1.5, 3, 6 and 7.5 months of age. **(b)** Quantification of blots demonstrated that GFAP levels were increased in transgenic retinas at all ages, after load normalization by tubulin levels. AU: arbitrary units. Values are expressed as the mean ±SEM of 2 animals/group. p*<0.05

In addition to GFAP upregulation, gliosis is characterized by proliferation of Müller cells (Dyer and Cepko, 2000). The activation and proliferation of Müller cells after a retinal injury is associated to the downregulation of $p27^{Kip}$, an inhibitor of cyclin kinases that avoids the entry into the S phase (Vázquez-Chona et al., 2011). $p27^{Kip}$ expression in the retina has been reported to be restricted to Müller cells (Dyer and Cepko, 2000). It has been reported that IGF-I can mediate the downregulation of $p27^{Kip}$ in several models, driven by the activation of its downstream signaling through the Akt/PI3 kinase pathway (Agudo et al., 2008; Mairet-Coello et al., 2009).

When retinal $p27^{Kip}$ levels were analyzed in TgIGF-I at different ages by quantitative PCR (qPCR), a significant decrease in $p27^{Kip}$ expression was found in transgenic retinas at 6 and 7.5 months of age when compared with Wt (Figure 20), suggesting that Müller cells were proliferating in TgIGF-I retinas at these ages.

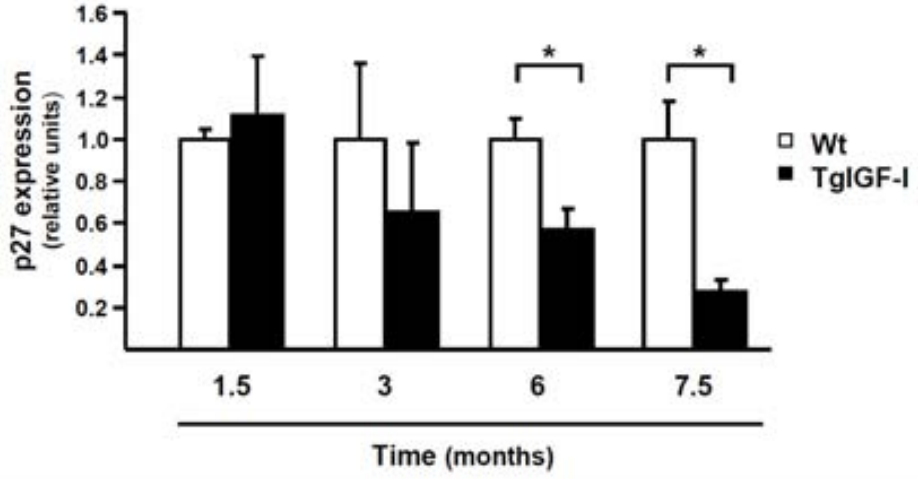

Figure 20. Analysis of $p27^{Kip}$ expression in Wt and TgIGF-I retinas according to age. Quantitative RT-PCR analysis revealed a decrease in the retinal levels of expression of $p27^{Kip}$ in transgenic mice at 6 and 7.5 months of age, when compared with Wt. Values are expressed as the mean ±SEM of 3-5 animals/group. p*<0.05

Microglial cells are the resident macrophages in the retina and become activated after retinal injury in several pathologies, including diabetic retinopathy (Krady et al., 2005). Immunostaining with tomato lectin (*Lycopersicon esculentum*) allowed the identification of retinal microglial cells. Positive cells were found in the GCL and the IPL of retinas from Wt and transgenic mice at different ages (Figure 21a, insets). The quantification of lectin+ cells revealed that a greater number of microglial cells infiltrated the retinas of transgenic mice, with clear differences being observed from 3 months of age (Figure 21b).

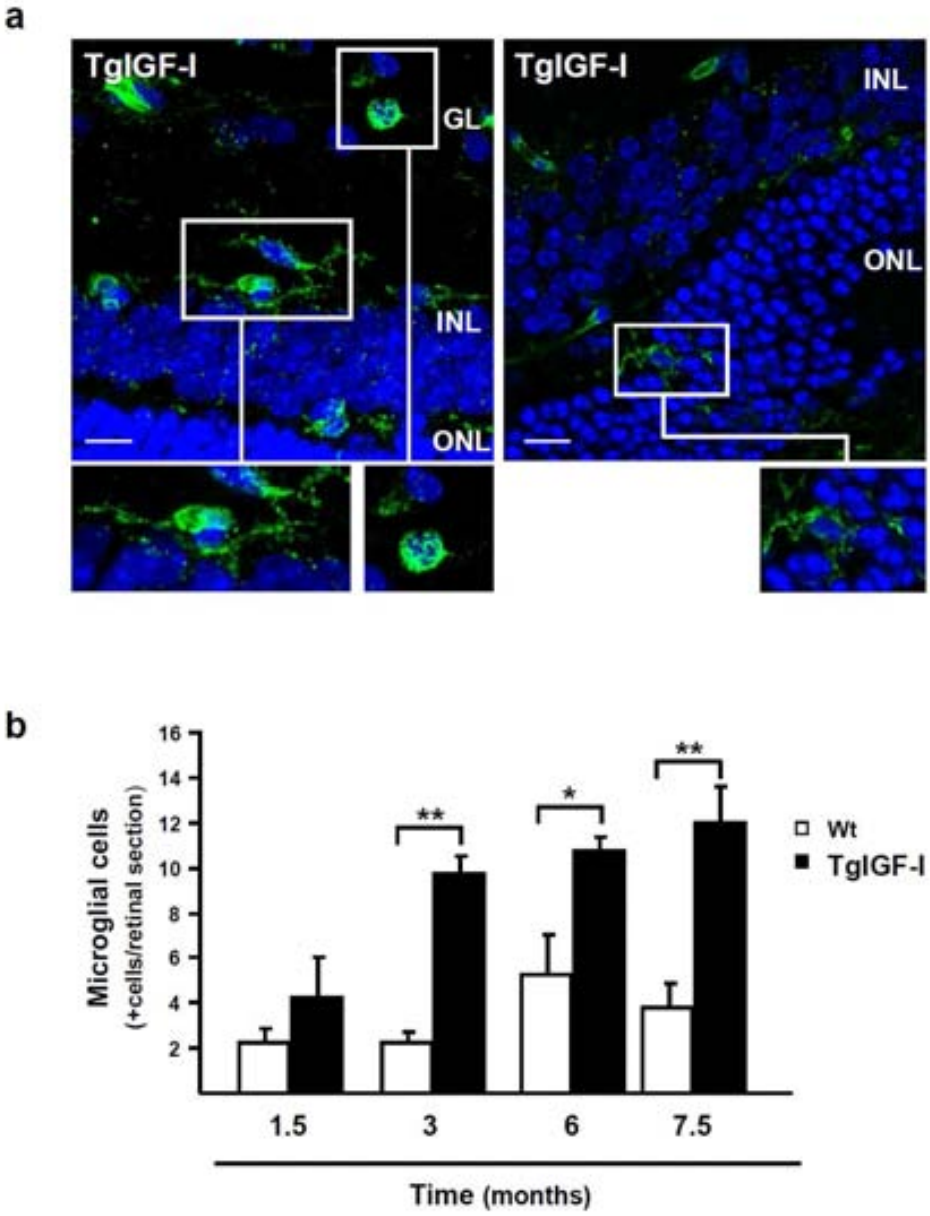

Figure 21. Retinal microglial cells in Wt and transgenic retinas at different ages. Immunofluorescence with the tomato lectin (*Lycopersicum esculentum*) allowed the identification of microglial cells in retinal sections from transgenic mice (green, insets). **(a)** Representative images obtained from retinas of transgenic mice at 7.5 months of age. The right inset in the left panel indicate round-shaped lectin+ cells, likely activated microglial cells. **(b)** The number of lectin positive cells per section was determined in complete medial retinal sections from Wt and transgenic retinas at 1.5, 3, 6 and 7.5 months of age, showing statistically significant differences in retinas of mice aged 3 months of age and older. Values are expressed as the mean ±SEM of 4 animals/group. p*<0.05, p**<0.01. Scale bar: 12.06 μm (left panel), 8.54 (right panel).

Moreover, some of these cells in transgenic retinas showed rounded morphology, characteristic of activated microglial cells (Fig 21, right inset, left panel).

2.2. RETINAL HOMEOSTASIS IN TgIGF-I RETINAS

As indicated in the Introduction, retinal glial cells, specially Müller cells, play several key roles in supporting neuronal function and maintaining retinal homeostasis, such as the control of pH and ionic homeostasis, the recycling of neurotransmitters, the production of neurotrophic factors and the detoxification of free-radicals (Bringmann et al., 2006). It has been reported that most of these essential functions can be impaired in gliosis, when Müller cells become reactive after a retinal injury (Giaume et al., 2007). In order to evaluate the status of glial functionality in TgIGF-I retinas, a careful assessment of these functions was undertaken.

2.2.1. Determination of glutamate recycling

Amongst other functions, retinal Müller cells are involved in the recycling of neurotransmitters, essentially glutamate and GABA, whose accumulation in the retinal milieu has been extensively associated to neurotoxicity (Bringmann et al., 2009b). Following its release from neurons, glutamate is taken up by Müller cells, rapidly converted to glutamine and shuttled back to neurons, where glutamine acts as the main precursor for the production of both glutamate and GABA (Bringmann et al., 2009b). It has been described that glutamate processing is impaired in reactive glial cells (Giaume et al., 2007). To evaluate

this in TgIGF-I retinas, glutamate content was determined in retinal extracts from Wt and transgenic mice at different ages (from 3 to 7.5 month-old) by monitoring of glutamate dehydrogenation through the measurement of NADH production. However, no clear differences could be observed in the glutamate content between Wt and transgenic mice at any of the ages analyzed (Figure 22).

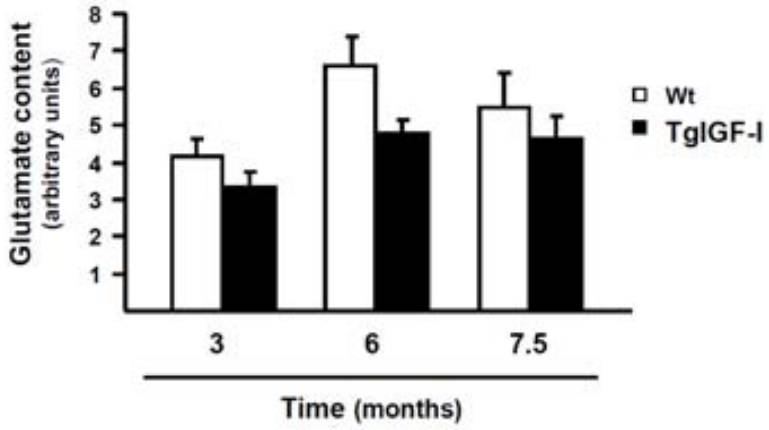

Figure 22. Levels of glutamate in the retinas of Wt and TgIGF-I mice. The total glutamate content was measured by mesuring NADH levels produced by glutamate dehydrogenation in retinas from Wt and transgenic mice, and no significant differences were observed between animals at any of the ages studied. Values are expressed as the mean ±SEM of 5 animals/group.

GLAST is the major glutamate transporter in Müller Cells and its expression and activity have been reported to be increased in pathological conditions, and also by extracellular glutamate content (Bringmann et al., 2009). GLAST expression was measured by quantitative RT-PCR in Wt and transgenic retinas at different ages. Although at all ages analyzed transgenic animals seemed to have higher expression of GLAST, no statistically significant differences were found in any case (Figure 23).

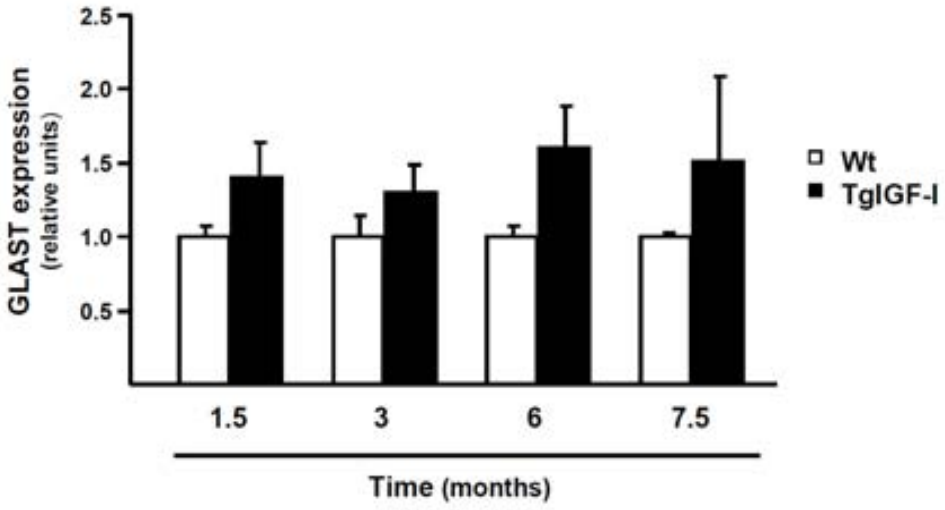

Figure 23. Expression of **GLAST in Wt and transgenic retinas.** Retinal expression of the glutamate transporter GLAST was assessed by quantitative RT-PCR in Wt and transgenic retinas at 1.5, 3, 6 and 7.5 months. Results suggested a higher expression of GLAST in transgenic retinas but not statistical differences were found. Values are expressed as the mean ±SEM of 3-4 animals/group.

Glutamine synthetase (GS) is the main enzyme that converts glutamate into glutamine in Müller cells. The activity of glutamine synthetase was assayed in retinal extracts from Wt and transgenic mice at different ages by spectrophotometric monitoring of γ-glutamyl hydroxamate production (Lund, 1971). Despite the observation of normal levels of glutamate and GLAST in transgenic retinas, a statistically significant decrease in the activity of glutamine synthetase was observed at all ages analyzed (Figure 24).

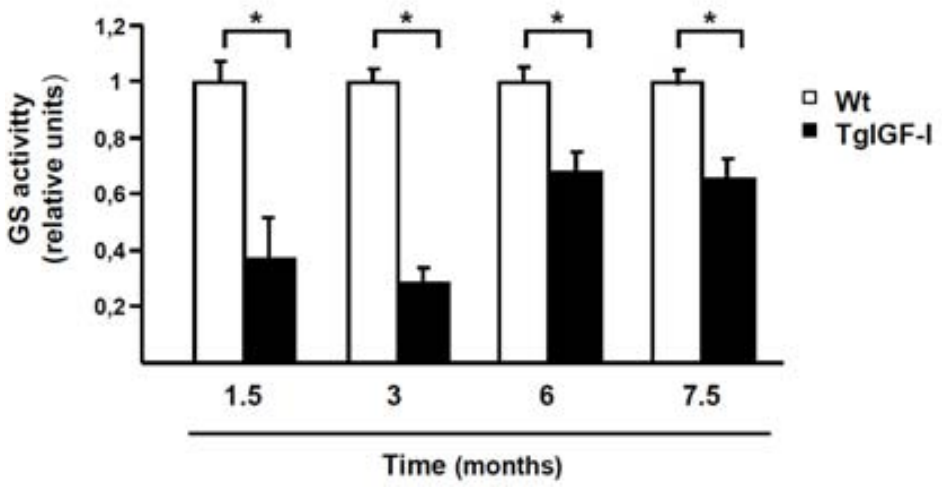

Figure 24. Reduced glutamine syntethase activity in retinal extracts from Wt and TgIGF-I mice at different ages. Retinal GS activity was assayed in Wt and TgIGF-I mice from 1.5 to 7.5 months of age, by spectrophotometric monitoring of γ-glutamyl hydroxamate generation. The retinal activity of this enzyme was significantly reduced in transgenic animals from early to advanced stages in the evolution of the pathology. Values are expressed as the mean ±SEM of 8-13 animals/group. p*<0.05

2.2.2. Determination of the oxidative stress in TgIGF-I retinas

Antioxidant protection is especially important in the retina, due to the high oxygen consumption of this tissue and the constant exposure to irradiation (Bringmann et al., 2009b). Glutathione acts as an scavenger of free radical and reactive oxygen species (ROS). Glutathione is mainly produce by Müller cells and astrocytes, and its production by Müller cells is dependent on the availability of glutamate and cystine (Reichelt et al., 1997b). In situations of oxidative stress, reduced glutathione is rapidly released from Müller cells and provided to retinal neurons where it is oxidized (Schütte and Werner, 1998).

To evaluate the oxidative status of transgenic retinas, the content of total and oxidized glutathione was analyzed in retinas of Wt and transgenic mice at

different ages by monitoring the activity of the enzyme glutathione reductase, as indicated in Methods. Total glutathione was increased in retinas of TgIGF-I mice at 6 and 7.5 months of age, but not in younger animals (Figure 25a). At all ages analyzed, however, increased levels of oxidized glutathione were detected in retinas of transgenic animals (3 months of age and older) (Figure 25b), indicating the presence of increased retinal oxidative stress in transgenic retinas from an early age.

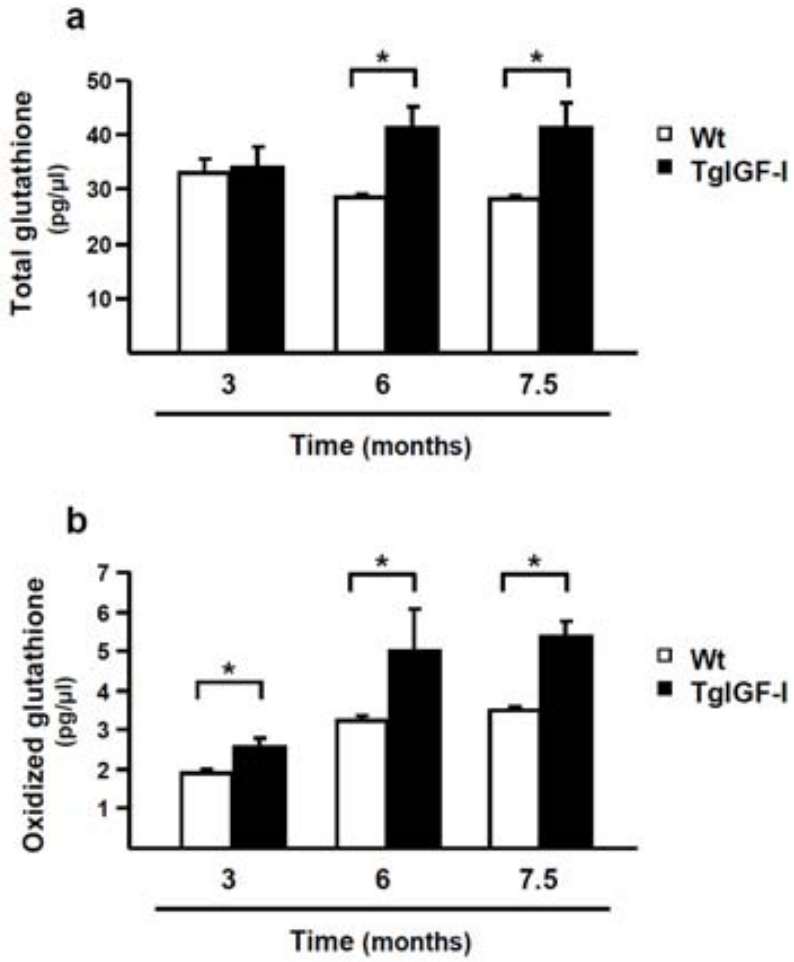

Figure 25. Retinal glutathione content in Wt and Tg mice. Total and oxidized glutathione were measured in retinal extracts of Wt and transgenic mice at 3, 6 and 7.5 months of age. **(a)** Statistically significant increases in total glutathione were observed in retinas from mice older than 6 months of age. **(b)** Oxidized glutathione levels were higher in transgenic retinas compared with Wt ones at all ages studied, suggesting the presence of oxidative stress in transgenic retinas. Values are expressed as the mean ±SEM of 5 animals/group. p*<0.05

Protein oxidation occurs when intracellular ROS production is increased, as a consequence of retinal oxidative stress. The observed increases in oxidized glutathione in TgIGF-I retinas suggested a greater production of ROS in transgenic retinas. To investigate whether it was happening in transgenic retinas, samples from Wt and transgenic animals at 6 and 7.5 months of age were analyzed for the measurement of carbonyl groups, which are introduced in protein chains by excessive amounts of ROS. The technique relies on the immunodetection using an antibody that binds specifically to carbonyl groups after a chemical treatment of the samples. Although a tendency to be higher was observed at both ages, no significant differences were observed in the content of oxidized proteins between Wt and transgenic retinas (Figure 26).

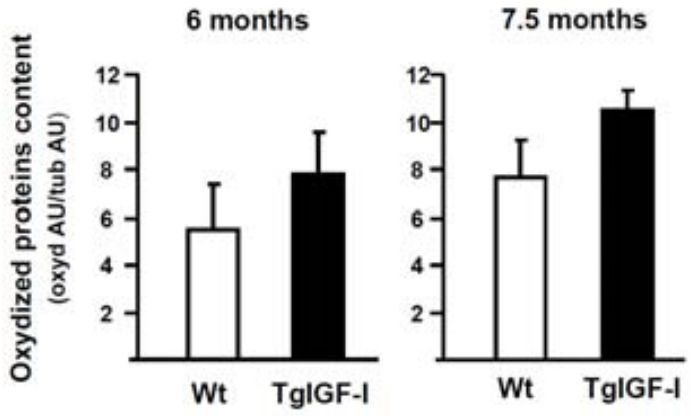

Figure 26. Detection of carbonyl groups as a measurement of the oxidation of proteins in retinal extracts from Wt and TgIGF-I mice. Oxidized proteins were measured in retinal extracts by Western blot, using an antibody that recognizes carbonyl groups after a chemical derivatization of the samples. Transgenic mice appeared to have higher content of oxidized proteins than Wt mice at 6 and 7.5 months of age although no statistically significant differences were observed among groups. Normalization with tubulin content attested equal loading of the samples. AU: arbitrary units. Values are expressed as the mean ±SEM of 4 animals/group.

Nitric oxide (NO) is a bioactive free radical involved in many physiological processes, such as signal transduction, regulation of vascular tone and neurotransmission (Abu El-Asrar et al., 2001). Basal levels of NO are normally produced by the calcium-dependent, constitutive forms of the nitric oxide synthases (NOS), expressed in neurons (nNOS) and endothelial cells (eNOS) (Brown, 2010). On the other hand, the inducible form of NOS, iNOS, produces large quantities of NO that are associated with neurotoxicity, inflammation and angiogenesis (Dawson and Dawson, 1996; Ziche et al., 1994). The overproduction of NO induces the formation of peroxynitrites, which cause DNA damage, depletion of reduced glutathione and lipid and protein modification (Behar-Cohen et al., 1996). Although stimulated endothelial cells and pericytes also express iNOS (Chakravarthy et al., 1995), iNOS is mainly expressed in retinal glial and microglial cells and its expression is induced by glial activation after the addition of lipopolysaccharide (LPS), interferon gamma and TNF-α (Goureau et al., 1994). For human diabetic retinopathy, it has been reported that there is upregulation of iNOS expression in Müller cells (Abu El-Asrar et al., 2001). When the expression of iNOS was analysed by quantitative RT-PCR in RNA retinal extracts from Wt and transgenic IGF-I mice at different ages, a marked increase in retinal iNOS expression in 7.5 month-old TgIGF-I mice was found (Figure 27). This observation suggested that there might be overproduction of NO in transgenic retinas that could contribute to neuronal death.

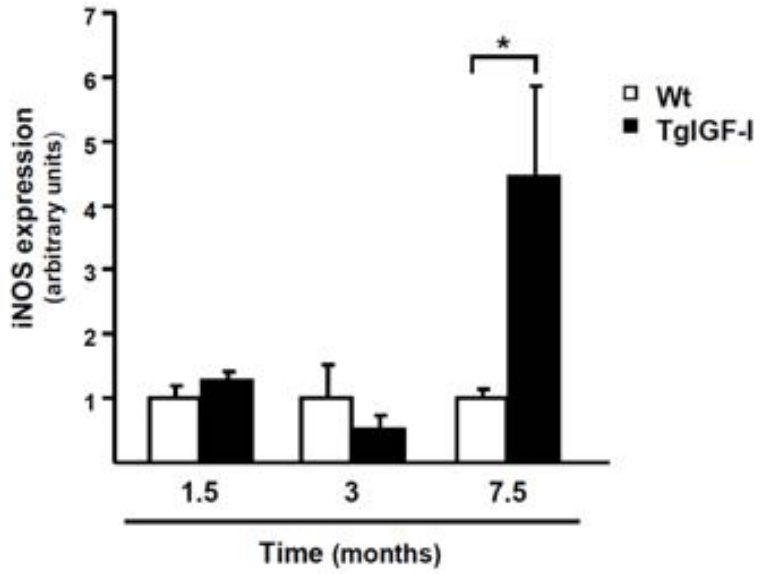

Figure 27. Expression of iNOS in Wt and transgenic retinas. Retinal expression of the enzyme iNOS was assessed by quantitative RT-PCR in Wt and transgenic retinas at 1.5, 3 and 7.5 months. Results indicated a marked increased in the expression of iNOS in transgenic retinas at 7.5 months of age, but not at earlier ages. Values are expressed as the mean ±SEM of 4-5 animals/group. p*<0.05

2.2.3. Study of the potassium homeostasis

Retinal Müller cells are also responsible for clearing the excess of potassium that is accumulated in synaptic layers as a result of neuronal activity (Pannicke et al., 2004; Bringmann et al., 2006; Giaume et al., 2007). This essential supportive function is carried out by distinct K+ channels located in the membrane of retinal Müller cells that control K+ influx (Kir 2.1) or efflux (Kir 4.1) from the cell (Kofuji et al., 2002). Kir 4.1 is mainly located in the areas that surround retinal vessels and in the inner and outer limiting membranes (Nagelhus et al., 1999). The excess of K+ is exported to blood vessels or to the vitreal or subretinal space through these channels. It has been reported that gliosis induces changes in K+ conductance and Kir4.1 localization in Müller

cells (Ulbricht et al., 2008). These observations have been also described in STZ-induced diabetic rats (Pannicke et al., 2006).

Kir 4.1 immunohistochemistry was performed in retinal sections from Wt and TgIGF-I mice at 3 and 7.5 months of age. In healthy mice, Kir 4.1 immunoreactivity was found specifically in Müller cells, specially in the inner and outer limiting membranes and in the perivascular areas (Figure 28a), as previously described (Nagelhus et al., 1999). However, retinal sections from transgenic mice at both 3 and 7.5 months of age showed a diffuse staining for this channel, maintaining strong inmunoreactivity only in the inner limiting membrane (Figure 28a). A semi-quantitative analysis of these samples was performed by assigning a numeric value to the degree of delocalization of Kir 4.1 immunostaining in each sample, being 0 total delocalization and 3 normal localization of Kir 4.1. A value was given to each of three specific retinal areas: the inner limiting membrane, the outer limiting membrane and the perivascular area. The total score for each sample resulted from the sum of the values assigned to each area evaluated. The score for Kir 4.1 localization was markedly decreased in TgIGF-I when compared with Wt mice at both 3 and 7.5 months of age, suggesting the existence of altered K+ homeostasis in transgenic retinas (Figure 28b).

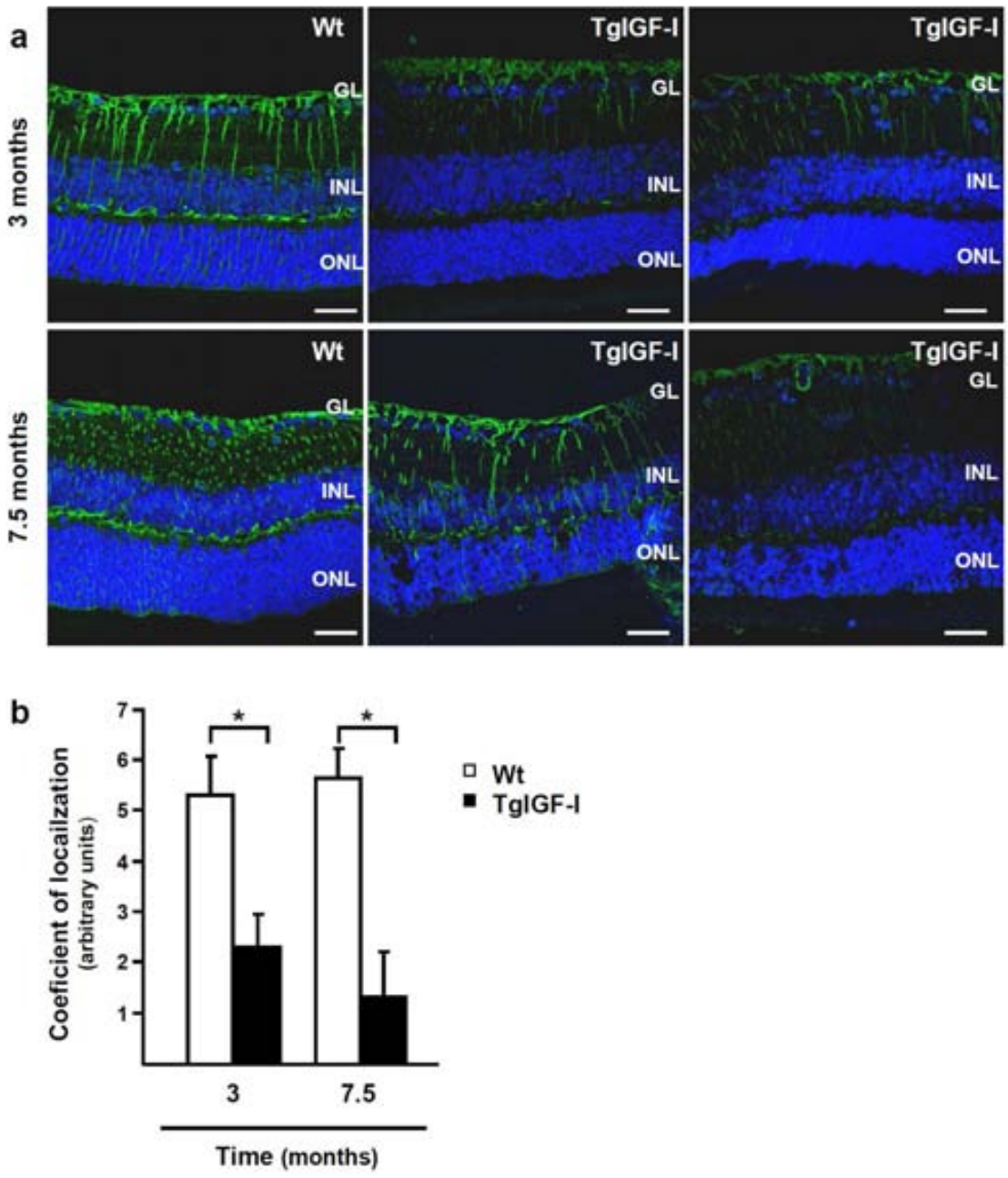

Figure 28. Retinal Kir 4.1 localization and content in Wt and TgIGF-I mice at different ages. (a) Representative images of Kir 4.1 inmunodetection in retinal sections from 7.5 month-old Wt mice showed a strong inmunoreactivity in the inner and the outer limiting membrane and the areas surrounding blood vessels. TgIGF-I retinas at the same age presented a diffuse pattern of staining. **(b)** Semiquantitative analysis of the Kir4.1 localization in Wt and TgIGF-I retinas revealed a marked decrease of the localization score in transgenic retinas at both 3 and 7.5 moths of age. Values are expressed as the mean ±SEM of 4 animals/group. Scale bar: 31.27 µm.

2.2.4. Analysis of the production of pro-inflammatory cytokines

It has been reported that both activated Müller and microglial cells can have direct neurotoxic effects by releasing pro-inflammatory cytokines such as Tumour Necrosis Factor alpha (TNF-α) and Monocyte Chemotactic Protein-1 (MCP-1) (de Kozak et al., 1997), which have been associated to the death of ganglion neurons (Lebrun-Julien et al., 2009) and photoreceptors (Nakazawa et al., 2007), respectively, in different models of retinal injury. The expression of TNF-α in the retina was analyzed in Wt and transgenic mice at different ages by quantitative RT-PCR. Transgenic mice aged 7.5 months showed an increase in TNF-α expression of more than 7-fold when compared to the levels observed in WT animals (Figure 29a).

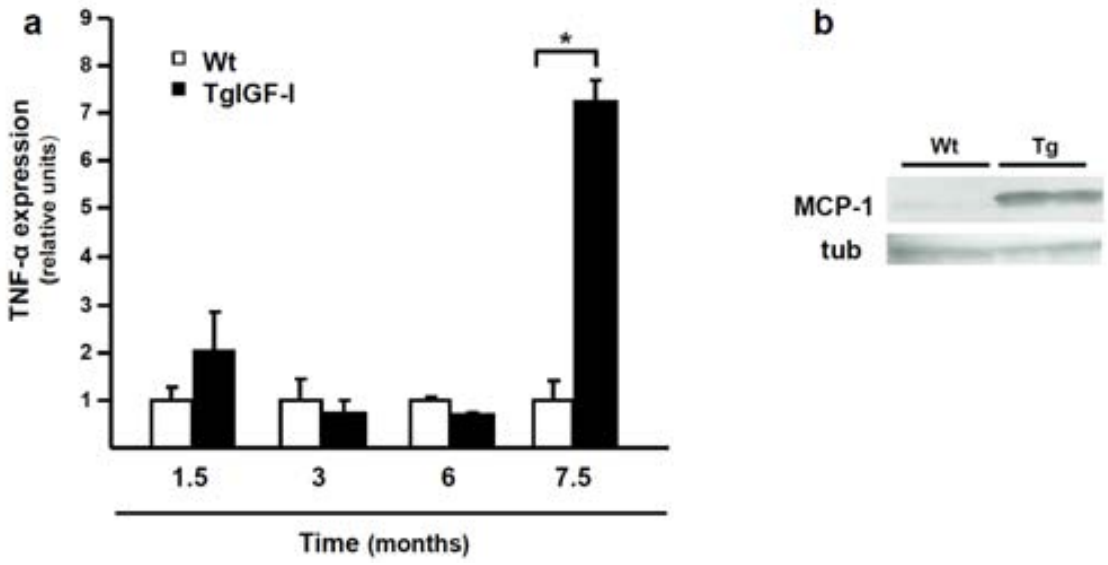

Figure 29. Pro-inflammatory cytokines in retinas of TgIGF-I mice. (a) Chronological analysis of TNF-α expression in Wt and TgIGF-I retinas by quantitative RT-PCR using specific primers. An approximately 7-fold increase was observed in the retinal levels of TNF-α expression in transgenic mice at 7.5 months of age. **(b)** Immunoblot corresponding to the detection of MCP-1 in protein extracts from individual retinas obtained from 7.5 month-old Wt and TgIGF-I mice. A marked increase in MCP-1 levels was observed in transgenic retinas when compared with healthy littermates. Unequal loading of the samples was corrected by tubulin blotting. Values are expressed as the mean ±SEM of 4-5 animals/group. p*<0.05

In addition, the quantification by Western Blot of the retinal content of MCP-1, a pro-inflammatory cytokine involved in the recruitment of macrophages, demonstrated a significantly higher level of MCP-1 in transgenic retinas at this age (Figure 29b). Altogether, these results indicated the presence of an inflammatory process in transgenic retinas.

The analysis of the glial and microglial alterations suggests that the neuronal dysfunction observed in transgenic IGF-I mice could arise as a consequence of either vascular, previously described (Ruberte et al., 2004; Haurigot et al., 2009) or glial alterations or both. Given that glial alterations appear very early in the course of the disease and that glial cells fulfill essential roles for optimal neuronal function, our results suggest that chronic gliosis has a greater impact on neuronal dysfunctionality in Tg-IGF-I retinas. Gliosis is known to alter some of the neuron-supportive functions normally carried out by glial cells, and as a consequence of gliosis transgenic mice showed alterations in the activity of GS, an enzyme key to glutamate metabolism, and signs of oxidative stress and impaired potassium buffering. In most cases, alterations showed a progressive pattern, worsening as animals aged. These changes in normal retinal metabolism may underlie neuronal dysfunction in transgenic retinas. In addition to their role in maintaining normal retinas homeostasis to support neuronal function, the increased production of cytokines by activated Müller cells, especially TNF-α, can also induce neuronal degeneration. Together with Müller cells, microglial cells could be another source of pro-inflammatory cytokines in transgenic eyes.

3. DISCUSSION

Diabetic retinopathy has been classically classified as a vascular pathology, probably due to the fact that vascular alterations are the first sign to be noted in standard clinical practice, as retinal blood vessels are easily visualized. However, it is known that, in humans, other retinal cell types are affected by hyperglycemia, like neurons or glial cells (Antonetti et al., 2006). These neuronal and glial alterations may be even previous to vascular damage and may actually influence the development of vascular disease. Retinal neuronal dysfunction (Shirao and Kawasaki, 1998) and reactive gliosis (Mizutani et al., 1998) have been observed in patients with early retinopathy, in which vascular alterations were not yet evident. The contribution of these pathological processes to the progression of diabetic retinopathy is difficult to determine by clinical observations. The study of the link between neuronal, glial and vascular alterations in the retina is, however, essential for the identification of the primary causes of the disease and for understanding the progression of the retinal alterations. Therefore, animal models that recapitulate the pathogenesis of human retinopathy are required to elucidate the molecular basis of the disease and identify new therapeutic targets, as well as for the pre-clinical evaluation of newly developed therapies. As described in the Introduction, many rodent models have been used for the study of diabetic retinopathy. Both spontaneous and STZ-induced hyperglycaemic models develop metabolic alterations similar to those of the human disease and many of them are also useful models of diabetic nephropathy and neuropathy. However, most of them only present a mild phenotype of diabetic retinopathy,

mainly characterized by non-proliferative vascular alterations, gliosis and, in a few models, late neuronal dysfunction (Barber et al., 2005; Danis and Yang, 1993; Feit-Leichman et al., 2005; Midena et al., 1989). It has been reported that the rodent retina, especially in mice, has a huge anti-oxidant potential when compared with human retinas, which would make rodent retinas capable of detoxifying diabetes-induced ROS overproduction (Obrosova et al., 2006). This may be an explanation for the phenotype highly resistant to the development of retinopathy of hyperglycaemic rodents.

IGF-I is increased in the vitreous of patients with proliferative diabetic retinopathy (Merimee et al., 1983; Grant et al., 1986; Inokuchi et al., 2001) and the disruption of IGF-I signalling prevents in rodents the development of retinal neovascularization under hypoxic conditions (Smith et al., 1999; Kondo et al., 2003), suggesting that IGF-I is involved in the development of proliferative diabetic retinopathy. Furthermore, intravitreal injection of IGF-I in rabbits and pigs results in the breakdown of the blood-retinal barrier and neovascularization (Grant et al., 1993; Danis and Bingaman, 1997). The transgenic mouse model used in the present work, which overexpresses IGF-I in the photoreceptors (TgIGF-I), develops many of the retinal vascular alterations of human diabetic retinal disease, despite not being hyperglycaemic (Ruberte et al., 2004; Haurigot et al., 2009). Although IGF-I is present in transgenic eyes from birth, only non-proliferative vascular alterations are found in young animals (2-3 months) and the phenotype progresses with age to overt pre-retinal neovascularization in adult mice at about 7-8 months of age (Ruberte et al., 2004). This temporary evolution resembles that of the human disease, and

allows for long-term evaluation of therapeutic strategies, facilitating the translation to the clinical setting of a chronic pathology such as retinopathy. In addition, VEGF, which is known to play a pivotal role in the development of proliferative retinopathy (Aiello et al., 1994; Pierce et al., 1995) is expressed by glial cells in TgIGF-I retinas, the same cells that contribute to the over-production of this factor in diabetic patients (Amin et al., 1997). The mechanism by which IGF-I, despite being present throughout the animal's life, induces this chronic and slow phenotype in TgIGF-I mice remains to be elucidated. It is known that IGF-I is able to induce VEGF expression in retinal cells (Treins et al., 2005) and that VEGF is increased in TgIGF-I retinas, in agreement with the vascular hyperpermeability and the proliferation of neovessels in transgenic retinas (Haurigot et al., 2009; Ruberte et al., 2004). But the continuous production of IGF-I likely has other earlier effects on transgenic retinas that may be contributors to the subsequent progression of vascular alterations. For this reason, the neuronal and glial phenotypes of TgIGF-I retinas needed to be further characterized. The present study addresses the characterization of neuronal and glial alterations in this animal model of retinopathy to further understand the initiation and progression mechanism that lead to the development of retinopathy.

TgIGF-I mice retinas a progressive decline in their electroretinographic responses that resulted in significantly impaired neuronal functionality in 7.5 month-old mice. Furthermore, all mice aged 9 months were completely blind. This loss of vision was accompanied by the observation of apoptotic cells in transgenic retinas and a progressive loss of neuronal populations that became

significant at 7.5 months of age. Gliosis and microgliosis were detected in transgenic mice at early ages and worsened as mice aged. Gliosis is associated with the loss of neuron-supportive functions performed by Müller cells that are essential for the visual process, such as the control of blood-flow, of the concentrations of ions and the recycling of neurotransmitters. Transgenic mice showed alterations in the activity of glutamine synthetase, an enzyme key to glutamate metabolism, and signs of oxidative stress, iNOS overexpression and impaired potassium buffering. In most cases, alterations showed a progressive pattern, worsening as animals aged. These changes in normal retinal metabolism may underlie neuronal dysfunction in transgenic retinas, which could be exacerbated by the increased production of pro-inflammatory cytokines such as TNF-α and MCP-1 observed in these mice.

Early changes in neuronal function have been observed in diabetic patients before any vascular pathology was clinically established (Shirao and Kawasaki, 1998). To determine if neuron functionality was also affected in mice overexpressing IGF-I in the retina, ERG measurements were performed in wild-type and transgenic mice at different ages, from 3 to 9 months of age. Although normal responses were recorded in 3 months-old TgIGF-I mice, all ERG parameters recorded were affected in transgenic mice at 6-7 months of age. The variability in the recorded responses at this age suggested that retinal neurologic dysfunction in transgenic mice developed in a very progressive manner, giving rise to slightly different time courses of development for each individual mouse. In contrast, in 9 month-old transgenic mice, ERG responses in all animals assessed were reduced by 80%. This suggests a general and

progressive alteration in retinal function, which was corroborated with histological results showing decreased populations of almost all types of retinal neurons at 7.5 months of age. As a result of these reduced populations, all parameters analyzed by ERG were affected in TgIGF-I retinas, in both scotopic and photopic conditions and at different light intensities. Even cone-driven responses were affected, despite arrestin levels suggested that this neuronal cell type was not affected. The alterations observed in bipolar and ganglion neurons could, however, be responsible of this generalized impaired responses, precluding the transmission of the signals from photoreceptors. The most consistent alterations found in the ERG analysis of diabetic patients implicate the oscillatory potentials (OPs) (Shirao and Kawasaki, 1998), generated by inner nuclear layer neurons; although reduced activity of photoreceptors has also been reported (Holopigian et al., 1997; Tyrberg et al., 2011). The first change detected in OPs in diabetic patients is the prolongation of the peak latency, which is observed in patients with no sign of funduscopic retinopathy and is directly caused by neuronal dysfunction (Shirao and Kawasaki, 1998). In humans, as vascular retinopathy progresses, OPs alterations become more evident, with reduced amplitude of the waves, which it has been suggested could be influenced by the development of angiopathy (Shirao and Kawasaki, 1998). Similarly, reduced OPs amplitudes were observed in 7.5 months-old TgIGF-I mice, which present advanced vascular disease at this age, whereas OPs responses were not altered in the absence of angiopathy (3 months of age).

Transgenic mice showed decreased populations of rod photoreceptors, bipolar, amacrine and ganglion neurons at 7.5 months of age. Only bipolar cells were significantly reduced at 6 months of age, suggesting an increased sensitivity of this neuronal population. It has been reported that bipolar cells totally depend on glutamine produced by Müller cells for their functionality (Pow and Robinson, 1994). As GS activity is markedly decreased in transgenic Müller cells, bipolar neurons could be specially affected by this glial alteration.

The loss of different retinal neuronal types, as well as the reduction in the length of the posterior segment of rod photoreceptors have both been observed in experimental models of diabetes (Park et al., 2003; Phipps et al., 2006; Barber et al., 1998; Aizu et al., 2002). Studies have been particularly focused on the loss of ganglion cells, which are known to be affected in human diabetic retinas (Kern and Barber, 2008). There are controversial results regarding the time of onset of neuronal degeneration in diabetic rodents, with reports ranging from 2 weeks to 7.5 months post hyperglycaemia development (Barber et al., 1998; Fletcher et al., 2007). In this study, although cell loss was clearly established, very few caspase-3 positive cells were found in transgenic retinas when studied at different ages. The slow progression of neuronal death in TgIGF-I retinas may make the observation of dying cells in these retinas difficult, due to the rapid clearance of dead cells by phagocytosis.

The extensive impairment of the functionality of transgenic retinal neurons could be the result of the compromise of glial functions in TgIGF-I retinas. Alterations in glial physiology are known to contribute to the onset and

progression of many neurodegenerative diseases (Yamanaka et al., 2008; Lioy et al., 2011). Müller cells are the most abundant macroglial cells in the retina and have a number of neuron-supportive functions essential for the visual process (Bringmann et al., 2006). Moreover, Müller cells maintain the homeostasis of the retinal milieu, controlling pH homeostasis, the concentrations of ions and the recycling of neurotransmitters (Bringmann et al., 2006). Müller cells also interact with the retinal vasculature, regulating blood-flow and secreting factors necessary for vascular integrity (Bringmann et al., 2006). However, all these essential functions can be impaired when gliosis is established. Initially, glial cells react against an injury by releasing antioxidant or neurotrophic factors in order to limit tissue damage (Bringmann et al., 2009a). But if this glial activation becomes chronic, as it may occur in diabetic retinopathy, these protective response may result in detrimental effects. As an example, low levels of VEGF in the retina have neuroprotective effects (Saint-Geniez et al., 2008), but overexpression of this factor leads to vascular hyperpermeability and pathological neovascularization (Pierce et al., 1995). In line with this concept, the chronic activation of glial cells has been reported to be essential to the progression of other neurodegenerative disorders, such as amyotrophic lateral sclerosis or Rett syndrome (Yamanaka et al., 2008; Lioy et al., 2011).

Reactive gliosis, identified by GFAP up-regulation, has been described as an early event in human retinopathy (Mizutani et al., 1998) and in experimental diabetes in rats (Lieth et al., 1998). In diabetes, gliosis is probably a consequence of the increased flux through the polyol pathway, the

accumulation of AGEs and oxidative stress-derived damage on Müller cells (Asnaghi et al., 2003; Curtis et al., 2011). The presence of gliosis in TgIGF-I retinas has been previously reported (Ruberte et al., 2004). However, the systematic evaluation performed here of GFAP up-regulation by inmunohistochemistry and Western blot at different ages has revealed that reactive gliosis is present in TgIGF-I retinas in animals as young as 1.5 months of age and maintained throughout the animal's life. The observation of gliosis at such early stages, when transgenic mice do not present any other alteration, neuronal or vascular, suggests that gliosis may be a direct consequence of IGF-I overexpression. In agreement with this, it has been described that the intraocular injection of the IGF-I protein can induce gliosis in Müller cells *in vivo* (Fischer et al., 2010).

The proliferation of Müller cells is another hallmark of reactive gliosis, and it has been associated with the development of epiretinal membranes in proliferative retinopathies (Sethi et al., 2005). $p27^{Kip}$ is an inhibitor of cyclin kinases that blocks the cellular transition from quiescent to proliferative state (Katayose et al., 1997). In healthy, adult retinas $p27^{Kip}$ is expressed specifically in Müller cells (Dyer and Cepko, 2000). After retinal injury, $p27^{Kip}$ is downregulated in Müller cells and the cell re-enters the cell cycle (Dyer and Cepko, 2000). Moreover, the retinal $p27^{Kip}$ knock-out presents reactive gliosis and vascular alterations from birth (Dyer and Cepko, 2000). It has been decribed that IGF-I action induces downregulation of $p27^{Kip}$ in several cell types, such in β-cells overexpressing IGF-I and in IGF-I-stimulated cortical neuronal precursors (Agudo et al., 2008; Mairet-Coello et al., 2009). Furthermore, it has

been proposed that mitogenic factors such as IGF-I and Platelet Derived Growth Factor (PDGF) contribute to Müller cell proliferation in experimental diabetes (Fletcher et al., 2007). When $p27^{Kip}$ expression was analyzed in TgIGF-I retinas, a marked reduction was observed in 6 and 7.5 month-old mice. This observation suggests that Müller cells of transgenic retinas are proliferating.

Microglial cells, considered the resident macrophages of the retina, also became activated early after retinal injury, which results in changes in their morphology and localization (Karlstetter et al., 2010). As previously described, the number of blood-derived microglial cells is increased in retinas from diabetic patients (Zeng et al., 2008) and also in 6 month-old TgIGF-I retinas (Haurigot et al., 2009). Having observed that gliosis was a very early event in transgenic retinas, the time-course of microglial infiltration was studied by immunofluorescent labeling with tomato lectin in Tg-IGF-I eyes. The number of tomato lectin positive microglial cells per retinal section was significantly increased in transgenic animals aged 3 months and older, confirming the existence of an inflammatory process in transgenic retinas. The increased microglial infiltration observed in transgenic retinas is in agreement with the increased expression of ICAM-1 in these transgenic retinas (Haurigot et al., 2009). ICAM-1 is also overexpressed in retinas from diabetic patients (McLeod et al., 1995) and in experimental diabetes (Adamis, 2002), and it is considered an indicator of inflammation. In addition, a careful evaluation of the morphology of microglial cells after tomato lectin labelling suggested that these microglial cells were activated, because activated microglial cells typically have rounded

shape and lack of processes. The activation of retinal microglia has also been described in human diabetes, particularly in areas of vascular injury (Zeng et al., 2008). These activated cells contribute to the progression of retinopathy secreting pro-inflammatory cytokines that may compromise both vascular and neuronal function (de Kozak et al., 1997; Nakazawa et al., 2007; Krady et al., 2005). In agreement with this, TNF-α and MCP-1 retinal levels were markedly increased in TgIGF-I retinas at 7.5 months of age.

The presence of chronic gliosis accompanied by microglial activation could cause the alteration of retinal homeostasis and the impairment of neuron-supportive functions of Müller cells in TgIGF-I retinas. Müller cells play an essential role in the recycling of neurotransmitters, a process fundamental for the normal functionality of synapses and to avoid neuronal excitoxicity. The latter refers to a state of neuronal overstimulation in the presence of increased levels of glutamate, the most important excitatory mediator in the retina (Bringmann et al., 2009b). Increased levels of the glutamate transporter GLAST and reduced activity of the enzyme glutamine synthetase, both involved in glutamate recycling, have been reported in experimental models of diabetes (Reichelt et al., 1997a; Lieth et al., 2000). Moreover, increased levels of glutamate have been detected in the vitreous cavity of diabetic patients suggesting that glutamate recycling is compromised in human retinopathy as well (Ambati et al., 1997). When analyzed in TgIGF-I retinas, the activity of glutamine synthase was reduced from early age, and this impaired activity was maintained throughout the observation period. The apparent increment of GS activity in transgenic retinas at 6 and 7.5 months of age in comparison with

younger transgenic mice could be associated with the likely proliferation of Müller cells in transgenic retinas, as indicated by $p27^{Kip}$ downregulation at this age. On the other hand, retinal expression of GLAST, the main glutamate transporter in Müller cells, showed a tendency to increase in transgenic retinas, although no statistically significant differences were attained. Increases in GLAST content have also been demonstrated in human diabetic retinas (Reichelt et al., 1997a), an observation that could be considered as a compensatory mechanism for the reduced functionality of this transporter. In this sense, decreased activity of the GLAST transporter has been reported in experimental diabetes (Li and Puro, 2002). Despite these marked alterations in glutamate recycling, no differences in the content of total glutamate were detected in transgenic retinas when compared with healthy controls. Possible explanations to this observation could be the technical difficulties inherent to glutamate measurement or the potential overactivation of other metabolic pathways in Müller cells that consume glutamate, such as production of glutathione, alanine or α-ketoglutarate ***(Scheme 1)*** (Bringmann et al., 2009b).

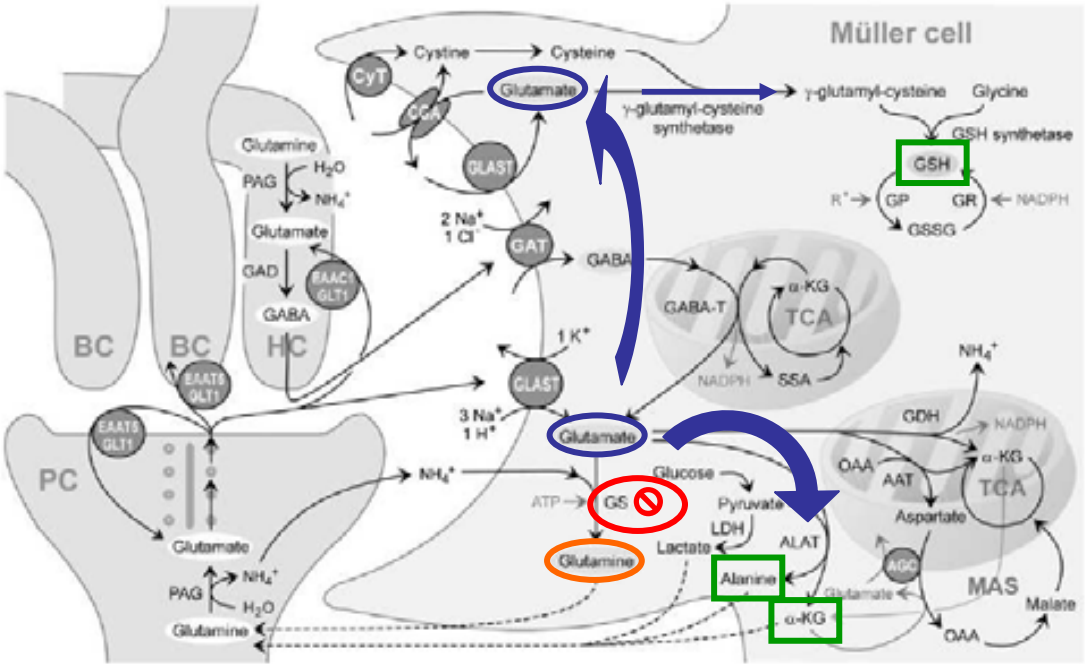

Scheme 1. Recycling of neurotransmitters in the outer plexiform layer of the mammalian retina. Uptake and metabolism of glutamate and gamma-aminobutyric acid (GABA) by Müller cells in the synaptic complex involving photoreceptors (PC), bipolar (BC) and horizontal cells (HC). Glutamate and GABA are transported to Müller cells and converted to glutamine, alanine, α-ketoglutarate or glutathione. These molecules are then released and taken up by neurons, which use them to generate neurotransmitters (glutamine), energy (alanine, α-ketoglutarate) or as an anti-oxidant (gluthatione). Impaired GS activity in Müller cells in TgIGF-I mice could be compensated by increased conversion of glutamate into alanine, α-ketoglutarate or glutathione, as suggested by increased levels of glutathione. Adapted from Bringmann et al. 2009b.

Increased ROS production and oxidative stress is a hallmark of diabetic complications (Brownlee, 2001). Glutathione is a major anti-oxidant molecule that protects retinal cells by scavenging free radicals. Together with horizontal cells and astrocytes, Müller cells are the main producers of glutathione, which constitutes about a 2% of the total protein in these cells (Paasche et al., 1998). In reactive gliosis and in hypoxic conditions glutathione levels are depleted in retinal Müller cells (Giaume et al., 2007; Huster et al., 2000). However, when analyzed in transgenic retinas, total glutathione levels were unchanged at 3 months of age and significantly increased in 6 and 7.5 month-old mice. This observation could be the consequence of two factors. First, the reduced

conversion of glutamate to glutamine due to decreased GS activity in transgenic Müller cells could induce the overproduction of glutathione in these cells, as an alternative pathway for glutamate metabolization. Secondly, $p27^{Kip}$ downregulation suggests that Müller cells are proliferating in older transgenic mice, and hence an increased number of these cells would result in increased levels of total retinal glutathione. On the other hand, oxidized glutathione was significantly increased in transgenic retinas at all ages studied, indicating the presence of oxidative stress in transgenic retinas. When the levels of carbonyl groups were analysed, only a non-statistically significant increase was observed in transgenic retinas in the levels of this compound that reflects the degree of oxidation of retinal proteins, suggesting mild oxidative stress. Given that TgIGF-I mice are not hyperglycaemic, the cause for any degree of oxidative stress that might be present in their retinas would be a direct consequence of cell dysfunction rather than excess substrate metabolization. An increase in the rate of production of nitric oxide (NO) by activated Müller and/or microglial cells could underlie this observation (Kobayashi et al., 2000; Krady et al., 2005). In this regard, iNOS expression was increased in 7.5 month-old TgIGF-I retinas, suggesting that increased production of NO could contribute to the formation of reactive species. The increase, however, was not observed in younger mice. iNOS expression is activated by TNF-α in retinal glial cells (Goureau et al., 1994), a cytokine which was also significantly increased in transgenic retinas by 7.5 months of age. High levels of NO cause neuronal death by inhibiting mitochondrial respiration, causing PARP activation or inducing excitotoxicity (reviewed in (Brown, 2010)). Thus, an increased rate of production of NO due to

iNOS upregulation in transgenic retinas could possibly play a role in the neuronal death detected.

Potassium homeostasis is essential for the maintenance of the membrane potential and, consequently, for proper neuronal function. Reactive gliosis is associated with inactivation of Kir 4.1, the main K+ channel in Müller cells, leading to impaired K+ conductance (Giaume et al., 2007). This observation has been reported by Pannicke et al. for three different models of reactive gliosis in rats, consequent to the development of ischemia, ocular inflammation and diabetes (Pannicke et al., 2004, 2005, 2006). Alterations in the distribution of Kir 4.1 immunoreactivity have also been observed in experimental models of gliosis (Pannicke et al., 2006; Ulbricht et al., 2008). The inactivation of the Kir4.1 channel resulted in altered potassium conductance, leading to retinal edema and impaired neuro-glia interaction due to reduced membrane hyperpolarization (Pannicke et al., 2006). In TgIGF-I retinas, Kir 4.1 inmunodetection showed a diffuse pattern of localization, when compared with healthy retinas in which the protein was observed mainly in the inner and outer limiting membrane and in perivascular areas, which suggests that the buffering of the potassium ions could be impaired in transgenic retinas.

Finally, both activated Müller and microglial cells can produce and secrete pro-inflammatory cytokines that contribute to the dysfunction of the blood-retinal barrier and can also directly cause neuronal death (Krady et al., 2005; Lebrun-Julien et al., 2009). Furthermore, activated microglia and activated Müller cells establish a positive feed-back for the production of pro-

inflammatory cytokines, stimulating each other (Wang et al., 2011). Amongst cytokines, TNF-α and MCP-1 have been reported to directly contribute to neuronal loss (Nakazawa et al., 2007; Lebrun-Julien et al., 2009). In human diabetic retinas and in experimental models of diabetic retinopathy, increases in TNF-α and MCP-1 as well as other cytokines have been observed (Suzuki et al., 2011; Joussen et al., 2002). In agreement with the significant gliosis and microgliosis observed in transgenic mice, the levels of both TNF-α and MCP-1 were increased at 7.5 months of age, an age that coincides with severe loss of vision according to ERG measurements and marked reductions in certain populations of retinal neurons, suggesting that these molecules could potentially contribute to the loss of neurons described in the transgenic retinas at this age.

As previously described, essential neuron-supportive functions that may compromise neuronal viability are defective from early ages in transgenic retinas ***(Scheme 2)***. However, neuronal activity was normal until advanced stages of the disease (6-7 months). It has to be taken into account that IGF-I is a pro-survival molecule that can act on neurons (D'Ercole et al., 1996). For its anti-apoptotic properties, IGF-I has been used to counteract neurodegeneration in experimental animal models of ischemic injury and vascular occlusion in the brain (Guan et al., 1993; Saatman et al., 1997; Liu et al., 2001). Thus, despite the profound alterations in retinal homeostasis caused by glial dysfunction, IGF-I overexpression may actually help neurons survive longer, which could provide an explanation for the lack of early alterations in neurons in TgIGF-I retinas. In addition, potential effectors of neuronal death, such as TNF-α and NO, are not increased until mice are 7.5 month-old, which could contribute to the marked

loss of neuronal populations and functionality observed at this age, but not earlier. At this stage, the IGF-I pro-survival effects could not be enough to overcome the retinal alterations present in the transgenic retinas. This hypothesis is summarized in the ***Scheme 3***, where the effects that IGF-I exerts on different cell types in the transgenic retinas are shown.

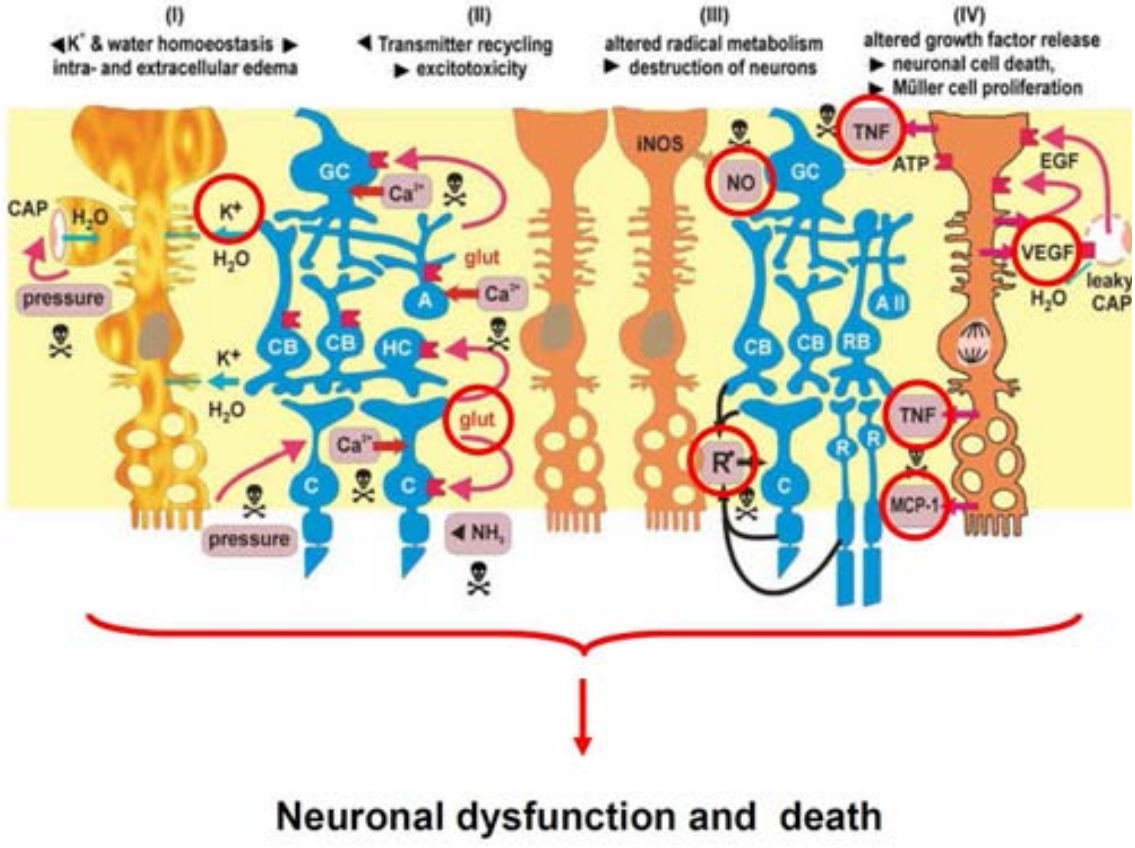

Scheme 2. Neuron-supportive functions altered in gliotic Müller cells underlying neuronal dysfunction and death in TgIGF-I retinas. Müller cell dysfunction can lead to neurodegeneration through different mechanisms. Indicated in red, impaired potassium buffering, alterations in the metabolism of glutamate, signs of oxidative stress and the production of pro-inflammatory cytokines may be causing neuronal dysfunction and death in TgIGF-I retinas. The vascular pathology observed in these mice can also contribute to the neurodegeneration. Adapted from Giaume et al. 2007.

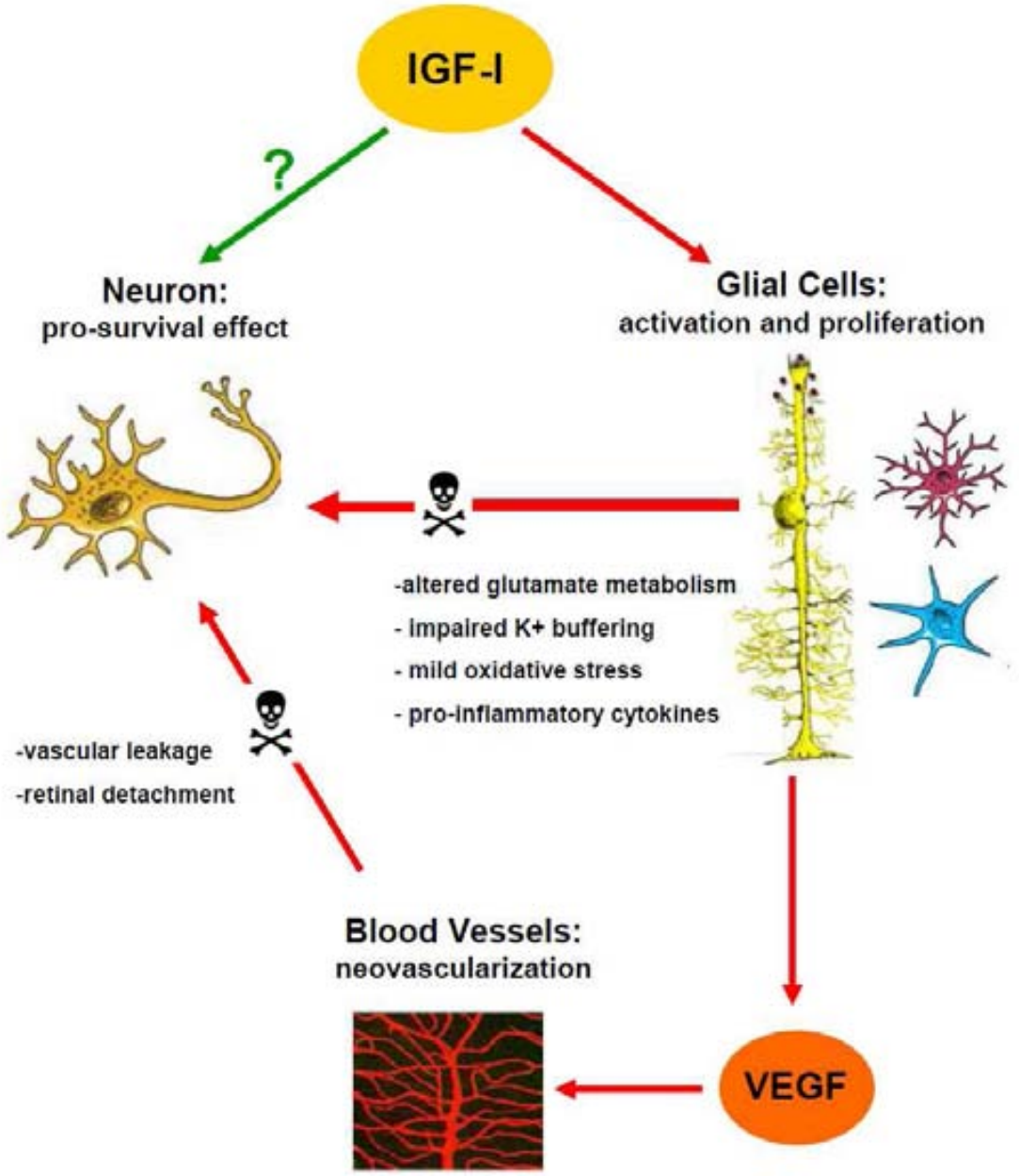

Scheme 3. IGF-I effects on different cell types in transgenic retinas. IGF-I acts on glial and microglial cells, activating them and disturbing their normal supportive functions, contributing to the neuronal death. IGF-I also stimulates VEGF production in glial cells (Ruberte et al., 2004), which participate in the development of the vascular pathology present in the transgenic retinas. Vascular leakage, the breakdown of the BRB and retinal detachment can also contribute to the loss of neuronal populations. In the other hand, IGF-I may exert neuroprotective effects in the transgenic retinas that delay the loss of neurons in this model.

In summary, transgenic mice overexpressing IGF-I in the retina present a phenotype characterized by the early alteration of glial cells that affects the maintenance of retinal homeostasis and neuron-supportive functions. These alterations may add to the vascular alterations that develop later to cause the progressive loss of retinal neuronal populations, with the concomitant loss of functionality, as demonstrated by ERG recordings. Most of these glial alterations are also present in experimental models of diabetes and in diabetic patients, in which alterations in ERG responses and loss of retinal neurons have also been described to precede vascular disease.

Part II: Evaluation of the Efficacy of Long-term PEDF Gene Expression in Counteracting Neovascularization and Neurodegeneration in TgIGF-I Retinas

The inhibition of ocular neovascularization is an unmet medical need in diabetic retinopathy and other proliferative diseases of the eye. The standard clinical practice, mainly based on photocoagulation and vitrectomy, is only able to delay the progression of vessel proliferation, and has serious adverse effects. New treatments with anti-VEGF drugs are being tested in patients, but their efficacy is dependent on the frequency of the readministrations. Repetitive intraocular injections can cause many problems in the treatment of a chronic disease like diabetic retinopathy. In contrast, AAV-based gene therapy offers the possibility of treating chronic diseases with a single administration of the vector.

The TgIGF-I model, but not other induced models of neovascularization, allows the long-term evaluation of the efficacy of antiangiogenic and neuroprotective therapeutic approaches, given the progressive evolution of its vascular, neuronal and glial alterations, resembling those of human diabetic patients. In the second part of this work, we examine the effects of a gene therapy protocol with an AAV2 vector containing the cDNA of PEDF, a potent antiangiogenic factor. In addition, PEDF have neuroprotective properties that may help to counteract the neuronal alterations present in both diabetic patients and the TgIGF-I mice. Thus, the efficacy of the intravitreal administration of AAV2-hPEDF in counteracting retinal neovascularization and neurodegeneration has been tested in TgIGF-I mice.

1. STUDY OF THE EFFECTS OF LONG-TERM PEDF OVEREXPRESSION ON COUNTERACTING NEOVASCULARIZATION AND NEURODEGENERATION IN TRANSGENIC TgIGF-I RETINAS

1.1. EXPERIMENTAL DESIGN OF THE AAV2-hPEDF GENE THERAPY APPROACH

Both diabetic retinopathy patients and TgIGF-I mice develop chronic pathologies, with slow progression, that start with almost undetectable vascular and neuronal alterations that worsen with time to an overt neovascular and fibrotic pathology with high risk of loss of vision (Antonetti et al., 2006; Ruberte et al., 2004; Haurigot et al., 2009). Taking this into account, it was hypothesized that a preventive therapy may be a useful approach to try and counteract this pathology/phenotype progression from early stages.

To this end, in this study, IGF-I transgenic animals of 1.5 months of age (with normal ERG, no neovascularization, only mild gliosis present) received intravitreal injections of AAV2-hPEDF vectors, carrying the cDNA of human PEDF, in the left eye ($6.4x10^8$ viral genomes (vg)/eye) and AAV2-null vectors, containing the same expression cassette but without coding cDNA, in the right eye ($2.4x10^8$ vg/eye). Non-proliferative aspects of the pathology were evaluated 2 months after the administration of the vectors. Six months after the treatment, at 7.5 months of age, ERG recordings were performed and animals were sacrificed and samples collected (Figure 30). As previously described, this is the age at which all TgIGF-I mice show clear neuronal, glial and vascular pathology, making this time point suitable for evaluation of therapeutic efficacy.

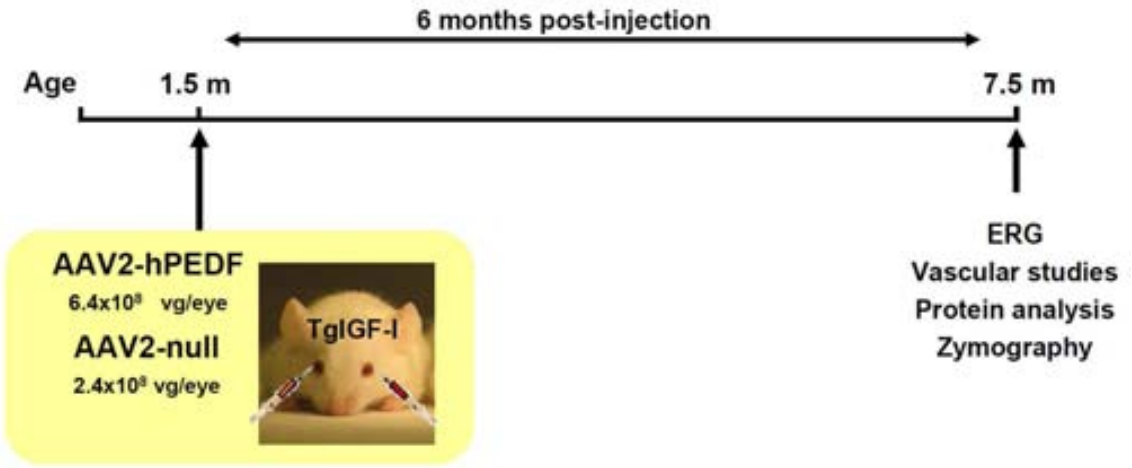

Figure 30. Experimental design of AAV2-hPEDF treatment in TgIGF-I mice. Animals received intravitreal injections of AAV2-hPEDF (left eye) and AAV2-null (right eye) at 1.5 months of age. Two months later, some of the animals were killed and pericytes were analysed. Six months after the treatment, ERG studies were performed, animals were sacrificed and samples were obtained for histological and molecular studies.

1.2. ANALYSIS OF THE AAV2 TROPISM IN TgIGF-I RETINAS

The tropism of AAV2 vectors after intravitreal injection has previously been described for wild-type rodent retina (Bennett et al., 1997; Hellström et al., 2009). It is known that in pathological conditions the tropism of a viral vector can be modified by changes in the profile of molecules in the target tissue that may act or not as putative receptors or co-receptors for the vector (Chen et al., 2009). To determine whether the pathology of TgIGF-I retinas (Ruberte et al., 2004; Haurigot et al., 2009) could alter the normal pattern of infection of AAV2 vectors after intravitreal injection, the expression of the reporter green fluorescent protein (GFP) was analysed after the delivery of AAV2-GFP ($6.2x10^7$ vg/eye) to 1.5-month-old transgenic mice. In this vector, the GFP gene was under the control of the ubiquitous hybrid CAG promoter, composed of the chicken beta actin and the citomegalovirus enhancer. A month after vector

administration, the majority of the cells on the retinal surface expressed GFP, as shown in flat-mounted retinas (Figure 31a). The protein was detected in cell bodies and also in superficial axons, indicating the transduction of ganglionar neurons whose axonal fibres converge to form the optic nerve (Figure 31a, arrows). When GFP immunostaining was performed on retinal sections (Figure 31b), the protein was also detected in cells located deeper in the retina (arrows in inset, Figure 31b) indicating that other cells, besides ganglion neurons, were expressing GFP.

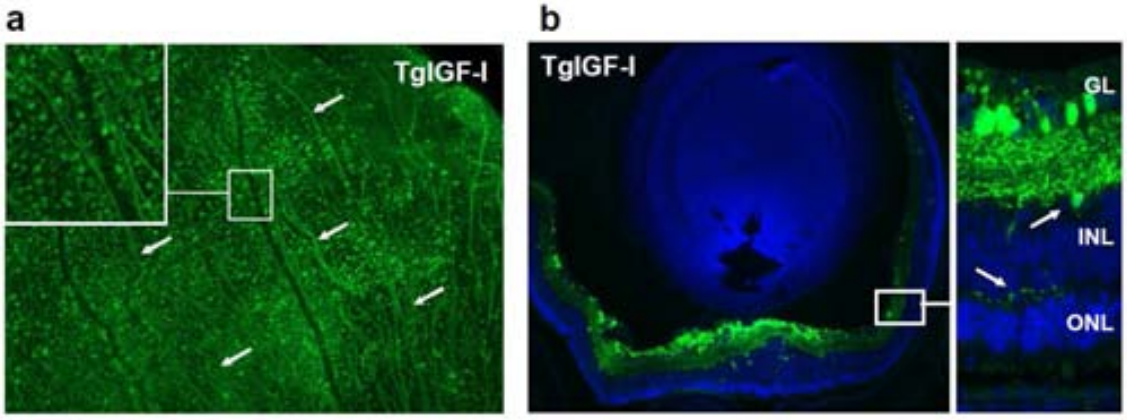

Figure 31. AAV2 tropism in TgIGF-I retinas a month after intravitreal injection. (a) Immunohistochemical detection of GFP (green) in flat-mounted retinas revealed extensive transduction of the cells located on the retinal surface. Long axons containing the GFP protein were also observed (arrows). **(b)** Retinal sections immunolabelled for GFP. Cells expressing GFP in the inner nuclear layer (INL) (inset, arrows) were detected. Nuclei were stained with TOPRO (blue). Original magnification: 10x (a), 2x (b).

To identify the cells expressing GFP in the inner layers of the retina, immunostaining with specific markers for each neuronal type was performed in retinal sections from transgenic mice 1 month post-injection of the vector. In addition to ganglionar cells, displaced amacrine neurons can also be found in the GCL of the retina (Jeon et al., 1998). These cells are a subpopulation of amacrine cells, the majority of which are located in the INL. As previously described, amacrine cells can be detected by calretinin expression (Kolb et al.,

2002). Cells co-expressing calretinin and GFP were observed in both the GCL and the INL in the AAV2GFP-injected transgenic retinas, indicating that the vector was able to transduce amacrine cells efficiently (Figure 32).

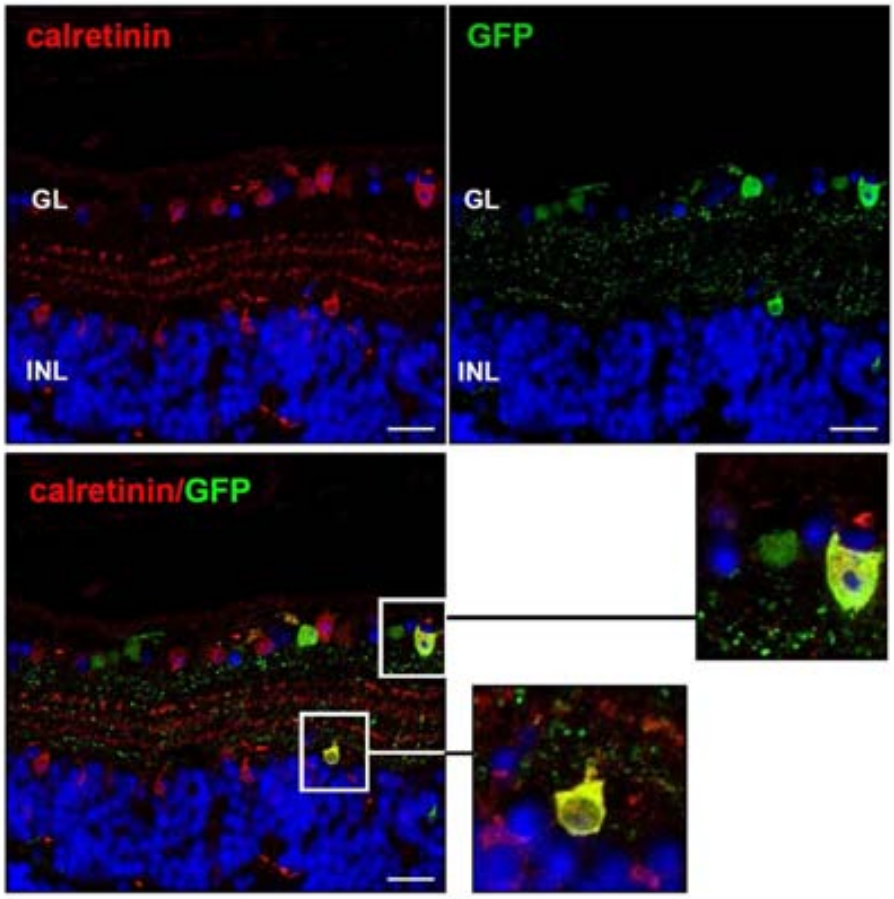

Figure 32. AAV2-GFP transduction of amacrine cells. Representative confocal images showing calretinin positive (red staining) amacrine cells co-expressing GFP (green staining) protein in both the GCL and the INL (insets) a month after intravitreal delivery of AA2-GFP vector, demonstrating that this vector is able to transduce amacrine cells. Nuclei were stained with TOPRO (blue). Scale bar: 33 μm.

Immunostaining with an antibody specific for calbindin allows the visualization of horizontal cells, placed in the outmost part of the INL, but also of certain subtypes of amacrine neurons (Wassle et al., 2000), which can be differentiated from calbindin-positive horizontal cells by their localization. One month after intravitreal administration of AAV2-GFP vectors, a few of the

calbindin-positive cells located in the outer INL also showed GFP expression indicating that these vectors had tropism for horizontal neurons (Figure 33). A few calbindin-positive amacrine cells located in the INL and the GCL also expressed GFP (Figure 33), confirming the previously observed tropism of AAV2 for amacrine cells (Figure 32).

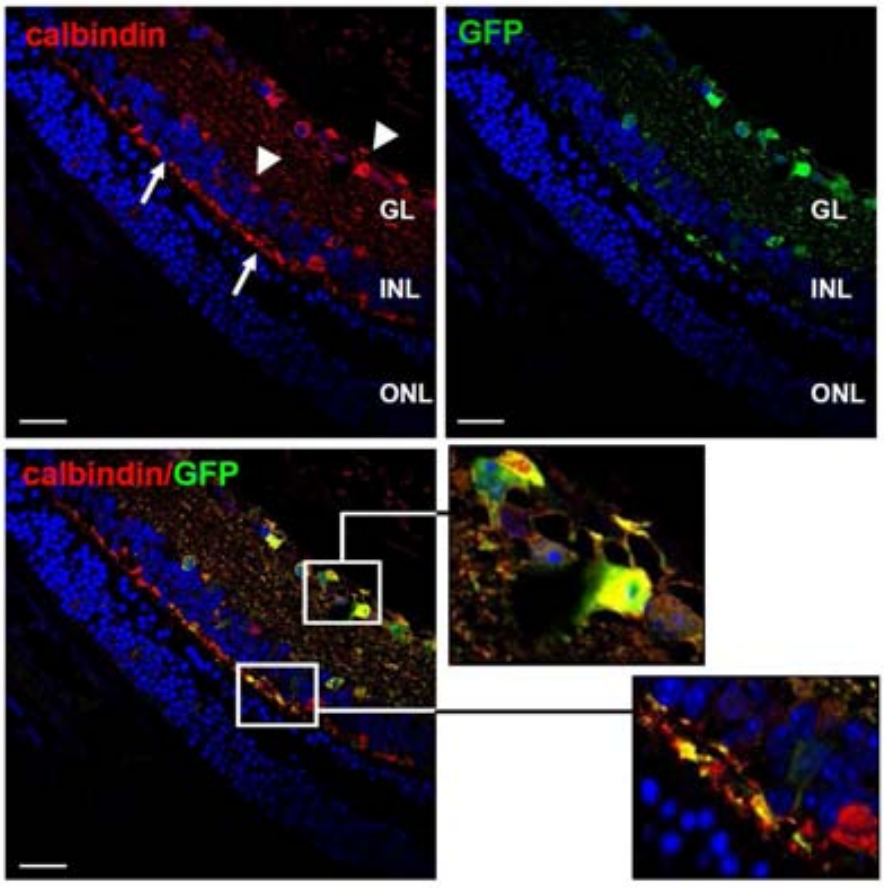

Figure 33. Transduction of calbindin-positive neurons by AAV2-GFP after intravitreal injection. Calbindin-positive horizontal cells were identified in the outmost portion of the INL (arrows). A few of these cells also expressed GFP (lower inset), revealing tropism of the AAV2 vector for this type of neurons after intravitreal injection in transgenic eyes. Certain subtypes of amacrine cells of the INL and GCL were also positive for calbindin immunostaining (arrowhead) and expressed GFP (upper inset), confirming the tropism of the AAV2 vector for these cells, as shown in Figure 32. Nuclei were stained with TOPRO (blue). Scale bar: 74 µm.

Bipolar neurons are detected by immunostaining with an antibody specific for protein kinase C alpha (PKCα) (Grunert et al., 1994). Despite the fact that bipolar cells are in close contact with the viral solution delivered to the

retinal surface after intravitreal administration, none of the PKCα-positive cells presented GFP co-localization when double PKCα/GFP immunostaining was performed in retinal sections a month after viral injection (Figure 34), indicating that AAV2 vectors are not able to transduce this type of retinal neurons in TgIGF-I retinas.

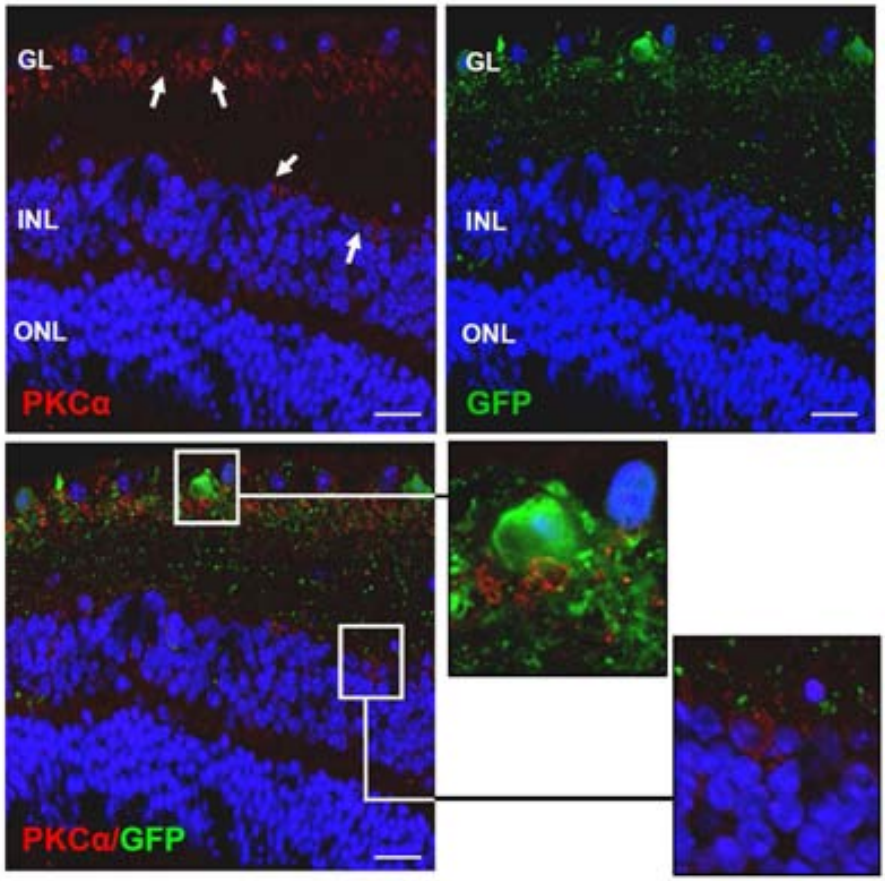

Figure 34. Bipolar neurons were not transduced by AAV2-GFP. Confocal images of PKC-α immunodetection in retinal sections from TgIGF-I mice receiving intravitreal AAV2-GFP. PKC-α positive bipolar cells did not show GFP expression in either the terminals in the GCL (upper inset) or in the cell bodies located in INL (lower inset). Nuclei were stained with TOPRO (blue). Scale bar: 33 μm.

As previously mentioned, Müller cells and astrocytes are the glial cells of the retina. Whereas Müller cell bodies span along the retina, from the ONL to the surface, astrocytes are found on the retinal surface, mostly surrounding

blood vessels. Both cells types are therefore in close contact with vector solution after intravitreal injection, but none of them were transduced by AAV2-GFP (Figures 33 and 34). No cells positive for glutamine syntethase (GS), a specific marker of Müller cells (Lewis et al., 1988) or S100, a specific marker of astrocytes (Casella et al., 2004) co-expressed GFP (Figures 35 and 36). This was likely due to the lack of AAV2-specific receptors on their cell-surfaces.

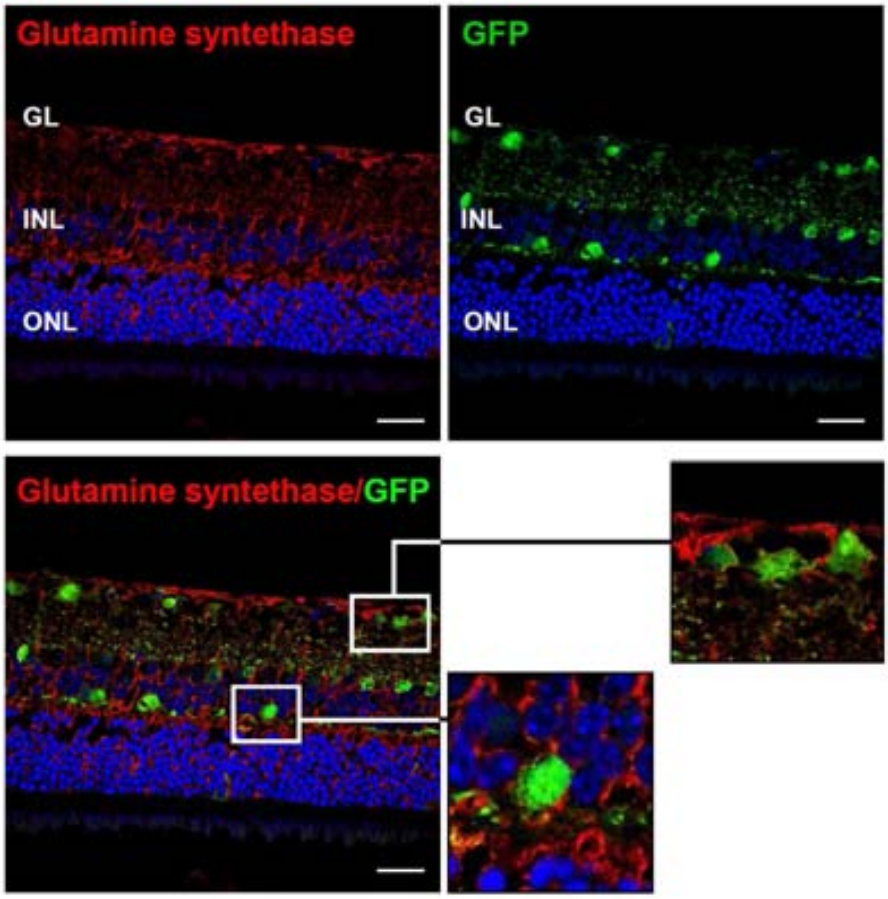

Figure 35. AAV2 vectors were not able to transduce Müller glial cells. Confocal images showed that glutamine synthetase (GS) positive Müller cells (red) did not exoress GFP (green) in either their end-feet processes in the GCL (upper inset) or in their cell bodies located in the INL (lower inset). Nuclei were stained with TOPRO (blue). Scale bar: 74 µm.

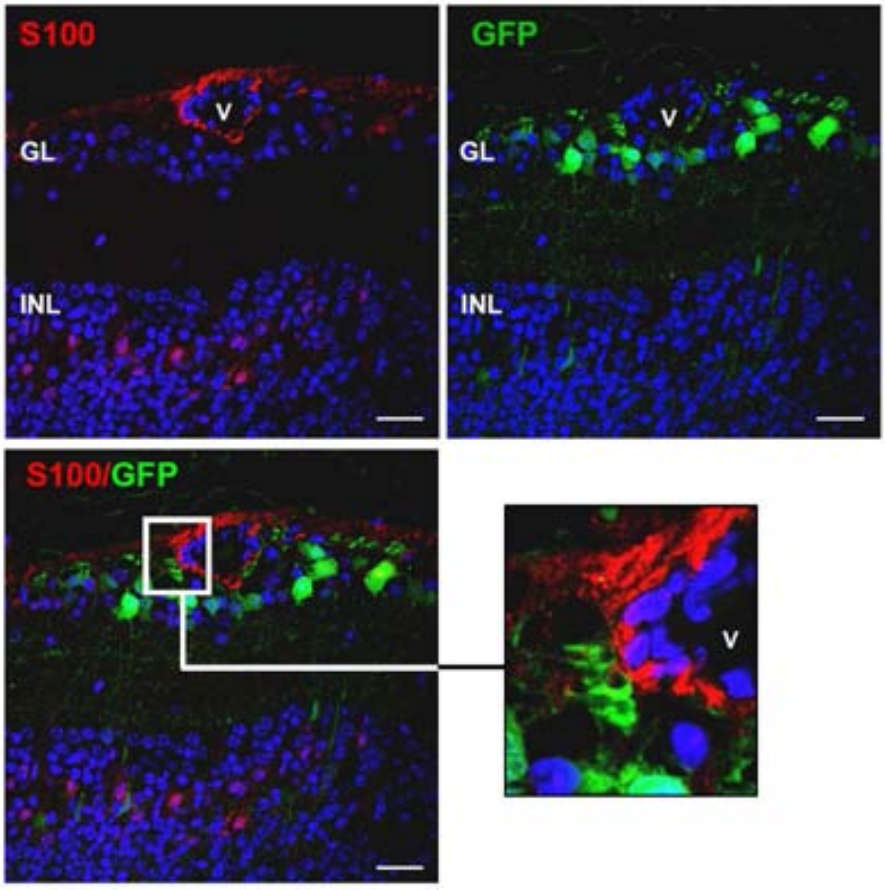

Figure 36. AAV2 vectors did not transduce astrocytes. A month after AAV2-GFP intravitreal delivery, no S100-positive astrocytes (red) showed GFP expression (green), as revealed by confocal imaging of transgenic retinal sections immunostained with S100 and GFP antibodies. Nuclei were stained with TOPRO (blue). Scale bar: 18 µm.

Collectively, the colocalization study with specific markers for the different populations of retinal cells indicated that intravitreal injection of AAV2 resulted in efficient transduction of TgIGF-I retinas, with expression of the transgene detected in ganglion, amacrine and horizontal neurons.

1.3. AAV-MEDIATED PEDF OVEREXPRESSION IN TgIGF-I RETINAS

It has been shown that AAV vectors allow prolonged and stable gene expression in the retina of rodents and large animal models (Bennett et al., 1997; Stieger et al., 2008). Both TgIGF-I mice and diabetic patients present a chronic pathology with slow progression that would require long-term production of the therapeutic agent in order to prevent the development of neovessels. To study the time-course of PEDF expression after AAV2 intravitreal administration, six week-old TgIGF-I mice received a single injection of $6.4x10^8$ vg of an AAV2-hPEDF and PEDF expression was evaluated at different time points post vector delivery. Using specific primers for human PEDF, that allow the detection of the transgene carried by the AAV2 vector but not the endogenous murine PEDF, quantitative RT-PCR showed high levels of PEDF in AAV2-hPEDF-injected retinas, whereas it remained undetectable in the retinas injected with AAV2-null vector (Figure 37). A steady level of expression of human PEDF was reached 2 months after vector administration and was maintained until at least 6 months after a single injection (Figure 37), confirming the long-term expression of the transgene after AAV2 delivery.

Six months after gene transfer, PEDF was detected by immunofluorescence with an antibody specific for PEDF in flat-mounted retinas, showing a pattern of expression similar to that observed in AAV2-GFP-injected retinas, with transduction of a high percentage of the superficial neurons (Figure 38a).

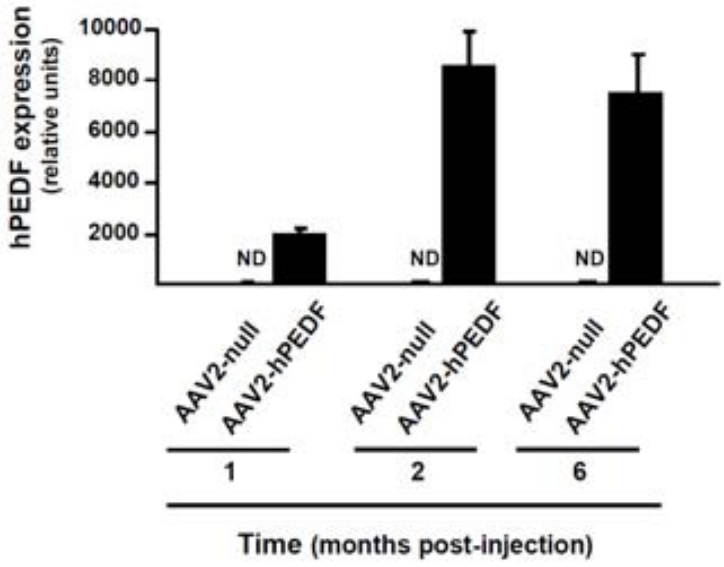

Figure 37. Time-course of hPEDF expression after a single intravitreal delivery of AAV2-hPEDF. Quantitative PCR analysis with transgene-specific primers revealed that hPEDF expression reached a plateau 2 months after a single injection of AAV2-hPEDF to 1.5-month-old TgIGF-I mice. hPEDF expression was undetectable in AAV2-null injected contralateral retinas. Sample load was normalized with ribosomal 36b4 expression levels. Values are expressed as the mean ±SEM of 3 animals/group.

PEDF was also measured by Western blot in retinal extracts 6 months after vector delivery (Figure 38b). Retinal levels of PEDF in transgenic mice receiving a single administration of AAV2-hPEDF vector were more than 6-fold higher than those of non-injected retinas (Figure 38b). Non-treated TgIGF-I mice also showed an increase in endogenous retinal PEDF expression (the antibody used recognized both human and murine PEDF). This suggested that the upregulation of endogenous PEDF may have been one of the mechanisms by which non-treated transgenic mice attempted to counteract the pro-angiogenic stimulus present in their eyes.

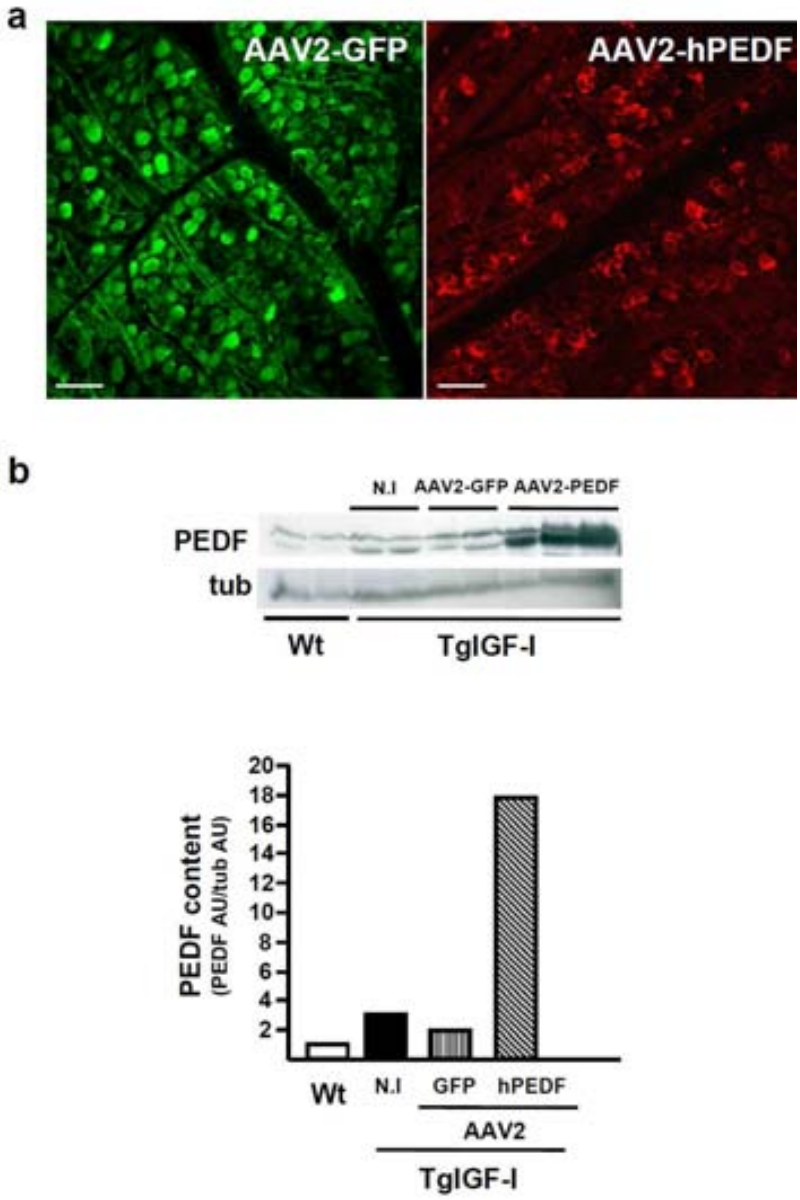

Figure 38. PEDF retinal content 6 months after a single intravitreal injection of AAV2-hPEDF. (a) Immunofluorescent detection of GFP (left panel) and PEDF (right panel) in retinal flat mounts 6 months after a single intravitreal injection of AAV2-GFP or AVV2-hPEDF demonstrating the expression of the exogenous transgenes. **(b)** PEDF detection by Western Blot in retinas of transgenic treated mice. Wild-type, non-injected and AAV2-GFP-treated transgenic mice were used as controls. Normalization by tubulin content corrected for loading differences. AU: arbitrary units. Values are expressed as the mean ±SEM of 4-6 animals/group. Scale bar: 33 μm (a).

The immunofluorescent detection of GFP and PEDF in retinal cells of animals aged 12 and 18 months, respectively, that received a single injection of vector at 1.5 months of age, confirmed the lifelong persistence of expression of the gene of interest after a single AAV administration to the rodent retina (Figure 39).

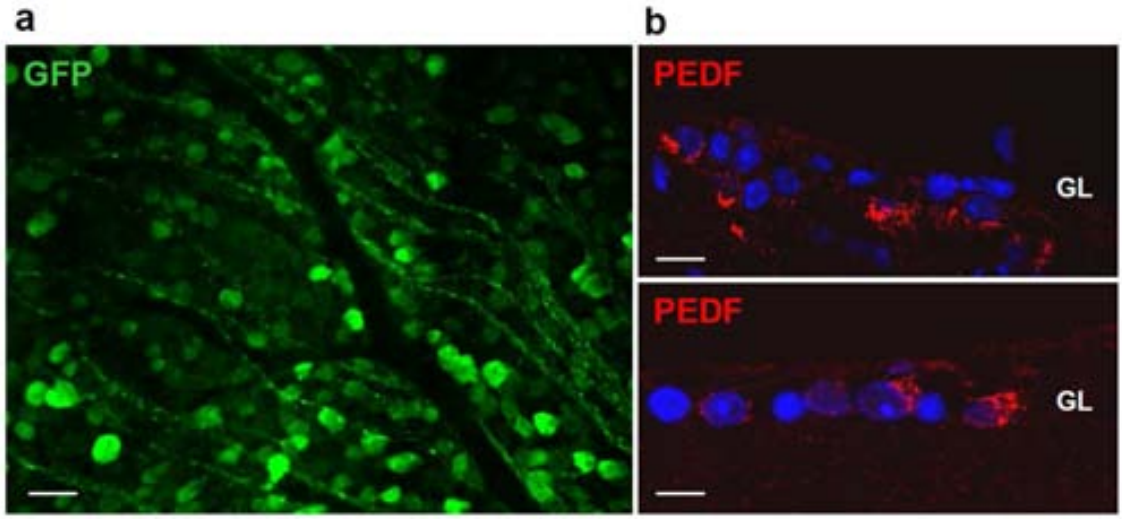

Figure 39. Long-term expression of exogenous genes after a single AAV2-mediated intravitreal gene delivery. (a) Inmunofluorescent detection of GFP (green, intracellular protein) in a flat-mounted retina 12 months after a single injection of AAV2-GFP to a wild-type mouse. **(b)** PEDF (red, secreted protein) inmunodetection in paraffin-embedded eye sections 18 months after a single intravitreal injection of AAV2-hPEDF to TgIGF-I. Scale bars: 66 μm (a), 105 μm (b, upper panel), 94 μm (b, lower panel).

1.4. STUDY OF THE EFFECTS OF PEDF OVEREXPRESSION ON THE RETINAL VASCULATURE OF TgIGF-I MICE

1.4.1. Effects of PEDF treatment on non-proliferative retinopathy

Pathological alterations characteristic of non-proliferative retinopathy, such as loss of pericytes and thickening of the vascular basement membrane (BM) have been reported in retinal capillaries of TgIGF-I mice (Ruberte et al., 2004). By transmission electron microscopy it was previously determined that the basement membrane of transgenic retinal vessels, more specifically of capillaries, was thickened at 2-3 months of age (Ruberte et al., 2004). This study was also performed in transgenic eyes with and without AAV2-hPEDF treatment 6 months after vector intravitreal delivery. Electron microscopy images of at least 5 retinal capillaries were obtained and the thickness of the BM was determined by morphometric analysis. The basement membrane in retinal capillaries appeared thinner in AAV2-hPEDF treated mice when compared with non-treated and AAV2-null treated mice (Figure 40a). Quantitative assessment revealed a slight reduction in the thickness of the vascular basement membrane in AAV2-hPEDF-treated eyes (Figure 40b). Although this reduction did not reach statistical significance, it suggested a beneficial effect of PEDF overexpression on the retinal capillaries of TgIGF-I mice.

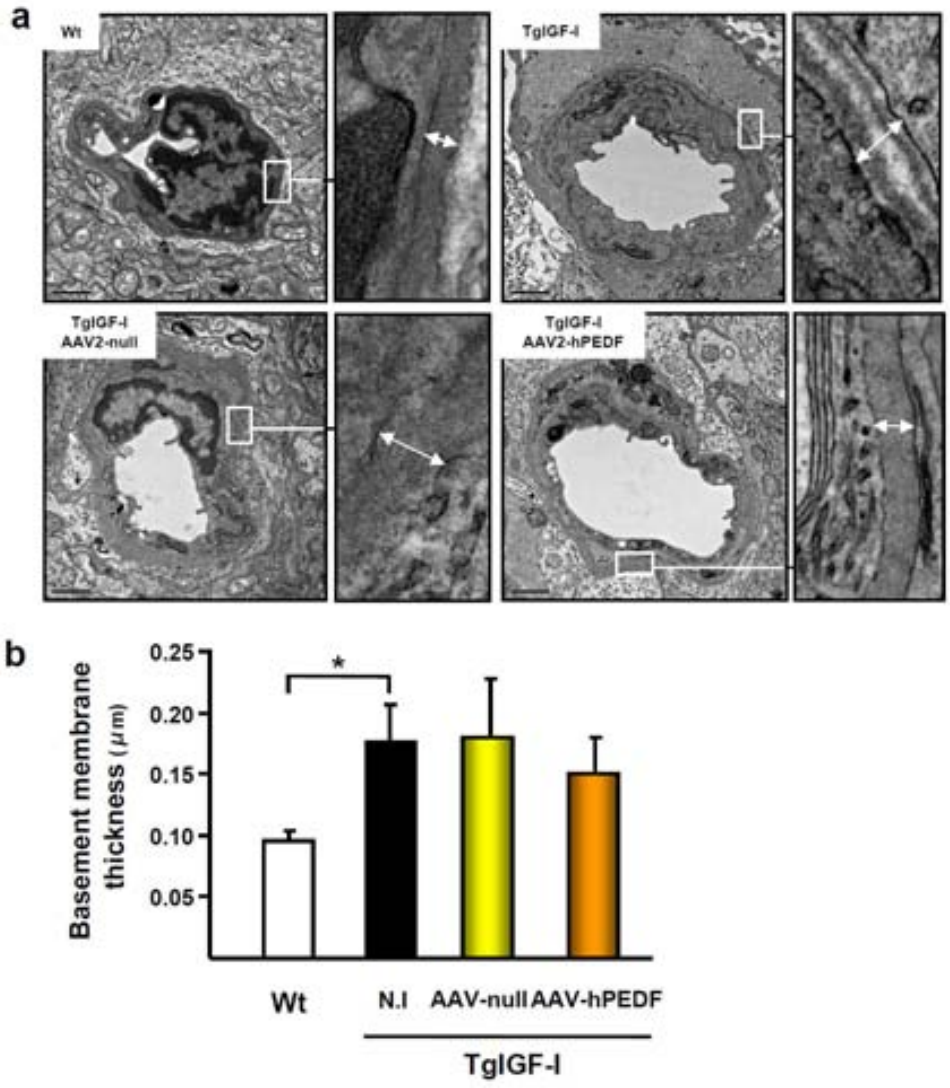

Figure 40. Effect of AAV2-hPEDF treatment on capillary basement membrane. (a) Transmission electron microscopy images showing capillary vessels from wild-type (Wt) and transgenic non-injected, AAV2-null-injected and AAV2-hPEDF-injected retinas 6 months after treatment. Right insets show areas of vascular basement membrane at high magnification. **(b)** Quantification of the thickness of the basement membrane in 5 capillary/retina. Twelve measurements were performed per vessel. AAV2-mediated hPEDF overexpression led to a statistically non-significant reduction of the basement membrane thickness in comparison with AAV-null injected animals. Values are expressed as the mean ±SEM of 3 animals/group. p*<0.05. Scale bar: 1 μm (a).

1.4.2. Evaluation of AAV2-hPEDF effects on intraretinal neovascularization

To study the antiangiogenic effects of PEDF on TgIGF-I retinas, fluorescein angiographies were performed in Wt and TgIGF-I mice with and without PEDF treatment. This technique allowed the evaluation of vascular morphology and the quantification of retinal capillary density. At 7.5 months of age, fluorescein angiographies of untreated and AAV2-null injected TgIGF-I mice revealed the presence of vascular abnormalities and areas of neovascularization in the retina (Figure 41a), as previously reported (Ruberte et al., 2004). AAV2-hPEDF treatment prevented the development of these retinal vascular alterations in treated TgIGF-I mice (Figure 41a). To quantify the inhibitory effects of PEDF on the intraretinal vasculature, retinal capillary density was determined by digital image analysis of fluorescein angiographies at high magnification. Twenty images at 40x were captured per retina, and the green area corresponding to capillaries was quantified with the NIS-Elements software. Representative images used for this morphometric analysis are presented in Figure 41c.

Figure 41. Inhibition of intraretinal neovascularization by AAV2-hPEDF treatment. (a) Representative whole-mounted retinal angiographies with fluorescein-conjugated dextran of Wt and IGF-I transgenic mice 6 months after intravitreal injection with AAV2-null or AAV2-hPEDF. AAV2-null injected transgenic retinas showed vascular abnormalities, characteristic of the neovascularization present in IGF-I transgenic mice (inset). The retinas of transgenic AAV2-hPEDF treated mice had a less pathological aspect suggesting a beneficial effect of PEDF on retinal vasculature. **(b)** Digital image quantification showed a significant increase in the retinal capillary density in transgenic animals compared with Wt. Six months after a single treatment with AAV2-hPEDF transgenic retinas showed a capillary density similar to that of Wt healthy retinas. **(c)** Representative images used for morphometric quantification of capillary density. Original magnification: 1x (a), 40x (c). Values are expressed as the mean ±SEM of 7 animals/group. $p^*<0.05$

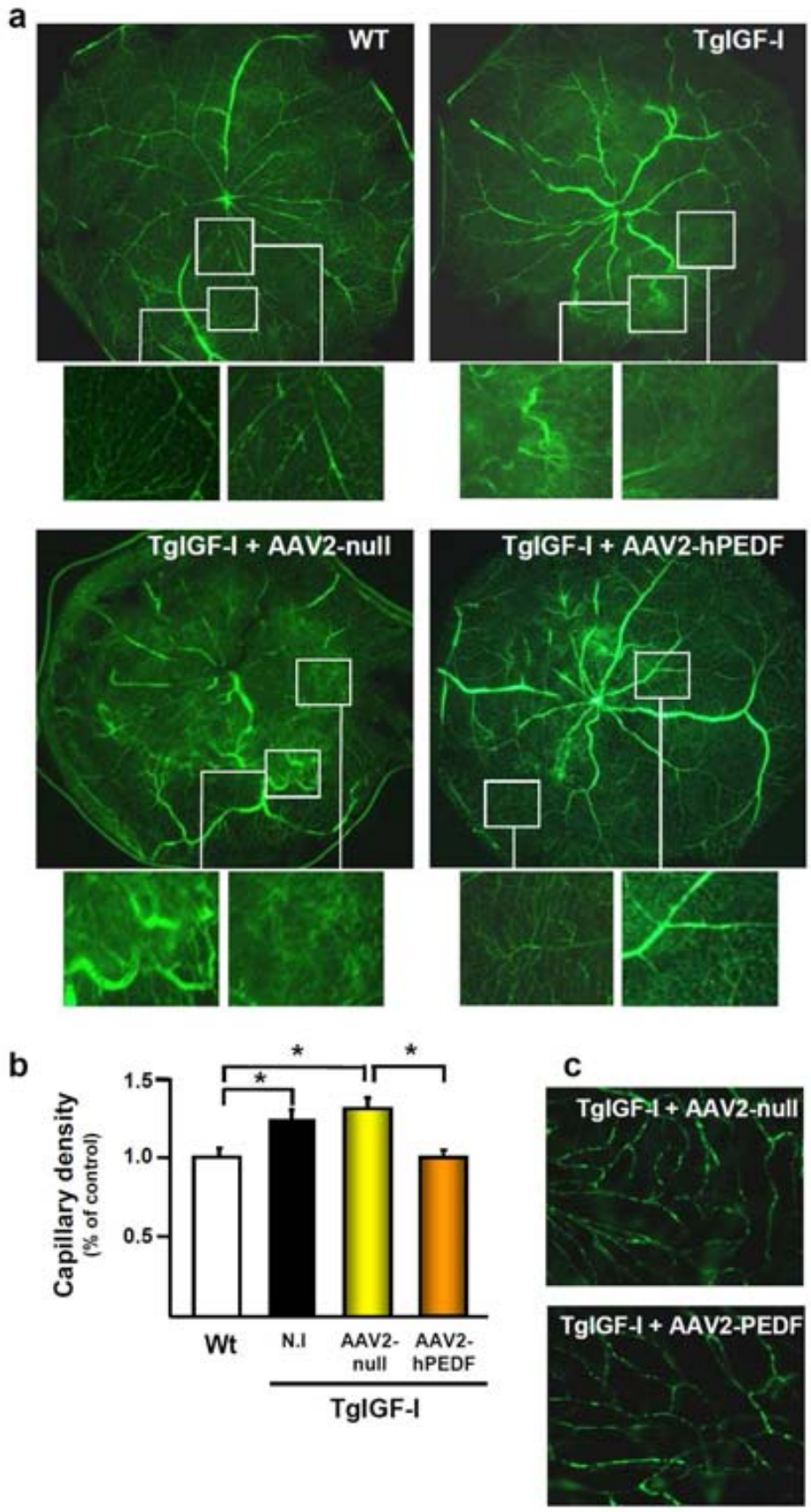
a
WT
TgIGF-I
TgIGF-I + AAV2-null
TgIGF-I + AAV2-hPEDF
b
Capillary density
(% of control)
1.5
1.0
0.5
*
*
*
Wt
N.I
AAV2-null
AAV2-hPEDF
TgIGF-I
c
TgIGF-I + AAV2-null
TgIGF-I + AAV2-PEDF

TgIGF-I mice showed an increment of 20% in the capillary density in comparison with age-matched Wt animals. Six months after treatment, transgenic retinas treated with hPEDF presented a capillary density similar to that of healthy retinas (Figure 41b). This suggested that vector-mediated PEDF overexpression succeeded in counteracting the ongoing neovascularization process present in transgenic retinas without affecting stable pre-existing vessels.

1.4.3. Evaluation of AAV2-hPEDF effects on intravitreal neovascularization

Intravitreal neovascularization is a hallmark of proliferative retinopathy and is highly associated with loss of vision due to retinal detachment (Porta and Bandello, 2002). Given the potentially deleterious consequences of the development of intravitreal neovascularization, it is important to develop new therapies that counteract the proliferation of vessels in the vitreous cavity. The intraocular accumulation of IGF-I in the TgIGF-I model results in abnormal growth of neovessels in the vitreous cavity (Ruberte et al., 2004). Two methods, in parallel, were used to characterize and quantify the effects of AAV2-hPEDF treatment on intravitreal neovascularization in TgIGF-I. First, eye sections were analysed after PAS staining, a standard method to identify and quantify intravitreal neovessels (Smith et al., 1994). Transgenic eyes from mice aged 7.5 months presented PAS positive intravitreal structures that were not present in Wt animals at the same age (Figure 42a). In transgenic eyes, it could be observed the presence of fibrotic tissue associated to the intravitreal vessel attached to the inner limiting membrane of the retina, in an area where the

retinal morphology appeared altered (inset Figure 42a). Double immunostaining with collagen type IV (ColIV) and CD105, markers of basement membrane and endothelial cells, respectively, was performed on Wt and transgenic retinal sections to ensure the vascular nature of these intravitreal structures. As showed in Figure 42b, in the vitreous cavity of transgenic eyes, CD105 positive cells formed a rounded structure that was surrounded by a ColIV positive ring. Therefore, the use of specific vascular markers allowed the identification of these intravitreal structures as neovessels formed by endothelial cells and surrounded by basement membrane.

.

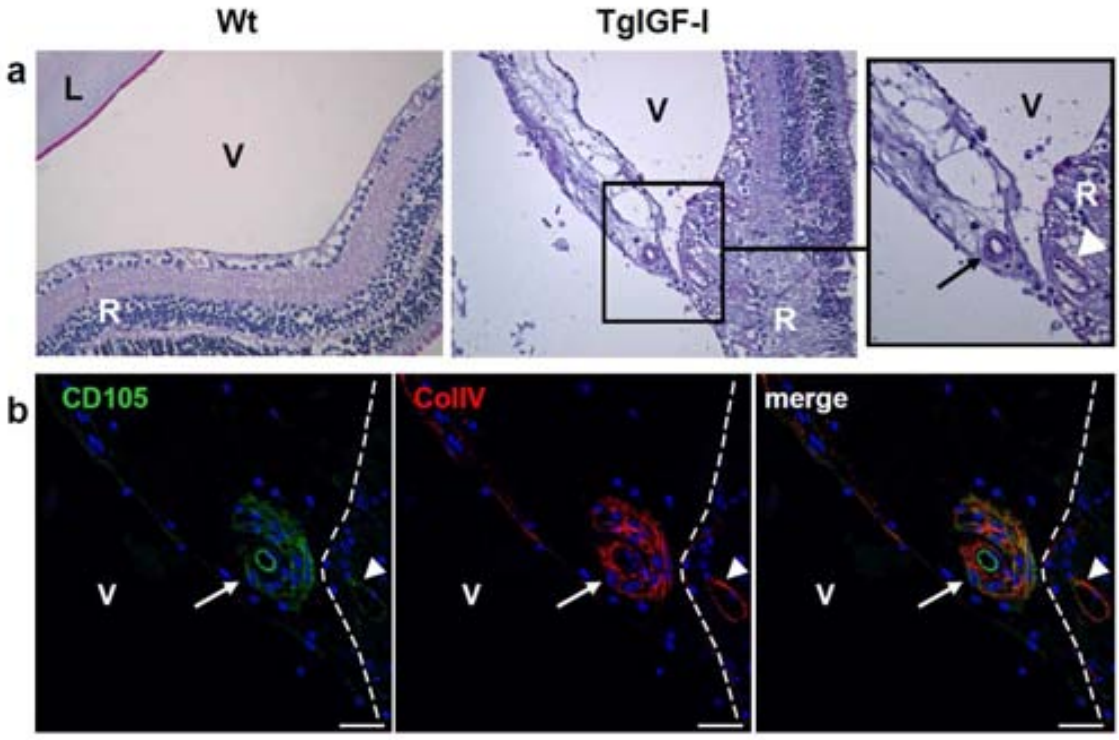

Figure 42. Intravitreal neovessels in 7.5 month-old TgIGF-I mice. (a) Representative image of PAS-stained sections of transgenic eyes showing intravitreal vessels. Wild-type eyes did not present vascular structures nor fibrosis in the vitreous cavity. **(b)** ColIV and CD105 inmunostaining in the same intravitreal neovessel corresponding to a transgenic mouse aged 7.5 months. Arrows indicate completely formed intravitreal neovessels. Arrowheads indicate a blood vessel within the retina. The dashed line indicates the limit between the retina and the vitreous. L, lenses, V, vitreous cavity, R, retina. Original magnification: 20x (a). Scale bar: 25 µm (b).

Then, AAV-injected eyes were investigated for the presence of intravitreal vessels 6 months after vector administration. As in non-treated TgIGF-I eyes, CD105+/Col-IV+ vascular structures were also detectable in the vitreous cavity of transgenic eyes receiving AAV2-null vector (Figure 43), but no vessels were observed in the vitreous cavity of any of the contralateral eyes treated with AAV2-hPEDF.

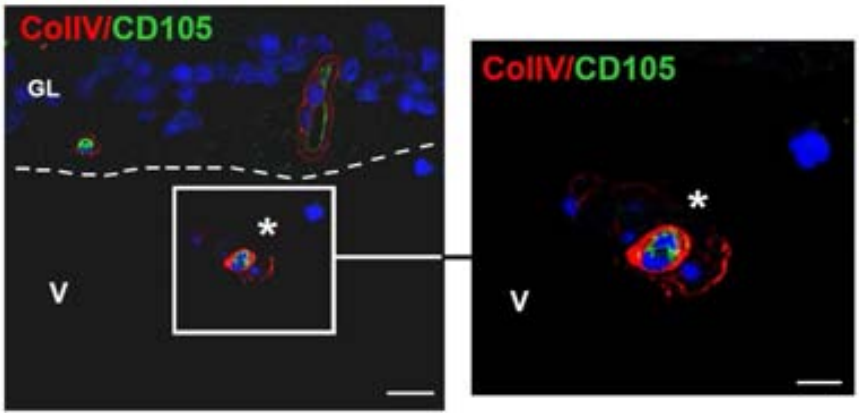

Figure 43. Inhibition of preretinal neovascularization by AAV2-hPEDF treatment. Double immunolabelling for CD105 and Collagen Type IV of retinal sections. Representative image of the CD105+/Col-IV+ vascular structures (asterisks) present in the vitreous cavity of AAV2-null injected eyes 6 months after delivery of the vectors. No such structures were observed in the contralateral PEDF-treated eyes. The dashed line indicates the limit between the retina and the vitreous. GCL, ganglion cell layer; L, lenses; V, vitreous. Scale bar: 25 µm (left pannel), 7.5 µm (right pannel).

Similarly, after PAS-haematoxylin staining, no vessels were observed in the vitreous cavity of the right, PEDF-injected eyes (Figure 44), whereas they were easily detected in the AAV2-null-injected eyes. Quantification of intravitreal PAS+ cells in eyes from the same animal receiving AAV2-null injection in the right eye and AAV2-hPEDF treatment in the left eye revealed that PEDF gene delivery led to a striking reduction in the number of these cells, likely vascular

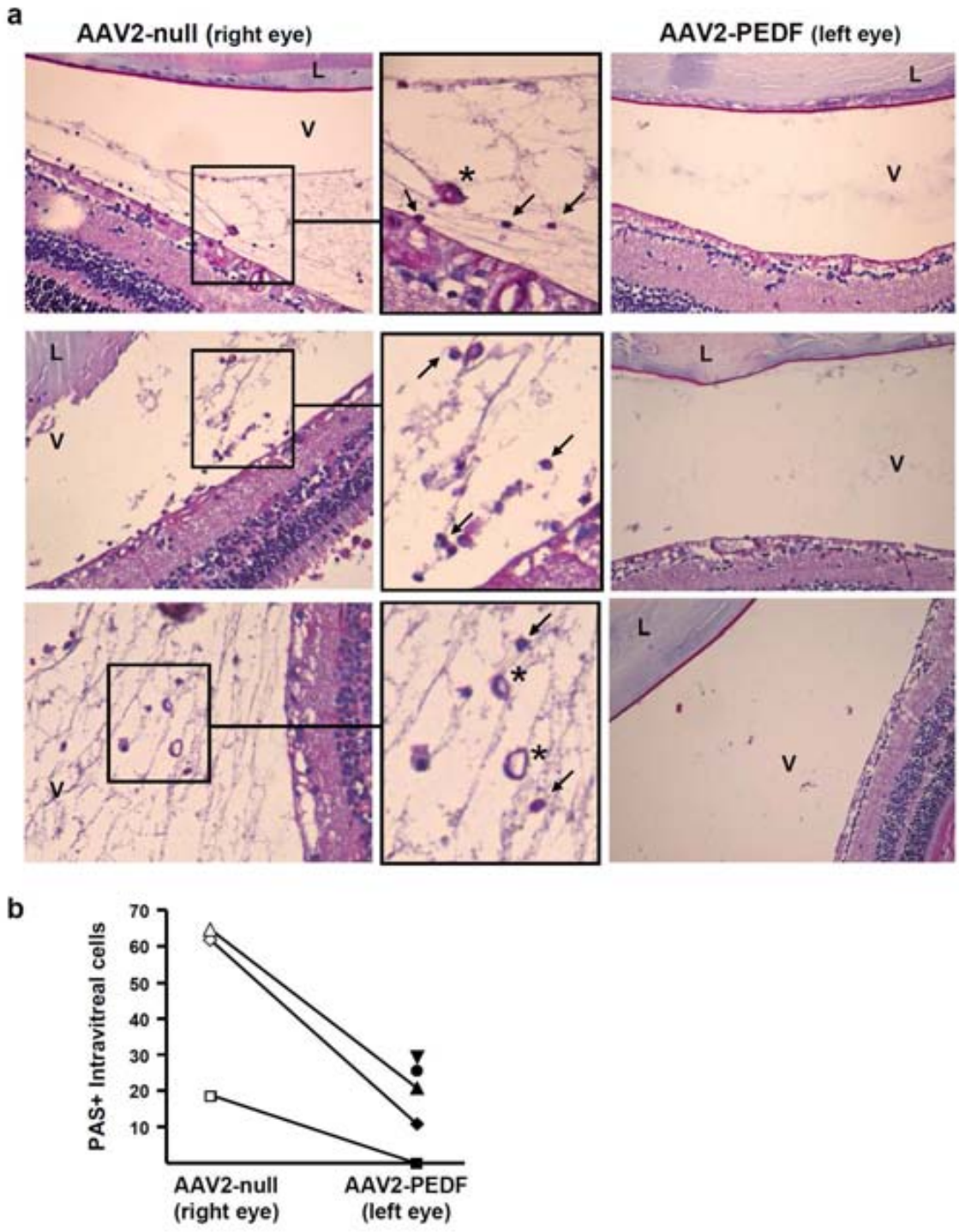

Figure 44. Inhibition of preretinal neovascularization by AAV2-hPEDF treatment. Representative micrographs of PAS-haematoxylin stained sections of the right (AAV2-null injected) and left (AAV2-hPEDF injected) eyes from TgIGF-I mice 6 months after delivery of the vectors. Note the presence of completely formed neovessels (insets, asterisks) in the vitreous cavity of AAV2-null-injected eyes. AAV2-hPEDF treated eyes showed a striking reduction in the number of intravitreal PAS positive cells when compared with their untreated contralateral eyes. Two null-injected transgenic eyes could not be analysed due to marked retinal detachment that impeded the counting of PAS+ cells in the vitreous cavity. Original magnification 20x.

cells (Smith et al., 1994), with respect to the untreated contralateral eye in all animals analysed. Two null-injected transgenic eyes could not be analysed due to marked retinal detachment that impeded the counting of PAS+ cells in the vitreous cavity.

1.5. STUDY OF THE INCIDENCE OF RETINAL DETACHMENT AFTER AAV2-hPEDF TREATMENT

Retinal detachment can occur in advanced diabetic retinopathy as a consequence of intravitreal neovascularization that tractionally detaches the neuroretina from the supporting pigment epithelium leading to visual loss (Agardh and Agardh, 2004). Old TgIGF-I mice present a high incidence of retinal detachment, characterized by folded areas in the retina and by the presence of subretinal cells, probably macrophages (Ruberte et al., 2004). In agreement with the inhibitory effect of PEDF on preretinal neovascularization, six months after vector injection the incidence of retinal detachment, determined by histological evaluation, was 83% for the AAV2-null treated eyes while it was only of 16.5% for the AAV2-hPEDF treated eyes. Representative histological images of AAV2-null-injected and AAV2-hPEDF-treated transgenic eyes are shown in Figure 45. Retinal folds and infiltrating cells were present in detached areas of AAV2-null treated retinas. These results clearly indicated that PEDF treatment, either directly or through the inhibition of intravitreal neovascularization was very efficacious in preventing retinal detachment, a sight-threatening complication of proliferative retinopathies.

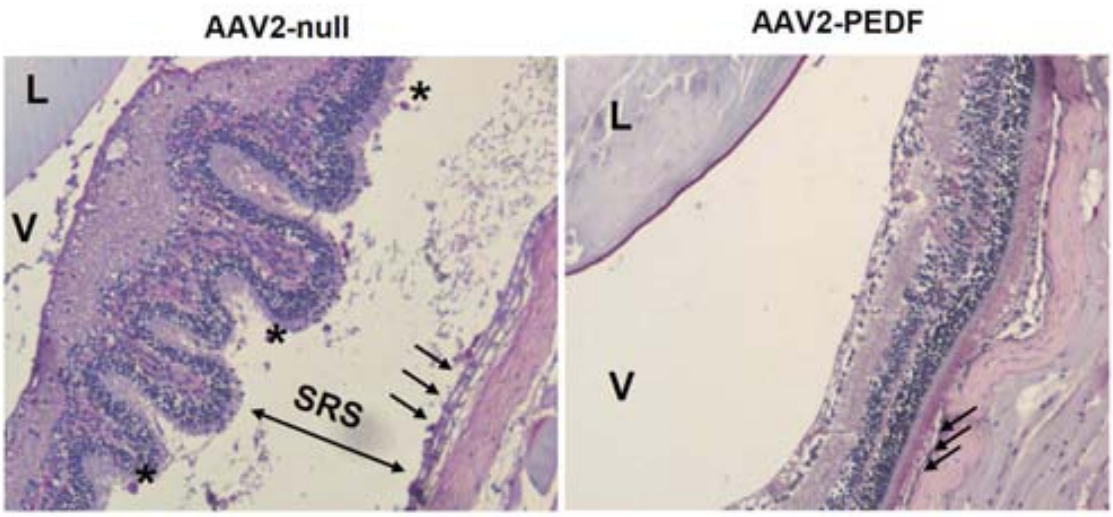

Figure 45. PEDF gene delivery prevents retinal detachment in TgIGF-I mice. Areas of retinal detachment were identified histologically by the presence of retinal folds. Infiltrating cells were observed in the subretinal space created around the detachment (left panel, asterisks). Black arrows indicate the monolayer of cells than constitute the Retinal Pigment Epithelium (RPE). Representative micrographs of the AAV2-null and AAV2-hPEDF injected eyes of the same animal are shown. L, lenses; V, vitreous,; SRS, Subretinal space. Original magnification: 10x.

1.6. MOLECULAR CHANGES IN TRANGENIC RETINAS INDUCED BY AAV2-hPEDF TREATMENT

The molecular mechanism by which PEDF exerts its anti-angiogenic properties has not been clearly identified. PEDF has been reported to interfere with VEGF pro-angiogenic signalling (Cai et al., 2006; Wang et al., 2006b). To determine the molecular changes underlying the anti-angiogenic effects of PEDF in transgenic retinas, the intraocular levels of VEGF and other up and downstream mediators of angiogenesis were analysed in 6 months after receiving AAV2-hPEDF.

1.6.1. Intraocular levels of VEGF

VEGF is the most potent angiogenic factor described (Ferrara, 2000) and it is increased in ocular fluids in patients with proliferative retinopathy and also in animal models of retinal neovascularization (Aiello et al., 1994; Pierce et al., 1995), including TgIGF-I mice (Ruberte et al., 2004; Haurigot et al., 2009). One possible mechanism for PEDF antiangiogenic action is the downregulation of VEGF expression (Wang et al., 2006b). Enzyme-linked immunosorbent assay (ELISA) for mouse VEGF was performed to elucidate if PEDF overexpression led to reduced intraocular levels of VEGF in TgIGF-I mice. It is unfeasible to obtain vitreous samples from mice due to the small size of this cavity in rodents; for this reason, VEGF detection was performed in aqueous humour samples. The measurement of concentrations in the aqueous humour is considered a good surrogate of the vitreous, and VEGF levels in the aqueous humour of human patients is proportional to those of the vitreous humour (Aiello et al., 1994). Then, VEGF concentration was measured by ELISA in aqueous humour samples from Wt and untreated, AAV2-null and AAV2-hPEDF treated TgIGF-I mice at 7.5 months of age to determine if PEDF treatment had any effect on VEGF ocular levels. Samples obtained from non-injected and AAV2-null injected TgIGF-I eyes showed a 50% increment in VEGF levels with respect to Wt eyes (Figure 46), which was in agreement with previous observations (Ruberte et al., 2004; Haurigot et al., 2009). In contrast, 6 months after a single administration of AAV2-hPEDF, VEGF levels were normalized in transgenic eyes (Figure 46). This reduction in VEGF levels was consistent with the inhibition of neovascularization observed by quantitative fluorescein angiography and PAS staining (Figures 41 and 44).

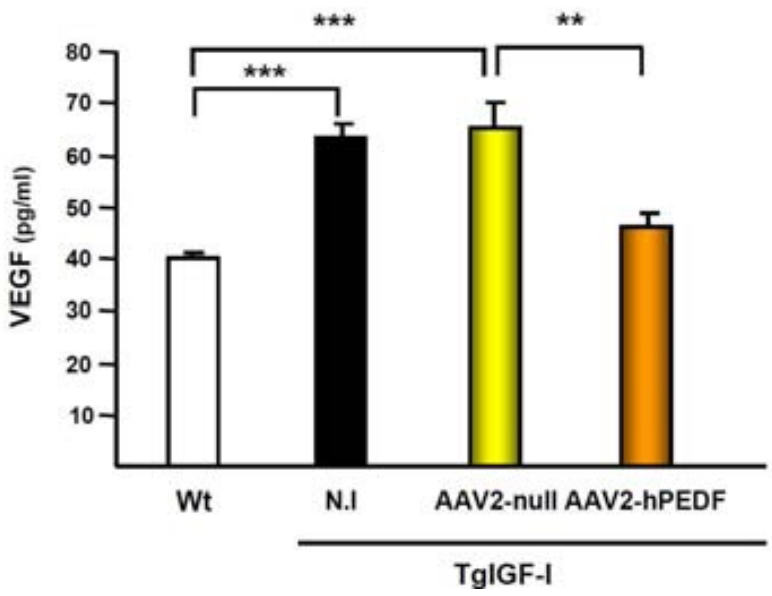

Figure 46. Effects of AAV2-hPEDF treatment on the intraocular levels of VEGF. Detection by enzyme-linked immunosorbent assay (ELISA) specific for mouse VEGF showed increased intraocular levels of VEGF in 7.5 month-old non-treated TgIGF-I when compared with age-matched Wt mice. VEGF levels were normalized in AAV2-hPEDF treated TgIGF-I mice 6 months after a single administration of the vector (7.5 months of age), whereas VEGF levels remained unchanged in AAV2-null injected TgIGF-I mice. Values are expressed as the mean ±SEM of 8-10 animals/group. p*<0.05, p**< 0.01, p***< 0.001

1.6.2. Effects of PEDF on HIF-1α content

Hypoxia-inducible factor 1 alpha (HIF-1α) is the main regulator of the hypoxic response and promotes neovascularization through upregulation of VEGF (Forsythe et al., 1996). HIF-1α can be also directly up-regulated by IGF-I, which stimulates HIF-1α accumulation, nuclear localization and the induction of VEGF expression (Treins et al., 2005). When HIF-1α was analysed in whole retinal extracts of TgIGF-I mice at different ages, an approximately 2-fold increase over Wt levels was observed in 7.5 month-old mice, which was not evident in younger animals (Figure 47).

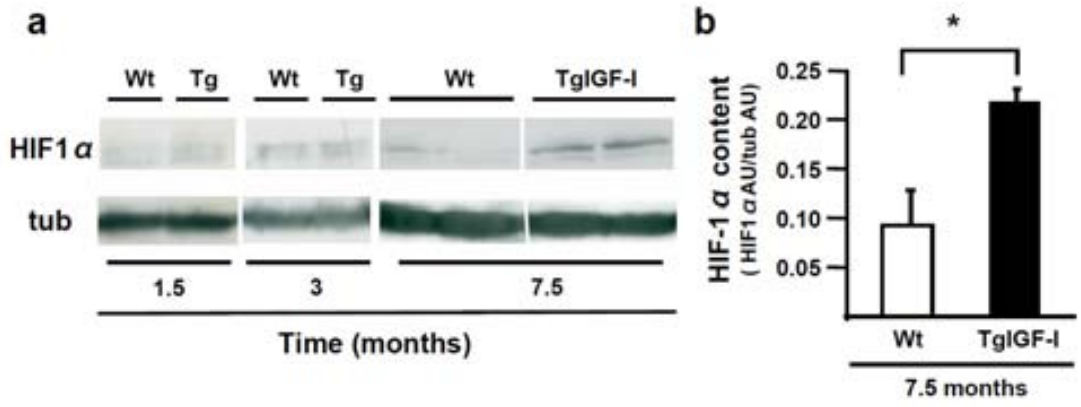

Figure 47. Time-course of retinal HIF-1α levels in TgIGF-I mice. (a) Western blot of whole retinal extracts from Wt and TgIGF-I mice at 3, 6 and 7.5 months of age. **(b)** Quantification of the bands obtained showed that HIF-1α protein was increased in retinas of 7.5 month-old TgIGF-I, remaining unaltered in younger animals. Normalization by tubulin content corrected for loading differences. AU: arbitrary units. Values are expressed as the mean ±SEM of 4 animals/group. $p^*<0.05$

The reductions in neovascularization and VEGF observed in the AAV2-hPEDF treated retinas may suggest that the HIF-1α stimulus present in transgenic retinas could be reduced in treated mice. However, HIF-1α levels remained unchanged six months after AAV2-hPEDF administration in TgIGF-I mice (Figure 48), suggesting that PEDF inhibitory actions on vascular growth were not mediated by a reduction in HIF-1α. This finding is consistent with a direct regulation of HIF-1α by IGF-I in TgIGF-I retinas.

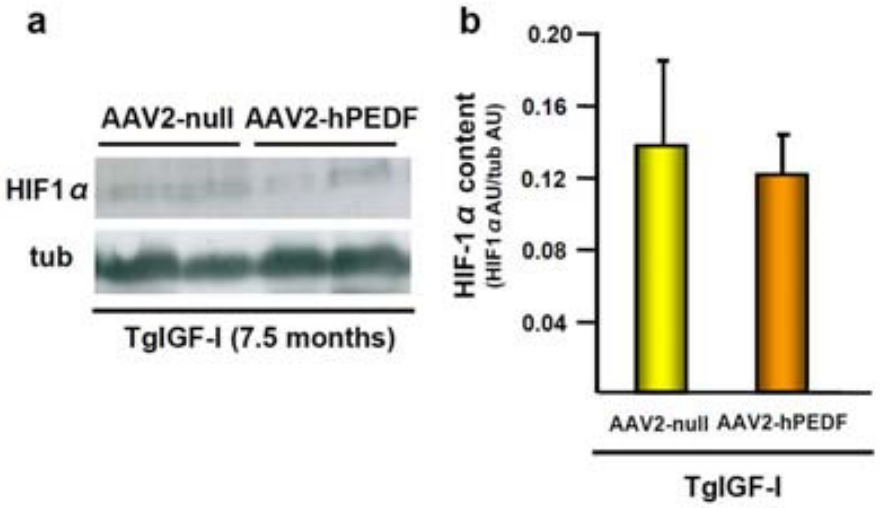

Figure 48. AAV2-hPEDF treatment did not alter the content of HIF-1α 6 months after injection of the vector. (a) Western blot of retinal extracts from AAV2-null and AAV2-hPEDF treated mice was performed 6 months after vector administration. **(b)** Densitometric quantification of HIF-1α bands revealed retinal levels were not changed 6 months after PEDF treatment and remained at the same levels of AAV2-null-injected retinas. AU: arbitrary units. Values were normalized by tubulin content and expressed as the mean ±SEM of 4 animals/group.

1.6.3. Effects of PEDF on angiogenesis-related factors

Matrix metalloproteinases (MMPs) are enzymes capable of degrading a variety of extracellular matrix proteins during tissue remodelling and other physiological processes. MMP2 and MMP9 are collagenases, essential for the degradation of the Collagen IV of vascular basement membranes during neovessel formation. It has been described that their expression is regulated by several factors including VEGF (Wang and Keiser, 1998). MMP2 and 9 can be produced by endothelial and Müller cells and are secreted to the extracellular space to perform their action. Their activity can be measured by zymography, a technique consisting in the separation of proteins by an electrophoresis performed on a gel containing gelatine that can be degraded by these enzymes.

After the electrophoresis, proteins are re-natured and incubated in an appropriate buffer for degradation of the gelatine. After gel staining, the areas of degradation, which will depend on the molecular weight of each gelatinase, can be easily observed (Figure 49a). The activity of MMP2 and MMP9 was evaluated in the aqueous humor of Wt and non-treated, AAV2-null and AAV2-hPEDF treated TgIGF-I eyes six months after vector administration. As with other soluble factors, the activity of these enzymes in the aqueous humor can be considered to reflect their activity in the retina. Consistent with the ongoing angiogenic process and with the elevated VEGF ocular levels, TgIGF-I mice had increased intraocular activity of both MMP2 and MMP9 at 7.5 months of age (Figure 49b). Six months after vector injection, a clear reduction in the activity of these gelatinases was observed in the aqueous humour samples from PEDF-treated mice but not from AAV2-null injected mice (Figure 49b). This reduction in metalloproteinases activity probably reflected the normalization of ocular VEGF observed in PEDF-treated animals.

In proliferative retinopathy, neovascularization may progress to a fibrotic phase that has been associated with elevated vitreous levels of Connective Tissue Growth Factor (CTGF) (Kuiper et al., 2008). This fibrosis is responsible for the formation of epiretinal membranes that can traction the retina, which implies a high risk of retinal detachment and loss of vision (Porta and Bandello, 2002). VEGF directly upregulates CTGF expression in retinal vascular cells (Suzuma et al., 2000).

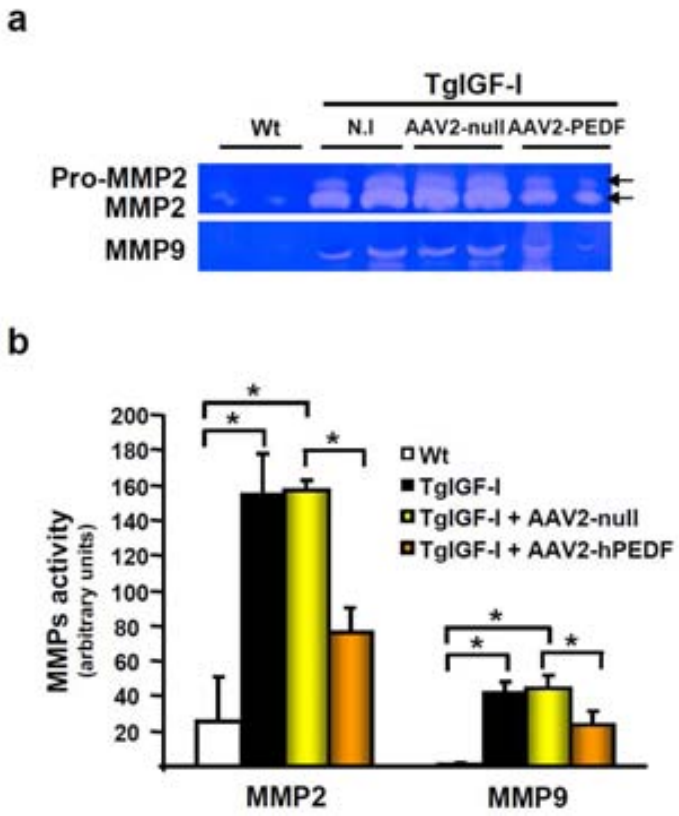

Figure 49. PEDF overexpression downregulates the activity of MMP2 and 9. (a) Gel zymography on 5 µl of aqueous humour showing the non-stained areas in which MMP2 and 9 had degraded gelatine. MMP2 showed a band of higher molecular weight that corresponds to the non-cleaved form of MMP2. **(b)** Quantification of the degraded areas revealed a reduction in the activity of MMP2 and 9 in aqueous humour from TgIGF-I mice 6 months after treatment with AAV2-hPEDF, whereas AAV2-null injected mice showed the same increased activity than age-matched non-treated transgenic eyes. Values are expressed as the mean ±SEM of 5 animals/group. p*<0.05

When the levels of CTGF protein were analysed by Western blot, TgIGF-I retinas showed an approximately 7-fold increase in this growth factor when compared to Wt eyes (Figure 50). In contrast, 6 months after treatment with AAV2-hPEDF CTGF levels were significantly reduced (Figure 50) in transgenic eyes, whereas AAV2-null injected animals had the same levels of a non-treated transgenics. Thus, PEDF overexpression may be an effective way of preventing neovascularization-related fibrosis by reduction of CTGF retinal content.

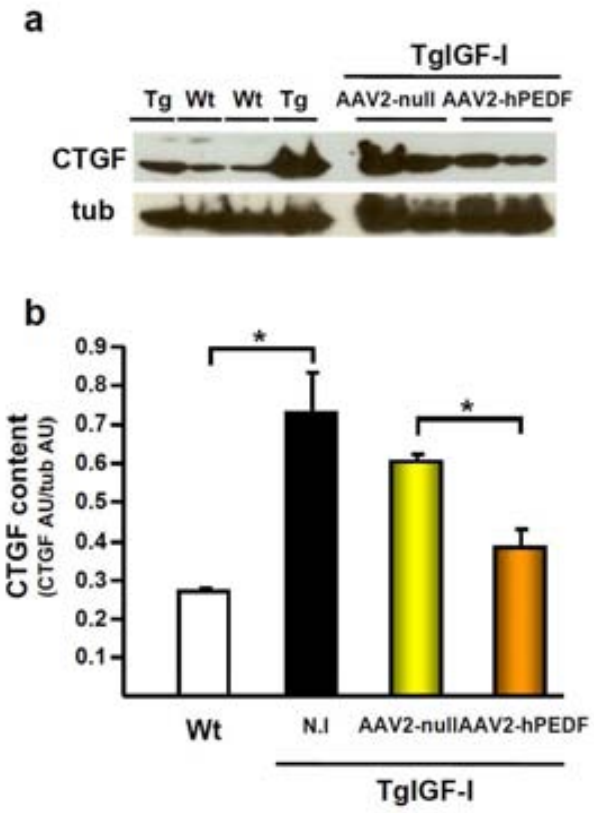

Figure 50. Decreased CTGF retinal content after 6 months of PEDF overexpression. (a) Western blot analysis of the retinal levels of CTGF in Wt and non-treated, AAV2-null and AAV2-hPEDF treated TgIGF-I mice at 7.5 months of age, 6 moths after vector administration. **(b)** After band intensity quantification and normalization by tubulin content, transgenic mice showed increased CTGF accumulation in comparison with Wt. CTGF levels were reduced 6 months after AAV2-hPEDF treatment, but not in AAV2-null injected eyes. AU: arbitrary units. Values are expressed as the mean ±SEM of 5 animals/group. $p^*<0.05$

1.7. ANALYSIS OF THE NEUROPROTECTIVE ACTION OF PEDF TREATMENT IN TgIGF-I RETINAS

The neuroprotective properties of PEDF have been extensively reported in several models of retinal neurodegeneration (Barnstable and Tombran-Tink, 2004). As described earlier, and similar to the vascular phenotype, the neuronal alterations in TgIGF-I retinas are progressive and affect several cell types,

being 7.5 months the age at which retinal dysfunction is clearly present in all transgenic animals.

1.7.1. Study of the effects of PEDF overexpression on the ERG responses

Retinal activity was recorded six months after vector administration, when animals were 7.5 month-old. Separated responses were obtained from the right eye (AAV2-null injected) and the left eye (AAV2-hPEDF treated eye). The amplitudes obtained in the different parameters analysed showed no recovery of retinal functionality in the AAV2-hPEDF treated eyes, presenting the same degree of dysfunction than the untreated TgIGF-I animals (about 40% of wild-type activity) (Figure 51).

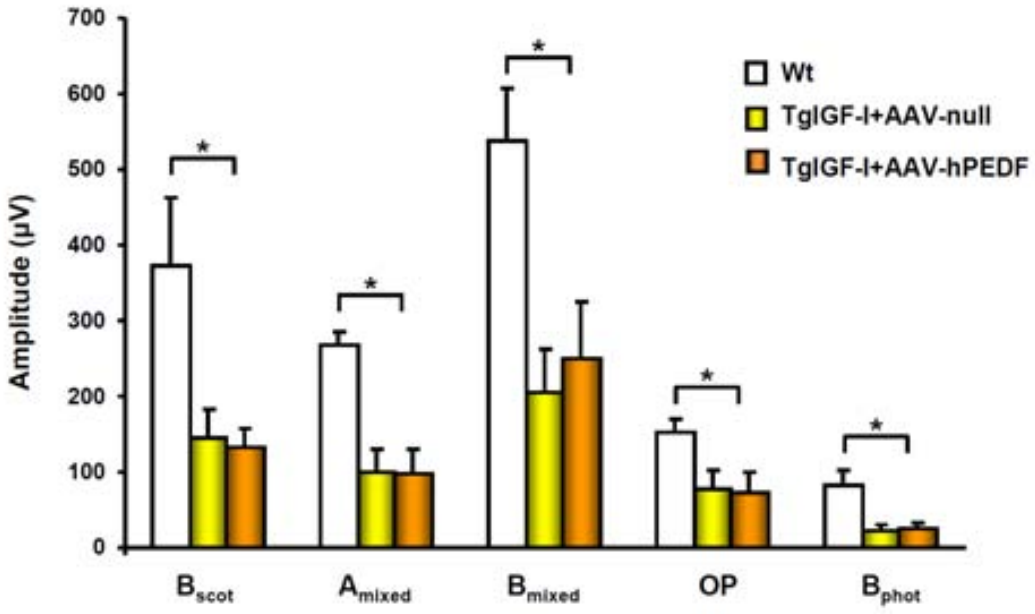

Figure 51. PEDF overexpression did not recover neuronal function in TgIGF-I retinas. ERG responses were recorded 6 months after intravitreal administration of AAV2-hPEDF (left eye) and AAV2-null (right eye) vectors to transgenic mice of 1.5 months of age. Age-matched Wt littermates served as controls. Scotopic b-wave, mixed a and b-waves, OPs and photopic b-wave were analyzed. PEDF overexpression was not able to ameliorate electroretinographic responses in transgenic eyes, which presented reduced amplitudes in all tests performed, similar to that of untreated transgenic mice. Values are expressed as the mean ±SEM of 7 animals/group. p*<0.05

These observations indicated that AAV2-mediated PEDF overexpression was unable to counteract neurodegeneration in transgenic animals overexpressing IGF-I in the retina.

1.7.2. Gliosis after AAV2-hPEDF treatment

Gliosis is detected in TgIGF-I retinas from an early age and worsens as animals age, as described in the first part of this work. This chronic gliosis likely affects the functionality of retinal Müller cells and the subsequent alteration of retinal physiology may be responsible, at least in part, of the neuronal degeneration observed. Glial activation was studied in transgenic retinas 6 months after receiving AAV2-null or AAV2-hPEDF administration. GFAP immunostaining showed similar levels of GFAP expression in Müller cells in AAV2-null and AAV2-hPEDF treated eyes (Figure 52a), indicating that gliosis was not counteracted by PEDF overexpression.

Expression of other gliosis-related genes which are known to be upregulated in TgIGF-I retinas, such as Gja1 (gap junction protein alpha 1, also connexin 43) and S100b also remained abnormal despite PEDF treatment, as determined by quantitative RT-PCR analysis (Figure 52b). These results indicated that PEDF was not able to ameliorate gliosis in retinas from animals overexpressing IGF-I receiving PEDF vector at 1.5 months of age.

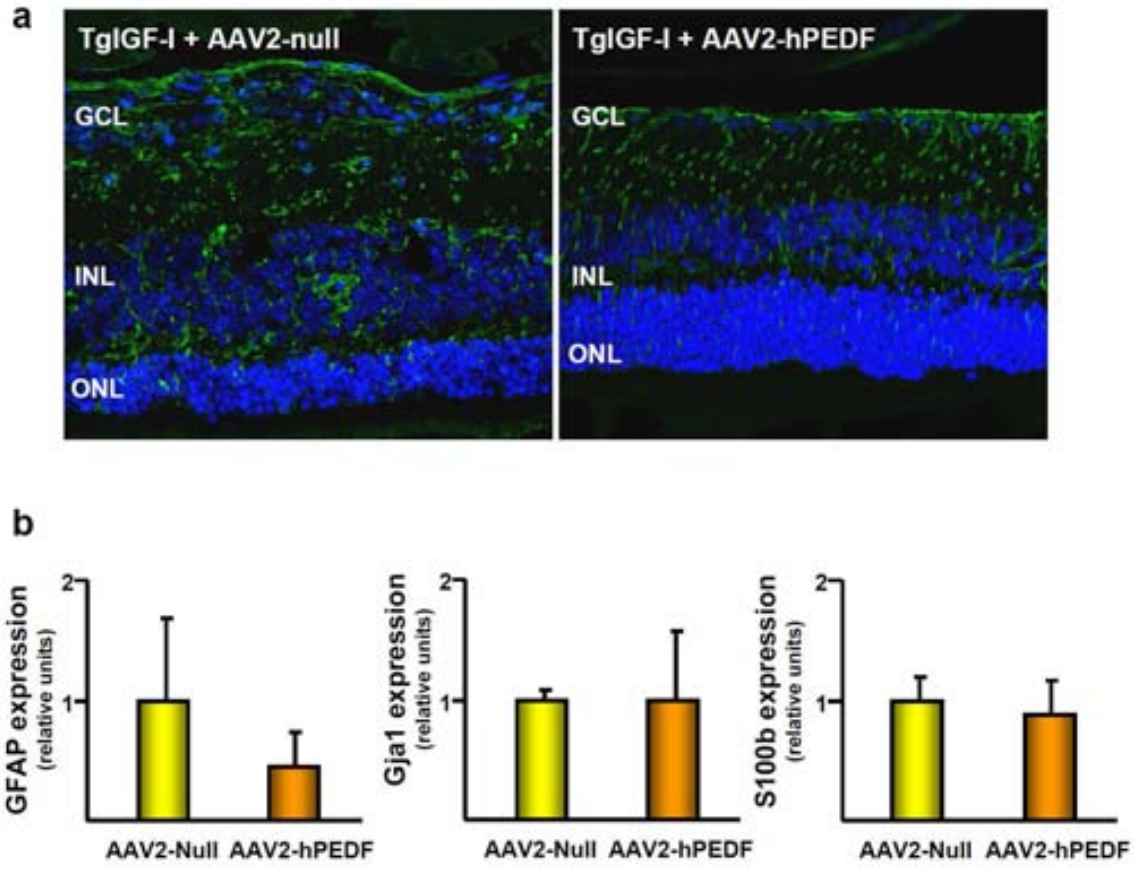

Figure 52. PEDF overexpression did not ameliorate gliosis in TgIGF-I retinas. (a) GFAP immunostaining (green) showing similar levels and distribution of GFAP in retinal sections from AAV2-null-injected and AAV2-hPEDF treated eyes, indicating that gliosis was unchanged after 6 months of treatment, consistent with the observation of GFAP in Müller cell processes. **(b)** Retinal expression of gliosis-related genes was determined by quantitative RT-PCR in total RNA extracts from AAV2-null injected and AAV2-hPEDF treated retinas. No changes were observed 6 months after the treatment. Nuclei were stained with DAPI (blue). Scale bar: 74 μm (a). Values are expressed as the mean ±SEM of 4 animals/group.

Therefore, these results indicate that PEDF overexpression was not able to recover neuronal functionality, likely owing to the persistence of gliosis in the treated retinas. The combination of the PEDF gene transfer with other anti-gliotic factors could lead to the recovery of the TgIGF-I retinal neuronal alterations. Nevertheless, this study demonstrates that a single intravitreal injection of AAV2-hPEDF led to long-term production of PEDF and to a striking

inhibition of intravitreal neovascularization, normalization of retinal capillary density and prevention of retinal detachment. This was parallel to a reduction in the intraocular levels of VEGF. Normalization of VEGF was consistent with a downregulation effectors of angiogenesis, such as the activity of MMP2 and 9 and the content of CTGF. These results demonstrate long-term efficacy of AAV-mediated PEDF overexpression in counteracting retinal neovascularization in a relevant model and provides evidence towards the use of this strategy to treat angiogenesis in DR and other chronic proliferative disorders,

2. DISCUSSION

Diabetic retinopathy is the leading cause of blindness in the working age population of Western societies. As diabetes incidence is dramatically increasing worldwide, in developed as well as developing countries, the number of patients affected by diabetes-induced ocular complications is expected to increase in the future (Shaw et al., 2010). Despite new therapeutic approaches to counteract disease progression have been tested in recent years, none of them has been able to clearly prevent the pathological events that lead to vision loss. Clearly, the development of new, effective therapies requires further investigations on disease pathogenesis, in addition to good animal models to assay the potential of experimental drugs. As previously discussed, transgenic mice overexpressing IGF-I in the retinas present vascular alterations that progress as animal age from non-proliferative to proliferative disease, with development of intraretinal and intravitreal neovascularization, making these mice an excellent animal model of proliferative vascular retinopathy (Ruberte et al., 2004).

The second part of this work has been focused on the development of a therapeutic approach to retinal proliferative vascular disease and neurodegeneration based on the overexpression of PEDF in TgIGF-I retinas by using AAV vectors. AAV2 vectors promoted efficient and long-term expression of PEDF in TgIGF-I eyes. Six months after a single injection of AAV2-hPEDF, transgenic mice showed significantly reduced intraretinal and intravitreal neovascularization, which results in reduced incidence of retina detachment. These observations were in agreement with normalized intraocular levels of

VEGF and other factors involved retinal angiogenesis. However, PEDF overexpression was not able to counteract neuronal degeneration in TgIGF-I, probably as a consequence of persisting gliosis.

Current standard treatments for diabetic retinopathy, particularly for advanced, proliferative forms in which there is high risk of loss of vision, are merely palliative. In the last few years, several molecules have been studied in order to determine their antiangiogenic potential in diabetic patients. Amongst them, anti-VEGF agents such as pegaptanib, ranibizumab and bevacizumab are the most tested in clinical assays (Nicholson and Schachat, 2010). These drugs have demonstrated their efficacy (alone or in combination with laser treatment) in short-duration trials carried out in diabetic patients refractive to standard therapies, with observation of reductions in vascular leakage and inhibition of the proliferation of neovessels (Nicholson and Schachat, 2010). However, the wide range of physiological functions that VEGF plays in the healthy retina should be taken into consideration when evaluating the safety of these therapies. VEGF acts as neuroprotective factor for retinal neurons (Saint-Geniez et al., 2008) and maintains the vascular integrity in many tissues (Kamba et al., 2006), including the choriocapillaries in the eye. In addition, systemic administration of bevacizumab, indicated for cancer treatments, has been associated with tromboembolic complications (Scappaticci et al., 2007). Likewise, in patients receiving intraocular treatment with ranibizumab for ocular vascular disease, an increased incidence of non-ocular haemorrhages and cebreovascular accidents has been reported (Gillies and Wong, 2007; Ueta et al., 2009).

In addition, due to the short half-life of proteins, the efficacy of these treatments decreases if the frequency of administration is too low (Regillo et al., 2008). The administration of periodical intravitreal injections for the treatment of a chronic pathology like diabetic retinopathy may have clinical adverse events, causing inflammation, infections and additional ocular problems to patients, which can compromise their compliance with the treatment (Schwartz et al., 2009). Gene therapy is a good therapeutic alternative to circumvent these limitations by offering the possibility of long-term production of the therapeutic agent after a single administration. Gene therapy has proven successful in the AAV2-based treatment of LCA patients in three independent clinical trials, in which partial recovery of vision in the treated eye was determined, in the absence of serious adverse effects (Bainbridge et al., 2008; Maguire et al., 2008; Hauswirth et al., 2008). Moreover, a recent follow-up report to one of the LCA trials demonstrated the feasibility and efficacy of the re-administration of AAV2 vectors in the previously non-treated eye of these patients (Bennett et al., 2012). These results confirm the safety and efficacy of AAV2-based gene therapy to treat retinal disorders.

AAV2 vectors have demonstrated their efficacy to transduce several types of retinal cells after intravitreal administration to healthy rodents (Bennett et al., 1997; Hellström et al., 2009). The physiological conditions of a tissue can, however, create specific molecular signatures that influence AAV vector tropism, by changing the expression of molecules that AAV vectors use to enter into the cell (Chen et al., 2009). Consequently, the first step in the design of an gene therapy approach for the treatment of retinopathy was the evaluation of

the tropism of AAV2 specifically in TgIGF-I retinas. Despite the fact that gliosis is already established in transgenic retinas at the time of vector administration (1.5 months of age), no differences were observed in the tropism of AAV2 vector after intravitreal injection in TgIGF-I mice compared with that previously reported for healthy mice (Dudus et al., 1999). Ganglion, amacrine and horizontal neurons were transduced in transgenic mice, whereas no glial cells expressed GFP, in agreement with the neuronal tropism of AAV2 in rodent retinas (Hellström et al., 2009). This observation is important as it suggests that this should be the tropism expected in a clinical setting in which AAV2 is administered to diseased retinas with active gliosis.

The previously reported long-term expression mediated by AAV vectors after intraocular delivery (Stieger et al., 2008) was confirmed in TgIGF-I mice, in which cells expressing the gene of interest where detected 18 months after a single injection of vectors, supporting the feasibility of a long-term therapy with only one intervention. Restricted immunologic conditions within the eye and the lack of replication of neurons are factors that contribute to the long-term expression of therapeutic agents in the retina after AAV delivery (Colella et al., 2009).

The antiangiogenic potential of PEDF gene transfer using AAV or adenoviral vectors has previously been demonstrated in experimental models of retinal neovascularization (Mori et al., 2002c; Raisler et al., 2002), as well as in human patients with neovascular macular degeneration (Campochiaro et al., 2006). An attractive feature of PEDF is that its action is restricted to proliferating

vessels, and does not affect quiescent vasculature (Volpert et al., 2002), avoiding the undesired side effects on vascular homeostasis that other antiangiogenic strategies, such as anti-VEGF therapies, present. Moreover, the neuroprotective properties of PEDF, which have been reported in several experimental models of neurodegeneration (Barnstable and Tombran-Tink, 2004), represent an additional advantage for PEDF in comparison with anti-VEGF molecules, which may compromise neuronal function by inhibiting the neuroprotective actions of VEGF (Saint-Geniez et al., 2008).

The experimental design of a gene transfer approach for the treatment of the vascular and neurological alterations present in TgIGF-I mice was conceived as a preventive therapy. Mice were treated at 1.5 months of age, when only mild gliosis is present, but neuronal or vascular alterations are not observed (Ruberte et al., 2004; Haurigot et al., 2009). In diabetic patients, the progression of the vascular pathology is slow. AAV2-hPEDF treatment would be indicated to patients showing very early retinopathy, with increased latencies in ERG and/or mild vascular alterations. In addition, better outcomes have been observed in clinical interventions when diabetic patients receive treatment at early stages of the pathology (Stefansson et al., 2000). The slowly progressive pattern of neovascularization development that the retinas of TgIGF-I mice show, in contrast with that of the OIR models (Smith et al., 1994), allowed the evaluation of the long-term efficacy of AAV2-hPEDF administration, an aspect important in the treatment of a chronic disease such as diabetic retinopathy or other proliferative retinopathies.

The dose of AAV2-hPEDF vector used was 6.4 x 10^8 vg/eye, which was able to transduce transgenic retinas with high efficiency. This dose is much lower than the doses used in the AAV2-based clinical trials (Bainbridge et al., 2008; Maguire et al., 2008; Hauswirth et al., 2008), indicating that no adverse effects in terms of inflammation should be associated to the administration of such vector dose in patients. PEDF protein was increased by 6 times in treated retinas, when compared with non-treated ones. Based on observations in a mouse model of CNV, it has been suggested that high levels of PEDF in the retina can actually have a stimulatory effect on vessel proliferation (Apte et al., 2004). The results obtained in the present work, however, indicate that the levels of PEDF achieved herein are efficient at inhibiting neovascularization rather than promoting it. Of note, non-treated TgIGF-I retinas showed increased levels of PEDF in comparison with wild-type retinas. This may indeed reflect an adaptive response to the chronic presence of pro-angiogenic stimuli in transgenic retinas.

Vascular alterations develop progressively in transgenic mice overexpressing IGF-I in the retina, showing pathological features related with non-proliferative retinopathy at early ages that advance to proliferative neovascularization (Ruberte et al., 2004). The thickening of the basement membrane is characteristic of both non-proliferative human retinopathy (Agardh and Agardh, 2004) and young TgIGF-I (Ruberte et al., 2004), affecting vascular stability and functionality (Roy et al., 2010). The thickening of the basement membrane (BM) was slightly reduced in TgIGF-I retinal capillaries 6 moths after treatment, although this reduction was not statistically significant (Figure 40).

Both IGF-I and CTGF are known to increase the deposit of collagen in the basement membrane in high-glucose conditions contributing to its thickening (Lam et al., 2003; Kuiper et al., 2008; Danis and Bingaman, 1997). Here, reduced levels of CTGF were observed after 6 months of AAV2-hPEDF treatment, which may be the explanation for the partial, but not total, amelioration of BM thickness in TgIGF-I mice. Again, PEDF overexpression may not be able to counteract the direct effects of IGF-I in transgenic retinas, but it may inhibit those alterations caused by VEGF overexpression, such as CTGF upregulation.

Neovascularization is a hallmark of proliferative retinopathies and is associated with a high risk of loss of vision. The potential of PEDF as an antiangiogenic has been demonstrated in several approaches, in both experimental models and clinical trials, demonstrating its efficacy in inhibiting neovessel formation and proliferation (Mori et al., 2002c; Raisler et al., 2002; Campochiaro et al., 2006). Much of the pre-clinical evidence on the antiangiogenic properties of PEDF on retinal vessels was obtained, however, in animal models that do not reproduce the time-course of neovascularization in humans. The results of this work indicate that PEDF counteracts angiogenesis in an animal model with progressive adult neovascularization. Intraretinal and pre-retinal neovascularization are present in transgenic eyes at 7.5 months of age, as determined by the quantification of the capillary area in angiograms performed after fluorescein-conjugated dextran perfusion and by quantification of PAS-positive cells in the vitreous cavity, respectively. Both methods of evaluation have extensively been used in several publications on retinal

neovascularization (Smith et al., 1994; Auricchio et al., 2002; Balaggan et al., 2006). Furthermore, immunohistochemistry with specific markers for endothelial cells and vascular basement membrane confirmed the vascular nature of the PAS+ intravitreal structures. Transgenic animals receiving AAV2-hPEDF treatment at 1.5 months of age showed normalization of the capillary density 6 months after gene transfer. The fact that the capillary density in PEDF-treated retinas was similar to that of healthy Wt retinas, and not less, agrees with published literature supporting the notion that PEDF effects are restricted to newly formed vessels and do not affect quiescent vessels (Volpert et al., 2002). Moreover, PEDF treatment led to a striking decrease in the number of vascular cells detected in the vitreous cavity of these mice. These data suggest that PEDF overexpression can counteract the ongoing intraretinal and intravitreal neovascularization that develops with age in TgIGF-I mice with no alteration of pre-existing vessels.

An additional beneficial effect of PEDF-mediated inhibition of pathological neovascularization is the reduced incidence of retinal detachment observed in treated transgenic mice. Due to the traction forces exerted by neovessels and epiretinal membranes, photoreceptors can be separated from the RPE, which is their main source of nutrients and oxygen, leading to the degeneration of the photoreceptors. Retinal detachment is the main process that causes loss of vision in diabetic patients (Porta and Bandello, 2002). The reduced intravitreal neovascularization in PEDF-treated transgenic mice results in a much lower incidence of retinal detachment. Despite the reduction in the incidence of retinal detachment, however, no recovery in visual functionality

was observed after treatment. Altogether, these observations further reinforce the idea that neuronal pathology in TgIGF-I eyes is probably more a consequence of the alterations in retinal homeostasis caused by chronic glial dysfunction than of vascular disease.

VEGF is a key factor in the development and progression of human diabetic retinopathy and also in TgIGF-I mice (Aiello et al., 1994; Pierce et al., 1995; Ruberte et al., 2004). Increased intraocular levels of VEGF have been detected in the ocular fluids of diabetic patients and in the aqueous humor of TgIGF-I mice (Aiello et al., 1994; Ruberte et al., 2004; Haurigot et al., 2009), which prompted the testing of anti-VEGF therapies in patients with diabetic macular edema or proliferative retinopathy (Nicholson and Schachat, 2010). PEDF overexpression induced a reduction in the intraocular levels of VEGF in treated TgIGF-I to levels of healthy mice. The maintenance of physiological levels of VEGF after PEDF overexpression would avoid the deleterious effects of VEGF depletion reported in retinal neuronal and vascular cells (Saint-Geniez et al., 2008; Tolentino, 2011). The molecular mechanism by which PEDF exerts its antiangiogenic action has not been elucidated yet but some reports indicate that this mechanism is based on the disruption of VEGF signalling (Wang et al., 2006b; Cai et al., 2006). Wang and colleagues also reported the suppression of VEGF expression by PEDF (Wang et al., 2006b). In TgIGF-I mice, the reduced intraocular levels of VEGF observed after AAV2-hPEDF treatment could in principle be a consequence of PEDF direct inhibition of VEGF expression. However, other possibilities should be considered such as increased rate of VEGF mRNA or protein degradation. IGF-I, and other growth factors, induce the

upregulation of VEGF by preventing the degradation of HIF-1α, mediating its nuclear translocation through the activation of the PI3 kinase pathway (Treins et al., 2005). In agreement with the intraocular accumulation of IGF-I, untreated transgenic retinas showed increased levels of HIF-α. HIF1-α binds to the hypoxia-binding elements present in the promoter of the VEGF gene, being HIF1-α the most potent regulator of VEGF expression (Forsythe et al., 1996). This mechanism of control of VEGF expression by hypoxic conditions or by the presence of growth factors has been well characterized in retinal cells (Treins et al., 2005). Interestingly, HIF1-α levels remained unchanged after AAV2-hPEDF administration to TgIGF-I. This result is in line with the concept that PEDF cannot directly inhibit IGF-I actions. In addition, because the levels of HIF1-α do not change after treatment, these observations give support to a mechanism of action in which PEDF acts downstream of VEGF expression to inhibit angiogenesis, either by promoting mRNA/protein degradation or by interfering with VEGF signalling, or both. Consequently PEDF would be able to inhibit neovascularization even in hypoxic environments in which HIF1-α is accumulated by acting directly at VEGF level. In this direction, the production and secretion of PEDF by Müller cells under strong hypoxic conditions has been reported, suggesting this is indeed a physiologic response to limit the action of proangiogenic molecules in hypoxia (Lange et al., 2008).

VEGF pro-angiogenic actions include the activation of many downstream effectors that mediate vascular remodelling and neovascularization. Amongst them, MMP2 and MMP9 are responsible for the extracellular matrix remodelling required for retinal neovascularization (Salzmann et al., 2000). The activity of

MMP2 and MMP9 is increased in TgIGF-I eyes and decreased after PEDF treatment, in agreement with a reduction of VEGF signalling after PEDF overexpression. The same pattern is observed for CTGF. CTGF is another downstream effector of VEGF whose increase in retinopathy underlies the development of fibrotic processes associated with retinal angiogenesis (Kuiper et al., 2008). Almost total normalization of CTGF levels was observed after PEDF treatment, which likely reflects the normalization of VEGF levels, although a direct effect of PEDF on CTGF regulation cannot be excluded. This anti-fibrogenic activity of PEDF has previously been reported after gene transfer to the kidney of diabetic rats (Wang et al., 2006a), but never before for the eye. Then, the normalization of VEGF levels after PEDF overexpression led to the inhibition of the neovascularization and the downregulation of downstream effectors of VEGF ***(Scheme 2)***.

Scheme 1. PEDF overexpression inhibits VEGF action in TgIGF-I retinas. AAV2-hPEDF treatment normalizes intraocular VEGF levels, leading to the inhibition of the angiogenic process present in the transgenic retinas.

Despite the clear beneficial effects observed on counteracting the vascular pathology, the visual function of TgIGF-I retinas was not recovered after AAV2-hPEDF treatment, although the well-described neurotrophic

properties of PEDF (Barnstable and Tombran-Tink, 2004)**.** ERG responses in TgIGF-I mice measured 6 months after the treatment were similar to those of non-treated TgIGF-I. Several factors may contribute to the inability of AAV2-hPEDF to ameliorate ERG responses. First, the levels of PEDF achieved after AAV2-hPEDF treatment, although sufficient to counteract vascular alterations, may not be enough to protect neurons. In other words, the biological threshold for neuroprotection may be higher than for inhibition of neovascularization. It has been suggested that PEDF actions on vascular and neuronal cells are mediated by different receptors or by different regions of the PEDF protein, and these could have different affinities and efficacies (Bernard et al., 2009; Notari et al., 2006). Second, the results presented here strongly suggest that neurodegeneration in TgIGF-I mice may be caused by glial alterations, which in turn seem to be a direct consequence of IGF-I overexpression. PEDF has been reported to interfere with VEGF signalling pathways (Wang et al., 2006b; Cai et al., 2006) and inhibit its action, but no direct inhibition of IGF-I signalling by PEDF has ever been reported. Then, PEDF would not be able to counteract the initial insult present in TgIGF-I retinas, as exemplified by the persistence of gliosis in AAV2-hPEDF treated transgenic mice, which would be the main contributor to neuronal dysfunction and death in transgenic retinas ***(Scheme 2)***. Finally, the overexpression PEDF driven by AAV vectors after intravitreal administration is restricted to the inner layers of the retina. Then, only the neurons located in the INL and the GL would be in exposed to the secreted PEDF protein, which may not reach photoreceptors in the ONL. If a partial recovery occurred in the neurons of inner retina by PEDF neuroprotective action, it would possibly be difficult to detect by ERG recordings unless

photoreceptors were also recovered, as these are the cells that initiate the electrical response after light stimulation during ERG recordings. Therefore, the treatment of neurodegenerative retinal disease in TgIGF-I mice may require the use of higher doses of intravitreal AAV2-hPEDF, or the concomitant administration of PEDF by subretinal delivery or the combination of PEDF with anti-gliotic factors.

In summary, in the second part of this study, the ability of PEDF to counteract angiogenesis in an adult model of retinal neovascularization with slow progression was clearly demonstrated. AAV-mediated gene transfer of PEDF to the eye resulted in normalization of intraocular levels of VEGF and other pro-angiogenic molecules. The advantage of the approach presented here resides in that this therapeutic effect was achieved after a single administration of AAV2-hPEDF, eliminating the need for repeated administrations of the therapeutic agent. These findings suggest that AAV2-hPEDF treatment may represent an effective therapy for diabetic retinopathy and other ocular diseases characterized by neovascularization.

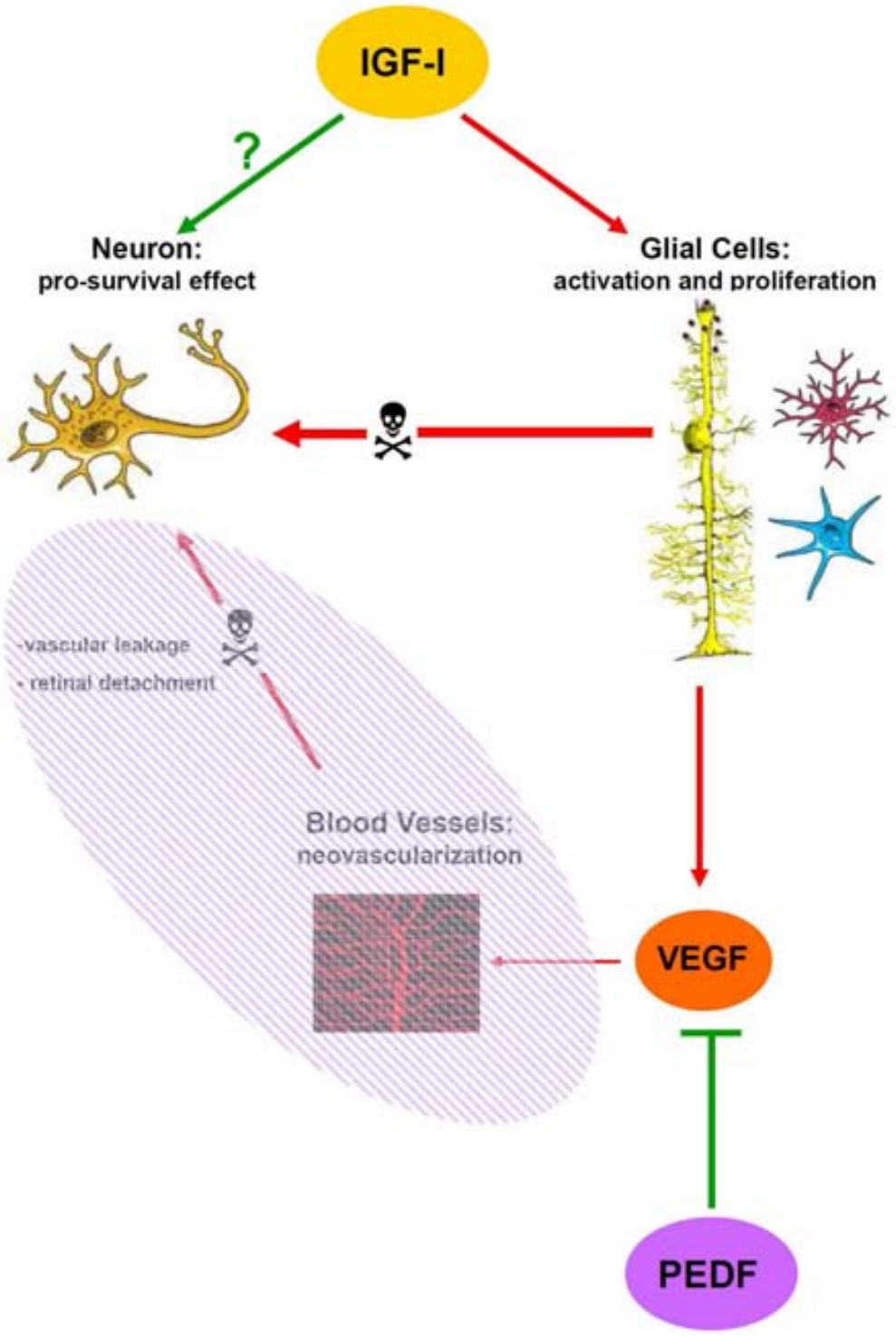

Scheme 2. PEDF overexpression is able to inhibit ocular neovascularization in TgIGF-I mice. AAV2-hPEDF treatment normalizes intraocular VEGF levels, counteracting the proliferation of neovessels in the transgenic eyes. However, the IGF-I –induced gliosis observed in the TgIGF-I retinas is not ameliorated after the treatment, which avoid the recovery of the neuronal functionality.

V. Conclusions

PART I. CHARACTERIZATION OF NEUROGLIAL ALTERATIONS IN MICE OVEREXPRESSING IGF-I IN THE RETINA.

1. Transgenic mice overexpressing IGF-I in the retina show a progressive decline in their electroretinographic responses, starting from normal recordings at early age that evolve to 80% reductions in response amplitudes in old transgenic mice.

2. TgIGF-I retinas show reduced thickness of the inner and outer nuclear layers at 7.5 months of age, associated with reduced populations of rod photoreceptors, bipolar, amacrine and ganglionar neurones.

3. Gliosis, characterized by GFAP up-regulation, is observed in transgenic retinas as early as 1.5 month of age and progresses as animals age. Downregulation of $p27^{Kip}$ expression in transgenic retinas suggests that the proliferation of Müller cells is partially responsible of the reactive gliosis.

4. Microglial infiltration is detected in IGF-I-overexpressing retinas as soon as 3 months of age and persists in old mice.

5. In agreement with gliosis, the activity of glutamine synthetase, an enzyme essential for glutamate recycling in Müller cells, is markedly reduced in transgenic retinas from early ages.

6. Transgenic mice present a high degree of delocalization of the potassium channel Kir 4.1 as soon as 3 months of age, suggesting impairment in the potassium buffering capacity in transgenic retinas.

7. Increased levels of oxidized glutathione are observed as soon as 3 months of age, suggesting the presence of oxidative stress in transgenic retinas.

8. The expression of iNOS is markedly upregulated in TgIGF-I retinas at 7.5 months of age, suggesting increased retinal levels of NO in transgenic mice that probably contribute to exacerbate oxidative stress, inflammation and neuronal death. The expression of iNOS is markedly upregulated in TgIGF-I retinas at 7.5 months of age, which may lead to an increment in NO that could exacerbate oxidative stress, inflammation and neuronal death.

9. Transgenic retinas present a significant increase in the levels of the pro-inflammatory cytokines TNF-α and MCP-1 at 7.5 months of age, which could also contribute to neurodegeneration.

10. Altogether, our study suggests that early glial alterations in TgIGF-I retinas may underlie the progressive loss of retinal neuronal populations, with the concomitant impairment in functionality. Most of these neuronal and glial alterations have also been described in human patients with retinopathy.

PART II. EVALUATION OF THE EFFICACY OF LONG-TERM PEDF GENE TRANSFER IN COUNTERACTING NEOVASCULARIZATION AND NEURODEGENERATION IN TRANSGENIC TgIGF-I RETINAS

1. AAV2 vectors are able to transduce TgIGF-I retinas with high efficiency after a single intravitreal administration. Long-term expression of the transgene was detected in ganglion, amacrine and horizontal cells, but not in glial cells.

2. The thickening of the basement membrane, a non-proliferative vascular alteration, is only partially inhibited by PEDF overexpression in TgIGF-I retinas.

3. The administration of AAV2-hPEDF normalizes retinal capillary density in TgIGF-I mice, showing values similar to those of healthy mice, which indicates that the quiescent vasculature is not affected by PEDF overexpression.

4. AAV2-hPEDF treatment inhibits pre-retinal neovascularization in TgIGF-I eyes, in which intravitreal vessels were not found and PAS^+ vascular cells were significantly decreased 6 months after vector injection.

5. The incidence of retinal detachment in PEDF-treated eyes is markedly reduced, likely as a consequence of the inhibition of pre-retinal neovascularization.

6. VEGF intraocular levels are significantly reduced after AAV2-hPEDF treatment to values similar to those of healthy mice, ensuring the maintenance

of physiological levels of VEGF required for normal neuronal and vascular integrity.

7. HIF-1α increases in TgIGF-I retinas at 7.5 months of age but not in younger animals. After AAV2-hPEDF administration, HIF-1α levels remain unchanged, indicating that PEDF inhibition of neovascularization is not mediated by reductions in HIF-1α content.

9. AAV2-hPEDF treatment reduces MMP2 and 9 activity in treated transgenic mice, in agreement with the observed reduction in the levels of VEGF.

10. AAV2-hPEDF treatment leads to a reduction in the content of CTGF which could also be a consequence of the decrease in intraocular VEGF.

11. Despite the beneficial effects on retinal vasculature, PEDF overexpression is not able to recover electrophysiological functionality in TgIGF-I retinas. Gliosis is not counteracted by the treatment either, and this could explain the lack of efficacy of PEDF treatment on neuronal dysfunction.

12. Taken together these results suggest that AAV2-hPEDF is able to counteract neovascularization and prevent the development of proliferative retinopathy. Nevertheless, to prevent neuroglial alterations a combined therapy with other therapeutic genes acting specifically on those alterations would be required for maximal therapeutic benefit.

VI. Materials and Methods

1. MATERIALS

1.1. ANIMALS

Heterozygous transgenic mice expressing IGF-I under the control of the rat insulin promoter in a CD1 genetic background and wild-type littermates were used (George et al., 2002). This colony was previously established in SER-CBATEG facility. All mice were fed ad libitum with a standard diet (2018S Teklad Global, Harlan Tecklad) and maintained under conditions of controlled temperature and light (12-hour light/dark cycles). Before sacrificing, animals were anesthetized with inhalational anesthetics (IsoFlo, Esteve) Animal care and experimental procedures were approved by the ethics committee in animal and human experimentation of the UAB.

1.2. REAGENTS

All of the molecular biology reagents were purchased from the following commercial suppliers: Roche, Invitrogen, Bio-Rad, Amersham (GE), Sigma-Aldrich, Promega, Panreac, Fluka, Thermo. dCTPs labelled with radioactive P^{32} were obtained from Perkin-Elmer.

1.3. DNA PROBES

In order to detect the presence of the transgene in the genomic DNA of RIP/IGF-I mice a specific DNA probe was used. This probe was a fragment of the mouse IGF-I cDNA obtained by EcoRI digestion of the plasmid containing

the quimeric gene used for the generation of the transgenic mice (ref george 2002b). GFP and PEDF cDNAs were used as probes for dot blot viral genome quantifications.

1.4. ANTIBODIES

The antibodies and other reagents used in the inmunohistochemichal or Western blot detections are listed in the following table:

Antibody	**Reactivity**	**Species**	**Supplier**	**dilution**
anti GFP (A6455)		goat	Abcam	IHC:1/300 *in toto:* 1/250
anti mouse calretinin (C 7479)	human, rat, chicken	rabbit	Sigma-Aldrich	IHC: 1/100
anti mouse rhodopsin (C 7479)	human, mouse, rat	mouse	Sigma-Aldrich	WB:1/100 IHC: 1/50
anti rat PKC α (P 4334)	mouse, rat	rabbit	Sigma-Aldrich	IHC:1/500 WB: 1/2000
anti rat calbindin (KD-15) (C 7354)	human, rat, chicken	rabbit	Sigma-Aldrich	IHC: 1/5000
anti mouse glutamine synthetase (G 2781)	mammalian	rabbit	Sigma-Aldrich	IHC: 1/500
anti human Kir 4.1 (apc-035)	human, mouse	rabbit	Alomone Labs	IHC:1/200 WB: 1/400
anti cow S100 (Z 0311)	cat, horse, mouse, rat	rabbit	DAKO Cytomation	IHC: 1/500
anti mouse CTGF (ab6992)	human, mouse, rat	rabbit	Abcam	WB:1/1000
anti human cleaved caspase-3 (9661)	human, mouse, rat	rabbit	Cell signaling	IHC: 1/250
anti human HIF1α (AB1536)	human, mouse	rabbit	R&D Systems	WB:1/2000
anti mouse CD105 (BAF1320)	human, mouse	goat	R&D Systems	IHC:1/7
anti rat MCP1 (ab25124)	mouse, rat	rabbit	Abcam	WB:1/2000
anti human Brn3a (sc-31984))	human, mouse, rat	goat	Santa Cruz Biotechnology	WB:1/100
Lycopersicon esculentum lectin (L0651)			Sigma-Aldrich	IHC: 1/100
anti cow GFAP (Z0334)	human, mouse, rat,...	rabbit	DAKO Cytomation	WB:1/500 IHC: 1/500

anti human PEDF (AF1177)	human	goat	R&D Systems	WB:1/100 IHC: 1/50
anti human tubulin (ab4074)	human, mouse, rat,...	rabbit	Abcam	WB:1/2000
Mouse on Mouse (MOM) kit (BMK-2202)	mouse		Vector Labs	
anti rabbit Ig- HRP (PO163)	rabbit	swine	DAKO Cytomation	WB:1/20000
anti goat Ig- HRP (PO163)	goat	rabbit	DAKO Cytomation	WB:1/20000
anti rabbit Ig- biotinilated (31820)	rabbit	goat	Pierce	IHC:1/300
anti goat Ig- biotinilated (sc-2042)	goat	donkey	Santa Cruz Biotechnology	IHC:1/300
Streptoavidine Alexa Fluor 568 (S-11226)			Molecular Probes	IHC:1/300
Streptoavidine Alexa Fluor 488 (S-11223)			Molecular Probes	IHC:1/300
To-pro 3 iodide (642/661)			Invitrogen	IHC:1/100
Hoechst (DAPI) (B2261)			Sigma-Aldrich	IHC:1/100

2. METHODS

2.1. RIP/IGF-I TRANSGENIC MICE GENOTYPING

Transgenic mice were identified by determining the presence of the transgene in the genomic DNA, extracted from a tail sample from animals aged 3 weeks. The sample was digested in a 1-5% v/v Proteinase K (Roche) buffered solution overnight at 56ºC. The digestion mixture was centrifuged 5 minutes at 13000g and the supernatant (600 µl) was clarified by addition of 250 µl of saturated NaCl solution. The mixture was incubated 15 minutes at 4ºC and centrifuged 15 min at 12000g. The supernatant was recovered and mixed with 420 µl of isopropanol, in order to precipitate genomic DNA. After 20 minutes of

centrifugation at 9800g, the DNA pellet was rinsed with 70% ethanol and the resuspended in 65 µl of deionizated water.

Once genomic DNA was obtained, analysis by Southern blot allowed to identified the presence of the transgene. To do so, 15 µl of genomic DNA were digested with the enzyme BamHI, overnight at 37º. BamHI restriction sites are known to flank IGF-I cDNA in the transgene. After digestion, samples were run in an agarose gel and once electrophoresis was finished, gel treatment was perfomed. The first step of the treatment was 15 minutes in 0.25 HCl to allow the depurinization of DNA; then, 15 minutes in alkaline solution to denature DNA and finally neutralizing solution for 30 minutes to recover the negative charge in DNA molecules.

Genomic DNA was transferred to a positively charged nylon membrane (Roche) using the Turboblotter system (Schleicher & Schuell), based on capillarity through absorbent papers with SSC buffer. After a minimum of 2 hours transferring, the membrane was irradiated in UV light in a UV-Stratalinker to attached covalently DNA to the nylon membrane and the stained with methylene blue solution to visualized the transferred genomic DNA.

For the radioactive detection of the transgene, the membrane was previously pre-hybridized for 2 hours at 65º to reduce unspecific binding. Hybridization with the specific probe of IGF-I cDNA radioactively labeled was performed overnight at 65ºC. For the probe labeling the kit Ready-to-Go DNA Labelling Beads (-dCTP^{32}) (Amersham, GE) was used, following manufacturer

instructions. Next morning, the membrane was washed with solutions with increasing astringency. First, two washes of ten minutes at room temperature with a low astringency solution and then 5 minutes of washing at 65ºC with a high astringency solution. Finally the blots were exposed to a photographic film (Amersham, GE) to obtain the signal corresponding to the presence of the transgene.

Solutions

- Tissue digestion: 100mM Tris-HCl pH 8.5; 5 mM EDTA pH 8; 0.2% w/v SDS; 200 mm NaCl; 1 mg/ml proteinase K.
- Electrophoresis buffer: 40 mM Tris-acetate pH 8.3; 1mM EDTA; 0.5 µg/ml ethidium bromide
- Loading buffer 10x: 50% v/v glycerol; 100 mM EDTA; 1% w/v SDS; 0.1% w/v bromophenol blue
- Alkaline solution: 1.5M NaCl and 0.5M NaOH
- Neutralizing solution: 1M Tris and 3M NaCl
- 20x SSC: 3 M NaCl; 0.3 M sodium citrate pH 7.4
- Hybridization solution: 0.25 mM Na_2HPO_4 pH 7.2; 10% w/v SDS; 1 mM EDTA; 0.5% w/v Blocking Reagent (Roche)
- Low astringency solution: 2x SSC; 0.1% w/v SDS
- High astringency solution: 0.1x SSC; 0.1% w/v SDS

2.2. ELECTRORETINOGRAPHY

Prior to electroretinogram (ERG) recording, the mice were maintained in darkness overnight and, subsequently, the set up procedures were conducted in dim red light, which was thereafter extinguished for the dark adapted studies. The mice were anaesthetized with an intraperitoneal injection of a solution of ketamine (95 mg/kg) and xylazine (5 mg/kg) and maintained on a heating pad at 37 ºC. The pupils were dilated by applying a topical drop of 1% tropicamide (Tropicamida, Alcon Cusí). A topical drop of 2% Methocel (Ciba Vision) was applied in each eye immediately before situating the corneal electrode. Flash-induced ERG responses were recorded from the right eye in response to light stimuli applied with a Ganzfeld stimulator. The intensity of light stimuli was measured with a photometer (Mavo Monitor USB, Gossen) at the level of the eye. At each light intensity, the average of 4-64 consecutive stimuli was obtained; the interflash interval in scotopic conditions ranged from 10 s for dim flashes and up to 60 s for the highest intensity stimuli. Under photopic conditions the interval between light flashes was fixed at 1 s. The ERG signals were amplified and band filtered between 0.3 and 1000 Hz with a Grass amplifier (CP511 AC amplifier, Grass Instruments, Quincy, MA). Electrical signals were digitized at 20 kHz with a Power Lab data acquisition board (AD Instruments, Chalgrove, UK). Bipolar recording was performed between an electrode fixed on a corneal lens (Burian-Allen electrode, Hansen Ophthalmic Development Lab, Coralville, IA) and a reference electrode located in the mouth, with a ground electrode located in the tail. Rod mediated responses were recorded under dark adaptation to light flashes of 2 log cd.s.m^{-2}. Mixed rod

and cone mediated responseswere recorded in response to light flashes of 0.48 log cd.s.m^{-2}. Oscillatory potentials (OP) were isolated using white flashes of 0.48 log cdm^2 and band pass filtered between 100e10,000 Hz. Cone mediated responses to light flashes of 1.48 log cd.s.m^{-2} on a rod saturating background of 30 cd.m^{-2} were recorded. Flicker responses (20 Hz) to light flashes of 1.48 log cd.s.m^{-2} were recorded under a rod-saturating background of 30 cdm^2. All parameters were defined and responses were recorded and analyzed with the software Scope v6.4 of Power Lab (ADInstruments Ltd). The amplitudes of the a-wave, b-waves, OP (peak to peak) and flicker response (peak to peak) were measured off-line and the results averaged. For simultaneous recording of both eyes in AAV-treated mice, a VERIS Multifocal System with Integrated Ganzfeld Stimulator (Electro-Diagnostic Imaging, Inc) was used, with equivalent protocols, settings and analysis that the rest of the recordings.

2.3. HISTOLOGICAL ANALYSES

2.3.1. Immunohistochemistry in paraffin-embedded tissue sections

After eye enucleation, corneas were partially removed to facilitate the entrance of liquids. Then, eyes were fixed in formalin overnight at 4ºC and then rinsed in PBS for 2 hours. Paraffin-embedding was performed during 3 days: after PBS washing, eyes were placed in 70% v/v ethanol for 3 hours and then changed to 96% v/v ethanol, for an overnight. Next morning, two incubations in 100% ethanol for 2 hours were performed. Once dehydration was finished, eyes

were transferred to xylol for 30 minutes and then to paraffin for overnight at 65ºC. In the third morning, an additional paraffin step of 2 hours was performed and then the paraffin blocks were solidified and sectioned.

For inmunohistochemical detection, sections were mounted in coverplates (Shandon Coverplates, Thermo), blocked for 30 minutes with a PBS solution containing 25% of normal serum and then incubated overnight at 4ºC with the specific antibody (see list, section 1.4) diluted in 10% normal serum PBS. After 3 washes of 5 minutes with PBS, sections were incubated for 1 hour at room temperature with the corresponding secondary antibodies (see list, section 1.4). After washing again, sections were incubated with fluorochrome (see list, section 1.4) for 1 hour at room temperature and nuclei were counterstained with DAPI and covered with mounting media for fluorescence (Fluoromount, Sigma-Aldrich).

For PAS staining, sections were incubated in a 5% w/v solution of periodic acid (Sigma-Aldrich) for 10 minutes, then rinsed in distilled water and incubated in Schiff reagent (Sigma-Aldrich) for 25 minutes. Sections were counterstained in hematoxylin.

2.3.2. Immunohistochemistry in *in toto* retinas

Retinas were dissected in PBS, flattened and fixed for an overnight at 4ºC in 10% formalin. Next morning, retinas were washed 4 times with PBT (PBS with 0.1% v/v IGEPAL, Sigma-Aldrich) for 1 hour at room temperature and the permeabilized with 0.1% TRITON X-100 (Sigma-Aldrich) in PBS, for 2 hour more. Then, samples were incubated overnight at 4ºC with the specific antibody (see list, section 1.4) diluted in PBS with 3 gr/L of BSA and 10% v/v of normal serum. The following day, four 1-hour washes with PBT were performed and the samples were incubated overnight at 4ºC with the corresponding secondary antibody. After this incubation, samples were washed as usual and incubated in the same conditions with the fluorochrome diluted in PBS and counterstained with TOPRO. After washing again, the samples were flattened on slides and covered with mounting medio for fluorescence (Fluoromount, Sigma-Aldrich).

2.3. MORPHOMETRIC ANALYSIS FOR EVALUATION OF NEURONAL POPULATIONS

Retinal layers (INL and ONL) length was measured with NIS Elements software (Nikon) in 6 central and 6 peripheral images (20x) from retinal sections showing the optic nerve. Three measurements were performed in each image for each layer, ensuring perpendicular distances between layer limits.

For quantification of specific neuronal populations, total positive cells were counted per 20 images of central retinal sections with optic nerve.

Alternative quantification of total positive cells/total nuclei underscored differences given the reduced number of total nuclei in transgenic retinas.

Semi-quantitative analysis of the degree of delocalization of Kir 4.1 was performed by assigning a numeric value to immunostaining in each sample, being 0 total delocalization and 3 normal localization of Kir 4.1. A value was given to each of three specific retinal areas: the inner limiting membrane, the outer limiting membrane and the perivascular area. The total score for each sample resulted from the sum of the values assigned to each area evaluated.

2.4. ANALYSIS OF PROTEIN EXPRESSION BY WESTERN BLOT

2.4.1. Protein extracts preparation and quantification

Retinas were homogenized in 75 µl of cold lysis buffer containing a protease inhibitor cocktail (Complete Mini EDTA-free, Roche, one table in 10 mL of buffer). Three pulses of 5 seconds were applied with the sonicator, putting sample on ice between each pulse to avoid overheating. After sonication, samples were centrifuged 10 minutes at 10000g (4ºC) and the supernatant was collected.

Protein concentration in homogenized samples was determined by Bradford method. A BSA standard solution was used to make a curve with concentrations from 0 to 15 µg of protein in a volume of 800 ul of water + 200 ul

of Bradford reagent (Bio-Rad). 1 µl of the homogenized samples was diluted in the same proportion and after a short incubation at room temperature, the absorbance at 594 nm was measured. The concentration of the samples was calculated using the standard curve.

2.4.2. SDS-PAGE

Two-phase polyacrilamide (acrylamide-bisacrylamide 30%, Bio-Rad) gels with SDS were used to separate proteins by electrophoresis. The upper or stacking gel, containing 4% of polyacrilamide, allowed sample loading in the wells and stacking of the proteins before separation. In the bottom, the resolving gel, containing 12% of polyacrilamide, separated the different proteins of the extract. Samples were thawed on ice and Laemmli loading buffer 4x was added. Before loading, samples were denatured 2 minutes at 90º and cooled down at room temperature. Until samples were running through the stacking gel, electrophoresis was carried out at 50V. Once the samples are in the resolving, the potency was increased to 100V. Molecular weight marker (Spectra Multicolor Broad Range Protein Ladder, Fermentas) were used to calculate the protein size in the gel.

2.4.3. Protein transfer to membranes and immunodetection

PVDF membranes (Hyperbond-P, Amersham, GH) were used to blot proteins from electrophoresis gel. Transfer was perfomed at 100V for 2 hours at 4ºC in towing buffer containing 20% methanol. After the blotting, membranes

were stained with Ponceau dye to check the presence and correct loading of the proteins. Red staining was completely removed with TBS-Tween 0.05% washing and then blots were blocked 1 hour at room temperature with blotto (10% w/v dried milk in TBS-Tween 0.05%) or 10% w/v BSA. Incubation with specific primary antibody (see list, section 1.4) diluted in 5% blotto or BSA solution was performed overnight at 4ºC. Next morning, excess of antibody was washed with TBS-Tween 0.05% (3 quick rinses + 2x 10 minutes) and the membranes were incubated with the corresponding secondary antibody, conjugated with HRP (see list, section 1.4), for 2 hours at room temperature. Then, the blots were washed again, adding a final 5 minute-rinse with TBS. Immobilon Western Blot Chemiluminiscence Kit (Millipore) was used to detect HRP signal in the blots, exposing them to a photographic film and developed to visualize de signal. Bands intensity was measured using GeneSnap software (Syngene).

2.4.4. Oxidized proteins detection

Oxidized proteins were detected by immunoblotting with the commercial kit Oxyblot (Millipore, cat. S7150) following manufacturer's intructions. Retinal protein extracts were prepared as previously described, but lysis buffer was supplemented with 2% v/v β-mercaptoethanol to prevent oxidation of the samples. Carbonyl groups were derivatized by incubation with 2,4-Dinitrophenylhydrazine (DNPH) and converted to DNP-hydrazone. Treated samples were loaded to standard electrphoresis gel in parallel with non-treated replicates. After transference, carbonyl groups were detected by immunoblotting

with an antibody specific for DNP-hydrazone following the standard protocol detailed in 2.4.3 section.

Solutions:

- Protein lysis buffer: 50mM Tris pH 7, 150 mM NaCl, SDS 1%, Igepal 1%, 1 mM EDTA, Aprotinina 1 µg/µl, 1 mM sodium ortovanadate
- Stacking buffer (pH 6.8): 0.5 M Tris-HCl, 0.4% w/v
- Resolving buffer (pH 8.8): 1.5 M Tris-HCl, 0.4% w/v
- Laemmli loading buffer: 50 mM phosphate buffer pH 7, 30% v/v glycerol, 10% v/v SDS, 5% v/v β-mercaptoethanol, bromophenol blue.
- Electrophoresis buffer: 125 mM Tris, 960 mM Glycine, 17 mM SDS
- Towing buffer: 25 mM Tris, 192 mM glycine, 20% v/v methanol

2.5. RNA EXTRACTION AND QUANTITATIVE REAL-TIME PCR

Retinas were homogenized in 200 µl of Tripure and retinal RNA was purified using RNeasy Mini Kit (QIAGEN Sciences). cDNA was synthesized with Transcriptor First Strand cDNA Synthesis Kit (Roche). Quantitative real-time PCR was performed using LightCycler® 480 SYBR Green I Master (Roche) with specific primers (Invitrogen) listed in the following table:

Gene	Primers (5'-3')
$p27^{Kip}$	Fw: AGGCGGTGCCTTTAATTGGG
	Rv: TTACGTCTGGCGTCGAAGGC
GLAST	Fw: GCTTCGGTTTCGTGATCG
	Rv: AGAAGAGGATGCCAGAGG
TNF-α	Fw: TCTTCTCATTCCTGCTTGTGG
	Rv: GGTCTGGGCCATAGAACTGA
iNOS	Fw: TGGTCCGCAAGAGAGTGCT
	Rv: CCTCATTGGCCAGCTGCTT
GFAP	Fw: ACAGACTTTCTCCAACCTCCAG
	Rv: CCTTCTGACACGGATTTGGT
Gja1	Fw: GTGCCGGCTTCACTTTCA
	Rv: GGAGTAGGCTTGGACCTTGTC
s100b	Fw: GGACTCCAGCAGCAAAGGT
	Rv: TTCAGCTTGTGCTTGTCACC
hPEDF	Fw: TACCGGGTGCGATCCAGCA
	Rv: TGGGCTGCTGATCAAGTCA

2.6. MEASUREMENTS OF RETINAL GLUTAMATE CONTENT

Retinas were weighted and homogenized in 50 µl of 5% perchloric acid, using pestle and 4 minutes of ultrasound bath (repeated twice). Then, samples were centrifuged 5 minutes at 12000g at 4ºC and the supernatant was collected in a new tube and weighted. Supernatant pH was neutralized with KOH and re-weighted to determine the dilution factor of each sample. 20 µl of each sample were added to 80 µl of reaction cocktail containing: 0.06M Tris pH 9, 0.1 mM ADP (Sigma-Aldrich), 0.12 mM EDTA, 3.12 µl/mL hydrazine hydrate (Sigma-Aldrich), 1.5 mM NAD^+ (Sigma-Aldrich) and basal absorbance of samples was measured at 340 nm in a microplate reader. 1.25 µl of glutamate dehydrogenase (Sigma-Aldrich) were added to each well and the plate was incubated 45 minutes at room temperature. After this time, the absorbance was read again and 340nm. The ΔOD represented the quantity of glutamate

degraded by the enzymatic reaction and then present in the sample. A standard curve with known concentrations of glutamate (0.25-1.75 mM) was performed in the same microplate and sample values were obtained by extrapolation. These values were corrected by the dilution factor of each sample and referred to mg of retina.

2.7. ANALYSIS OF GLUTAMINE SYNTHETASE ACTIVITY

Protein extracts were obtained as in Western blot analysis. 40 µl of a 1/10 dilution of the extracts was added to the reaction cocktail containing: 50mM sodium glutamate (Sigma-Aldrich), 20 mM $MgCl_2$ (Panreac), 15 mM ATP (Sigma-Aldrich), 100 mM imidazol pH 7.2 (Fluka), 1 µl β-mercaptoethanol, 10 mM creatine phosphate (Sigma-Aldrich), 1 µl creatin-phosphokinase (CPK) (Sigma-Aldrich). The mixture was preincubate at 37ºC for 1-2 minutes and then, the reaction was started by adding 8 µl of 125mM hydroxylamine. Ten minutes later, the reaction was stopped with 120 µl of ferric chloride solution (0.37M $FeCl_3$, 0.67M HCl, 0.20M trichloroacetic acid) and put on ice for 5 minutes. Then, the microplate was centrifuged 5 min at low speed, the supernatant was collected from the wells and absorbance at 525 nm was read. Values were corrected by protein concentration of each sample and represented as percentage of the wild-type values.

2.8. GLUTATHIONE MEASUREMENT

Total and oxidized glutathione content was determined in retinal extracts using the Glutathione (total) Detection kit from Enzo Life Sciences (cat. ADI-900-160). Samples were homogenized in 5% w/v metaphosphoric acid (Sigma-Aldrich) following manufacture's instructions. The detection is based on the measurement of the activity of the enzyme glutathione reductase. The slope of the kinetic curve obtained after the spectrophotometric measurement of 5-thio-2-nitrobenzoic acid at 414 nm during 10 minutes was extrapolated to glutathione content by means of an standard curve with known quantities of glutathione. For the determination of oxidized glutathione, samples were pre-treated with 2 M 4-vinylpyridine (Sigma-Aldrich), that blocks free thiols in the reaction, avoiding the cycling reaction of that would reduce oxidized glutathione.

2.9. PREPARATION OF AAV2 VECTORS

Vectors were generated by helper virus-free transfection of HEK293 cells with three plasmids (Xiao et al., 1998). PEI transfection was performed in 140 mm plates with a mixture of the following contructions: (1) a vector plasmid carrying the expression cassette flanked by the viral ITRs corresponding to AAV2; (2) a packaging plasmid carrying the AAV2 rep and cap genes; and (3) a helper plasmid carrying the adenovirus helper functions (PXX6). The expression cassette contained the ubiquitous CAG promoter (hybrid of CMV early enhancer/ chicken ß actin promoter), GFP or human PEDF cDNA (provided by

Dr. Susan Crawford, Northwestern University, USA) and WPRE element. Three days after transfection, cells were collected and lysated with 3 cycles of freezing-thawing. Viral particles were purified by a gradient of 15%, 25%, 40% and 60% v/v iodixanol solutions and centrifuged 1 hour at 69.000 rpm and 18ºC in a type 70 Ti rotor. The clear interphase containing AAV particles was aspirated with a 18G needle.

In order to determine the titer of the viral preparations viral genomes were measured by Dot Blot. To do so, 1 y 5 µl of viral solution were treated with DNAsa I (QiagenMR), following manufacturer's instructions. This step ensured the elimination any cellular o plasmidic DNA remaining in the viral preparation. Then, Proteinase K digestion allowed the release of viral genomes from the viral particles. DNA was obtained with a 25:24:1 phenol/chloroform/isoamilic alcohol solution and precipitated 30 minutes at -80ºC with 0.1 volumes of sodic acetate 3M and 2.5 volumes of 100% ethanol in presence of glycogen (Sigma-Aldrich) as carrier. After washing with 70% etanol, DNA pellet was resuspending in 40 µl of 0.4M NaOH and 10 mM EDTA. Serial dilution of the plasmids used for AAV production were prepared (0; 0.07; 0.15; 0.3; 0.6; 1.2; 2.5; 5; 10; 20 and 40 ng of DNA) in a final volume of 40 µl of 0.4M NaOH and 10 mM EDTA. Samples were denatured 5 minutes at 100ºC , quickly put on ice and transferred to nylon membranes Hybond-XL (Amersham Biosciences) using a vacuum source. Once transferenced was finished, membranas were washed with 2x SSC and wet 2 hours at 80ºC. Blot hibridization was performed using the kit AlkPhos Direct (Amersham Biosciences), following manufacturer's instructions and using probes corresponding to GFP and PEDF cDNA. Blot signal was obtained with

the reactive CDP-Star (Amersham Biosciences). Spots intensity was determined by densitometry and viral genomes were calculated by extrapolation of the standard curve of each plasmid.

2.10. INTRAVITREAL ADMINISTRATION OF AAV VECTORS

Under a dissecting microscope, 2 µl of viral solution were delivered to the vitreous cavity of deeply anesthetized mice (100 mg/kg ketamine/10 mg/kg xylazine) using a 10-mm 33-gauge needle mounted on a 5 µl Hamilton syringe (Hamilton Bonaduz AG). The needle was advanced through the sclera near to the corneoscleral limbus. Pupils were previously dilated with Tropicamide (Alcon Cusí) and antibiotic and anti-inflammatory drops (Tobradex, Alcon Cusí,) were administered after the injection. Animals showing signs of trauma or ocular bleeding after the injection were excluded from the study.

2.11. BASEMENT MEMBRANE ANALYSIS BY TRANSMISSION ELECTRON MICROSCOPY

Retinas were dissected and a peripheral area of 1 mm2 was cut and fixed in 2.5% glutaraldehyde and 2% paraformaldehyde for 2 hours at 4℃. After washing in cold phosphate buffer 0.1M, the specimens were post-fixed in 1% osmium tetroxide, dehydrated through a graded acetone series and embedded in epoxy resin. Ultrathin sections (600–800 Å) were stained using lead citrate and analyzed with a transmission electron microscope (Hitachi H-7000). Five capillary were analysed per retina and the thickness of the basement

membrane was measured in 12 sites per vessel (NIS Elements, Nikon Instruments).

2.12. ASSESSMENT OF NEOVASCULARIZATION

For retinal angiograms, animals received a tail vein injection of 50 mg/ml FITC-conjugated Dextran (Sigma-Aldrich). Ten minutes later, animals were sacrificed and retinas were dissected, flat-mounted and fixed overnight in 10% formalin at 4ºC, protected from light. Twenty images (40x) of the capillary network that excluded major vessels were captured per retina (Nikon Eclipse 90i), and the area corresponding to the capillary area was calculated using software tools (NIS Elements, Nikon Instruments) as percentage of green area over total retinal area. Pre-retinal vessels were analyzed in PAS-stained eye sections. The number of PAS+ intravitreal cells on the vitreal side of the internal limiting membrane was counted in 6 non-consecutive sections/eye.

2.13. VEGF DETECTION

For VEGF detection in aqueous humor (pooled from 2-3 eyes) 10 µl of sample were analyzed with the Mouse VEGF ELISA kit (QIA52, Calbiochem) following manufacturer's instructions.

2.14. ZYMOGRAPHY ANALYSIS

3 µl of aqueous humor were directly loaded into 12% polyacrylamide running gels containing 0.1 mg/ml of porcine gelatin (BioRad) and ran as standard protein electrophoresis. Gels were removed from glass plates, rinsed with 1M Tris-HCl pH 7.5 with 12.5% v/v Triton X-100 and incubated in 1M Tris-HCl pH 7.5, 0.5M CaCl2 for 18 h at 37ºC. After incubation, gels were stained in 0.1% Coomassie Blue, 10% v/v acetic acid, 10% v/v isopropanol for 2 h and then destained in 10% v/v acetic acid, 10% v/v isopropanol until the bands were clearly visible. Bands intensity was measured using GeneSnap software (Syngene).

2.15. STATISTICAL ANALYSIS

Values are expressed as the mean ± SEM. Differences between groups were compared by unpaired Student t test. Differences were considered statistically significant at P values less than 0.05.

VII. Bibliography

ADA (2010). Standards of medical care in diabetes--2010. Diabetes care 33 Suppl 1, S11–S61.

ADA (2005). Standards of medical care in diabetes. Diabetes care 28 Suppl 1, S4–S36.

Abu El-Asrar, A. M., Desmet, S., Meersschaert, A., Dralands, L., Missotten, L., and Geboes, K. (2001). Expression of the inducible isoform of nitric oxide synthase in the retinas of human subjects with diabetes mellitus. American journal of ophthalmology 132, 551–556.

Abu-El-Asrar, A. M., Dralands, L., Missotten, L., Al-Jadaan, I. A., and Geboes, K. (2004). Expression of apoptosis markers in the retinas of human subjects with diabetes. Investigative ophthalmology & visual science 45, 2760–2766.

Acland, G. M., Aguirre, G. D., Bennett, J., Aleman, T. S., Cideciyan, A. V., Bennicelli, J., Dejneka, N. S., Pearce-Kelling, S. E., Maguire, A. M., Palczewski, K., et al. (2005). Long-term restoration of rod and cone vision by single dose rAAV-mediated gene transfer to the retina in a canine model of childhood blindness. Molecular therapy 12, 1072–1082.

Adamis, A. P. (2002). Is diabetic retinopathy an inflammatory disease? The British journal of ophthalmology 86, 363–365.

Adamis, A. P., Altaweel, M., Bressler, N. M., Cunningham, E. T., Davis, M. D., Goldbaum, M., Gonzales, C., Guyer, D. R., Barrett, K., and Patel, M. (2006). Changes in retinal neovascularization after pegaptanib (Macugen) therapy in diabetic individuals. Ophthalmology 113, 23–28.

Agardh, C. D., Agardh, E., Zhang, H., and Ostenson, C. G. (1997). Altered endothelial/pericyte ratio in Goto-Kakizaki rat retina. Journal of diabetes and its complications 11, 158–162.

Agardh, E., and Agardh, C. D. (2004). Diabetic Retinopathy. In International Textbook of Diabetes Mellitus, R. A. DeFronzo, H. Ferrannini, H. Keen, and P. Zimmet, eds. (John Wiley & Sons), pp. 1187–1206.

Agudo, J., Ayuso, E., Jimenez, V., Salavert, A., Casellas, A., Tafuro, S., Haurigot, V., Ruberte, J., Segovia, J. C., Bueren, J., et al. (2008). IGF-I mediates regeneration of endocrine pancreas by increasing beta cell replication through cell cycle protein modulation in mice. Diabetologia 51, 1862–1872.

Aiello, L. P., Avery, R. L., Arrigg, P. G., Keyt, B. A., Jampel, H. D., Shah, S. T., Pasquale, L. R., Thieme, H., Iwamoto, M. A., and Park, J. E. (1994). Vascular endothelial growth factor in ocular fluid of patients with diabetic retinopathy and other retinal disorders. The New England journal of medicine 331, 1480–1487.

Aizu, Y., Oyanagi, K., Hu, J., and Nakagawa, H. (2002). Degeneration of retinal neuronal processes and pigment epithelium in the early stage of the streptozotocin-diabetic rats. Neuropathology 22, 161–170.

Alvarez, R. D., Gomez-Navarro, J., Wang, M., Barnes, M. N., Strong, T. V., Arani, R. B., Arafat, W., Hughes, J. V., Siegal, G. P., and Curiel, D. T. (2000). Adenoviral-mediated suicide gene therapy for ovarian cancer. Molecular therapy 2, 524–530.

Ambati, J., Chalam, K. V., Chawla, D. K., D'Angio, C. T., Guillet, E. G., Rose, S. J., Vanderlinde, R. E., and Ambati, B. K. (1997). Elevated gamma-aminobutyric acid, glutamate, and vascular endothelial growth factor levels in the vitreous of patients with proliferative diabetic retinopathy. Archives of ophthalmology 115, 1161–1166.

Amin, R. H., Frank, R. N., Kennedy, A., Eliott, D., Puklin, J. E., and Abrams, G. W. (1997). Vascular endothelial growth factor is present in glial cells of the retina and optic nerve of human subjects with nonproliferative diabetic retinopathy. Investigative ophthalmology & visual science 38, 36–47.

Andrieu-Soler, C., Bejjani, R.-A., de Bizemont, T., Normand, N., BenEzra, D., and Behar-Cohen, F. (2006). Ocular gene therapy: a review of nonviral strategies. Molecular vision 12, 1334–1347.

Antonetti, D. A., Barber, A. J., Bronson, S. K., Freeman, W. M., Gardner, T. W., Jefferson, L. S., Kester, M., Kimball, S. R., Krady, J. K., LaNoue, K. F., et al. (2006). Diabetic retinopathy: seeing beyond glucose-induced microvascular disease. Diabetes 55, 2401–2411.

Apte, R. S., Barreiro, R. A., Duh, E., Volpert, O., and Ferguson, T. A. (2004). Stimulation of neovascularization by the anti-angiogenic factor PEDF. Investigative ophthalmology & visual science 45, 4491–4497.

Ashton, N. (1966). Oxygen and the growth and development of retinal vessels. In vivo and in vitro studies. The XX Francis I. Proctor Lecture. American journal of ophthalmology 62, 412–435.

Asnaghi, V., Gerhardinger, C., Hoehn, T., Adeboje, A., and Lorenzi, M. (2003). A role for the polyol pathway in the early neuroretinal apoptosis and glial changes induced by diabetes in the rat. Diabetes 52, 506–511.

Augustin, A. J., Dick, H. B., Koch, F., and Schmidt-Erfurth, U. (2002). Correlation of blood-glucose control with oxidative metabolites in plasma and vitreous body of diabetic patients. European journal of ophthalmology 12, 94–101.

Auricchio, A. (2003). Pseudotyped AAV vectors for constitutive and regulated gene expression in the eye. Vision research 43, 913–918.

Auricchio, A., Behling, K. C., Maguire, A. M., O'Connor, E. M., Bennett, J., Wilson, J. M., and Tolentino, M. J. (2002). Inhibition of retinal neovascularization by intraocular viral-mediated delivery of anti-angiogenic agents. Molecular therapy 6, 490–494.

Bainbridge, J.W., Tan, M.H., Ali, R.R. (2006) Gene therapy progress and prospects: the eye. Gene Therapy 13,1191-7.

Bainbridge, J. W. B., Smith, A. J., Barker, S. S., Robbie, S., Henderson, R., Balaggan, K., Viswanathan, A., Holder, G. E., Stockman, A., Tyler, N., et al. (2008). Effect of gene therapy on visual function in Leber's congenital amaurosis. The New England journal of medicine 358, 2231–2239.

Balaggan, K. S., Binley, K., Esapa, M., Maclaren, R. E., Iqball, S., Duran, Y., Pearson, R. A., Kan, O., Barker, S. E., Smith, A. J., et al. (2006). EIAV vector-mediated delivery of endostatin or angiostatin inhibits angiogenesis and vascular hyperpermeability in experimental CNV. Gene Therapy 13, 1153–1165.

Barber, A. J., Antonetti, D. A., Kern, T. S., Reiter, C. E. N., Soans, R. S., Krady, J. K., Levison, S. W., Gardner, T. W., and Bronson, S. K. (2005). The Ins2Akita mouse as a model of early retinal complications in diabetes. Investigative ophthalmology & visual science 46, 2210–2218.

Barber, A. J., Antonetti, D. A., and Gardner, T. W. (2000). Altered expression of retinal occludin and glial fibrillary acidic protein in experimental diabetes. The Penn State Retina Research Group. Investigative ophthalmology & visual science 41, 3561–3568.

Barber, A. J., Gardner, T. W., and Abcouwer, S. F. (2011). The significance of vascular and neural apoptosis to the pathology of diabetic retinopathy. Investigative ophthalmology & visual science 52, 1156–1163.

Barber, A. J., Lieth, E., Khin, S. A., Antonetti, D. A., Buchanan, A. G., and Gardner, T. W. (1998). Neural apoptosis in the retina during experimental and human diabetes. Early onset and effect of insulin. The Journal of clinical investigation 102, 783–791.

Barnstable, C. J., and Tombran-Tink, J. (2004). Neuroprotective and antiangiogenic actions of PEDF in the eye: molecular targets and therapeutic potential. Progress in retinal and eye research 23, 561–577.

Bearse, M. A., Adams, A. J., Han, Y., Schneck, M. E., Ng, J., Bronson-Castain, K., and Barez, S. (2006). A multifocal electroretinogram model predicting the development of diabetic retinopathy. Progress in retinal and eye research 25, 425–448.

Becerra, S. P., Sagasti, A., Spinella, P., and Notario, V. (1995). Pigment epithelium-derived factor behaves like a noninhibitory serpin. Neurotrophic activity does not require the serpin reactive loop. The Journal of biological chemistry 270, 25992–25999.

Behar-Cohen, F. F., Heydolph, S., Faure, V., Droy-Lefaix, M. T., Courtois, Y., and Goureau, O. (1996). Peroxynitrite cytotoxicity on bovine retinal pigmented epithelial cells in culture. Biochemical and biophysical research communications 226, 842–849.

Bell, D. S. H. (2003). Diabetic cardiomyopathy. Diabetes care 26, 2949–2951.

Bennett, J., Ashtari, M., Wellman, J., Marshall, K. A., Cyckowski, L. L., Chung, D. C., McCague, S., Pierce, E. A., Chen, Y., Bennicelli, J. L., et al. (2012). AAV2 Gene Therapy Readministration in Three Adults with Congenital Blindness. Science translational medicine 4, 120ra15.

Bennett, J., Duan, D., Engelhardt, J. F., and Maguire, A. M. (1997). Real-time, noninvasive in vivo assessment of adeno-associated virus-mediated retinal transduction. Investigative ophthalmology & visual science 38, 2857–2863.

Bennett, J., Wilson, J., Sun, D., Forbes, B., and Maguire, A. (1994). Adenovirus vector-mediated in vivo gene transfer into adult murine retina. Investigative ophthalmology & visual science 35, 2535–2542.

Bernard, A., Gao-Li, J., Franco, C.-A., Bouceba, T., Huet, A., and Li, Z. (2009). Laminin Receptor Involvement in the Anti-angiogenic Activity of Pigment Epithelium-derived Factor. The Journal of biological chemistry 284, 10480–10490.

Bilak, M. M., Corse, A. M., Bilak, S. R., Lehar, M., Tombran-Tink, J., and Kuncl, R. W. (1999). Pigment epithelium-derived factor (PEDF) protects motor neurons from chronic glutamate-mediated neurodegeneration. Journal of neuropathology and experimental neurology 58, 719–728.

Boscia, F. (2010). Current approaches to the management of diabetic retinopathy and diabetic macular oedema. Drugs 70, 2171–2200.

Bouck, N. (2002). PEDF: anti-angiogenic guardian of ocular function. Trends in molecular medicine 8, 330–334.

Bringmann, A., Francke, M., Pannicke, T., Biedermann, B., Kodal, H., Faude, F., Reichelt, W., and Reichenbach, A. (2000). Role of glial K(+) channels in ontogeny and gliosis: a hypothesis based upon studies on Müller cells. Glia 29, 35–44.

Bringmann, A., Iandiev, I., Pannicke, T., Wurm, A., Hollborn, M., Wiedemann, P., Osborne, N. N., and Reichenbach, A. (2009a). Cellular signaling and factors involved in Müller cell gliosis: neuroprotective and detrimental effects. Progress in retinal and eye research 28, 423–451.

Bringmann, A., Pannicke, T., Biedermann, B., Francke, M., Iandiev, I., Grosche, J., Wiedemann, P., Albrecht, J., and Reichenbach, A. (2009b). Role of retinal glial cells in neurotransmitter uptake and metabolism. Neurochemistry international 54, 143–160.

Bringmann, A., Pannicke, T., Grosche, J., Francke, M., Wiedemann, P., Skatchkov, S. N., Osborne, N. N., and Reichenbach, A. (2006). Müller cells in the healthy and diseased retina. Progress in retinal and eye research 25, 397–424.

Broadhead, M. L., Dass, C. R., and Choong, P. F. M. (2009). Cancer cell apoptotic pathways mediated by PEDF: prospects for therapy. Trends in molecular medicine 15, 461–467.

Broderick, C. A., Smith, A. J., Balaggan, K. S., Georgiadis, A., Georgarias, A., Buch, P. K., Trittibach, P. C., Barker, S. E., Sarra, G.-M., Thrasher, A. J., et al. (2005). Local administration of an adeno-associated viral vector expressing IL-10 reduces monocyte infiltration and subsequent photoreceptor damage during experimental autoimmune uveitis. Molecular therapy□: the journal of the American Society of Gene Therapy 12, 369–373.

Brown, G. C. (2010). Nitric oxide and neuronal death. Nitric Oxide 23, 153–165.

Brownlee, M. (2001). Biochemistry and molecular cell biology of diabetic complications. Nature 414, 813–820.

Brownlee, M. (2005). The pathobiology of diabetic complications: a unifying mechanism. Diabetes 54, 1615–1625.

Buch, P.K., Bainbridge, J.W., Ali, R.R. (2008) AAV-mediated gene therapy for retinal disorders: from mouse to man. Gene Therapy 15, 849-57.

Budenz, D. L., Bennett, J., Alonso, L., and Maguire, A. (1995). In vivo gene transfer into murine corneal endothelial and trabecular meshwork cells. Investigative ophthalmology & visual science 36, 2211–2215.

Cai, J., Jiang, W. G., Grant, M. B., and Boulton, M. (2006). Pigment epithelium-derived factor inhibits angiogenesis via regulated intracellular proteolysis of vascular endothelial growth factor receptor 1. The Journal of biological chemistry 281, 3604–3613.

Cai, J., and Boulton, M. (2002). The pathogenesis of diabetic retinopathy: old concepts and new questions. Eye (London, England) 16, 242–260.

Calcutt, N. A., Willars, G. B., and Tomlinson, D. R. (1988). Axonal transport of choline acetyltransferase and 6-phosphofructokinase activities in genetically diabetic mice. Muscle & nerve 11, 1206–1210.

Campochiaro, P. A., Brown, D. M., Awh, C. C., Lee, S. Y., Gray, S., Saroj, N., Murahashi, W. Y., and Rubio, R. G. (2011). Sustained benefits from ranibizumab for macular edema following central retinal vein occlusion: twelve-month outcomes of a phase III study. Ophthalmology 118, 2041–2049.

Campochiaro, P. A., Nguyen, Q. D., Shah, S. M., Klein, M. L., Holz, E., Frank, R. N., Saperstein, D. A., Gupta, A., Stout, J. T., Macko, J., et al. (2006). Adenoviral vector-delivered pigment epithelium-derived factor for neovascular age-related macular degeneration: results of a phase I clinical trial. Human gene therapy 17, 167–176.

Cao, W., Tombran-Tink, J., Chen, W., Mrazek, D., Elias, R., and McGinnis, J. F. (1999). Pigment epithelium-derived factor protects cultured retinal neurons against hydrogen peroxide-induced cell death. Journal of neuroscience research 57, 789–800.

Cao, W., Tombran-Tink, J., Elias, R., Sezate, S., Mrazek, D., and McGinnis, J. F. (2001). In vivo protection of photoreceptors from light damage by pigment epithelium-derived factor. Investigative ophthalmology & visual science 42, 1646–1652.

Carmo, A., Cunha-Vaz, J. G., Carvalho, A. P., and Lopes, M. C. (2000). Nitric oxide synthase activity in retinas from non-insulin-dependent diabetic Goto-Kakizaki rats: correlation with blood-retinal barrier permeability. Nitric oxide□: biology and chemistry / official journal of the Nitric Oxide Society 4, 590–596.

Casella, G. T. B., Bunge, M. B., and Wood, P. M. (2004). Improved immunocytochemical identification of neural, endothelial, and inflammatory cell types in paraffin-embedded injured adult rat spinal cord. Journal of neuroscience methods 139, 1–11.

Cayouette, M., Smith, S. B., Becerra, S. P., and Gravel, C. (1999). Pigment epithelium-derived factor delays the death of photoreceptors in mouse models of inherited retinal degenerations. Neurobiology of disease 6, 523–532.

Chakravarthy, U., Stitt, A. W., McNally, J., Bailie, J. R., Hoey, E. M., and Duprex, P. (1995). Nitric oxide synthase activity and expression in retinal capillary endothelial cells and pericytes. Current eye research 14, 285–294.

Challa, P., Luna, C., Liton, P. B., Chamblin, B., Wakefield, J., Ramabhadran, R., Epstein, D. L., and Gonzalez, P. (2005). Lentiviral mediated gene delivery to the anterior chamber of rodent eyes. Molecular vision 11, 425–430.

Charonis, A. S., Reger, L. A., Dege, J. E., Kouzi-Koliakos, K., Furcht, L. T., Wohlhueter, R. M., and Tsilibary, E. C. (1990). Laminin alterations after in vitro nonenzymatic glycosylation. Diabetes 39, 807–814.

Chen, Y. H., Chang, M., and Davidson, B. L. (2009). Molecular signatures of disease brain endothelia provide new sites for CNS-directed enzyme therapy. Nature medicine 15, 1215–1218.

Cheung, A. K. H., Fung, M. K. L., Lo, A. C. Y., Lam, T. T. L., So, K. F., Chung, S. S. M., and Chung, S. K. (2005). Aldose reductase deficiency prevents diabetes-induced blood-retinal barrier breakdown, apoptosis, and glial reactivation in the retina of db/db mice. Diabetes 54, 3119–3125.

Cheung, N., Mitchell, P., and Wong, T. Y. (2010). Diabetic retinopathy. Lancet 376, 124–136.

Cho, W. B., Oh, S. B., Moon, J. W., and Kim, H. C. (2009). Panretinal photocoagulation combined with intravitreal bevacizumab in high-risk proliferative diabetic retinopathy. Retina (Philadelphia, Pa.) 29, 516–522.

Chun, D. W., Heier, J. S., Topping, T. M., Duker, J. S., and Bankert, J. M. (2006). A pilot study of multiple intravitreal injections of ranibizumab in patients with center-involving clinically significant diabetic macular edema. Ophthalmology 113, 1706–1712.

Chévez-Barrios, P., Chintagumpala, M., Mieler, W., Paysse, E., Boniuk, M., Kozinetz, C., Hurwitz, M. Y., and Hurwitz, R. L. (2005). Response of retinoblastoma with vitreous tumor seeding to adenovirus-mediated delivery of thymidine kinase followed by ganciclovir. Journal of clinical oncology 23, 7927–7935.

Clark, J. B., Palmer, C. J., and Shaw, W. N. (1983). The diabetic Zucker fatty rat. Proceedings of the Society for Experimental Biology and Medicine. Society for Experimental Biology and Medicine (New York, N.Y.) 173, 68–75.

Clements, R. S., Robison, W. G., and Cohen, M. P. (1998). Anti-glycated albumin therapy ameliorates early retinal microvascular pathology in db/db mice. Journal of diabetes and its complications 12, 28–33.

Colella, P., Cotugno, G., and Auricchio, A. (2009). Ocular gene therapy: current progress and future prospects. Trends in molecular medicine 15, 23–31.

Cooper, M. E. (1998). Pathogenesis, prevention, and treatment of diabetic nephropathy. Lancet 352, 213–219.

Coupland, S. G. (1987). A comparison of oscillatory potential and pattern electroretinogram measures in diabetic retinopathy. Documenta ophthalmologica. Advances in ophthalmology 66, 207–218.

Crawford, S. E., Stellmach, V., Ranalli, M., Huang, X., Huang, L., Volpert, O., De Vries, G. H., Abramson, L. P., and Bouck, N. (2001). Pigment epithelium-derived factor (PEDF) in neuroblastoma: a multifunctional mediator of Schwann cell antitumor activity. Journal of cell science 114, 4421–4428.

Cunningham, E. T., Adamis, A. P., Altaweel, M., Aiello, L. P., Bressler, N. M., D'Amico, D. J., Goldbaum, M., Guyer, D. R., Katz, B., Patel, M., et al. (2005). A phase II randomized double-masked trial of pegaptanib, an anti-vascular endothelial growth factor aptamer, for diabetic macular edema. Ophthalmology 112, 1747–1757.

Curtis, T. M., Hamilton, R., Yong, P.-H., McVicar, C. M., Berner, A., Pringle, R., Uchida, K., Nagai, R., Brockbank, S., and Stitt, A. W. (2011). Müller glial dysfunction during diabetic retinopathy in rats is linked to accumulation of advanced glycation end-products and advanced lipoxidation end-products. Diabetologia 54, 690–698.

DCCT (1993). The effect of intensive treatment of diabetes on the development and progression of long-term complications in insulin-dependent diabetes mellitus. The Diabetes Control and Complications Trial Research Group. The New England journal of medicine 329, 977–986.

DRSV Report 5 (1990). Early vitrectomy for severe vitreous hemorrhage in diabetic retinopathy. Four-year results of a randomized trial: Diabetic Retinopathy Vitrectomy Study Report 5. Archives of ophthalmology 108, 958–964.

Daneman, D. (2006). Type 1 diabetes. Lancet 367, 847–858.

Danis, R. P., and Bingaman, D. P. (1997). Insulin-like growth factor-1 retinal microangiopathy in the pig eye. Ophthalmology 104, 1661–1669.

Danis, R. P., and Yang, Y. (1993). Microvascular retinopathy in the Zucker diabetic fatty rat. Investigative ophthalmology & visual science 34, 2367–2371.

Dawson, D. W. (1999). Pigment Epithelium-Derived Factor: A Potent Inhibitor of Angiogenesis. Science 285, 245–248.

Dawson, V. L., and Dawson, T. M. (1996). Nitric oxide neurotoxicity. Journal of chemical neuroanatomy 10, 179–190.

Defronzo, R. A. (2009). Banting Lecture. From the triumvirate to the ominous octet: a new paradigm for the treatment of type 2 diabetes mellitus. Diabetes 58, 773–795.

Dejana, E. (2004). Endothelial cell-cell junctions: happy together. Nature reviews. Molecular cell biology 5, 261–270.

Devendra, D., Liu, E., and Eisenbarth, G. S. (2004). Type 1 diabetes: recent developments. BMJ (Clinical research ed.) 328, 750–754.

Devesa, S. S. (1975). The incidence of retinoblastoma. American journal of ophthalmology 80, 263–265.

Doll, J. A., Stellmach, V. M., Bouck, N. P., Bergh, A. R. J., Lee, C., Abramson, L. P., Cornwell, M. L., Pins, M. R., Borensztajn, J., and Crawford, S. E. (2003). Pigment epithelium-derived factor regulates the vasculature and mass of the prostate and pancreas. Nature medicine 9, 774–780.

Du, X., Matsumura, T., Edelstein, D., Rossetti, L., Zsengellér, Z., Szabó, C., and Brownlee, M. (2003). Inhibition of GAPDH activity by poly(ADP-ribose) polymerase activates three major pathways of hyperglycemic damage in endothelial cells. The Journal of clinical investigation 112, 1049–1057.

Dudus L, Anand V, Acland GM, Chen SJ, Wilson JM, Fisher KJ, Maguire AM, Bennett J. (1999) Persistent transgene product in retina, optic nerve and brain after intraocular injection of rAAV. Vision Research 39, 2545-53.

Dyer, M. A., and Cepko, C. L. (2000). Control of Müller glial cell proliferation and activation following retinal injury. Nature neuroscience 3, 873–880.

D'Ercole, A. J., Ye, P., Calikoglu, A. S., and Gutierrez-Ospina, G. (1996). The role of the insulin-like growth factors in the central nervous system. Molecular neurobiology 13, 227–255.

Eisenfeld, A. J., Bunt-Milam, A. H., and Sarthy, P. V. (1984). Müller cell expression of glial fibrillary acidic protein after genetic and experimental photoreceptor degeneration in the rat retina. Investigative ophthalmology & visual science 25, 1321–1328.

Elman, M. J., Aiello, L. P., Beck, R. W., Bressler, N. M., Bressler, S. B., Edwards, A. R., Ferris, F. L., Friedman, S. M., Glassman, A. R., Miller, K. M., et al. (2010). Randomized trial evaluating ranibizumab plus prompt or deferred laser or triamcinolone plus prompt laser for diabetic macular edema. Ophthalmology 117, 1064–1077.e35.

Evcimen, N. D., and King, G. L. (2007). The role of protein kinase C activation and the vascular complications of diabetes. Pharmacological research□: the official journal of the Italian Pharmacological Society 55, 498–510.

Feit-Leichman, R. A., Kinouchi, R., Takeda, M., Fan, Z., Mohr, S., Kern, T. S., and Chen, D. F. (2005). Vascular damage in a mouse model of diabetic retinopathy: relation to neuronal and glial changes. Investigative ophthalmology & visual science 46, 4281–4287.

Ferrara, N. (2000). Vascular endothelial growth factor and the regulation of angiogenesis. Recent progress in hormone research 55, 15–35.

Filleur, S., Nelius, T., de Riese, W., and Kennedy, R. C. (2009). Characterization of PEDF: a multi-functional serpin family protein. Journal of cellular biochemistry 106, 769–775.

Fischer, A. J., Scott, M. A., Zelinka, C., and Sherwood, P. (2010). A novel type of glial cell in the retina is stimulated by insulin-like growth factor 1 and may exacerbate damage to neurons and Müller glia. Glia 58, 633–649.

Fletcher, E. L., Phipps, J. A., Ward, M. M., Puthussery, T., and Wilkinson-Berka, J. L. (2007). Neuronal and glial cell abnormality as predictors of progression of diabetic retinopathy. Current pharmaceutical design 13, 2699–2712.

Forrester, J. (2002). The Eye. Basic science in practice Second Edi. (Saunders, Elsevier).

Forsythe, J. A., Jiang, B. H., Iyer, N. V., Agani, F., Leung, S. W., Koos, R. D., and Semenza, G. L. (1996). Activation of vascular endothelial growth factor gene transcription by hypoxia-inducible factor 1. Molecular and cellular biology 16, 4604–4613.

Friedman, E. A. (1996). Renal syndromes in diabetes. Endocrinology and metabolism clinics of North America 25, 293–324.

Fujimaki, T., Huang, Z.-Y., Kitagawa, H., Sakuma, H., Murakami, A., Kanai, A., McLaren, M. J., and Inana, G. (2004). Truncation and mutagenesis analysis of the human X-arrestin gene promoter. Gene 339, 139–147.

Funatsu, H., Yamashita, H., Nakamura, S., Mimura, T., Eguchi, S., Noma, H., and Hori, S. (2006). Vitreous levels of pigment epithelium-derived factor and vascular endothelial growth factor are related to diabetic macular edema. Ophthalmology 113, 294–301.

Gale, E. A. M. (2002). The rise of childhood type 1 diabetes in the 20th century. Diabetes 51, 3353–3361.

Gehlbach, P., Demetriades, A. M., Yamamoto, S., Deering, T., Duh, E. J., Yang, H. S., Cingolani, C., Lai, H., Wei, L., and Campochiaro, P. A. (2003). Periocular injection of an adenoviral vector encoding pigment epithelium-derived factor inhibits choroidal neovascularization. Gene Therapy 10, 637–646.

George, M., Ayuso, E., Casellas, A., Costa, C., Devedjian, J. C., and Bosch, F. (2002). Beta cell expression of IGF-I leads to recovery from type 1 diabetes. The Journal of clinical investigation 109, 1153–1163.

Gerhardinger, C., Costa, M. B., Coulombe, M. C., Toth, I., Hoehn, T., and Grosu, P. (2005). Expression of acute-phase response proteins in retinal Müller cells in diabetes. Investigative ophthalmology & visual science 46, 349–357.

Giaume, C., Kirchhoff, F., Matute, C., Reichenbach, A., and Verkhratsky, A. (2007). Glia: the fulcrum of brain diseases. Cell death and differentiation 14, 1324–1335.

Gillies, M. C., and Wong, T. Y. (2007). Ranibizumab for neovascular age-related macular degeneration. The New England journal of medicine 356, 748–749; author reply 749–750.

Golden, S. H. (2011). Emerging therapeutic approaches for the management of diabetes mellitus and macrovascular complications. The American journal of cardiology 108, 59B-67B.

González, V. H., Giuliari, G. P., Banda, R. M., and Guel, D. A. (2009). Intravitreal injection of pegaptanib sodium for proliferative diabetic retinopathy. The British journal of ophthalmology 93, 1474–1478.

Gonçalves, M. A. F. V. (2005). Adeno-associated virus: from defective virus to effective vector. Virology journal 2, 43.

Goto, Y., Suzuki, K., Ono, T., Sasaki, M., and Toyota, T. (1988). Development of diabetes in the non-obese NIDDM rat (GK rat). Advances in experimental medicine and biology 246, 29–31.

Gottfredsdóttir, M. S., Stefánsson, E., Jónasson, F., and Gíslason, I. (1993). Retinal vasoconstriction after laser treatment for diabetic macular edema. American journal of ophthalmology 115, 64–67.

Goureau, O., Hicks, D., Courtois, Y., and De Kozak, Y. (1994). Induction and regulation of nitric oxide synthase in retinal Müller glial cells. Journal of neurochemistry 63, 310–317.

Grant, M. B., Mames, R. N., Fitzgerald, C., Ellis, E. A., Aboufriekha, M., and Guy, J. (1993). Insulin-like growth factor I acts as an angiogenic agent in rabbit cornea and retina: comparative studies with basic fibroblast growth factor. Diabetologia 36, 282–291.

Grant, M., Russell, B., Fitzgerald, C., and Merimee, T. (1986). Insulin-like growth factors in vitreous. Studies in control and diabetic subjects with neovascularization. Diabetes 35, 416–420.

Greenberg, K. P., Geller, S. F., Schaffer, D. V., and Flannery, J. G. (2007). Targeted transgene expression in muller glia of normal and diseased retinas using lentiviral vectors. Investigative ophthalmology & visual science 48, 1844–1852.

Grünert, U., Martin, P. R., and Wässle, H. (1994). Immunocytochemical analysis of bipolar cells in the macaque monkey retina. The Journal of comparative neurology 348, 607–627.

Guan, J., Williams, C., Gunning, M., Mallard, C., and Gluckman, P. (1993). The effects of IGF-1 treatment after hypoxic-ischemic brain injury in adult rats. Journal of cerebral blood flow and metabolism : official journal of the International Society of Cerebral Blood Flow and Metabolism 13, 609–616.

Hammes, H. P., Martin, S., Federlin, K., Geisen, K., and Brownlee, M. (1991). Aminoguanidine treatment inhibits the development of experimental diabetic retinopathy. Proceedings of the National Academy of Sciences of the United States of America 88, 11555–11558.

Harati, Y. (1996). Diabetes and the nervous system. Endocrinology and metabolism clinics of North America 25, 325–359.

Haurigot, V., Villacampa, P., Ribera, A., Llombart, C., Bosch, A., Nacher, V., Ramos, D., Ayuso, E., Segovia, J. C., Bueren, J. A., et al. (2009). Increased intraocular insulin-like growth factor-I (IGF-I) triggers blood-retinal barrier breakdown. The Journal of biological chemistry 284, 22961–22969.

Hauswirth, W. W., Aleman, T. S., Kaushal, S., Cideciyan, A. V., Schwartz, S. B., Wang, L., Conlon, T. J., Boye, S. L., Flotte, T. R., Byrne, B. J., et al. (2008). Treatment of Leber Congenital Amaurosis Due to RPE65 Mutations by Ocular Subretinal Injection of Adeno-Associated Virus Gene Vector: Short-Term Results of a Phase I Trial. Human Gene Therapy 19, 979–990.

Haverkamp, S., and Wässle, H. (2000). Immunocytochemical analysis of the mouse retina. The Journal of comparative neurology 424, 1–23.

Heilig, C. W., Concepcion, L. A., Riser, B. L., Freytag, S. O., Zhu, M., and Cortes, P. (1995). Overexpression of glucose transporters in rat mesangial cells cultured in a normal glucose milieu mimics the diabetic phenotype. The Journal of clinical investigation 96, 1802–1814.

Helbig, H. (2007). Surgery for diabetic retinopathy. Ophthalmologica. Journal international d'ophtalmologie. International journal of ophthalmology. Zeitschrift für Augenheilkunde 221, 103–111.

Hellström, M., Ruitenberg, M. J., Pollett, M. A., Ehlert, E. M. E., Twisk, J., Verhaagen, J., and Harvey, A. R. (2009). Cellular tropism and transduction properties of seven adeno-associated viral vector serotypes in adult retina after intravitreal injection. Gene therapy 16, 521–532.

Holländer, H., Makarov, F., Dreher, Z., van Driel, D., Chan-Ling, T. L., and Stone, J. (1991). Structure of the macroglia of the retina: sharing and division of labour between astrocytes and Müller cells. The Journal of comparative neurology 313, 587–603.

Holopigian, K., Greenstein, V. C., Seiple, W., Hood, D. C., and Carr, R. E. (1997). Evidence for photoreceptor changes in patients with diabetic retinopathy. Investigative ophthalmology & visual science 38, 2355–2365.

Houenou, L. J., D'Costa, A. P., Li, L., Turgeon, V. L., Enyadike, C., Alberdi, E., and Becerra, S. P. (1999). Pigment epithelium-derived factor promotes the survival and differentiation of developing spinal motor neurons. The Journal of comparative neurology 412, 506–514.

Huster, D., Reichenbach, A., and Reichelt, W. (2000). The glutathione content of retinal Müller (glial) cells: effect of pathological conditions. Neurochemistry international 36, 461–469.

Inokuchi, N., Ikeda, T., Imamura, Y., Sotozono, C., Kinoshita, S., Uchihori, Y., and Nakamura, K. (2001). Vitreous levels of insulin-like growth factor-I in patients with proliferative diabetic retinopathy. Current eye research 23, 368–371.

Jablonski, M. M., Tombran-tink, J., Mrazek, D. A., and Iannaccone, A. (2001). Pigment epithelium-derived factor supports normal Müller cell development and glutamine synthetase expression after removal of the retinal pigment epithelium. Glia 35, 14–25.

Jeon, C. J., Strettoi, E., and Masland, R. H. (1998). The major cell populations of the mouse retina. The Journal of neuroscience 18, 8936–8946.

Joussen, A. M., Poulaki, V., Mitsiades, N., Kirchhof, B., Koizumi, K., Döhmen, S., and Adamis, A. P. (2002). Nonsteroidal anti-inflammatory drugs prevent early diabetic retinopathy via TNF-alpha suppression. The FASEB journal 16, 438–440.

Kaiser, N., Sasson, S., Feener, E. P., Boukobza-Vardi, N., Higashi, S., Moller, D. E., Davidheiser, S., Przybylski, R. J., and King, G. L. (1993). Differential regulation of glucose transport and transporters by glucose in vascular endothelial and smooth muscle cells. Diabetes 42, 80–89.

Kakehashi, A., Saito, Y., Mori, K., Sugi, N., Ono, R., Yamagami, H., Shinohara, M., Tamemoto, H., Ishikawa, S.-e, Kawakami, M., et al. (2006). Characteristics of diabetic retinopathy in SDT rats. Diabetes/metabolism research and reviews 22, 455–461.

Kamba, T., Tam, B. Y. Y., Hashizume, H., Haskell, A., Sennino, B., Mancuso, M. R., Norberg, S. M., O'Brien, S. M., Davis, R. B., Gowen, L. C., et al. (2006). VEGF-dependent plasticity of fenestrated capillaries in the normal adult microvasculature. American journal of physiology. Heart and circulatory physiology 290, H560–H576.

Karakousis, P. C., John, S. K., Behling, K. C., Surace, E. M., Smith, J. E., Hendrickson, A., Tang, W. X., Bennett, J., and Milam, A. H. (2001). Localization of pigment epithelium derived factor (PEDF) in developing and adult human ocular tissues. Molecular vision 7, 154–163.

Karlstetter, M., Ebert, S., and Langmann, T. (2010). Microglia in the healthy and degenerating retina: insights from novel mouse models. Immunobiology 215, 685–691.

Kasiske, B. L., Cleary, M. P., O'Donnell, M. P., and Keane, W. F. (1985). Effects of genetic obesity on renal structure and function in the Zucker rat. The Journal of laboratory and clinical medicine 106, 598–604.

Katayose, Y., Kim, M., Rakkar, A. N., Li, Z., Cowan, K. H., and Seth, P. (1997). Promoting apoptosis: a novel activity associated with the cyclin-dependent kinase inhibitor p27. Cancer research 57, 5441–5445.

Kawano, K., Hirashima, T., Mori, S., Saitoh, Y., Kurosumi, M., and Natori, T. (1992). Spontaneous long-term hyperglycemic rat with diabetic complications. Otsuka Long-Evans Tokushima Fatty (OLETF) strain. Diabetes 41, 1422–1428.

Kempen, J. H., O'Colmain, B. J., Leske, M. C., Haffner, S. M., Klein, R., Moss, S. E., Taylor, H. R., and Hamman, R. F. (2004). The prevalence of diabetic retinopathy among adults in the United States. Archives of ophthalmology 122, 552–563.

Kent, D., Vinores, S. A., and Campochiaro, P. A. (2000). Macular oedema: the role of soluble mediators. The British journal of ophthalmology 84, 542–545.

Kern, T. S., Miller, C. M., Tang, J., Du, Y., Ball, S. L., and Berti-Matera, L. (2010). Comparison of three strains of diabetic rats with respect to the rate at which retinopathy and tactile allodynia develop. Molecular vision 16, 1629–1639.

Kern, T. S., and Barber, A. J. (2008a). Retinal ganglion cells in diabetes. The Journal of physiology 586, 4401–4408.

Kobayashi, M., Kuroiwa, T., Shimokawa, R., Okeda, R., and Tokoro, T. (2000) Nitric oxide synthase expression in ischemic rat retinas. Japanese journal of ophthalmology 44, 235–244.

Kochanek, S., Schiedner, G., and Volpers, C. (2001). High-capacity "gutless" adenoviral vectors. Current opinion in molecular therapeutics 3, 454–463.

Kodama, H., Fujita, M., and Yamaguchi, I. (1994). Development of hyperglycaemia and insulin resistance in conscious genetically diabetic (C57BL/KsJ-db/db) mice. Diabetologia 37, 739–744.

Kofuji, P., Biedermann, B., Siddharthan, V., Raap, M., Iandiev, I., Milenkovic, I., Thomzig, A., Veh, R. W., Bringmann, A., and Reichenbach, A. (2002). Kir potassium channel subunit expression in retinal glial cells: implications for spatial potassium buffering. Glia 39, 292–303.

Kolb, H. (1995). Simple Anatomy of the Retina. In Webvision: The Organization of the Retina and Visual System, H. Kolb, E. Fernandez, and R. Nelson, eds. (University of Utah Health Sciences Center).

Kolb, H., Zhang, L., Dekorver, L., and Cuenca, N. (2002). A new look at calretinin-immunoreactive amacrine cell types in the monkey retina. The Journal of comparative neurology 453, 168–184.

Kondo, T., Vicent, D., Suzuma, K., Yanagisawa, M., King, G. L., Holzenberger, M., and Kahn, C. R. (2003). Knockout of insulin and IGF-1 receptors on vascular endothelial cells protects against retinal neovascularization. The Journal of clinical investigation 111, 1835–1842.

Kosano, H., Okano, T., Katsura, Y., Noritake, M., Kado, S., Matsuoka, T., and Nishigori, H. (1999). ProMMP-9 (92 kDa gelatinase) in vitreous fluid of patients with proliferative diabetic retinopathy. Life sciences 64, 2307–2315.

Kostic, C., Chiodini, F., Salmon, P., Wiznerowicz, M., Deglon, N., Hornfeld, D., Trono, D., Aebischer, P., Schorderet, D. F., Munier, F. L., et al. (2003). Activity analysis of housekeeping promoters using self-inactivating lentiviral vector delivery into the mouse retina. Gene therapy 10, 818–821.

de Kozak, Y., Cotinet, A., Goureau, O., Hicks, D., and Thillaye-Goldenberg, B. (1997). Tumor necrosis factor and nitric oxide production by resident retinal glial cells from rats presenting hereditary retinal degeneration. Ocular immunology and inflammation 5, 85–94.

Krady, J. K., Basu, A., Allen, C. M., Xu, Y., LaNoue, K. F., Gardner, T. W., and Levison, S. W. (2005). Minocycline reduces proinflammatory cytokine expression, microglial activation, and caspase-3 activation in a rodent model of diabetic retinopathy. Diabetes 54, 1559–1565.

Kreppel, F., Luther, T. T., Semkova, I., Schraermeyer, U., and Kochanek, S. (2002). Long-term transgene expression in the RPE after gene transfer with a high-capacity adenoviral vector. Investigative ophthalmology & visual science 43, 1965–1970.

Kuiper, E. J., Van Nieuwenhoven, F. A., de Smet, M. D., van Meurs, J. C., Tanck, M. W., Oliver, N., Klaassen, I., Van Noorden, C. J. F., Goldschmeding, R., and Schlingemann, R. O. (2008). The angio-fibrotic switch of VEGF and CTGF in proliferative diabetic retinopathy. PLoS ONE 3, e2675.

Kumagai, A. K., Glasgow, B. J., and Pardridge, W. M. (1994). GLUT1 glucose transporter expression in the diabetic and nondiabetic human eye. Investigative ophthalmology & visual science 35, 2887–2894.

Kuroki, T., Isshiki, K., and King, G. L. (2003). Oxidative stress: the lead or supporting actor in the pathogenesis of diabetic complications. Journal of the American Society of Nephrology 14, S216–S220.

Lam, S., van der Geest, R. N., Verhagen, N. A. M., van Nieuwenhoven, F. A., Blom, I. E., Aten, J., Goldschmeding, R., Daha, M. R., and van Kooten, C. (2003). Connective tissue growth factor and igf-I are produced by human renal fibroblasts and cooperate in the induction of collagen production by high glucose. Diabetes 52, 2975–2983.

Lange, J., Yafai, Y., Reichenbach, A., Wiedemann, P., and Eichler, W. (2008). Regulation of pigment epithelium-derived factor production and release by retinal glial (Müller) cells under hypoxia. Investigative ophthalmology & visual science 49, 5161–5167.

Langmann, T. (2007). Microglia activation in retinal degeneration. Journal of leukocyte biology 81, 1345–1351.

Lebherz C, Maguire A, Tang W, Bennett J, Wilson JM. (2008) Novel AAV serotypes for improved ocular gene transfer. Journal of Gene Medicine 10, 375-82.

Lebrun-Julien, F., Duplan, L., Pernet, V., Osswald, I., Sapieha, P., Bourgeois, P., Dickson, K., Bowie, D., Barker, P. A., and Di Polo, A. (2009). Excitotoxic death of retinal neurons in vivo occurs via a non-cell-autonomous mechanism. The Journal of neuroscience 29, 5536–5545.

Lee, A. Y., and Chung, S. S. (1999). Contributions of polyol pathway to oxidative stress in diabetic cataract. FASEB journal 13, 23–30.

Lewis, G. P., Erickson, P. A., Kaska, D. D., and Fisher, S. K. (1988). An immunocytochemical comparison of Müller cells and astrocytes in the cat retina. Experimental eye research 47, 839–853.

Li, Q., and Puro, D. G. (2002). Diabetes-induced dysfunction of the glutamate transporter in retinal Müller cells. Investigative ophthalmology & visual science 43, 3109–3116.

Lieth, E., Barber, A. J., Xu, B., Dice, C., Ratz, M. J., Tanase, D., and Strother, J. M. (1998). Glial reactivity and impaired glutamate metabolism in short-term experimental diabetic retinopathy. Penn State Retina Research Group. Diabetes 47, 815–820.

Lieth, E., LaNoue, K. F., Antonetti, D. A., and Ratz, M. (2000). Diabetes reduces glutamate oxidation and glutamine synthesis in the retina. The Penn State Retina Research Group. Experimental eye research 70, 723–730.

Like, A. A., Butler, L., Williams, R. M., Appel, M. C., Weringer, E. J., and Rossini, A. A. (1982). Spontaneous autoimmune diabetes mellitus in the BB rat. Diabetes 31, 7–13.

Lindström, P. (2007). The physiology of obese-hyperglycemic mice [ob/ob mice]. TheScientificWorldJournal 7, 666–685.

Lioy, D. T., Garg, S. K., Monaghan, C. E., Raber, J., Foust, K. D., Kaspar, B. K., Hirrlinger, P. G., Kirchhoff, F., Bissonnette, J. M., Ballas, N., et al. (2011). A role for glia in the progression of Rett's syndrome. Nature 475, 497–500.

Liu, X. F., Fawcett, J. R., Thorne, R. G., and Frey, W. H. (2001). Non-invasive intranasal insulin-like growth factor-I reduces infarct volume and improves neurologic function in rats following middle cerebral artery occlusion. Neuroscience letters 308, 91–94.

Lu, Z.-Y., Bhutto, I. A., and Amemiya, T. (2003). Retinal changes in Otsuka long-evans Tokushima Fatty rats (spontaneously diabetic rat)--possibility of a new experimental model for diabetic retinopathy. Japanese journal of ophthalmology 47, 28–35.

Lukason, M., DuFresne, E., Rubin, H., Pechan, P., Li, Q., Kim, I., Kiss, S., Flaxel, C., Collins, M., Miller, J., et al. (2011). Inhibition of choroidal neovascularization in a nonhuman primate model by intravitreal administration of an AAV2 vector expressing a novel anti-VEGF molecule. Molecular therapy 19, 260–265.

Lund, P. (1971). Control of glutamine synthesis in rat liver. The Biochemical journal 124, 653–660.

Maeda, M., Yabuki, A., Suzuki, S., Matsumoto, M., Taniguchi, K., and Nishinakagawa, H. (2003). Renal lesions in spontaneous insulin-dependent diabetes mellitus in the nonobese diabetic mouse: acute phase of diabetes. Veterinary pathology 40, 187–195.

Maguire, A. M., High, K. A., Auricchio, A., Wright, J. F., Pierce, E. A., Testa, F., Mingozzi, F., Bennicelli, J. L., Ying, G.-shuang, and Rossi, S. (2009). Age-dependent effects of RPE65 gene therapy for Leber's congenital amaurosis: a phase 1 dose-escalation trial. The Lancet 6736, 1–9.

Maguire, A. M., Simonelli, F., Pierce, E. A., Pugh, E. N., Mingozzi, F., Bennicelli, J., Banfi, S., Marshall, K. A., Testa, F., Surace, E. M., et al. (2008). Safety and efficacy of gene transfer for Leber's congenital amaurosis. The New England journal of medicine 358, 2240–2248.

Maik-Rachline, G., and Seger, R. (2006). Variable phosphorylation states of pigment-epithelium-derived factor differentially regulate its function. Blood 107, 2745–2752.

Mairet-Coello, G., Tury, A., and DiCicco-Bloom, E. (2009). Insulin-like growth factor-1 promotes G(1)/S cell cycle progression through bidirectional regulation of cyclins and cyclin-dependent kinase inhibitors via the phosphatidylinositol 3-kinase/Akt pathway in developing rat cerebral cortex. The Journal of neuroscience 29, 775–788.

Malchiodi-Albedi, F., Feher, J., Caiazza, S., Formisano, G., Perilli, R., Falchi, M., Petrucci, T. C., Scorcia, G., and Tombran-Tink, J. (1998). PEDF (pigment epithelium-derived factor) promotes increase and maturation of pigment granules in pigment epithelial cells in neonatal albino rat retinal cultures. International journal of developmental neuroscience 16, 423–432.

Malecaze, F., Clamens, S., Simorre-Pinatel, V., Mathis, A., Chollet, P., Favard, C., Bayard, F., and Plouet, J. (1994). Detection of vascular endothelial growth factor messenger RNA and vascular endothelial growth factor-like activity in proliferative diabetic retinopathy. Archives of ophthalmology 112, 1476–1482.

Masland, R. H. (2011). Cell populations of the retina: the Proctor lecture. Investigative ophthalmology & visual science 52, 4581–4591.

McLeod, D., Lefer, D., Merges, C., and Lutty, G. (1995). Enhanced expression of intracellular adhesion molecule-1 and P-selectin in the diabetic human retina and choroid. Am J Pathol 147, 642–653.

Merimee, T., Zapf, J., and Froesch, E. (1983). Insulin-like growth factors. Studies in diabetics with and without retinopathy. N Engl J Med 309, 527–530.

Meyer, C., Notari, L., and Becerra, S. P. (2002). Mapping the type I collagen-binding site on pigment epithelium-derived factor. Implications for its antiangiogenic activity. The Journal of biological chemistry 277, 45400–45407.

Midena, E., Segato, T., Radin, S., di Giorgio, G., Meneghini, F., Piermarocchi, S., and Belloni, A. S. (1989). Studies on the retina of the diabetic db/db mouse. I. Endothelial cell-pericyte ratio. Ophthalmic research 21, 106–111.

Mizutani, M., Gerhardinger, C., and Lorenzi, M. (1998). Müller cell changes in human diabetic retinopathy. Diabetes 47, 445–449.

Mori, K., Duh, E., Gehlbach, P., Ando, A., Takahashi, K., Pearlman, J., Yang, H. S., Zack, D. J., Ettyreddy, D., Brough, D. E., et al. (2001). Pigment epithelium-derived factor inhibits retinal and choroidal neovascularization. Journal of cellular physiology 188, 253–263.

Mori, K., Gehlbach, P., Ando, A., Mcvey, D., Wei, L., and Campochiaro, P. A. (2002a). Regression of ocular neovascularization in response to increased expression of pigment epithelium-derived factor. Investigative ophthalmology & visual science 43, 2428–2434.

Mori, K., Gehlbach, P., Ando, A., Wahlin, K., Gunther, V., McVey, D., Wei, L., and Campochiaro, P. A. (2002b). Intraocular adenoviral vector-mediated gene transfer in proliferative retinopathies. Investigative ophthalmology & visual science 43, 1610–1615.

Mori, K., Gehlbach, P., Yamamoto, S., Duh, E., Zack, D. J., Li, Q., Berns, K. I., Raisler, B. J., Hauswirth, W. W., and Campochiaro, P. A. (2002c). AAV-mediated gene transfer of pigment epithelium-derived factor inhibits choroidal neovascularization. Investigative ophthalmology & visual science 43, 1994–2000.

Morsy, M. A., Gu, M., Motzel, S., Zhao, J., Lin, J., Su, Q., Allen, H., Franlin, L., Parks, R. J., Graham, F. L., et al. (1998). An adenoviral vector deleted for all viral coding sequences results in enhanced safety and extended expression of a leptin transgene. Proceedings of the National Academy of Sciences of the United States of America 95, 7866–7871.

Murakami, Y., Ikeda, Y., Yonemitsu, Y., Onimaru, M., Nakagawa, K., Kohno, R.-i., Miyazaki, M., Hisatomi, T., Nakamura, M., Yabe, T., et al. (2008). Inhibition of Nuclear Translocation of Apoptosis-Inducing Factor Is an Essential Mechanism of the Neuroprotective Activity of Pigment Epithelium-Derived Factor in a Rat Model of Retinal Degeneration. American Journal Of Pathology 173, 1326–1338.

Nagelhus, E. A., Horio, Y., Inanobe, A., Fujita, A., Haug, F. M., Nielsen, S., Kurachi, Y., and Ottersen, O. P. (1999). Immunogold evidence suggests that coupling of K+ siphoning and water transport in rat retinal Müller cells is mediated by a coenrichment of Kir4.1 and AQP4 in specific membrane domains. Glia 26, 47–54.

Nakazawa, T., Hisatomi, T., Nakazawa, C., Noda, K., Maruyama, K., She, H., Matsubara, A., Miyahara, S., Nakao, S., Yin, Y., et al. (2007). Monocyte chemoattractant protein 1 mediates retinal detachment-induced photoreceptor apoptosis. Proceedings of the National Academy of Sciences of the United States of America 104, 2425–2430.

Neubauer, A. S., and Ulbig, M. W. (2007). Laser treatment in diabetic retinopathy. Ophthalmologica. Journal international d'ophtalmologie. International journal of ophthalmology. Zeitschrift für Augenheilkunde 221, 95–102.

Nguyen, Q. D., Shah, S. M., Heier, J. S., Do, D. V., Lim, J., Boyer, D., Abraham, P., and Campochiaro, P. A. (2009). Primary End Point (Six Months) Results of the Ranibizumab for Edema of the mAcula in diabetes (READ-2) study. Ophthalmology 116, 2175–2181.e1.

Nicholson, B. P., and Schachat, A. P. (2010). A review of clinical trials of anti-VEGF agents for diabetic retinopathy. Graefe's archive for clinical and experimental ophthalmology 248, 915–930.

Nolan, C. J., Damm, P., and Prentki, M. (2011). Type 2 diabetes across generations: from pathophysiology to prevention and management. Lancet 378, 169–181.

Notari, L., Baladron, V., Aroca-Aguilar, J. D., Balko, N., Heredia, R., Meyer, C., Notario, P. M., Saravanamuthu, S., Nueda, M.-L., Sanchez-Sanchez, F., et al. (2006). Identification of a lipase-linked cell membrane receptor for pigment epithelium-derived factor. The Journal of biological chemistry 281, 38022–38037.

Obrosova, I. G., Drel, V. R., Kumagai, A. K., Szábo, C., Pacher, P., and Stevens, M. J. (2006). Early diabetes-induced biochemical changes in the retina: comparison of rat and mouse models. Diabetologia 49, 2525–2533.

Ogata, N., Nishikawa, M., Nishimura, T., Mitsuma, Y., and Matsumura, M. (2002). Unbalanced vitreous levels of pigment epithelium-derived factor and vascular endothelial growth factor in diabetic retinopathy. American journal of ophthalmology 134, 348–353.

Ohno-Matsui, K., Hirose, A., Yamamoto, S., Saikia, J., Okamoto, N., Gehlbach, P., Duh, E. J., Hackett, S., Chang, M., Bok, D., et al. (2002). Inducible expression of vascular endothelial growth factor in adult mice causes severe proliferative retinopathy and retinal detachment. The American journal of pathology 160, 711–719.

Oshima, Y., Oshima, S., Nambu, H., Kachi, S., Hackett, S. F., Melia, M., Kaleko, M., Connelly, S., Esumi, N., Zack, D. J., et al. (2004a). Increased expression of VEGF in retinal pigmented

epithelial cells is not sufficient to cause choroidal neovascularization. Journal of cellular physiology 201, 393–400.

Oshima, Y., Takahashi, K., Oshima, S., Saishin, Y., Saishin, Y., Silva, R. L., Liang, X., Reddy, P. S., Ganesh, S., Brann, T., et al. (2004b). Intraocular gutless adenoviral-vectored VEGF stimulates anterior segment but not retinal neovascularization. Journal of cellular physiology 199, 399–411.

Paasche, G., Huster, D., and Reichenbach, A. (1998). The glutathione content of retinal Müller (glial) cells: the effects of aging and of application of free-radical scavengers. Ophthalmic research 30, 351–360.

Pannicke, T., Iandiev, I., Uckermann, O., Biedermann, B., Kutzera, F., Wiedemann, P., Wolburg, H., Reichenbach, A., and Bringmann, A. (2004). A potassium channel-linked mechanism of glial cell swelling in the postischemic retina. Molecular and cellular neurosciences 26, 493–502.

Pannicke, T., Iandiev, I., Wurm, A., Uckermann, O., vom Hagen, F., Reichenbach, A., Wiedemann, P., Hammes, H.-P., and Bringmann, A. (2006). Diabetes alters osmotic swelling characteristics and membrane conductance of glial cells in rat retina. Diabetes 55, 633–639.

Pannicke, T., Uckermann, O., Iandiev, I., Wiedemann, P., Reichenbach, A., and Bringmann, A. (2005). Ocular inflammation alters swelling and membrane characteristics of rat Müller glial cells. Journal of neuroimmunology 161, 145–154.

Park, S.-H., Park, J.-W., Park, S.-J., Kim, K.-Y., Chung, J.-W., Chun, M.-H., and Oh, S.-J. (2003). Apoptotic death of photoreceptors in the streptozotocin-induced diabetic rat retina. Diabetologia 46, 1260–1268.

Paunescu, K., Wabbels, B., Preising, M. N., and Lorenz, B. (2005). Longitudinal and cross-sectional study of patients with early-onset severe retinal dystrophy associated with RPE65 mutations. Graefe's archive for clinical and experimental ophthalmology = Albrecht von Graefes Archiv für klinische und experimentelle Ophthalmologie 243, 417–426.

Pechan, P., Rubin, H., Lukason, M., Ardinger, J., DuFresne, E., Hauswirth, W. W., Wadsworth, S. C., and Scaria, A. (2009). Novel anti-VEGF chimeric molecules delivered by AAV vectors for inhibition of retinal neovascularization. Gene therapy 16, 10–16.

Penn, J. S., Tolman, B. L., and Lowery, L. A. (1993). Variable oxygen exposure causes preretinal neovascularization in the newborn rat. Investigative ophthalmology & visual science 34, 576–585.

Petersen, S. V., Valnickova, Z., and Enghild, J. J. (2003). Pigment-epithelium-derived factor (PEDF) occurs at a physiologically relevant concentration in human blood: purification and characterization. The Biochemical journal 374, 199–206.

Peterson, R. (2001). The Zucker diabetic fatty (ZDF) rat. In Animal Models of Diabetes-A Primer, A. Sima and E. Shafrir, eds. (Harwood Academic Publishers), pp. 109–128.

Phipps, J. A., Yee, P., Fletcher, E. L., and Vingrys, A. J. (2006). Rod photoreceptor dysfunction in diabetes: activation, deactivation, and dark adaptation. Investigative ophthalmology & visual science 47, 3187–3194.

Pierce, E. A., Avery, R. L., Foley, E. D., Aiello, L. P., and Smith, L. E. (1995). Vascular endothelial growth factor/vascular permeability factor expression in a mouse model of retinal neovascularization. Proceedings of the National Academy of Sciences of the United States of America 92, 905–909.

Poitry-Yamate, C. L., Poitry, S., and Tsacopoulos, M. (1995). Lactate released by Müller glial cells is metabolized by photoreceptors from mammalian retina. The Journal of neuroscience□: the official journal of the Society for Neuroscience 15, 5179–5191.

Porta, M., and Bandello, F. (2002). Diabetic retinopathy. A clinical update. Diabetologia 45, 1617–1634.

Pow, D. V., and Robinson, S. R. (1994). Glutamate in some retinal neurons is derived solely from glia. Neuroscience 60, 355–366.

Punglia, R., Lu, M., Hsu, J., Kuroki, M., Tolentino, M., Keough, K., Levy, A., Levy, N., Goldberg, M., D'Amato, R., et al. (1997). Regulation of vascular endothelial growth factor expression by insulin-like growth factor I. Diabetes 46, 1619–1626.

Raisler, B. J., Berns, K. I., Grant, M. B., Beliaev, D., and Hauswirth, W. W. (2002). Adeno-associated virus type-2 expression of pigmented epithelium-derived factor or Kringles 1-3 of angiostatin reduce retinal neovascularization. Proceedings of the National Academy of Sciences of the United States of America 99, 8909–8914.

Rand, L., Cavallerano, J., and Aiello, L. P. (2004). Nonretinal Ocular Complications of Diabetes Mellitus. In International Textbook of Diabetes Mellitus, R. DeFronzo, E. Ferrannini, Keen, and Z. P, eds. (John Wiley & Sons), pp. 1207–1218.

Raymond, N. T., Varadhan, L., Reynold, D. R., Bush, K., Sankaranarayanan, S., Bellary, S., Barnett, A. H., Kumar, S., and O'Hare, J. P. (2009). Higher prevalence of retinopathy in diabetic patients of South Asian ethnicity compared with white Europeans in the community: a cross-sectional study. Diabetes care 32, 410–415.

Redmond, T. M., Yu, S., Lee, E., Bok, D., Hamasaki, D., Chen, N., Goletz, P., Ma, J. X., Crouch, R. K., and Pfeifer, K. (1998). Rpe65 is necessary for production of 11-cis-vitamin A in the retinal visual cycle. Nature genetics 20, 344–351.

Regillo, C. D., Brown, D. M., Abraham, P., Yue, H., Ianchulev, T., Schneider, S., and Shams, N. (2008). Randomized, double-masked, sham-controlled trial of ranibizumab for neovascular age-related macular degeneration: PIER Study year 1. American journal of ophthalmology 145, 239–248.

Reichel, M. B., Ali, R. R., Thrasher, A. J., Hunt, D. M., Bhattacharya, S. S., and Baker, D. (1998). Immune responses limit adenovirally mediated gene expression in the adult mouse eye. Gene therapy 5, 1038–1046.

Reichelt, W., Pannicke, T., Biedermann, B., Francke, M., and Faude, F. (1997a). Comparison between functional characteristics of healthy and pathological human retinal Müller glial cells. Survey of ophthalmology 42 Suppl 1, S105–S117.

Reichelt, W., Stabel-Burow, J., Pannicke, T., Weichert, H., and Heinemann, U. (1997b). The glutathione level of retinal Müller glial cells is dependent on the high-affinity sodium-dependent uptake of glutamate. Neuroscience 77, 1213–1224.

Reinehr, T., Kiess, W., Kapellen, T., Wiegand, S., and Holl, R. W. (2010). Children with diabetes mellitus type 2 in Europe: an underserved population. Archives of disease in childhood 95, 954.

DRS Report 8 (1981). Photocoagulation treatment of proliferative diabetic retinopathy. Clinical application of Diabetic Retinopathy Study (DRS) findings, DRS Report Number 8. The Diabetic Retinopathy Study Research Group. Ophthalmology 88, 583–600.

Robson, J. G., and Frishman, L. J. (1998). Dissecting the dark-adapted electroretinogram. Documenta ophthalmologica. Advances in ophthalmology 95, 187–215.

Rossini, A. A., Appel, M. C., Williams, R. M., and Like, A. A. (1977). Genetic influence of the streptozotocin-induced insulitis and hyperglycemia. Diabetes 26, 916–920.

Roy, S., Ha, J., Trudeau, K., and Beglova, E. (2010). Vascular basement membrane thickening in diabetic retinopathy. Current eye research 35, 1045–1056.

Ruberte, J., Ayuso, E., Navarro, M., Carretero, A., Nacher, V., Haurigot, V., George, M., Llombart, C., Casellas, A., Costa, C., et al. (2004). Increased ocular levels of IGF-1 in transgenic mice lead to diabetes-like eye disease. J Clin Invest 113, 1149–1157.

Saatman, K. E., Contreras, P. C., Smith, D. H., Raghupathi, R., McDermott, K. L., Fernandez, S. C., Sanderson, K. L., Voddi, M., and McIntosh, T. K. (1997). Insulin-like growth factor-1 (IGF-1) improves both neurological motor and cognitive outcome following experimental brain injury. Experimental neurology 147, 418–427.

Saint-Geniez, M., Maharaj, A. S. R., Walshe, T. E., Tucker, B. A., Sekiyama, E., Kurihara, T., Darland, D. C., Young, M. J., and D'Amore, P. A. (2008). Endogenous VEGF is required for visual function: evidence for a survival role on müller cells and photoreceptors. PLoS ONE 3, e3554.

Saishin, Y., Silva, R. L., Saishin, Y., Kachi, S., Aslam, S., Gong, Y. Y., Lai, H., Carrion, M., Harris, B., Hamilton, M., et al. (2005). Periocular gene transfer of pigment epithelium-derived factor inhibits choroidal neovascularization in a human-sized eye. Human gene therapy 16, 473–478.

Saito, Y., Park, L., Skolik, S. A., Alfaro, D. V., Chaudhry, N. A., Barnstable, C. J., and Liggett, P. E. (1997). Experimental preretinal neovascularization by laser-induced venous thrombosis in rats. Current eye research 16, 26–33.

Salzmann, J., Limb, G. A., Khaw, P. T., Gregor, Z. J., Webster, L., Chignell, A. H., and Charteris, D. G. (2000). Matrix metalloproteinases and their natural inhibitors in fibrovascular membranes of proliferative diabetic retinopathy. The British journal of ophthalmology 84, 1091–1096.

Sasase, T. (2010). Pathophysiological characteristics of diabetic ocular complications in spontaneously diabetic torii rat. Journal of ophthalmology 2010, 615641.

Scappaticci, F. A., Skillings, J. R., Holden, S. N., Gerber, H.-P., Miller, K., Kabbinavar, F., Bergsland, E., Ngai, J., Holmgren, E., Wang, J., et al. (2007). Arterial thromboembolic events in patients with metastatic carcinoma treated with chemotherapy and bevacizumab. Journal of the National Cancer Institute 99, 1232–1239.

Schwartz, S. G., Flynn, H. W., and Scott, I. U. (2009). Endophthalmitis after intravitreal injections. Expert opinion on pharmacotherapy 10, 2119–2126.

Schütte, M., and Werner, P. (1998). Redistribution of glutathione in the ischemic rat retina. Neuroscience letters 246, 53–56.

Sethi, C. S., Lewis, G. P., Fisher, S. K., Leitner, W. P., Mann, D. L., Luthert, P. J., and Charteris, D. G. (2005). Glial remodeling and neural plasticity in human retinal detachment with proliferative vitreoretinopathy. Investigative ophthalmology & visual science 46, 329–342.

Sharma, K., McCue, P., and Dunn, S. R. (2003). Diabetic kidney disease in the db/db mouse. American journal of physiology. Renal physiology 284, F1138–F1144.

Shaw, J. E., Sicree, R. A., and Zimmet, P. Z. (2010). Global estimates of the prevalence of diabetes for 2010 and 2030. Diabetes research and clinical practice 87, 4–14.

Shields, C. L., De Potter, P., Himelstein, B. P., Shields, J. A., Meadows, A. T., and Maris, J. M. (1996). Chemoreduction in the initial management of intraocular retinoblastoma. Archives of ophthalmology 114, 1330–1338.

Shinohara, M., Masuyama, T., and Kakehashi, A. (2007). The Spontaneously Diabetic Torii (SDT) rat with retinopathy lesions resembling those of humans. In Animal Models of Diabetes: Frontiers in Research, E. Shafrir, ed. (Boca Raton, Fla, USA: CRC Press), pp. 311–321.

Shirao, Y., and Kawasaki, K. (1998). Electrical responses from diabetic retina. Progress in retinal and eye research 17, 59–76.

Sima, A. A., Chakrabarti, S., Garcia-Salinas, R., and Basu, P. K. (1985). The BB-rat--an authentic model of human diabetic retinopathy. Current eye research 4, 1087–1092.

Smith, A. J., Bainbridge, J. W., and Ali, R. R. (2009). Prospects for retinal gene replacement therapy. Trends in Genetics 25, 156–165.

Smith, L. E., Shen, W., Perruzzi, C., Soker, S., Kinose, F., Xu, X., Robinson, G., Driver, S., Bischoff, J., Zhang, B., et al. (1999). Regulation of vascular endothelial growth factor-dependent retinal neovascularization by insulin-like growth factor-1 receptor. Nature medicine 5, 1390–1395.

Smith, L. E., Wesolowski, E., McLellan, A., Kostyk, S. K., D'Amato, R., Sullivan, R., and D'Amore, P. A. (1994). Oxygen-induced retinopathy in the mouse. Investigative ophthalmology & visual science 35, 101–111.

Smith, R., Hawes, N., Chang, B., and Nishina, P. (2002). Systematic Evaluation of the Mouse Eye R. Smith, ed. (Boca Raton, Florida, USA: CRC Press).

Spector, K. S. (1998). Diabetic cardiomyopathy. Clinical cardiology 21, 885–887.

Steele, F. R., Chader, G. J., Johnson, L. V., and Tombran-Tink, J. (1993). Pigment epithelium-derived factor: neurotrophic activity and identification as a member of the serine protease inhibitor gene family. Proceedings of the National Academy of Sciences of the United States of America 90, 1526–1530.

Stefansson, E., Bek, T., Porta, M., Larsen, N., Kristinsson, J. K., and Agardh, E. (2000). Screening and prevention of diabetic blindness. Acta ophthalmologica Scandinavica 78, 374–385.

Stellmach, V., Crawford, S. E., Zhou, W., and Bouck, N. (2001). Prevention of ischemia-induced retinopathy by the natural ocular antiangiogenic agent pigment epithelium-derived factor. Proceedings of the National Academy of Sciences of the United States of America 98, 2593–2597.

Stieger, K., Schroeder, J., Provost, N., Mendes-Madeira, A., Belbellaa, B., Meur, G. L., Weber, M., Deschamps, J.-Y., Lorenz, B., Moullier, P., et al. (2008). Detection of Intact rAAV Particles up to 6 Years After Successful Gene Transfer in the Retina of Dogs and Primates. Molecular Therapy 17, 516–523.

Strauss, O. (2005). The retinal pigment epithelium in visual function. Physiological reviews 85, 845–881.

Sung, M. W., Yeh, H. C., Thung, S. N., Schwartz, M. E., Mandeli, J. P., Chen, S. H., and Woo, S. L. (2001). Intratumoral adenovirus-mediated suicide gene transfer for hepatic metastases from colorectal adenocarcinoma: results of a phase I clinical trial. Molecular therapy□: the journal of the American Society of Gene Therapy 4, 182–191.

Suzuki, Y., Nakazawa, M., Suzuki, K., Yamazaki, H., and Miyagawa, Y. (2011). Expression profiles of cytokines and chemokines in vitreous fluid in diabetic retinopathy and central retinal vein occlusion. Japanese journal of ophthalmology 55, 256–263.

Suzuma, K., Naruse, K., Suzuma, I., Takahara, N., Ueki, K., Aiello, L. P., and King, G. L. (2000). Vascular endothelial growth factor induces expression of connective tissue growth factor via KDR, Flt1, and phosphatidylinositol 3-kinase-akt-dependent pathways in retinal vascular cells. The Journal of biological chemistry 275, 40725–40731.

Takahashi, K., Saishin, Y., Saishin, Y., Silva, R. L., Oshima, Y., Oshima, S., Melia, M., Paszkiet, B., Zerby, D., Kadan, M. J., et al. (2003). Intraocular expression of endostatin reduces VEGF-induced retinal vascular permeability, neovascularization, and retinal detachment. FASEB journal 17, 896–898.

Takenaka, K., Yamagishi, S.-I., Jinnouchi, Y., Nakamura, K., Matsui, T., and Imaizumi, T. (2005). Pigment epithelium-derived factor (PEDF)-induced apoptosis and inhibition of vascular endothelial growth factor (VEGF) expression in MG63 human osteosarcoma cells. Life sciences 77, 3231–3241.

Takita, H., Yoneya, S., Gehlbach, P. L., Duh, E. J., Wei, L. L., and Mori, K. (2003). Retinal neuroprotection against ischemic injury mediated by intraocular gene transfer of pigment epithelium-derived factor. Investigative ophthalmology & visual science 44, 4497–4504.

Taniwaki, T., Becerra, S. P., Chader, G. J., and Schwartz, J. P. (1995). Pigment epithelium-derived factor is a survival factor for cerebellar granule cells in culture. Journal of neurochemistry 64, 2509–2517.

Terakita, A. (2005). The opsins. Genome biology 6, 213.

Tolentino, M. (2011) Systemic and ocular safety of intravitreal anti-VEGF therapies for ocular neovascular disease. Survey of ophthalmology 56, 95–113.

Tombran-Tink, J., Mazuruk, K., Rodriguez, I. R., Chung, D., Linker, T., Englander, E., and Chader, G. J. (1996). Organization, evolutionary conservation, expression and unusual Alu density of the human gene for pigment epithelium-derived factor, a unique neurotrophic serpin. Molecular vision 2, 11.

Tombran-Tink, J., Pawar, H., Swaroop, A., Rodriguez, I., and Chader, G. J. (1994). Localization of the gene for pigment epithelium-derived factor (PEDF) to chromosome 17p13.1 and expression in cultured human retinoblastoma cells. Genomics 19, 266–272.

Tombran-Tink, J., Shivaram, S. M., Chader, G. J., Johnson, L. V., and Bok, D. (1995). Expression, secretion, and age-related downregulation of pigment epithelium-derived factor, a serpin with neurotrophic activity. The Journal of neuroscience 15, 4992–5003.

Tombran-Tink, J., and Johnson, L. V. (1989). Neuronal differentiation of retinoblastoma cells induced by medium conditioned by human RPE cells. Investigative ophthalmology & visual science 30, 1700–1707.

Tonello, M., Costa, R. A., Almeida, F. P. P., Barbosa, J. C., Scott, I. U., and Jorge, R. (2008). Panretinal photocoagulation versus PRP plus intravitreal bevacizumab for high-risk proliferative diabetic retinopathy (IBeHi study). Acta ophthalmologica 86, 385–389.

Towler, H., and Lightman, S. (2003). Clinical features and management of diabetic eye disease. In Textbook of Diabetes, J. Pickup and G. Williams, eds. (Blackwell Publishing).

Treins, C., Giorgetti-Peraldi, S., Murdaca, J., Monthouël-Kartmann, M.-N., and Van Obberghen, E. (2005). Regulation of hypoxia-inducible factor (HIF)-1 activity and expression of HIF hydroxylases in response to insulin-like growth factor I. Molecular endocrinology 19, 1304–1317.

Tschernutter, M., Schlichtenbrede, F. C., Howe, S., Balaggan, K. S., Munro, P. M., Bainbridge, J. W. B., Thrasher, A. J., Smith, A. J., and Ali, R. R. (2005). Long-term preservation of retinal function in the RCS rat model of retinitis pigmentosa following lentivirus-mediated gene therapy. Gene therapy 12, 694–701.

Tsubota, K., Inoue, H., Ando, K., Ono, M., Yoshino, K., and Saito, I. (1998). Adenovirus-mediated gene transfer to the ocular surface epithelium. Experimental eye research 67, 531–538.

Tyrberg, M., Lindblad, U., Melander, A., Lövestam-Adrian, M., Ponjavic, V., and Andréasson, S. (2011). Electrophysiological studies in newly onset type 2 diabetes without visible vascular retinopathy. Documenta ophthalmologica. Advances in ophthalmology 123, 193–198.

UKPDS (1998). Intensive blood-glucose control with sulphonylureas or insulin compared with conventional treatment and risk of complications in patients with type 2 diabetes (UKPDS 33). UK Prospective Diabetes Study (UKPDS) Group. Lancet 352, 837–853.

Uehara, H., Miyamoto, M., Kato, K., Ebihara, Y., Kaneko, H., Hashimoto, H., Murakami, Y., Hase, R., Takahashi, R., Mega, S., et al. (2004). Expression of pigment epithelium-derived factor decreases liver metastasis and correlates with favorable prognosis for patients with ductal pancreatic adenocarcinoma. Cancer research 64, 3533–3537.

Ueta, T., Yanagi, Y., Tamaki, Y., and Yamaguchi, T. (2009). Cerebrovascular accidents in ranibizumab. Ophthalmology 116, 362.

Ulbricht, E., Pannicke, T., Hollborn, M., Raap, M., Goczalik, I., Iandiev, I., Härtig, W., Uhlmann, S., Wiedemann, P., Reichenbach, A., et al. (2008). Proliferative gliosis causes mislocation and inactivation of inwardly rectifying K(+) (Kir) channels in rabbit retinal glial cells. Experimental eye research 86, 305–313.

Venters, H. D., Tang, Q., Liu, Q., VanHoy, R. W., Dantzer, R., and Kelley, K. W. (1999). A new mechanism of neurodegeneration: a proinflammatory cytokine inhibits receptor signaling by a survival peptide. Proceedings of the National Academy of Sciences of the United States of America 96, 9879–9884.

Volpert, O. V., Zaichuk, T., Zhou, W., Reiher, F., Ferguson, T. A., Stuart, P. M., Amin, M., and Bouck, N. P. (2002). Inducer-stimulated Fas targets activated endothelium for destruction by anti-angiogenic thrombospondin-1 and pigment epithelium-derived factor. Nature medicine 8, 349–357.

Vázquez-Chona, F. R., Swan, A., Ferrell, W. D., Jiang, L., Baehr, W., Chien, W.-M., Fero, M., Marc, R. E., and Levine, E. M. (2011). Proliferative reactive gliosis is compatible with glial metabolic support and neuronal function. BMC neuroscience 12, 98.

Wachtmeister, L. (1998). Oscillatory potentials in the retina: what do they reveal. Progress in retinal and eye research 17, 485–521.

Wang, A., Nomura, M., Patan, S., and Ware, J. A. (2002). Inhibition of protein kinase Calpha prevents endothelial cell migration and vascular tube formation in vitro and myocardial neovascularization in vivo. Circulation research 90, 609–616.

Wang, H., and Keiser, J. A. (1998). Vascular endothelial growth factor upregulates the expression of matrix metalloproteinases in vascular smooth muscle cells: role of flt-1. Circulation research 83, 832–840.

Wang, J. J., Zhang, S. X., Mott, R., Knapp, R. R., Cao, W., Lau, K., and Ma, J.-X. (2006a). Salutary effect of pigment epithelium-derived factor in diabetic nephropathy: evidence for antifibrogenic activities. Diabetes 55, 1678–1685.

Wang, J., Zhang, S. X., Gao, G., Park, K., and Ma, J. (2006b). Pigment epithelium-derived factor downregulates vascular endothelial growth factor (VEGF) expression and inhibits VEGF-VEGF receptor 2 binding in diabetic retinopathy. Journal of Molecular Endocrinology 37, 1–12.

Wang, M., Ma, W., Zhao, L., Fariss, R. N., and Wong, W. T. (2011). Adaptive Müller cell responses to microglial activation mediate neuroprotection and coordinate inflammation in the retina. Journal of neuroinflammation 8, 173.

Wellner, M., Maasch, C., Kupprion, C., Lindschau, C., Luft, F. C., and Haller, H. (1999). The proliferative effect of vascular endothelial growth factor requires protein kinase C-alpha and protein kinase C-zeta. Arteriosclerosis, thrombosis, and vascular biology 19, 178–185.

Wells, L., and Hart, G. W. (2003). O-GlcNAc turns twenty: functional implications for post-translational modification of nuclear and cytosolic proteins with a sugar. FEBS letters 546, 154–158.

Wilson, G. L., Patton, N. J., McCord, J. M., Mullins, D. W., and Mossman, B. T. (1984). Mechanisms of streptozotocin- and alloxan-induced damage in rat B cells. Diabetologia 27, 587–591.

Wong, T. Y., Klein, R., Islam, F. M. A., Cotch, M. F., Folsom, A. R., Klein, B. E. K., Sharrett, A. R., and Shea, S. (2006). Diabetic retinopathy in a multi-ethnic cohort in the United States. American journal of ophthalmology 141, 446–455.

Wu, Y. Q., and Becerra, S. P. (1996). Proteolytic activity directed toward pigment epithelium-derived factor in vitreous of bovine eyes. Implications of proteolytic processing. Investigative ophthalmology & visual science 37, 1984–1993.

Xia, P., Inoguchi, T., Kern, T. S., Engerman, R. L., Oates, P. J., and King, G. L. (1994). Characterization of the mechanism for the chronic activation of diacylglycerol-protein kinase C pathway in diabetes and hypergalactosemia. Diabetes 43, 1122–1129.

Xie, Q., Bu, W., Bhatia, S., Hare, J., Somasundaram, T., Azzi, A., and Chapman, M. S. (2002). The atomic structure of adeno-associated virus (AAV-2), a vector for human gene therapy. Proceedings of the National Academy of Sciences of the United States of America 99, 10405–10410.

Yabe, T., Wilson, D., and Schwartz, J. P. (2001). NFkappaB activation is required for the neuroprotective effects of pigment epithelium-derived factor (PEDF) on cerebellar granule neurons. The Journal of biological chemistry 276, 43313–43319.

Yamada, H., Yamada, E., Higuchi, A., and Matsumura, M. (2005). Retinal neovascularisation without ischaemia in the spontaneously diabetic Torii rat. Diabetologia 48, 1663–1668.

Yamanaka, K., Boillee, S., Roberts, E. A., Garcia, M. L., McAlonis-Downes, M., Mikse, O. R., Cleveland, D. W., and Goldstein, L. S. B. (2008). Mutant SOD1 in cell types other than motor neurons and oligodendrocytes accelerates onset of disease in ALS mice. Proceedings of the National Academy of Sciences of the United States of America 105, 7594–7599.

Yoshioka, M., Kayo, T., Ikeda, T., and Koizumi, A. (1997). A novel locus, Mody4, distal to D7Mit189 on chromosome 7 determines early-onset NIDDM in nonobese C57BL/6 (Akita) mutant mice. Diabetes 46, 887–894.

Yu, D.-Y., and Cringle, S. J. (2005). Retinal degeneration and local oxygen metabolism. Experimental eye research 80, 745–751.

Zeng, H.-yang, Green, W. R., and Tso, M. O. M. (2008). Microglial activation in human diabetic retinopathy. Archives of ophthalmology 126, 227–232.

Ziche, M., Morbidelli, L., Masini, E., Amerini, S., Granger, H. J., Maggi, C. A., Geppetti, P., and Ledda, F. (1994). Nitric oxide mediates angiogenesis in vivo and endothelial cell growth and migration in vitro promoted by substance P. The Journal of clinical investigation 94, 2036–2044.

Zimmerman, M. A., Haskins, K., Bradley, B., Gilman, J., Gamboni-Robertson, F., and Flores, S. C. (2011). Autoimmune-mediated vascular injury occurs prior to sustained hyperglycemia in a murine model of type I diabetes mellitus. The Journal of surgical research 168, e195–e202.